

THE HYDRAULICS OF AN IRRIGATION
DISTRIBUTION CHANNEL

By

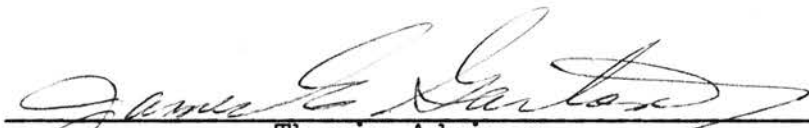
ALBERT LEE MINK

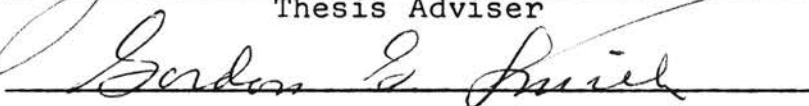
Bachelor of Science
Arkansas State College
Jonesboro, Arkansas
1961


Master of Science
Louisiana State University
Baton Rouge, Louisiana
1963


Submitted to the faculty of the
Graduate College
of the Oklahoma State University
in partial fulfillment of the
requirements for the degree
of
DOCTOR OF PHILOSOPHY
May, 1967

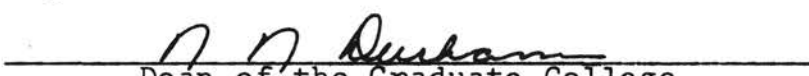
THE HYDRAULICS OF AN IRRIGATION
DISTRIBUTION CHANNEL


Thesis Adviser








Dean of the Graduate College

JAN 16 1968

ACKNOWLEDGMENTS

The work upon which this research is based was supported in part by funds provided by the United States Department of the Interior as authorized under the Water Resources Research Act of 1964, Public Law 88-379.

The author is especially grateful to his major adviser, Dr. James E. Garton, for his capable guidance during this study. His suggestions and comments were an inspiration to me from the initiation of the study through the preparation of the manuscript.

A special thanks is extended to Professor E. W. Schroeder, Head of the Agricultural Engineering Department, for serving on the advisory committee and to the Department for providing an assistantship throughout the study.

To the other members of the advisory committee, Dr. John F. Stone, Professor Gordon G. Smith, and the late Professor Roger F. Flanders, I thank you for your criticism and suggestions.

Thanks is extended to Mr. W. O. Ree of the Agricultural Research Service of the United States Department of Agriculture and his staff for their cooperation and for providing a desirable location for the experimental setup.

Appreciation is extended to Jack Fryrear and Don McCrackin for their assistance with the drafting of the figures.

I wish to thank Bill Allison, John Sweeten, Owen Maddux, and Larry Hada for their assistance in the gathering of the experimental data.

I am grateful to my wife, Loyce, for typing the rough draft of the manuscript and to Mrs. Sandra Carroll for typing the final draft of the manuscript.

TABLE OF CONTENTS

Chapter	Page
I. INTRODUCTION	1
The Problem	2
Objectives	4
Experimental Plan	5
Definition of Symbols	6
II. REVIEW OF LITERATURE	9
Equation of Motion	12
Bernoulli Equation	15
Gradually Varied Flow	17
Momentum Equation	21
Energy Equation	25
Spatially Varied Flow	28
Decreasing Spatially Varied Flow	34
Non-uniformity Coefficient	39
Open Channel Formulas	43
A Note on Manning's Formula	50
Resistance	52
Calculation of the Roughness Coefficient n	60
Dimensionless Parameters	61
Irrigation	64
The Concrete Lined Channel	67
Siphon Tubes	69
III. THEORY	73
General Energy Equation	74
Decreasing Spatially Varied Flow Equation	77
Discussion	81
IV. PRELIMINARY INVESTIGATION	82
Results	83
Summary	86
V. EXPERIMENTAL DISTRIBUTION CHANNEL SETUP	91
Distribution Channel	93
Gauge Wells and Reference System	93
Siphon Tube Mount	98

Chapter	Page
Check Gate	100
Velocity Distribution Measurements	100
Orifice Meter and Manometer.	103
VI. EXPERIMENTAL PROCEDURE	107
Gauge Zero and Channel Bottom	107
Geometric Channel Elements	108
Counter Test	109
Velocity Distribution and Resistance	111
Resistance	112
Siphon Tubes	114
Spatially Varied Flow Tests	114
VII. ANALYSIS AND DISCUSSION OF DATA	119
Siphon Tubes	119
Non-uniformity Coefficients	124
Alpha Without Tubes	132
Alpha With Siphon Tubes	135
Linear Model.	135
Dimensionless Model	137
Multivariant Model	140
Resistance	141
Resistance Without Tubes	142
Resistance With Tubes	149
Functional Model.	149
Dimensionless Model	154
Multivariant Model	157
Spatially Varied Flow Tests	159
Spatially Varied Profile n-cal and $\alpha = 1$	161
Water Surface Profile with Adjusted \bar{n}	165
Effective n For the Experimental Channel	171
Water Surface Profiles With n-cal and α -cal	171
Water Surface Profile for Sloping	
Prismatic Channels	174
Constant Tube Elevation	174
Tube Elevation 1.224 Feet Above	
Channel Bottom	180
VIII. SUMMARY AND CONCLUSIONS	194
Summary	194
Conclusions	196
Suggestions For Further Research	199
BIBLIOGRAPHY	200

Chapter	Page
APPENDIX A	205
APPENDIX B	209
APPENDIX C	212
APPENDIX D	215
APPENDIX E	217
APPENDIX F	234
APPENDIX G	239
APPENDIX H	248

LIST OF TABLES

Table	Page
I. Proposed Design Values of α And β From Kolupaila	41
II. Proposed Open Channel Formulas	45
III. An Analysis of the Variation of the Five Time Treatments at Five Velocities	110
IV. Experimental Design With Siphon Tubes	115
V. Spatially Varied Flow Tests	117
VI. Values of the Q Versus h_o Relationships for Different Siphon Tube Diameter.	121
VII. Non-Uniformity Coefficients for the Experimental Channel Without Siphon Tubes (Steady Gradually Varied Flow).	126
VIII. Non-Uniformity Coefficients at Station 0 + 60 for the Experimental Channel With Siphon Tubes (Steady Gradually Varied Flow).	128
IX. Non-Uniformity Coefficients Spatially Varied Flow Test Tube Location 1.0 Foot From Channel Bottom.	131
X. Coefficients for α Versus N_R for the Experimental Channel Without Tubes	133
XI. Values of n , n_α , f and f_α for Reach 0 + 00 to 1 + 80 Without Tubes	143
XII. Values of n , n_α , f and f_α for Reach 0 + 00 to 1 + 80 With Tubes	144
XIII. Resistance Values, Depths, Water Surface Elevations and Entering Q's for Various Tube Diameters in the Spatially Varied Flow Tests, 90 Tubes, 40-Inch Spacing	170

LIST OF FIGURES

Figure	Page
1. Infinitesimal Parallelepiped of Fluid	10
2. Infinitesimal Parallelepiped of Fluid with Velocity and Pressure Components in the x Direction	13
3. Graphic Illustration of Gradually Varied Flow . .	19
4. Free Body of an Elementary Fluid Volume	22
5. Elementary Fluid Volume	26
6. Graphic Illustration of Increasing Spatially Varied Flow	36
7. α and β for Wide Channels	44
8. The f to N_R Relationship for Flow in Rough Channels (after Chow)	53
9. Relationship of a Trapezoidal Channel in which the Bottom and Sides Have Different Roughness Characteristics	58
10. Elevation Drawing Showing the System of Cut-Back Furrow Irrigation Using One Cut-Back.	66
11. Proposed Standard Trapezoidal Canal and Ditch Sections	68
12. The Discharge of Plastic Siphon Tubes as a Function of Tube Diameter and Head.	71
13. Graphic Illustration of Decreasing Spatially Varied Flow	78
14. Change in the Water Surface Between the Ends of Level Distribution Bays of Various Depths Having 100 Tubes with a 3.33 Foot Spacing, a Manning n of 0.020 and $\alpha = 1.0$	84

Figure	Page
15. Change in the Water Surface Between the Ends of Level Distribution Bays Having Different Roughness.	85
16. The Effect of the Number of Tubes on the Depth Required for Equal Water Surface Elevation Between the Ends of a Distribution Bay. Tube Discharge = 0.02 cfs. Tube Spacing, 40 Inches.	87
17. The Depth Required for the Same Water Surface Elevation Between the Ends of a Level Distribution Bay for Different Numbers of Tubes and Different Roughness.	88
18. A Generalized Relationship of Depth Required for the Same Water Surface Elevation Between the Ends of Level Distribution Bays for Different Numbers of Tubes, Roughness, Tube Discharge and α	89
19. A General View of the Experimental Setup Showing the Water Supply Line, Orifice, Manometer, Gauge Wells, and Channel With the 2-Inch Tubes in Place for a Roughness Test	92
20. A View of the Wind Panels in Place During a Spatially Varied Flow Test. The Panels Were Used to Eliminate Wind Effects on the Water Surface Profile	94
21. A View of the Test Section of the Channel, the Siphon Tube Mounts, and the Concrete Apron	95
22. The Gauge Well at Station 0 + 00 With a FW-1 Water Stage Recorder and a 3-Foot Point Gauge. The Plumbing Seen on the Well Was Used to Obtain Gauge Zeros From a Common Water Surface	96
23. The Gauge Well at Station 0 + 90 With a 2-Foot Point Gauge. The Gauge Well is Typical of the Wells at the Other 9 Stations Along the Test Channel	97
24. A Brass Plug Embedded in the Channel Bottom. The Plug Was Used to Determine the Bottom Elevation of the Channel	99

Figure	Page
25. The Overflow Check Dam at the Downstream End of the Channel. In the Down Position the Dam Offers Little Resistance to Flow.	101
26. The Check Dam in an Up Position. The Dam was Used to Control the Depth in the Steady Flow Tests.	102
27. Point Velocity Measuring Apparatus. The Component Parts Are: 8-Inch Aluminum H Beam, Carriage, 3-Foot Point Gauge, OTT Laboratory Current Meter, and OTT F-4 Revolution Counter.	104
28. The Orifice Meter Used to Measure the Inflow. .	105
29. The Discharge Control Valve and 60-Inch Manometer	106
30. An Arrangement for a Typical Velocity Traverse	113
31. The Pump and Flexible Hose Used to Prime the Siphon Tube in the Spatially Varied Flow Tests	118
32. Relationship of Discharge Versus Head for Plastic Siphon Tubes	122
33. Relationship of C Versus Tube Diameter for Plastic Siphon Tubes	123
34. N_R/α Versus N_R for Channel Without Tubes . . .	134
35. A Plot of the Alpha Observed Versus Alpha Calculated from the Linear Model.	136
36. Alpha Observed Versus Alpha Calculated From the Dimensionless Model	139
37. Relationships of $N_R R^{1/6}/n$ Versus N_R for the Channel Without Tubes	147
38. Relationship of n Versus N_R for the Data of the Fall, 1965 and June, 1966	148
39. Average n as a Function of Tube Diameter at a Fixed Tube Location	150
40. Slope Versus Tube Location From Channel Bottom	152

Figure	Page
41. n Observed Versus n Calculated from Equation 24	153
42. Π_0 Versus Π_2 for Various Values of Q	155
43. Slopes from Figure 42 Versus $\bar{\Pi}_3$	156
44. n Observed Versus n As Calculated from Equation 25	158
45. f Versus N_R For Various Tube Diameters and Hydraulic Radii	163
46. The Relationship of f Versus N_R Used in the Water Surface Profile Computations	164
47. Water Surface Elevations as Observed and Calculated for the Channel with 2-Inch Tubes in the Spatially Varied Flow Tests	166
48. Water Surface Elevations as Observed and Calculated for the Channel with 1.5- Inch Tubes in the Spatially Varied Flow Tests.	167
49. Water Surface Elevations as Observed and Calculated for the Channel with 1.25- Inch Tubes in the Spatially Varied Flow Tests	168
50. Water Surface Elevations as Observed and Calculated for the Channel with 1.0- Inch Tubes in the Spatially Varied Flow Tests	169
51. The Functional Relationship of n_e Versus \bar{n}	172
52. Change in Water Surface Elevation Between the Upstream and Downstream End of the Prismatic Channel as a Function of Slope for the 2- Inch Tubes with Various Depths and Entering Q 's.	176
53. Change in Water Surface Elevation Between the Upstream and Downstream End of the Prismatic Channel as a Function of Slope for the 1.5- Inch Tubes with Various Depths and Entering Q 's.	177

Figure	Page
54. Change in Water Surface Elevation Between the Upstream and Downstream End of the Prismatic Channel as a Function of Slope for the 1.25-Inch Tubes with Various Depths and Entering Q's	178
55. Change in Water Surface Elevation Between the Upstream and Downstream End of the Prismatic Channel as a Function of Slope for the 1.0-Inch Tubes with Various Depths and Entering Q's	179
56. Percentage Change in the 2.00-Inch Tube Discharge for Tubes At a Constant Elevation in a Prismatic Channel with Various Slopes	181
57. Percentage Change in the 1.5-Inch Tube Discharge for Tubes At a Constant Elevation in a Prismatic Channel with Various Slopes	182
58. Percentage Change in the 1.25-Inch Tube Discharge for Tubes At a Constant Elevation in a Prismatic Channel with Various Slopes	183
59. Percentage Change in the 1.0-Inch Tube Discharge for Tubes At a Constant Elevation in a Prismatic Channel with Various Slopes	184
60. Δw_s As a Function of Slope for a Prismatic Channel With 2.0-Inch Siphon Tubes. The Tube Outlets Were 1.224 Feet Above the Channel Bottom	185
61. Δw_s As a Function of Slope for a Prismatic Channel with 1.5-Inch Siphon Tubes. The Tube Outlets Were 1.224 Feet Above the Channel Bottom	186
62. Δw_s As a Function of Slope for a Prismatic Channel with 1.25-Inch Siphon Tubes. The Tube Outlets Were 1.224 Feet Above the Channel Bottom	187
63. Δw_s As a Function of Slope for a Prismatic Channel with 1.0-Inch Siphon Tubes. The Tube Outlets Were 1.224 Feet Above the Channel Bottom	188

Figure	Page
64. Percentage Change in the 2.00-Inch Tube Discharge for a Prismatic Channel with Various Slopes. The Tube Outlets Were 1.224 Feet From the Channel Bottom.	190
65. Percentage Change in the 1.5-Inch Tube Discharge for a Prismatic Channel with Various Slopes. The Tube Outlets Were 1.224 Feet From the Channel Bottom.	191
66. Percentage Change in the 1.25-Inch Tube Discharge for a Prismatic Channel with Various Slopes. The Tube Outlets Were 1.224 Feet From the Channel Bottom.	192
67. Percentage Change in the 1.00-Inch Tube Discharge for a Prismatic Channel with Various Slopes. The Tube Outlets Were 1.224 Feet From the Channel Bottom.	193

CHAPTER I

INTRODUCTION

About half of the fresh water usage in the United States is for irrigation. The general consensus among researchers (17,18,23)* is that less than 40 per cent of the water diverted from the sources is made available to the crop where the depth of water applied is from 4 to 5 inches. An added decrease in efficiency can be expected with an increase in depths of application greater than 5 inches.

A reduction in water losses would result in a more efficient irrigation system and an increase in the total national water supply. A large contributor to water loss is uneven distribution. Thus, one way to reduce water loss would be to distribute the water more uniformly at the ditch.

A popular method of furrow irrigation is to use a concrete-lined channel in conjunction with siphon tubes. Its popularity is a result of the ease with which water can be taken from the distribution channel with siphon tubes and the low initial cost of the channel.

*Number in parentheses refers to the bibliography.

An effective way to achieve more uniform water application with a furrow irrigation system is to supply the furrows with a high initial inflow until they have watered through the field then decrease the inflow to a rate that is approximately equal to the in-take rate of the soil.

The purpose, regardless, of the design of an irrigation system is usually to store water in the root zone. The most desirable irrigation system is one that applies water to the soil uniformly while minimizing soil erosion, water losses, labor, and land used for the system.

The Problem

A furrow irrigation system generally has a conveyance and distribution channel. The hydraulic problems encountered in the conveyance channel are relatively simple. There are equations relating the pertinent quantities of the channel that give reliable estimates of the desired hydraulic properties.

In the distribution channel where the water is transferred from the channel to the furrows, the hydraulic problems become more complex. If the water is transferred from the channel along the distribution section, the resulting flow is known as decreasing spatially varied flow. The mathematical model and the hydraulic properties used in describing spatially varied flow have not been determined for small irrigation channels.

Decreasing spatially varied flow in a steady state condition has been studied for short channels in sewage disposal plants, channels with a bottom rack, and channels with a side weir; but little work has been done in applying the theories that have been developed for decreasing spatially varied flow to irrigation distribution channels where siphon tubes are used to transfer the water from the channel to the furrow.

The equations that supposedly describe decreasing spatially varied flow show the water surface elevation as a function of channel slope, roughness, quantity of water flowing, the amount of water taken out of the channel per unit distance, and non-uniformity coefficient (α). Thus, the water surface elevation is influenced by several factors and is subject to change.

Assuming siphon tubes are used as a means of transporting the water from the channel to the soil, then the water surface elevation becomes important due to the Q vs h relationship of the siphon tubes. To maintain a more nearly constant head on the tubes and a more nearly constant discharge for each tube one must be able to predict the water surface elevation for a channel.

Most of the distribution ditches in use today have slope. If siphon tubes were set at the same location relative to the ditch, slope would cause the siphon tube discharge to be less at the higher end of the channel, provided the water surface elevation was constant.

Compensation for the unequal discharge of the tubes accomplished by raising or lowering the outlet of the tubes would result in additional expense to the operation of the system. Without equalizing the heads, the system would not provide uniform water application.

A distribution channel, constructed as a series of level bays should result in a level water surface and provide uniform water application when the siphon tube outlets are at the same elevation.

The purpose of this study was to investigate the validity of this hypothesis theoretically with existing mathematical models and experimentally with a level distribution channel.

Objectives

To obtain a more effective and efficient design of a distribution channel with siphon tubes, the hydraulic properties should be determined. Also, the mathematical models that supposedly describe such a spatially varied flow system should be examined and modified if the experimental results from such a system indicate that sufficient accuracy cannot be obtained with the present mathematical models. Thus, the objectives of this study are as follows:

1. To predict water surface profiles for spatially varied flow with decreasing discharge in a

- concrete irrigation distribution channel using the theory of spatially varied flow.
2. Determine the water surface profiles in the distribution channel for spatially varied steady flow for various inflows, siphon tube sizes, and tube submergence.
 3. To modify, if necessary, the present theory of decreasing spatially varied flow to more accurately predict the measured water surface profile.
 4. Determine if a level irrigation channel distributes the water more uniformly than a sloping channel.

Experimental Plan

The experimental plan contains the following steps:

1. Construct a small concrete-lined channel covering the range of dimensions currently used in distribution channels.
2. Instrument the channel to obtain accurate measurements of the hydraulic properties, water surface profiles, and siphon tube elevations.
3. Determine the hydraulic properties of the channel from steady flow tests.

4. Determine suitable functional relationships of the hydraulic properties of the channel from steady flow tests.
5. Determine if the present theoretical models in conjunction with the functional relationships accurately describe the condition of decreasing spatially varied flow in the distribution channel.
6. Apply the information obtained from the level distribution channel to sloping channels.

Definition of Symbols

<u>Symbol</u>	<u>Quantity</u>	<u>Dimensions</u>
a	acceleration	ft./sec. ²
A	area	ft. ²
A _{avg}	average area	ft. ²
C	coefficient, Chezy	ft. ^{1/2} sec.
C	coefficient, discharge	ft. ^{1/2} sec.
C	coefficient, exponent	nonhomogeneous
d	depth normal to channel bottom	ft.
D	diameter	ft.
D	hydraulic depth	ft.
e	bulk modulus	lb./ft. ²
f	resistance coefficient, Darcy - Weisbach	dimensionless
F _B	total force on a body	lb.

<u>Symbol</u>	<u>Quantity</u>	<u>Dimensions</u>
F	force (basic quantity)	lb.
F _g	force, gravitational	lb.
F _p	force, pressure	lb.
F _s	force, shearing	lb.
g	gravitational acceleration	ft./sec. ²
h	head	ft.
h _L	head, resistance	ft.
H	head, total (Bernoulli)	ft.
k	roughness height	ft.
k	constant	dimensionless
L	length (channel reach)	ft.
m	mass (basic quantity)	lb. sec. ² /ft.
m	coefficient in Bazin formula	nonhomogeneous
n	coefficient in Manning formula ¹	ft. ^{1/6}
n	coefficient in Kutter formula	nonhomogeneous
n	coefficient, exponent	dimensionless
N _C	Cauchy number	dimensionless
N _E	Euler number	dimensionless
N _F	Froude number	dimensionless
N _M	Mach number	dimensionless
N _R	Reynolds number	dimensionless
N _W	Weber number	dimensionless
P	pressure	lb./ft. ²
P	perimeter	ft.
q	discharge per foot of length	ft. ³ /sec./ft.

¹See Chapter II, Review of Literature.

<u>Symbol</u>	<u>Quantity</u>	<u>Dimensions</u>
Q	discharge	ft. ³ /sec.
R	hydraulic radius (A/P)	ft.
s	distance along stream tube	ft.
S _o	slope, bed	dimensionless
S _s	slope, shear	dimensionless
t	time	sec.
T	top width	ft.
v	local velocity	ft./sec.
V	mean velocity	ft./sec.
V _o	volume	ft. ³
x	arbitrary direction	ft.
x	coordinate in direction of flow	ft.
y	depth of flow	ft.
y _m	depth, mean	ft.
w	weight	lb.
z	vertical distance from a datum	ft.
α	Coriolis coefficient	dimensionless
β	Boussinesq coefficient	dimensionless
γ	specific weight	lb./ft. ³
γ	specific heat ratio	dimensionless
θ	inclination angle of channel bottom	dimensionless
μ	viscosity, dynamic	lb. sec./ft. ²
ν	viscosity, kinematic	ft. ² /sec.
ρ	density	lb. sec. ² /ft. ⁴
∇	vector differential operator	

CHAPTER II

REVIEW OF LITERATURE

The subject matter in this chapter, Review of Literature, contains a brief resume' of the fundamental concepts of fluid mechanics, gradually varied flow, spatially varied flow, nonuniformity coefficients, open channel formulas, resistance coefficients and siphon tube discharge.

Continuity Equation

A mass of fluid can neither be created or destroyed by virtue of its motion. Therefore, in ideal flow between solid boundaries or a stream tube¹, the rate of passage of fluid moving through successive cross sections is a constant. Page (43) showed this by considering a small infinitesimal parallelepiped of fluid in a body shown in Figure 1. The sides have length dx , dy , and dz .

¹A streamline is a line drawn through a flowing fluid such that every point along its length is tangent to the velocity vector. Thus, the streamline imposes a boundary condition on the adjacent flow, i.e., flow cannot cross a streamline.

A stream tube is a closed surface formed of streamlines. Since the stream tube surface is composed of streamlines there can be no flow across or through a stream tube.

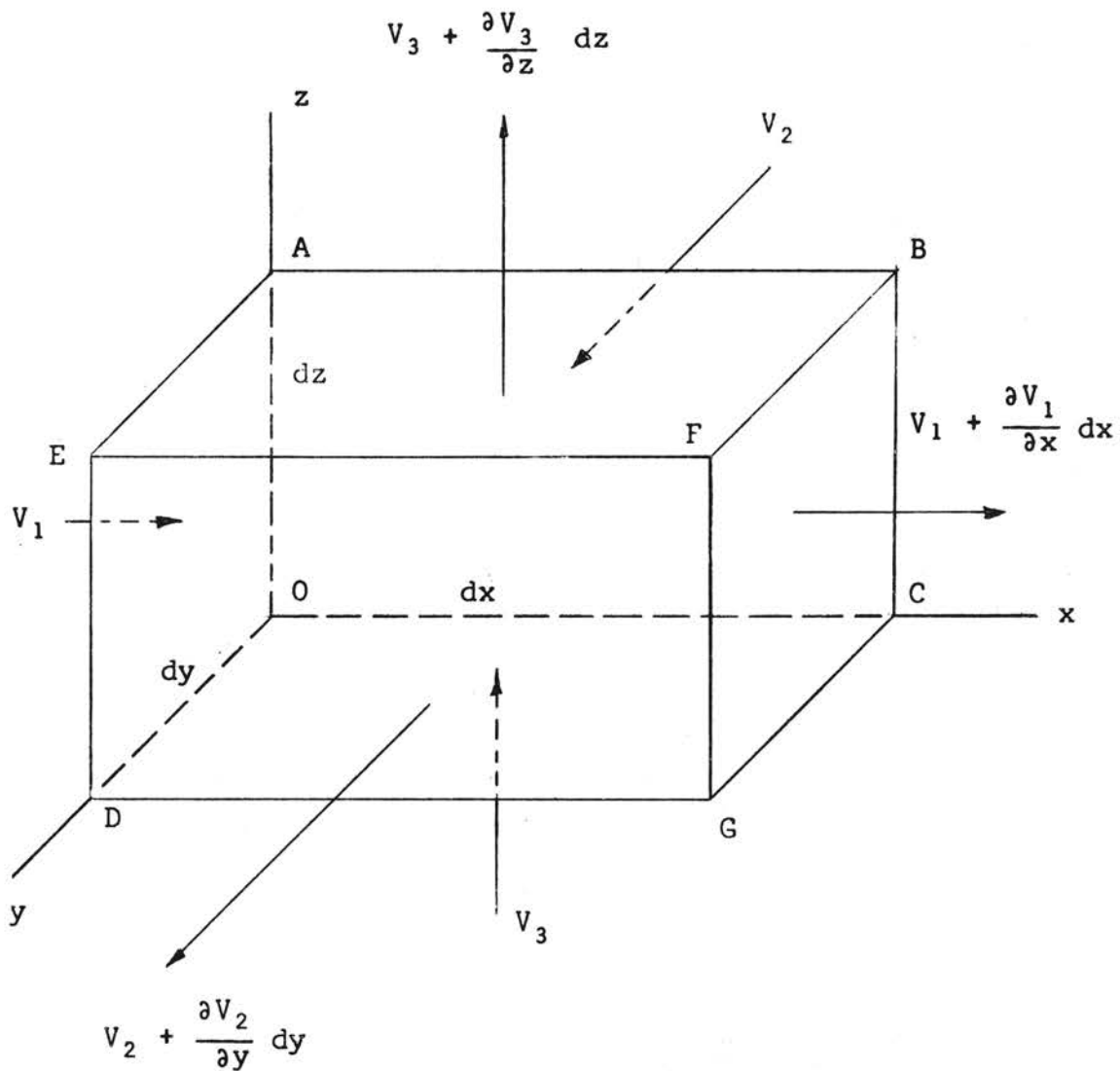


Figure 1. Infinitesimal Parallelepiped of Fluid

Assume the vector \vec{V} , \vec{V} = mass of fluid flowing through a unit cross sectional area perpendicular to the flow per unit time. If the fluid has a density of ρ and a velocity of \vec{v} then

$$\vec{V} = \rho \vec{v}$$

where

$$\begin{aligned}\vec{V} &= V_1 \vec{i} + V_2 \vec{j} + V_3 \vec{k} \\ \vec{v} &= v_1 \vec{i} + v_2 \vec{j} + v_3 \vec{k}\end{aligned}$$

Consider first the mass flow per unit of time in the x direction. The mass entering the left face through the area AEDO is $V_1 dy dz$ while the mass flowing through the area BFGC is

$$\left(V_1 + \frac{\partial V_1}{\partial x} dx \right) dy dz$$

Thus, the net gain of fluid mass in the x direction inside the infinitesimal volume is

$$V_1 dy dz - \left(V_1 + \frac{\partial V_1}{\partial x} dx \right) dy dz = - \frac{\partial V_1}{\partial x} dx dy dz$$

It follows that the net gain in mass in the y and z directions are

$$- \frac{\partial V_2}{\partial y} dy dz dx \text{ and } - \frac{\partial V_3}{\partial z} dz dy dx$$

respectively. Hence, the net increase of mass inside the volume is

$$- \left(\frac{\partial V_1}{\partial x} + \frac{\partial V_2}{\partial y} + \frac{\partial V_3}{\partial z} \right) dx dy dz$$

The foregoing equation represents the change of mass in a unit volume in a unit time which can be represented by

$$\frac{\partial \rho}{\partial t} dx dy dz$$

If there is to be no creation of mass then the total mass rate of flow across the closed boundary must be zero. So, the equation of continuity becomes

$$\frac{\partial \rho}{\partial t} + \nabla \cdot \vec{V} = 0 \quad (1)$$

Equation of Motion

A mathematical description of fluid motion is useful in the solution of fluid motion problems. Newton's second law is the basis for the equations of fluid motion, $F = Ma$. The quantities that act independently and cause fluid motion are pressure (a property of state), density, viscosity, surface tension, and elasticity (properties of the fluid).

Binder (7) is one of the many authors that used an adequate and standard approach to derive an equation of fluid motion. Consider an infinitesimal parallelepiped in a body of fluid as shown in Figure 2. The sides have the lengths of dx , dy , and dz . If the fluid is ideal or frictionless, the force effects, viscosity, surface tension and elasticity can be neglected. First, sum the forces acting on the fluid element in the x direction.

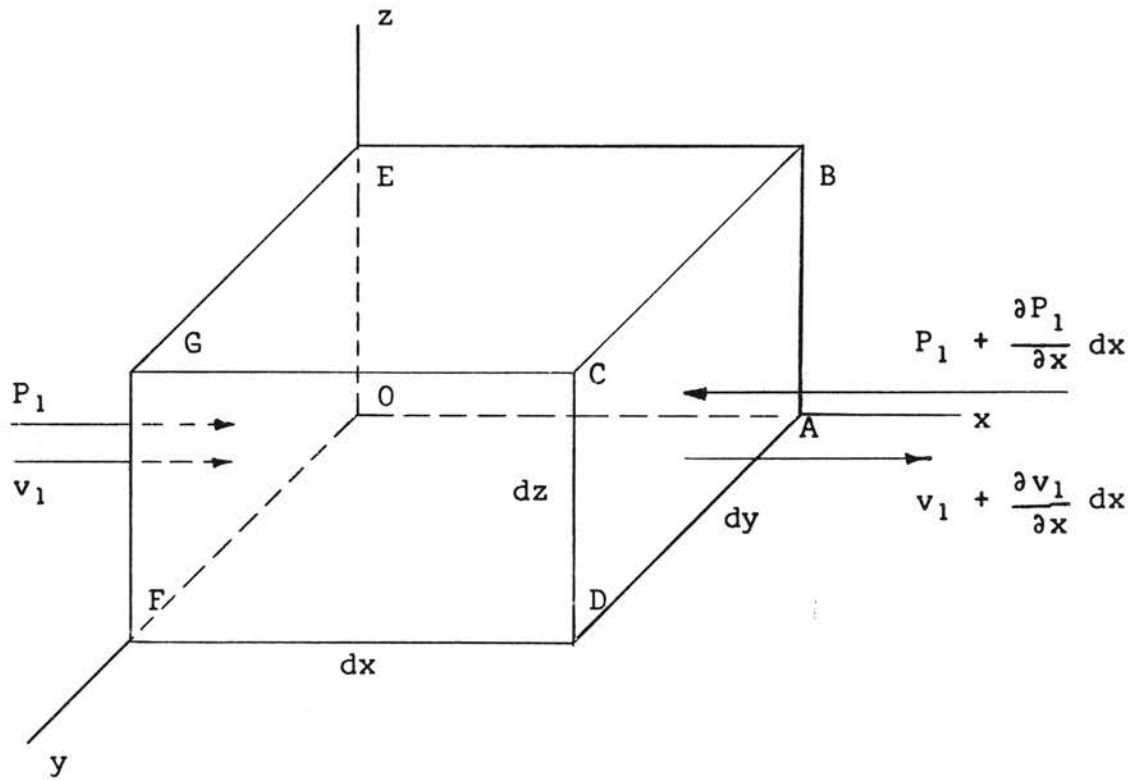


Figure 2. Infinitesimal Parallelepiped of Fluid with Velocity and Pressure Components in the x Direction

The pressure force on the left face OEGF is $P_1 dy dz$. The pressure force on the right face ABCD is $(P_1 + \frac{\partial P_1}{\partial x} dx) dy dz$. Thus, the net pressure force acting in the positive x direction is $-\frac{\partial P}{\partial x} dx dy dz$. Similarly, pressure forces acting in the positive y and z directions are $-\frac{\partial P}{\partial y} dx dy dz$ and $-\frac{\partial P}{\partial z} dz dx dy$, respectively. The pressure gradient of the element can be represented by $-\nabla P$. If the body forces are U, Q, and R representing the x, y, and z components of the body forces per unit mass, such that

$$\vec{F}_B = U\vec{i} + Q\vec{j} + R\vec{k}$$

then the sum of the total forces per unit volume that cause motion of the element is

$$\sum \vec{F} = \vec{F}_B - \nabla P$$

If the velocity of the fluid element is \vec{v} , then from Newton's second law

$$\sum \vec{F} = m\vec{a} = \rho dx dy dz \frac{d\vec{v}}{dt}$$

Substituting for $\sum \vec{F}$ the equation becomes

$$\rho \frac{d\vec{v}}{dt} = \vec{F}_B - \nabla P$$

which is known as Euler's equation of motion. It should be noted that in Eulerian coordinates the total derivative exists only if $\nabla \times \vec{v} = 0$ which is a condition of irrotational flow.

Bernoulli Equation

A complete derivation of the Bernoulli equation is given by Aris (1). He considers a steady barotropic flow¹ of a frictionless fluid. Using Euler's equation of motion expressed in material coordinates (Lagrangean coordinates)

$$\rho \frac{d\vec{v}}{dt} = -\nabla p + \rho \vec{F}$$

The transformation of coordinates gives

$$\rho \frac{d\vec{v}}{dt} = \frac{\partial \vec{v}}{\partial t} + \rho(\vec{v} \cdot \nabla)\vec{v} = -\nabla p + \rho \vec{F}$$

Substituting

$$(\vec{v} \cdot \nabla)\vec{v} = \nabla\left(\frac{\vec{v} \cdot \vec{v}}{2}\right) - \vec{v} \times (\nabla \times \vec{v})$$

Euler's equation of motion becomes

$$\rho\left\{\frac{\partial \vec{v}}{\partial t} + \nabla\left(\frac{\vec{v} \cdot \vec{v}}{2}\right) - \vec{v} \times (\nabla \times \vec{v})\right\} = -\nabla p + \rho \vec{F}$$

If F is derivable from a potential function, $\vec{F} = -\nabla\phi$ and $\nabla p = \nabla P$ (in barotropic flow) then substituting and dividing by ρ yields

$$\frac{\partial \vec{v}}{\partial t} - \vec{v} \times (\nabla \times \vec{v}) = -\nabla\left[\left(\frac{\vec{v} \cdot \vec{v}}{2}\right) + P + \phi\right] = -\nabla H$$

where $-\nabla H$ is called the total specific energy. Since,

¹Barotropic flow is a flow within which the pressure and density are directly related (Example: For an isentropic flow $p = k\rho^\gamma$), Aris (1, pp. 130).

$$\vec{v} \times (\nabla \times \vec{v}) = - (\nabla \times \vec{v}) \times \vec{v}$$

the equation is

$$\frac{\partial \vec{v}}{\partial t} + (\nabla \times \vec{v}) \times \vec{v} = - \nabla H$$

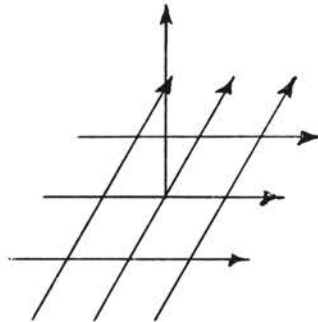
For steady flow $\frac{\partial \vec{v}}{\partial t}$ is equal to zero and the equation is

$$(\vec{w} \times \vec{v}) = - \nabla H$$

where

$$\vec{w} = \nabla \times \vec{v}$$

is defined as the vorticity. Physically, the expression is called the Lamé surface.



Bernoulli theory states that along any streamline the total specific energy is a constant, i.e., $\nabla H = \text{constant}$. Examination of the Bernoulli expression

$$\nabla H = \left[\frac{\vec{v} \cdot \vec{v}}{2} + P + \phi \right] \quad (2)$$

shows that the terms on the right are kinetic energy per unit mass, pressure energy per unit mass, and potential energy per unit mass. Assume further irrotational flow, i.e., $\nabla \times \vec{v} = \vec{w} = 0$. Then $\nabla H = 0$ or H is a constant. This is a reasonable assumption since shear is not

accounted for in Euler's equation and fluid shear is the quantity that starts rotation.

Gradually Varied Flow

Gradually varied flow is by definition a flow which is steady and the depth varies gradually along the length of the channel. The conditions for gradually varied flow are:

1. The flow must be steady, i.e., the same Q passing through each cross section per unit time
2. The streamlines are approximately parallel such that hydrostatic pressure exists over the channel section.

The theoretical analysis of gradually varied flow consists of either the momentum or energy approach. Both approaches are based on Newton's second law. Regardless of the approach used in development of a gradually varied flow equation, the basic assumptions according to Chow (11, pp. 217-218) are as follows:

1. The head loss at a section is the same as for a uniform flow having the same velocity and hydraulic radius of the section.
2. The slope of the channel is small so that:
 - a. The difference between the vertical depth and normal depth is negligible.

- b. The pressure correction factor, $\cos \theta$, is negligible.
 - c. The assumption of no air entrainment can be made.
3. The channel is prismatic.
 4. The velocity distribution coefficients are constant, i.e., the velocity is constant at a given point in the channel after a steady flow condition is attained.
 5. The conveyance $K = CAR^n$ and section factor $Z = A\sqrt{D}$ are exponential functions of the depth of flow.
 6. The roughness coefficient is independent of the depth of flow and constant throughout the reach.

Chow points out that according to assumption (1) the uniform flow equation may be used to evaluate the energy slope of gradually varied flow at a given channel section and the corresponding roughness coefficient is applicable to the flow. He notes that the assumption is probably more correct for varied flow with increasing velocities than for decreasing velocities because of the more pronounced eddy losses expected with decreasing velocities.

Chow (11, p. 218) derived a gradually varied flow equation by considering an elementary length dx of an open channel shown in Figure 3. The total head at the upstream end of the element is described by

$$H = z + d \cos \theta + \frac{\alpha V^2}{2g}$$

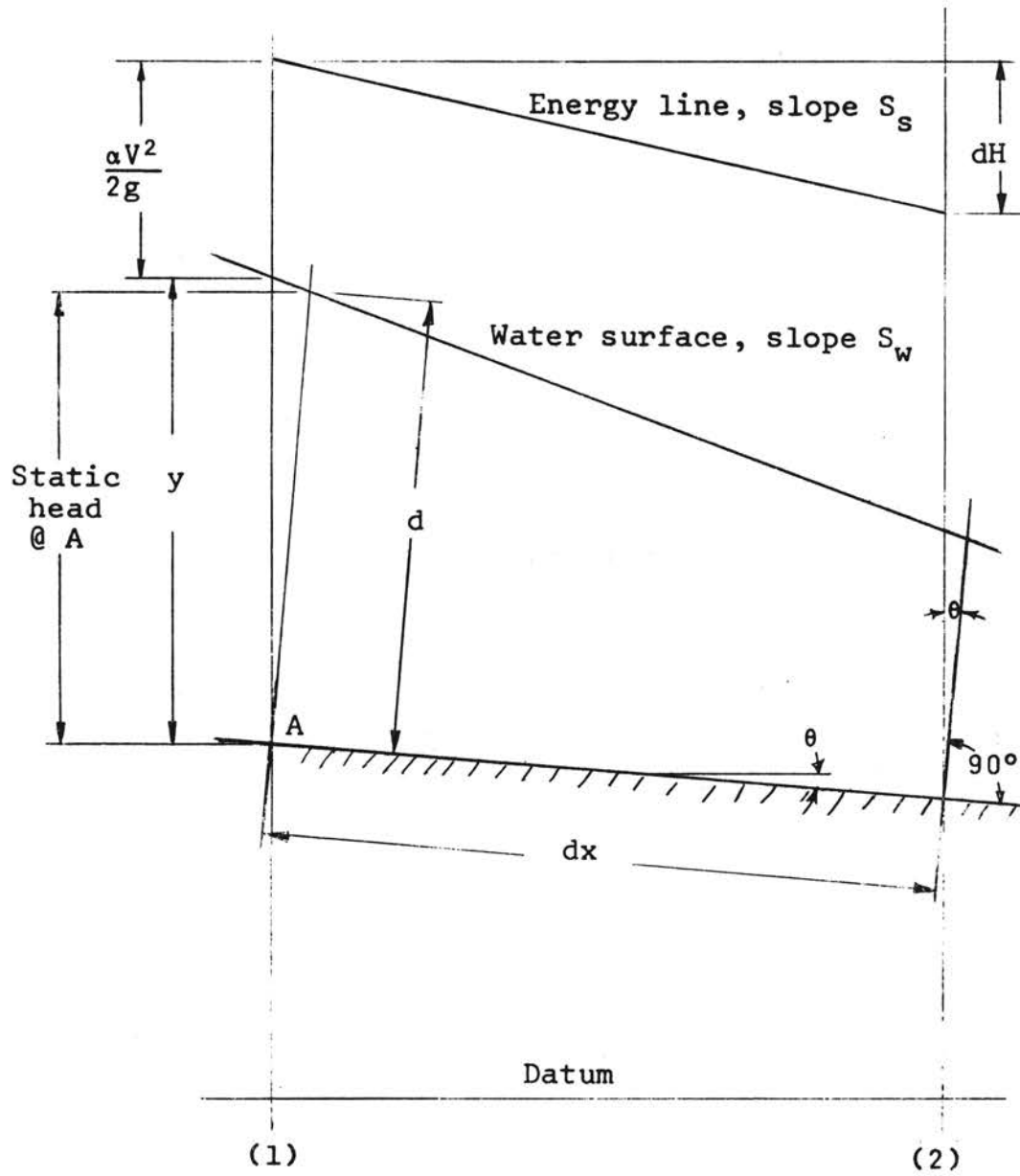


Figure 3. Graphic Illustration of Gradually Varied Flow

By assuming that α and θ were constant throughout the length of the channel and differentiating the equation with respect to the length, results in the equation

$$\frac{dH}{dx} = \frac{dz}{dx} + \cos \theta \frac{dd}{dx} + \frac{d\left(\frac{\alpha V^2}{2g}\right)}{dx}$$

by substituting

$$\frac{dH}{dx} = -S_s$$

and assuming that

$$\sin \theta = -\frac{dz}{dx} \sim S_o, \quad \cos \theta \sim 1, \quad d \sim y \quad \text{and}$$

$$\frac{dd}{dx} \sim \frac{dy}{dx}$$

equation becomes

$$\frac{dy}{dx} = \frac{S_o - S_s}{1 + \alpha \frac{d\left(\frac{V^2}{2g}\right)}{dy}} \quad (3)$$

The velocity head term

$$\alpha \frac{d\left(\frac{V^2}{2g}\right)}{dy}$$

with the aid of the relationships

$$V = \frac{Q}{A}, \quad \frac{dA}{dy} = T$$

can be rewritten in the following form

$$\alpha \frac{d\left(\frac{V^2}{2g}\right)}{dy} = -\alpha \frac{Q^2}{A^3} \frac{dA}{dy} = -\alpha \frac{Q^2}{A^2 Dg}$$

Substituting in Equation 3 the resulting equation yields

$$\frac{dy}{dx} = \frac{S_0 - S_s}{1 - \frac{\alpha Q^2}{gA^2D}} \quad (4)$$

which is the gradually varied flow equation. Using Equation 4, Chow explains the characteristics of water surface profiles.

Momentum Equation

Kindsvater (30, pp. 42-64) gives an adequate development of the momentum equation. He takes a fluid element as shown in Figure 4. The volume of the element is $dV_0 = ds \, dA = v \, dt \, dA = dQ \, dt$, where v is the mean velocity of the infinitesimal streamtube of length ds .

The weight of the fluid is $dw = \gamma ds \, dA = \gamma dQ \, dt$. From Newton's second law, the sum of the external forces (neglecting friction) acting on the elementary volume is equal to the inertial reaction. Substituting the pressure force $dF_p = dP dA$ and the gravitational force $dF_g = \gamma da \, dA$ the equation becomes

$$-\left[\frac{d}{ds} (P + \gamma z)\right] ds \, dA = \frac{\rho}{2} \left[\frac{d(v^2)}{ds}\right] ds \, dA \quad (5)$$

But, $\frac{dv^2}{ds} = 2v \frac{dv}{ds}$, where $\frac{dv}{ds}$ is the velocity gradient in the s direction. Substituting into the term on the right in Equation 5

$$\rho v \left(\frac{dv}{ds}\right) ds \, dA = \rho v \, dv \, dA = \rho \, dQ \, dv$$

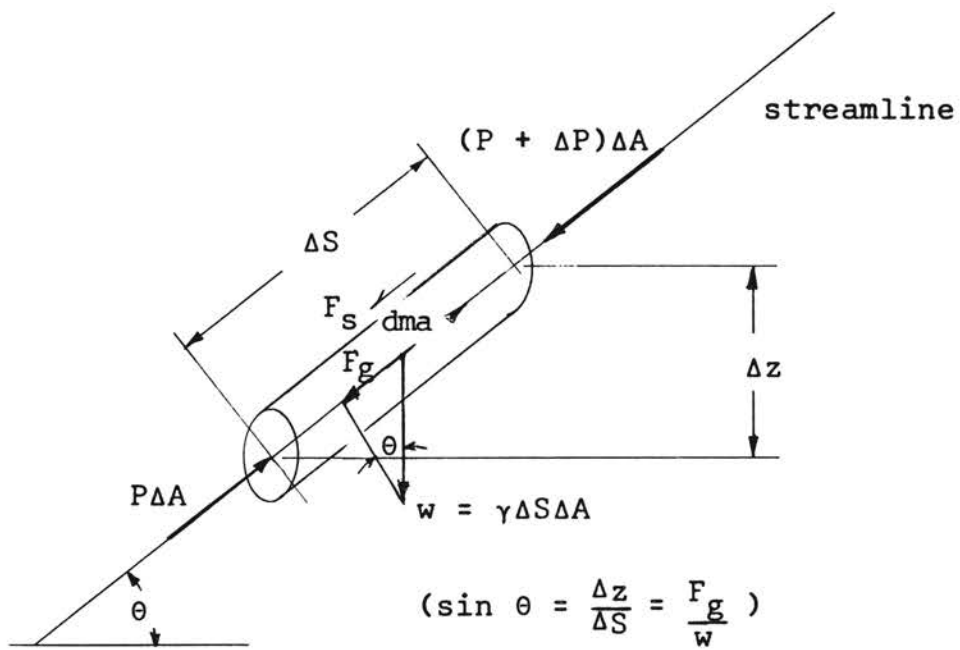


Figure 4. Free Body of an Elementary Fluid Volume

in which dQ is the rate of flow in the infinitesimal streamtube and dv is the change in velocity over the length ds of the element. The quantity ρdQ is equivalent to $\frac{dm}{dt}$ where dm is the mass of the element. The right hand member in the equation is the rate of change of momentum. This is the origin of the name "momentum equation". The rate of flow in the infinitesimal streamtube is a constant; therefore, the equation is really integrable. Integrating in the x direction the equation becomes

$$\Delta F_x = \rho dQ v_{x2} - \rho dQ v_{x1}$$

where ΔF_x is the resultant of all the external forces on the streamtube between sections 1 and 2. Integrating over the total area at sections 1 and 2 and substituting $dQ = v dA$ yields

$$\int \Delta F_x = \rho \int^{A^2} v_{x2} v_2 dA_2 - \rho \int^{A^1} v_{x1} v_1 dA_1$$

This equation is not integrable unless the relationship between v and A is attainable. Thus, an approximation to the integral can be written as

$$\sum F_x \sim \sum^Q Q \rho v_{x2} \Delta Q - \sum^Q Q \rho v_{x1} \Delta Q$$

or

$$\sum F_x = Q \rho \beta_2 V_{x2} - Q \rho \beta_1 V_{x1} \quad (6)$$

where

$$\beta = \frac{1}{QV_x} \int^Q v_x dQ \sim \frac{1}{QV_x} \sum^Q v_x \Delta Q$$

For a uniform flow condition the sum of the external forces in Equation 6 would equal zero, i.e. $\beta_2 V_{x2} = \beta_1 V_{x1}$.

A gradually varied flow equation of the Bernoulli type is presented by Stoker (48). He begins a unidirectional momentum equation

$$\sum F_x = \rho Q (\beta_2 V_2 - \beta_1 V_1)$$

The external forces $\sum F_x$ are considered to be the resultant of pressure, gravitation, and shear forces, i.e., $\sum F_x = F_{px} + F_g - F_{sx}$ where $F_{px} = \gamma A_{avg} \Delta x \frac{\partial y}{\partial x}$ is the pressure force acting on the element of fluid in the channel. The gravitational force is given by

$$F_g = \gamma A_{avg} \Delta x \tan \theta$$

By considering small angles such that $\tan \theta \sim \sin \theta = \frac{\Delta z}{\Delta x}$ the gravitational force becomes $F_g = \gamma A_{avg} \Delta z$. If the variations between sections 1 and 2 are assumed linear then

$$V = \frac{V_1 + V_2}{2} \quad A_{avg} = \frac{A_1 + A_2}{2} \quad \frac{\partial y}{\partial x} \sim \frac{y_1 - y_2}{\Delta x}$$

Substitution into the momentum equation gives

$$\begin{aligned} \sum F_x &= \rho A_{avg} \left(\frac{V_1 + V_2}{2} \right) (\beta_2 V_2 - \beta_1 V_1) \\ &= \frac{\rho A_{avg}}{2} (\beta_2 V_2^2 - \beta_1 V_1^2 + \beta_2 V_1 V_2 - \beta_1 V_1 V_2) \end{aligned}$$

If the difference between momentum coefficients is small, then

$$\sum F_x = \frac{\rho A_{avg}}{2} (\beta_2 V_2^2 - \beta_1 V_1^2)$$

Collecting all terms the equation becomes

$$\gamma A_{avg} (y_1 - y_2) + \gamma A_{avg} (z_1 - z_2) - F_s =$$

$$\frac{\rho A_{avg}}{2} (\beta_2 V_2^2 - \beta_1 V_1^2)$$

Rearranging the equation, the following Bernoulli-type equation is obtained

$$\frac{\beta_1 V_1^2}{2g} + y_1 + z_1 = \frac{\beta_2 V_2^2}{2g} + y_2 + z_2 + \frac{F_{sx}}{\gamma A_{avg}}$$

Energy Equation

An energy-type Bernoulli equation was derived by Rouse and McNown (47). Take a free body of a fluid element as shown in Figure 5. Consider the external forces, pressure, shear and weight of fluid acting upon the fluid element. Equate the rate of change of energy to the rate at which work is done on the fluid by the external forces. The rate of change of energy is the result of acceleration and energy dissipation. The rate of change of energy due to acceleration is

$$\rho \, dsdA \, \frac{d\left(\frac{v^2}{2}\right)}{dt}$$

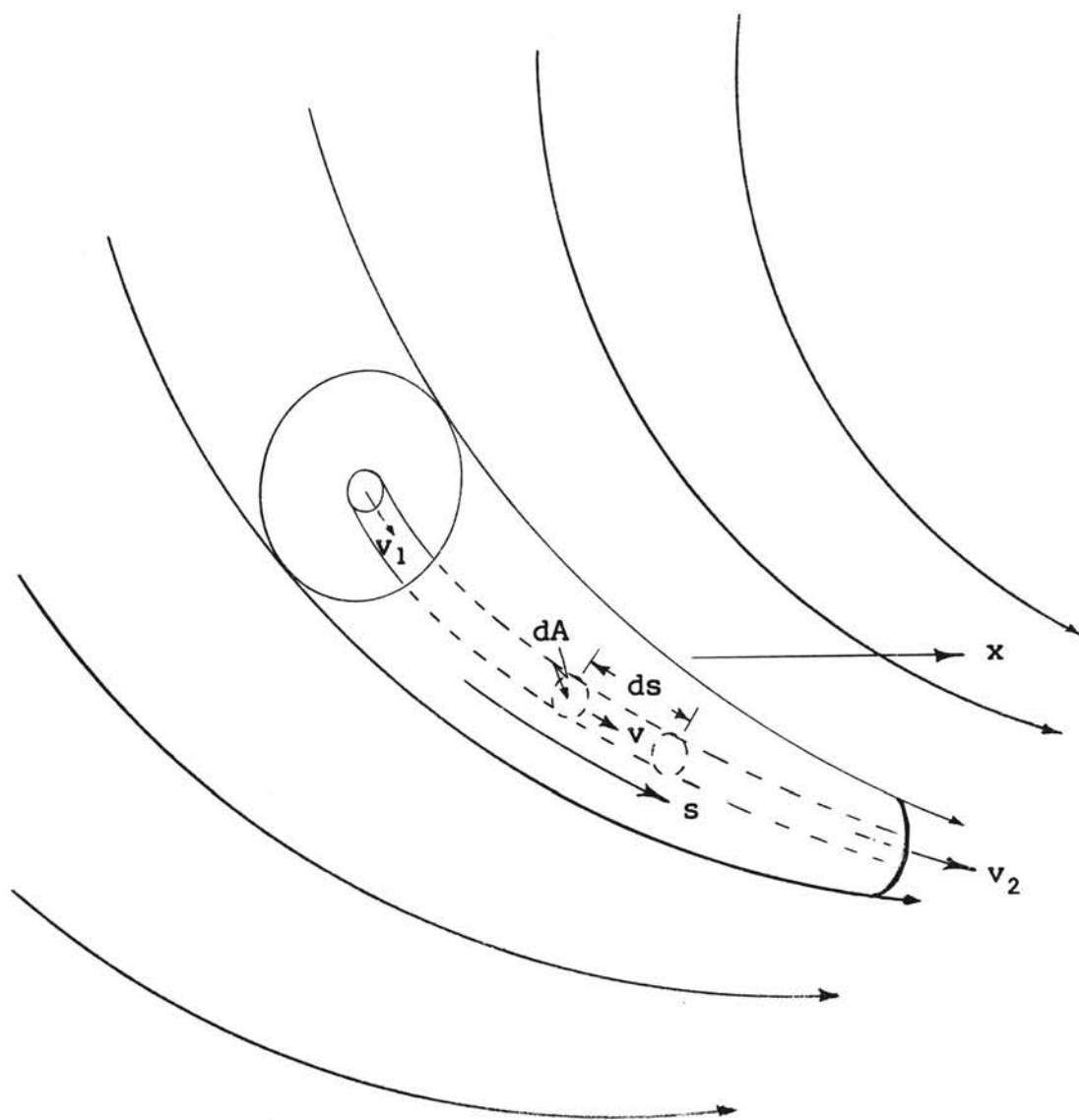


Figure 5. Elementary Fluid Volume

and due to dissipation is

$$\gamma dsdA \frac{dH}{dt}$$

where $\frac{dH}{dt}$ is the rate of change of total head. The total work done along a streamline is $\int (dF_s)v_s$. Equating rate of work done to rate of energy change yields

$$\int (dF_s)v_s = \rho dsdA \frac{d(\frac{v^2}{2})}{dt} - \gamma dsdA \frac{dH}{dt}$$

Substituting

$$dsdA = dQdt, \quad \frac{d(\frac{v^2}{2})}{dt} = \frac{\partial(\frac{v^2}{2})}{\partial x} \frac{ds}{dt}, \quad \text{and} \quad \frac{dH}{dt} = \frac{\partial H}{\partial t} \frac{ds}{dt} \quad \text{and}$$

rearranging the terms on the right, the equation becomes

$$\int (dF_s)v_s = \rho \frac{\partial(\frac{v^2}{2})}{\partial s} dsdQ - \gamma \frac{\partial H}{\partial s} dsdQ$$

The equation is integrable because dQ is constant along a streamline. Integrating with respect to s yields

$$\int_{s_1}^{s_2} \int (dF_s)v_s = \frac{\rho}{2} [v_2^2 - v_1^2]dQ - \gamma(H_1 - H_2)dQ$$

Integrating over all streamtubes, the equation becomes

$$\begin{aligned} \int_A \int_{s_1}^{s_2} \int (dF_s)v_s &= \int_{A_1} (\frac{v_2^2}{2g} - H_2)v_2 dA - \\ \int_{A_1} (\frac{v_1^2}{2g} - H_1)v_1 da &= \int_{A_1} (\frac{P_1}{\gamma} + Z_1)v_1 dA \\ - \int_{A_2} (\frac{P_2}{\gamma} + Z_2)v_2 dA \end{aligned}$$

where $Z = y + z$. The assumptions made for gradually varied flow reduces the equation to the Bernoulli equation

$$\frac{\alpha_1 V_1^2}{2g} + \frac{P_1}{\gamma} + Z_1 = \frac{\alpha_2 V_2^2}{2g} + \frac{P_2}{\gamma} + Z_2 + h_L$$

where

$$h_L = \frac{1}{A_1} \int_{A_1} H_1 \frac{v_1}{V_1} dA - \frac{1}{A_2} \int_{A_2} H_L \frac{v_2}{V_2} dA$$

The momentum and energy equation are derived from the same differential equation. They are independent in the sense that the momentum equation is independent of the energy losses due to internal viscous shear while the energy equation is independent of the external boundary shear. However, there is disagreement among authors about the independence of the energy and momentum equations. For a comprehensive coverage of the momentum and energy concepts, the reader is referred to McCool (37, p. 20-39).

Spatially Varied Flow

Steady spatially varied flow is flow with increasing or decreasing discharge along the channel. The hydraulics of spatially varied flow is more complicated than uniform flow due to the disturbance of the energy and/or momentum.

Many hydraulicians have contributed to the present theory of spatially varied flow. Among the first to present a spatially varied flow equation was Hinds.

Hinds (19) developed a differential equation for increasing spatially varied flow for the design of lateral spillways. The equation was based upon the law of conservation of linear momentum. He considered an incremental length of spillway channel, then equated the change in momentum to the external forces across the incremental length while letting the length become infinitely small.

The assumptions made by Hinds were:

1. All the energy due to impact is lost.
2. The fluid entering the channel has no component of momentum in the direction of flow.

During the development of the equation shear losses were not considered; however, a method of correcting for shear losses was shown at the time of evaluation of the water surface profile. The method developed by Hinds is applicable to any channel, prismatic or non-prismatic. A solution is obtainable by step computation with successive approximations. Verification of the theory came from field data taken at Arrowhead Reservation Spillway and 15 tests of the spillway model with a scale ratio of approximately 4:1.

Beij (3) studied the flow in roof gutters. First, he took the pertinent quantities that were needed to describe the flow in the gutters and formed them into dimensionless groups. With dimensionless groups he was only able to obtain a prediction equation for semi-circular and rectangular gutters with zero bottom slope.

He proceeded to obtain an analytical solution for flow in roof gutters using the principle of linear momentum. The time rate of change in momentum was set equal to the external forces, gravity and shearing, acting on the fluid. The pressure force was not included as an external force.

The general equation derived as a result of his efforts was not integrable. Solutions were only obtainable when shearing force was neglected. A comparison of the measured and calculated depths showed that the measured depths were consistently higher than the calculated depths as a result of an analytical solution without the shearing term included.

Camp (9) analyzed the flow of a prismatic channel with uniform inflow along its length. The procedure and assumptions made by Camp were similar to those presented by Hinds. The basic difference in their differential equation for increasing spatially varied flow was the shearing loss term included in Camp's equation. Camp presented a graphical solution to the increasing spatially varied flow equation for a rectangular channel and a method for solution to flow in channels with parallel sides.

Keulegan (29) using the conservation of mass arrived at a continuity equation for increasing spatially varied flow. He then proceeded to develop a general dynamic equation for spatially varied flow. By combining the general equation and continuity equation and an equation

for resistance he developed a general expression for increasing spatially varied flow. According to Keulegan, the velocity coefficients for both energy and momentum would be included in the general expression in order for it to be an exact equation representing increased spatially varied flow.

He was able to discard some of the terms in the general expression if the flow were turbulent, the length large, and the depth small. An approximate solution could be obtained after the terms were eliminated provided a relationship between the friction factor and Reynolds number had been determined.

Li (35) investigated straight prismatic channels with various slopes while water was added uniformly along the channel. The principle of the conservation of momentum was used to develop a differential equation for increasing spatially varied flow. He assumed that the momentum component of the entering flow would balance the shearing component at the channel's walls.

He investigated the effect of friction on the channel flow and concluded that the frictional effect could be neglected in many of the cases with the exception of channels with level or gradual slopes. He computed curves representing the percentage increase in the upstream depth as a result of friction for horizontal channels. Chow (11, p. 336) states that an increase

up to 10 per cent can be expected for effluent channels around sewage plants.

A general expression of unsteady spatially varied flow was developed in King's Handbook of Hydraulics (32). The principle of conservation of momentum was used in the derivation of the equation. The usual three forces, pressure, gravity, and shear, were considered with the addition of a shear force due to air friction. However, air friction was not included in the final analysis.

The case of steady spatially varied flow was then considered. The resulting equation was similar to the equation presented by Chow (11, p. 341) with the exception of the nonuniformity coefficient β which was omitted from the development. No comment was made as to the reason for omitting the nonuniformity coefficient.

As in the development of the gradually varied flow equation, two approaches have been used, that of linear momentum and energy. Regardless of which approach is used, the following assumptions according to Chow (11, p. 329) were made in order to derive the present day spatially varied flow equations.

1. The flow is unidirectional, actually there are strong cross currents present in the form of spiral flow, particularly in lateral spillway channels. The effects of these currents and of the accompanying turbulence cannot be easily evaluated but will be included in the computation

if the momentum principle is used. The lateral unevenness of the water surface, as a result of cross currents, is ignored.

2. The velocity distribution across the channel section is constant and uniform; i.e., the velocity distribution coefficient is taken as unity. However, proper values of the coefficient may be introduced if necessary.
3. The pressure in the flow is hydrostatic, i.e., the flow is parallel. The flow at the outlet, however, may be curvilinear and deviate greatly from the parallel-flow assumption if a hydraulic drop occurs. In such cases, proper values of the pressure distribution coefficients may be introduced if necessary.
4. The slope of the channel is relatively small, so its effects on the pressure head and on the force of channel section are negligible. If the slope is appreciable, corrections for these effects may be applied.
5. The Manning formula is used to evaluate the friction loss due to the shear developed along the channel wall.
6. The effect of air entrainment is neglected. A correction, however, may be applied to the computed result when necessary.

Decreasing Spatially Varied Flow

To analyze decreasing spatially varied flow the energy principle is applicable. Chow (11, p. 332) used the energy equation at a channel section as the starting point for the development of a decreasing spatially varied flow equation. Differentiating the equation with respect to x gives

$$\frac{dH}{dx} = \frac{dz}{dx} + \frac{dy}{dx} + \frac{\alpha}{2g} \left(\frac{2Q}{A} \frac{dQ}{dx} - \frac{2Q^2}{A^3} \frac{dA}{dx} \right) \quad (9)$$

Substituting

$$\frac{dA}{dx} = \frac{dA}{dy} \frac{dy}{dx} = T \frac{dy}{dx}, \quad \frac{dH}{dx} = -S_s, \quad \frac{dz}{dx} = -S_o, \quad \text{and}$$

$$\frac{dQ}{dx} = q$$

into Equation 9 and collecting terms results in an expression for the rate of change of the water surface elevation with respect to the length of the channel

$$\frac{dy}{dx} = \frac{S_o - S_s - \frac{\alpha Q q}{g A^2}}{1 - \frac{\alpha Q^2}{g A^2 D}} \quad (10)$$

Chow also derived Equation 10 using the momentum approach. The assumption was made that no momentum was added to the water, thus the term dQ was eliminated from the momentum equation

$$\frac{w}{g} [QdV + (V + dV) dQ] = \sum F_x$$

and the resulting equation was the same as Equation 10 if the energy coefficient α is substituted into the final equation.

In the development of increasing spatially varied flow equation, Chow used the momentum approach. The energy coefficient α was substituted in the final equation. The justification for using α was that the energy slope S_g was evaluated by the Manning formula for energy loss.

A complete derivation of the increasing spatially varied flow equation was presented by McCool (37). In the derivation, the change in momentum for a finite length as shown in Figure 6 was equated to the sum of the external forces acting on the fluid. The assumptions made were: (1) the flow entering the channel has no velocity and thus no momentum component in the direction of the main flow; (2) flow at the end of the reach is essentially in the same direction; and, (3) the variation in depth and area between the two ends of the reach is approximately linear. Using the momentum equation

$$\sum F_x = Q\rho(\beta_2 V_2 - \beta_1 V_1) = \rho(\beta_2 V_2^2 A_2 - \beta_1 V_1^2 A_1)$$

where the sum of the external force is

$$\sum F_x = F_p + F_g - F_s$$

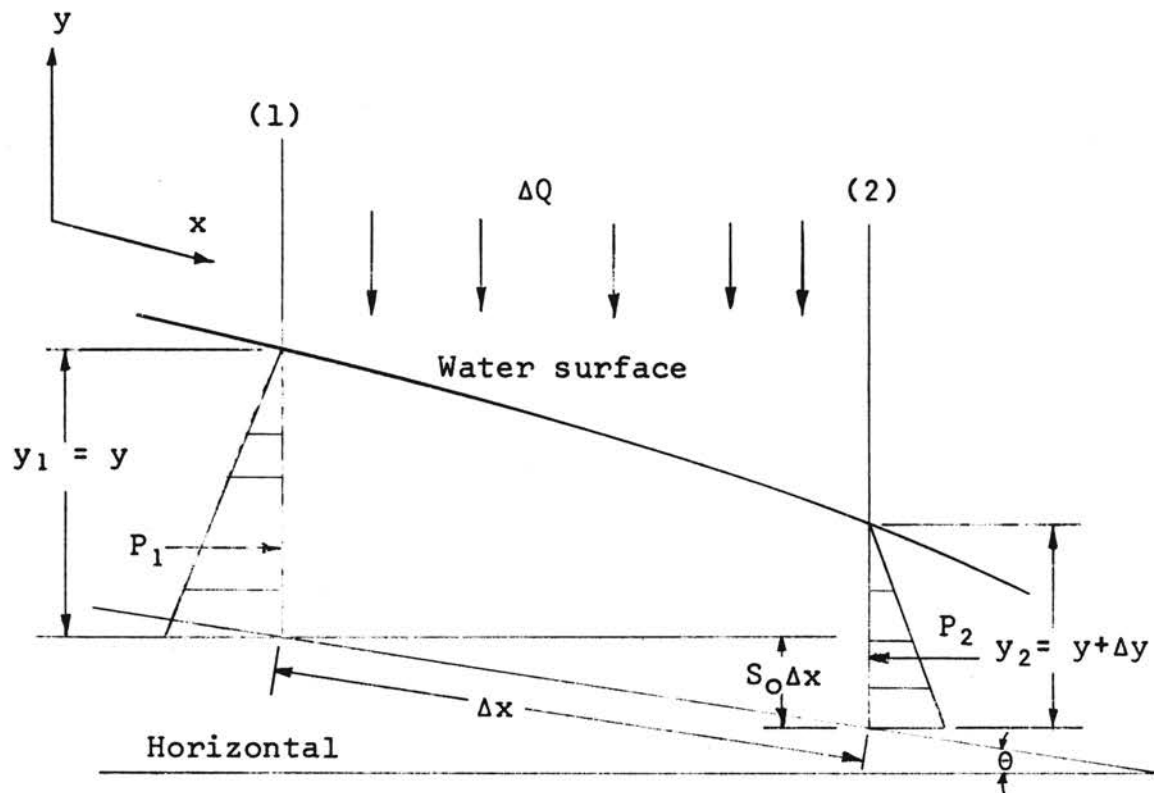


Figure 6. Graphic Illustration of Increasing Spatially Varied Flow

From the assumption of linear variation with depth,

$$F_p = \gamma A_{\text{avg}} \Delta x \frac{dy}{dx} = \gamma A_{\text{avg}} \Delta y;$$

$$F_s = \gamma A_{\text{avg}} \Delta x S_s$$

$$F_g = \gamma A_{\text{avg}} \Delta x \tan \theta = \gamma A_{\text{avg}} \Delta x S_o$$

Substituting into momentum equation gives

$$\rho (\beta_2 V_2^2 A_2 - \beta_1 V_1^2 A_1) = \gamma A_{\text{avg}} (\Delta y + \Delta x S_o - \Delta x S_s)$$

Dividing by γA_{avg} and solving for Δy the equation becomes

$$y = - \left(\frac{\beta_2 V_2^2 A_2 - \beta_1 V_1^2 A_1}{g A_{\text{avg}}} \right) + (S_o - S_s) \Delta x \quad (11)$$

Substituting

$$\begin{aligned} A_{\text{avg}} &= \frac{Q_1 + Q_2}{V_1 + V_2}, \quad V_1 A_1 = Q_1, \quad \text{and} \quad V_2 A_2 = Q_2 \\ &= Q_1 + \Delta Q \end{aligned}$$

into Equation 11 yields

$$\begin{aligned} \Delta y &= -Q \left(\frac{V_1 + V_2}{Q_1 + Q_2} \right) (\beta_2 V_2 - \beta_1 V_1 + \frac{\beta_2 V_2}{Q_1} \Delta Q) \\ &\quad + (S_o - S_s) \Delta x \end{aligned}$$

Substituting

$$\begin{aligned} Q_1 &= Q, \quad Q_2 = Q + \Delta Q, \quad V_1 = V, \quad V_2 = V + \Delta V, \\ A_{\text{avg}} &= A + \frac{1}{2} \Delta A, \quad \text{and} \quad \beta_1 = \beta_2 = \beta \end{aligned}$$

into Equation 12 and ignoring incremental products, Δy becomes

$$\Delta y = - \frac{\beta Q}{g} \left(\frac{Q\Delta V + V\Delta Q}{Q \left(A + \frac{1}{2} \Delta A \right)} \right) + (S_o - S_s) \Delta x \quad (12)$$

then by substituting Δv from

$$v + \Delta v = \frac{Q + \Delta Q}{A + \Delta A}$$

the equation can be written as

$$\Delta y = - \frac{\beta}{g} \left(\frac{2Q\Delta Q - QV\Delta A + V\Delta Q\Delta A}{\left(A + \frac{1}{2} \Delta A \right) \left(A + \Delta A \right)} \right) + (S_o - S_s) \Delta x$$

If the product of $A\Delta A$ and incremental products are negligible, then the equation becomes

$$\frac{y}{x} = - \frac{\beta}{g} \left(\frac{2Q}{A^2} \frac{\Delta Q}{\Delta x} - \frac{Q^2}{A^3} \frac{\Delta A}{\Delta x} \right) + S_o - S_s$$

Let $\Delta x \rightarrow 0$ then the expression becomes

$$\frac{dy}{dx} = \frac{S_o - S_s - 2\beta Qq/gA^2}{1 - \beta Q^2/gA^2D}$$

This is an expression for increasing spatially varied steady flow. The equation includes the momentum coefficient β whereas the equation derived by Chow has the energy coefficient α .

Considerable disagreement among hydraulicians exists as to what nonuniformity coefficient (α or β) should be

used with the spatially varied and gradually varied flow equations.

Non-uniformity Coefficients

Rouse (46) defines the momentum coefficient as

$$\beta = \frac{1}{A} \int_A \left(\frac{v}{\bar{v}}\right)^2 dA$$

and the energy coefficient as

$$\alpha = \frac{1}{A} \int_A \left(\frac{v}{\bar{v}}\right)^3 dA$$

The integrals can be evaluated only if knowledge of the velocity distribution exists. If the velocity distribution is parabolic, coefficients as high as $\beta = 1.33$ and $\alpha = 2.0$ can result. However, for most exploratory work α and β are generally considered to be unity. It should be noted that in areas of reverse flow negative contributions are made to α and positive contributions to β as the results of the squared and cubed term in the integrals. Thus, it is possible, but unlikely, to obtain a value of $\alpha \leq \beta$.

According to Chow (11), G. Coriolis was the first to propose the energy coefficient α and J. Boussinesq was the first to propose the momentum coefficient β . Chow showed the approximation to α and β as

$$\alpha \sim \frac{\sum v^3 \Delta A}{\bar{v}^3 A} \quad \text{and} \quad \beta \sim \frac{\sum v^2 \Delta A}{\bar{v}^2 A}$$

For channels of regular cross section and fairly straight alignment the effect of the nonuniform velocity head is small in comparison to the other uncertainties involved in the computation. So, the coefficients are often assumed to be unity.

If a logarithmic velocity distribution is assumed as in Chow (11, p. 203), the values of α and β may be computed by the formulas

$$\alpha = 1 + 3\epsilon^2 - 2\epsilon^3 \text{ and } \beta = 1 + \epsilon^2$$

where

$$\epsilon = \frac{V_{\max}}{V - 1}$$

For straight prismatic channels, the values generally obtained for the coefficient are $1.03 < \alpha < 1.36$ and $1.01 < \beta < 1.12$. Higher values of the coefficient are expected in small channels. Table 1 contains coefficients from Kolupaila (33, pp. 12-18) that were given by Chow as possible design values.

O'Brien and Johnson (42) developed and used a graphical procedure for determining the energy and momentum coefficients. The procedure is as follows:

1. Construct a cross section of the channel and the measured water surface.
2. Plot velocity data on the channel cross-section.
3. Construct isovels (continuous line of equal velocity).

TABLE I

PROPOSED DESIGN VALUES OF α AND β FROM KOLUPAILA

<u>Channels</u>	Value of α			Value of β		
	<u>Min.</u>	<u>Av.</u>	<u>Max.</u>	<u>Min.</u>	<u>Av.</u>	<u>Max.</u>
Regular channels, flumes, spillways	1.10	1.15	1.20	1.03	1.05	1.07
Natural streams and torrents	1.15	1.30	1.50	1.05	1.10	1.17
Rivers under ice cover	1.20	1.50	2.00	1.07	1.17	1.33
River valleys, overflowed	1.50	1.75	2.00	1.17	1.25	1.33

4. Planimeter the area between the isovels and construct velocity, velocity squared, and velocity cubed vs mass area curves.
5. Divide the area under the velocity squared vs mass area curve by V^2A to obtain β . The area under the velocity cubed vs mass area curve divided by V^3A is equal to α .

When the velocity head is of the same order of magnitude as the other terms in the Bernoulli equation, the energy coefficient α should be used. An important application of the coefficient is in the computation of friction factors from measured friction losses in open channels. The tabular values presented by O'Brien for α and β were from 1.04 to 1.35 and 1.01 to 1.121, respectively. The low and high values of α and β were obtained at the Sudbury Aqueduct and the Rhine River.

Streeter (50) considered an extremely wide channel with a velocity distribution

$$\frac{v}{V} = 1.0 + 2.5 \sqrt{\frac{g}{C}} + 2.5 \sqrt{\frac{g}{C}} \ln \frac{y_0}{y}$$

where y_0 equals distance from bottom of the channel.

Substituting $\frac{v}{V}$ into the equation

$$\alpha = \frac{1}{A} \int_A \left(\frac{v}{V}\right)^3 dA$$

and integrating he obtained

$$\alpha = 1 + \frac{75}{4} \left(\frac{g}{C^2}\right) - \frac{125}{4} \frac{g^{3/2}}{C}$$

In an analogous manner β was found to be

$$\beta = 1 + \frac{6.251 g}{C^2} = 1 + .78 f = 1.283 g \frac{n^2}{y^{1/3}}$$

A graph of the function is shown in Figure 7.

Open Channel Formulas

During the latter half of the nineteenth century numerous empirical formulas were proposed for computation of flow and for a characteristic roughness coefficient for open channels. The open channel formulas proposed up to 1918 were reviewed by Houk (21). As a convenience to the reader, some of the formulas will be listed under the classification given by Houk. A discussion of the merit of the various equations is found in Houk.

Houk's Conclusions:

After a detailed study of the above channel formulas as applied to a wide range of channels, Houk concluded that:

1. Of the German formulas which have been developed on the assumption that a roughness coefficient is not necessary, not one possesses sufficient merit to warrant its adoption as a general formula.

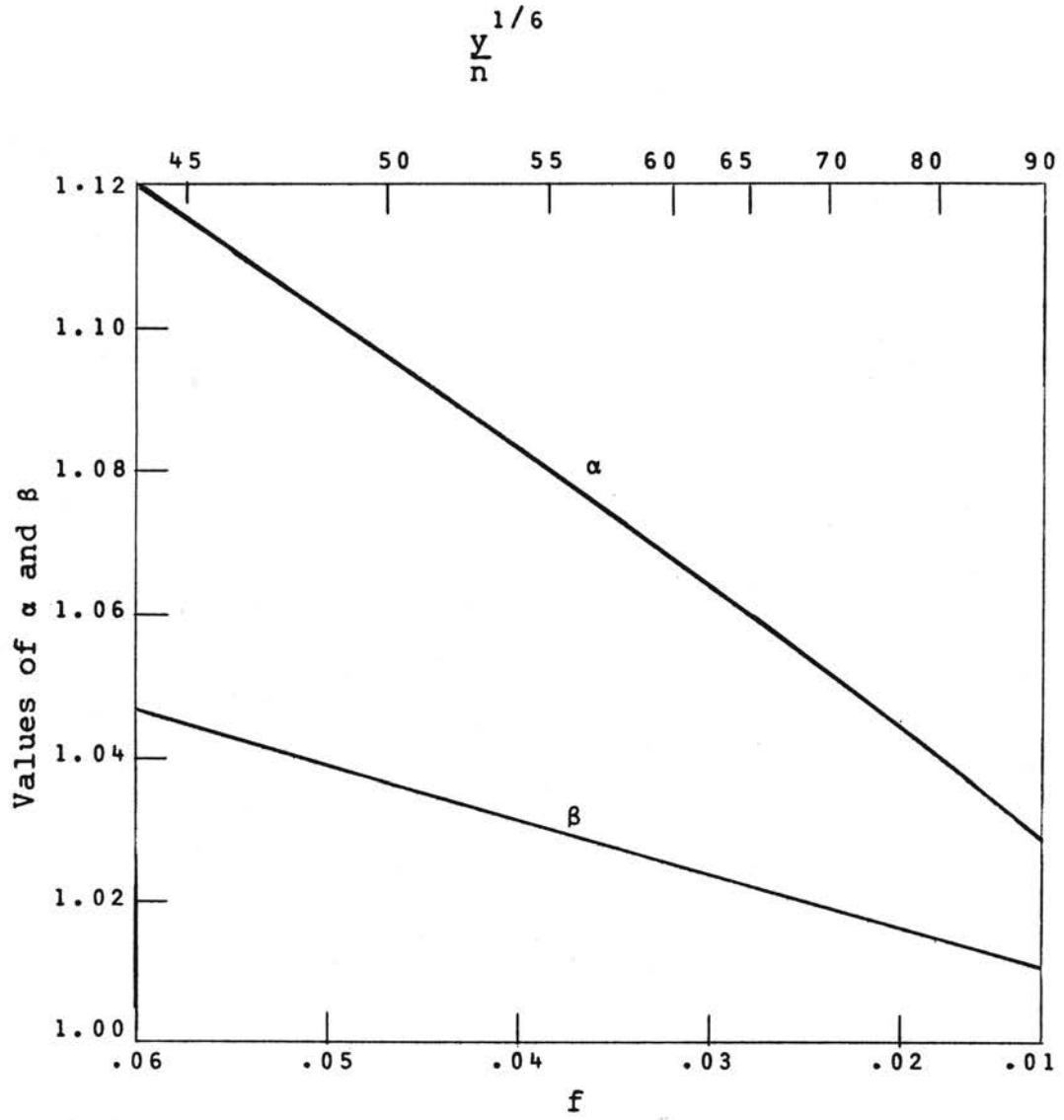


Figure 7. α and β for Wide Channels

TABLE II
PROPOSED OPEN CHANNEL FORMULAS

Class I:

German formulas developed on the assumption that a roughness factor is unnecessary.

Name	Proposed Formula	Remarks
Siedek	<p>Basic Formula:</p> $V' = \frac{20 D\sqrt{s}}{\sqrt{B} \sqrt{.001}}$ <p>General Expression:</p> $V = V' + \frac{D - D_m}{a} + \frac{S_s - S_{sm}}{b(S_s + S_{sm})} + V' \left(\frac{D_m - D}{C} \right)$	<p>B = Breadth of the cross section B = 3.0 meters B > 3.0 meters m - subscript means average a,b,c are coefficients D = average depth</p>
Gröger	$V = K D^m S_s^n$	K,m,n were obtained graphically.
Hessele	$V = 25 \left(1 + \frac{1}{2} \sqrt{R} \right) \sqrt{RS_s}$	25 $\left(1 + \frac{1}{2} \sqrt{R} \right)$ corresponds to Chezy's C
Christen	$V = m\sqrt{DS} \frac{8}{\sqrt{B/2}}$	m depends on channel roughness
Hermanek's	$V = 30.7 \sqrt{D} \sqrt{DS_s}$ $V = 34 \sqrt[4]{\sqrt{DS_s}}$ $V = (50.2 + D/2) \sqrt{DS_s}$	<p>D < 1.5 meters 1.5 < D < 6.0 meters 1 < D < 6.0 meters</p>

TABLE II (Continued)

Name	Proposed Formula	Remarks
Matakiewicz	$V = C' S_S^m D^n$	
Lindboe	$V = K [M + q (\frac{D}{B})^P] D^n S_S$	The exponents (n,P) and the constants (q,M,K) were found graphically.
Teubent	$V = 46.91 \sqrt{S_S} \sqrt[3]{D}$	
Harder	$V = (36.27 + 7.254 \sqrt{R}) \sqrt{R S_S}$	

Class II:

Formulas of the exponential type in which roughness conditions are accounted for by a coefficient.

Chezy	$V = C \sqrt{R S_S}$	
Williams & Hazen	$V = C' R^{.63} S_S^{.54} .001^{-.04}$	The quantity $.001^{-.04}$ was included so that C' would equal Chezy's C at $R = 1$.
Barnes	$V = 58.4 R^{.694} S_S^{.496}$	For earth channels and channels without vegetation.
Ellis	$V = C' R^{.69} S_S^{.5}$	

TABLE II (Continued)

Class III:

Miscellaneous formulas.

Name	Proposed Formula	Remarks
Manning	$V = C_1 \sqrt{S_s g} [R^{.50} + \frac{(.22)}{m^{.5}}(R - .15)]$	C_1 is a coefficient that varies with the nature of the bed.
Biel	$V = \sqrt{\frac{3281}{.12 + \frac{1.811f}{R}}} \sqrt{RS_s}$	Basic equation without temperature term. f is the equivalent roughness factor.

Class IV:

Formula of Bazin and that of Kutter.

Kutter	$V = C \sqrt{RS_s}$ <p>where</p> $C = \frac{41.6 + \frac{1.811}{n} + \frac{.00281}{S_s}}{1 + (41.6 + \frac{.00281}{S_s}) \frac{n}{\sqrt{R}}}$	
Bazin	$V = \frac{8.7 \sqrt{RS_s}}{.552 + \frac{m}{\sqrt{R}}}$	m depends on the channel lining.

2. It is not possible to develop a satisfactory formula for velocities in open channels without introducing therein a variable term to allow for changes in roughness.
3. No exponential formula so far advanced could be recommended for general use.
4. The effect of temperature should not be introduced into a formula for the flow of water in open channels unless its magnitude is greater than that assumed by Biel.
5. Manning's formula in its original form is practically as good as Kutter's for small channels of ordinary dimensions, but inferior to Kutter's for large rivers. Although its algebraic form is somewhat more simple than Kutter's equation, it does not seem advisable to adopt it for use even in ordinary instances, since the latter formula is now in general use and, moreover, is applicable to extreme cases.
6. No definite effect of the slope on the Chezy coefficient is shown by experimental data for small open channels.
7. Data available at present shows a decrease in C with an increase in S in large rivers with flat slopes.

8. The Bazin formula is inferior to Kutter's for all types of open channels. The constancy of the factor M is less than that of the factor N in all instances.
9. Although the Kutter formula is not ideal, it is the best equation available at the present time.

Since 1918 two formulas which have been used sparingly have been proposed by Powell and Pavlovskii. A resume of their investigations is given in Chow (11). Both men proposed an empirical formula to describe Chezy coefficient.

The equation proposed by Powell for the roughness of artificial channels was

$$C = -42 \log \left(\frac{C}{N_R} + \frac{\epsilon}{R} \right)$$

where ϵ is roughness in feet. As can be seen, C is an implicit function and a trial and error solution is required to obtain a value of C.

In 1925 Pavlovskii proposed a uni-flow formula that is widely used in the Union of Soviet Socialist Republics. The equation for C is $C = \frac{1}{n} R^y$ where $y = 2.5 \sqrt{n} - .13 - .75 \sqrt{R} (\sqrt{n} - .10)$ and for practical purposes

$$y = 1.5 \sqrt{n}, R < 1.0$$

$$y = 1.3 \sqrt{n}, R > 1.0$$

A Note on Manning's Formula

The Manning formula presented in its original form has been modified and is a widely used open channel formula today. The modified form of the equation in English units is

$$V = \frac{1.486}{n} R^{2/3} S_s^{1/2}$$

The hydraulician's acceptance of the modified Manning formula is probably due to its ability to yield satisfactory results to practical hydraulic problems and its simplicity.

Chow (10) gave the following discussion on the modification of the Manning formula. The formula as first published took the form

$$V = C \sqrt{S_s} g [R^{0.5} + (.22/m^{0.5})(R - .15)]$$

Comparison of this formula with seven other formulas was made for actual observation. Finally, based on Bazin's (3) data and application to 170 experiments, a simple form was established as follows:

$$V = C S_s^{1/2} R^{2/3}$$

Manning, however, mentioned that this simple form was also previously developed independently by Hagen. He acknowledged this credit to Hagen by quoting a statement by Cunningham (12).

The Manning formula was later modified and expressed in metric units as

$$V = \frac{1}{n} R^{2/3} S_s^{1/2}$$

where n is the coefficient of roughness, and V is in meters per second and R in meters. Since one meter equals 3.2808 feet, the formula in English units obtains its coefficient as $(3.2808)^{1/3} = 1.4856$. The Manning formula presented in most hydraulics textbooks now appears in the form

$$V = \frac{1.486}{n} R^{2/3} S_s^{1/2}$$

Considering the approximations involved in the derivation of this formula and the uncertainty of the value of n , it seems to be not justifiable to carry the numerical coefficient, 1.486, to more than three significant figures. A value equal to 1.49 is sufficiently accurate for practical purposes. Several very recent publications have adopted this suggested value.

Rouse (45) shows that the factor 1.49 and n in the Manning formula must have the dimensions of \sqrt{g} and $L^{1/6}$ respectively. He also plotted the parameter

$$\frac{1.49}{\sqrt{g}} \frac{R^{1/6}}{n}$$

versus the dimensionless friction factor f . He commented that the deviation between the more nearly correct Karman and Prandtl resistance equation and Manning equation was

an indication of the error encountered while using the Manning formula. He concluded that the Manning formula is most dependable for intermediate values of relative roughness and least dependable at low values of Reynolds number because of the exclusion of viscosity.

Resistance

Chow (10) presents an f versus N_R relationship from data gathered by hydraulicians for flow in rough channels shown in Figure 8. N_R is the Reynolds number. Observations from the figure are as follows:

1. The value of K for $\frac{K}{N_R}$ in the laminar region is higher for rough channels.
 - a. For smooth channels K ranges 14 to 24
 - b. For rough channels K ranges 33 to 60
2. When the degree of roughness is constant and the flow is turbulent, the friction factor decreases approximately in the order of rectangular, triangular, trapezoidal, and circular channels. This shows the pronounced effect of channel shape on the friction.
3. For values of high Reynolds number some plots become approximately parallel at the stage where the flow is completely turbulent and f is independent of Reynolds number. Then f is a function only of the shape and hydraulic radius of the channel.

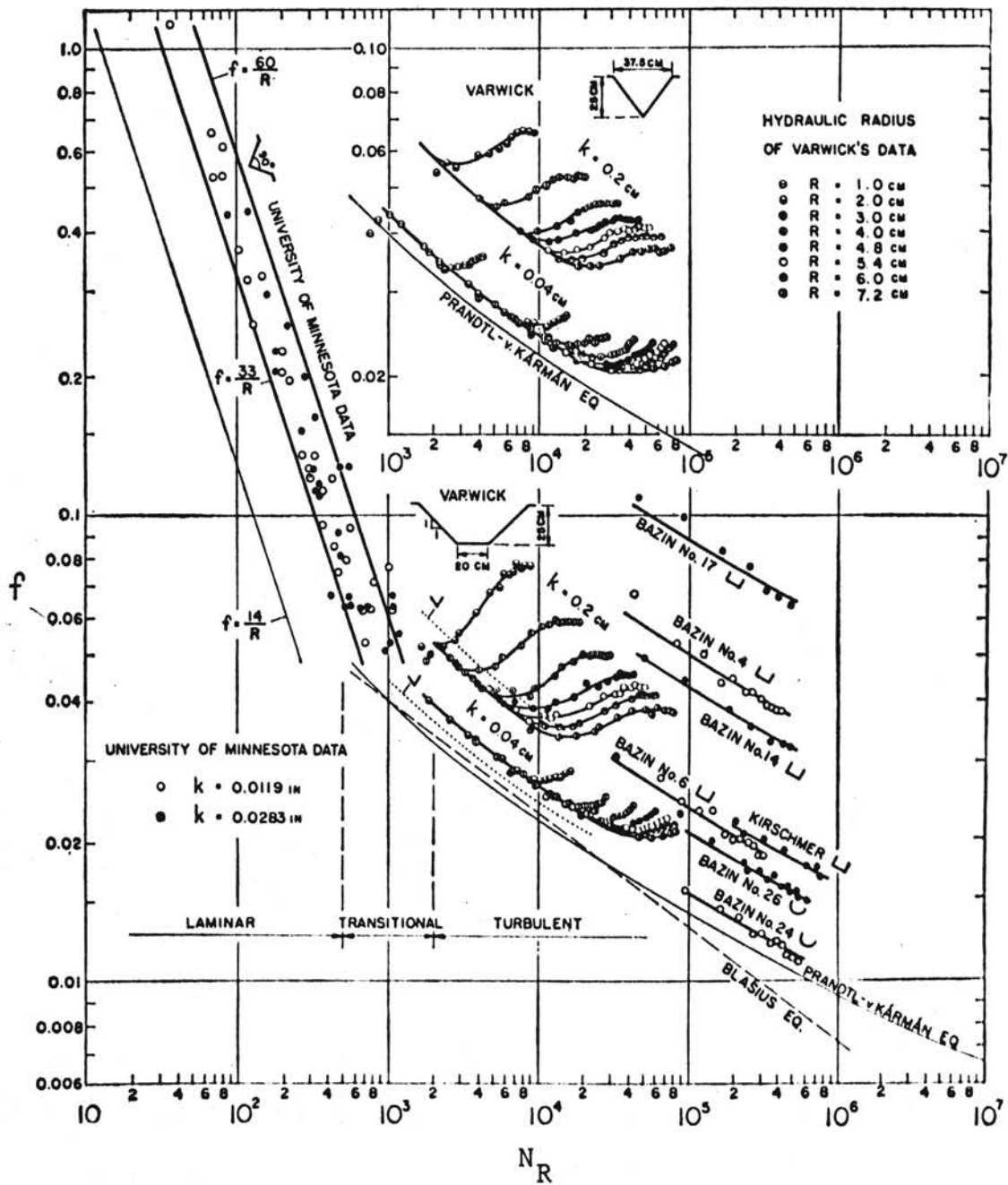


Figure 8. The f to N_R Relationship for Flow in Rough Channels (after Chow)

Chow discussed the predominate factors that influenced the coefficient of roughness of both artificial and natural channels. The factors are surface roughness, vegetation, channel irregularity, channel alignment, silting and scouring, obstructions, size and shape of channel, suspended material and bed load.

Woo (53) investigated sheet flow or overland flow for two roughnesses; namely, masonite and sand (1 mm). The range of critical Reynolds numbers or apparent departure from laminar flow varied from a Reynolds number of 400 to 900 depending on the slope. He concluded that in view of this variation that additional experimentation with different roughness was needed.

Kruse (34) examined the resistance to flow in a series of laboratory tests of channels similar to irrigation furrows. The primary factors affecting resistance were considered to be the degree of turbulence, boundary roughness, and channel shape. Seven parabolic and ten rectangular channels were tested. A fine sand was used to form the channel boundaries in a 60 foot tilting flume. After the formation of the desired boundary roughness, the sand was sprayed with a chemical application to prevent erosion. The slope of the flume was varied from .01 to .05 per cent. The following conclusions were drawn from an analysis of the data:

1. The transition of laminar to turbulent flow occurs at a Reynolds number between 400 and 700 depending on the channel roughness.
2. The standard deviation of the boundary elevation measurement used as an expression of the height of the roughness element is sufficient to predict the flow resistance coefficient. However, if the roughness shape and spacing could be measured adequately the resistance estimate could be improved.
3. The effect of channel slope, within the ranges of shapes of natural irrigation furrows exert negligible influence on flow resistance as compared to the effect of the boundary roughness.

Bettess (5,6) obtained a friction factor and Reynolds number relationship for nonuniform flow in a test channel 0.5 feet deep and .52 foot wide and 15.5 feet long. He used the gradually varied flow equation to calculate a value of the friction factor f . However, the velocity distribution coefficient normally included in the non-uniform flow equation was not used. The flow was turbulent and the channel smooth. The equation obtained was

$$f = .0246 N_R^{-.153}$$

A relationship obtained previously for uniform flow on a similar channel was

$$f = .0234 N_R^{-.15}$$

He concluded that the f to N_R relationship obtained for uniform flow could be used in nonuniform flow computations.

Boyer (8) combined Manning's equation

$$V = \frac{1.486}{n} y_m^{2/3} S^{1/2}$$

and a velocity distribution for turbulent flow

$$V = 2.5 (gy_m S)^{1/2} \left(\ln \frac{y_m}{y'} - 1 \right)$$

The resulting equation was

$$\frac{n}{y_m^{1/6}} = \frac{.105}{\ln \left(\frac{y_m}{y'} \right) - 1}$$

For turbulent flow $y' = \frac{k}{30}$ where k is equivalent to a mean sand grain diameter. He stated that Manning's n expressed in terms of the height of channel roughness would reduce the error in field estimates of the roughness coefficient because a 1000-fold variation in the roughness height produces a 4-fold variation in n .

Robinson (44) stated that 13 pertinent quantities affected the flow in open channels. The pertinent quantities were combined into dimensionless groups and all but three groups were eliminated. The dimensionless groups considered being the resistance coefficient $\frac{C}{\sqrt{g}}$ relative roughness parameter $\frac{y}{a}$, and Reynolds number

$\frac{VR}{v}$ where a is the height of artificial roughness. From a plot of $\frac{C}{\sqrt{g}}$ versus N_R at different values of $\frac{y}{a}$ he concluded that $\frac{C}{\sqrt{g}}$ remained constant over the range of N_R used in the test. (Range: Lower limit, $3500 < N_R < 30,000$; Upper limit, $N_R \sim 2.5 \times 10^5$) The prediction equation obtained from the plots of $\frac{C}{\sqrt{g}}$ versus N_R and $\frac{C}{\sqrt{g}}$ versus $\frac{y}{a}$ was $C = 26.65 \log (1.891 \frac{y}{a})$. The equation is said to be applicable for a 4-fold variation in roughness ($4 < \frac{y}{a} < 17$) and for a 2-fold variation in the roughness coefficient.

Some open channels have bottoms and sides made of different materials. Horton (20) separated the roughness values n of the sides and bottom of a channel. To solve for the resistance coefficients of the sides and bottom of the channel requires two values of the apparent n and of a parameter Z where Z is the ratio of the side length L of a section at a depth y and the bottom width. The equation given to calculate an apparent n with a given n_s of the sides and n_b of the bottom is

$$n = \left(\frac{n_b^{3/2} + 2 Z n_s^{3/2}}{1 + 2 Z} \right)^{2/3}$$

It is evident from this equation that n will vary with depth if n_b and n_s are constant. A typical plot is shown in Figure 9.

Straub (49) investigated the flow in open channels at low Reynolds numbers ($N_R < 4 \times 10^4$). The tests were conducted with rectangular, 90 degree triangular,

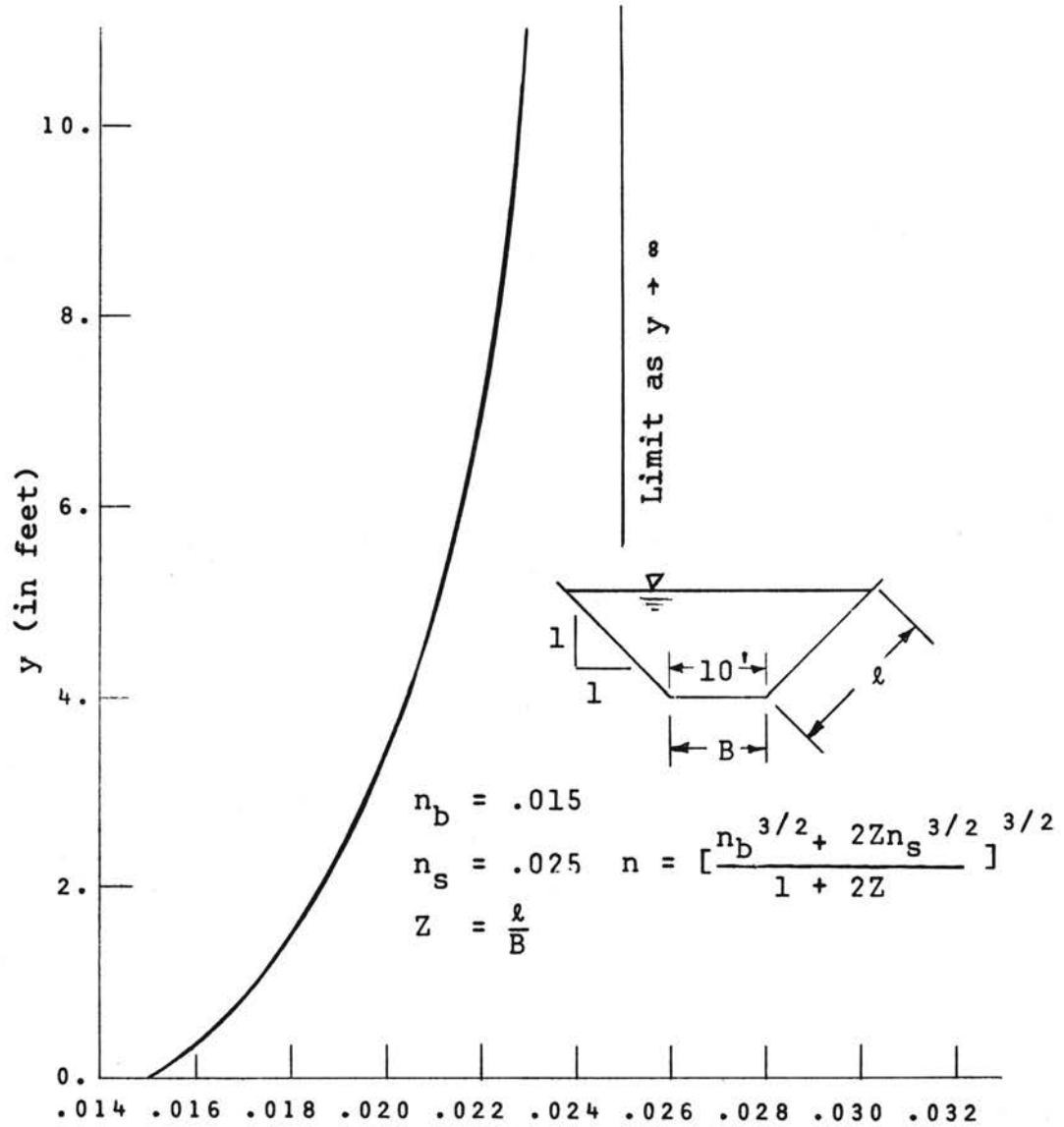


Figure 9. Relationship of a Trapezoidal Channel in which the Bottom and Sides Have Different Roughness Characteristics

variable triangular and circular channel cross sections. The channels ranged in length from 15 to 23 feet. While the accuracy of measurement was .001 foot.

The hydraulic depth was used as the characteristic length in the Reynolds number. They considered smooth laminar and smooth turbulent, rough turbulent and rough laminar flow as well as the transition from laminar to turbulent flow. The conclusions drawn from the investigation were as follows:

1. Friction and velocity distribution for flow in smooth, open channels at small Reynolds numbers are quantitatively equal to the corresponding values for flow in closed conduits with similar fixed boundaries when the Reynolds number based on hydraulic diameter is used as the correlating parameter. The foregoing applies to a sufficient degree of accuracy to both laminar and turbulent flow.
2. Friction in rough channels may be similar to friction in rough pipes or on rough plates, but because there is no suitable correlating parameter for rough flow available even for pipes, it is not feasible to make a comparison. There is a great need for the development of a means to correlate rough-flow data in the region in which viscous influences are still important.

3. The shape of the channel does not have an important influence on friction for turbulent flow in smooth channels at small Reynolds numbers. However, it does have some effect on friction in rough channels. Shape is quite important for laminar flow. The effect of shape in laminar flow can be estimated theoretically.
4. The lower critical Reynolds number for transition between laminar flow and turbulent flow in smooth channels depends to some extent on channel shape. The value ranges from 2,000 to more than 3,000 being generally larger than the value for closed-conduit flow.

Calculation of the Roughness Coefficient n

The computation of a roughness coefficient for both natural and artificial channels requires a value of the energy slope. The energy slope is usually calculated by

$$S_s = \frac{h_L}{L} = \frac{1}{L} \left[\left(\frac{V_1^2}{2g} - \frac{V_2^2}{2g} \right) + (y_1 - y_2) + (z_1 - z_2) \right]$$

The two assumptions made in the expression for S_s are:

1. The energy loss varies linearly over the reach L under consideration.
2. The energy (or Bernoulli) equation without velocity distribution coefficients is applicable.

Thus the error in these assumptions is included in the resistance coefficient. Since the Manning equation used to compute the resistance is empirical, it appears doubtful whether the Manning formula is either an energy or momentum formula. Regardless of the equation used in calculating S_s , the errors due to the assumptions in the momentum equation or the energy equation would finally be absorbed by the resistance coefficient n .

Dimensionless Parameters

Experimentation is usually necessary to determine the relative influence of each variable which produces a phenomenon. A methodical approach used by many hydraulicians is dimensional analysis in conjunction with the Buckingham Pi theorem. Dimensional analysis is a powerful tool in experimental design. The advantages of such an experimental design are (1) the possibility of describing all the contributing factors of a physical system by a single equation and (2) saving time by allowing the experimenter to obtain useful data with a minimum of experimental and computational effort. Murphy (38) lists the pertinent variable of a general fluid system. The variables will be presented in appropriate categories:

Kinematic Variables:

v - velocity

P - pressure

G - acceleration of gravity

Dimensions:

LT^{-1}

FL^{-2}

LT^{-1}

Fluid Variables	Dimensions:
γ - viscosity	$ML^{-1}T^{-1}$
ρ - density	ML^{-3}
e - bulk modulus	FL^{-2}
σ - surface tension	LT^{-2}

Geometrical Variables:

l - control distance	l
λ - outline dimension	L
η - cross-section dimension	L

Grouping the pertinent quantities into dimensionless parameters in accordance with the Buckingham Pi theorem, the expression for a general fluid system becomes

$$\frac{P}{\rho v^2} = f\left(\frac{\lambda}{l}, \frac{\eta}{l}, \frac{\rho v l}{\mu}, \frac{v^2}{l}, \frac{\rho v^2 l}{\sigma}, \frac{\rho v^2}{e}\right)$$

$$N_E = f\left(\frac{\lambda}{l}, \frac{\eta}{l}, N_R, N_F, N_W, N_e\right)$$

The first two parameters in the expression are geometrical and the others named in order are the Reynolds number, the Froude number, the Weber number, and the Cauchy number. The dependent parameter is called the Euler number.

The Reynolds number is distinguishable from the others by the fact that it contains the viscosity of the fluid. In other problems parameters containing viscosity can be transformed into the Reynolds number.

Dimensionally, the Reynolds number is proportional to the ratio of the inertia force to the viscous force of the fluid system. In model testing the N_R of the model must be equal to the N_R of the prototype. This is equivalent to requiring that the ratio of the inertia to viscous force be equal in the model and prototype which precludes the possibility of laminar flow in the prototype being represented by turbulent flow in the model, and vice versa.

Reynolds number for open channels is defined as $N_R = \frac{VR}{\nu}$. R , the hydraulic radius, is the characteristic length.

The Froude number is different from the other parameters in that it contains the acceleration of gravity. Since many fluid systems are acting under the direct influence of gravity, the N_F is sometimes used as the criterion for model design. The Froude number is defined as $N_F = \frac{V}{\sqrt{gD}}$ where D , the hydraulic depth, is the characteristic length. N_F is an expression of the ratio of the inertial forces to the gravitation force of the fluid system.

The Weber number is dimensionally equivalent to the ratio of the inertial force to the surface tension force. Where the surface tension force is important, N_W serves as a criterion for design. In channels of large depth the N_W is usually neglected. The Weber number is defined

as $N_W = \frac{\rho v^2 \ell}{\sigma}$. For sheet flow or overland flow, ℓ may be the thickness of the sheet while ℓ may be diameter of a drop of liquid in simulated rainfall.

The Cauchy number is distinguishable from the other parameters because it contains the compressibility force of the fluid. The Cauchy number is defined by $N_C = \frac{\rho v^2}{e}$. N_C is the ratio of the inertia force to the compressibility forces of a fluid. N_C is unimportant for an incompressible fluid. Compressibility effects are considered important for a $C \sim 1.0$ and negligible for $C \leq 0.1$.

The Euler number is the ratio of the pressure force to the inertial force of a fluid system. It is defined as $N_E = \frac{P}{\rho v^2}$. N_E is unimportant in problems related to open channel hydraulics.

Irrigation

The hydraulics of surface irrigation has the complexities of unsteady flow and variable intake rate. These complexities offer a great challenge to the designer of a furrow irrigation system. To add further complications, the economics of the entire farming operation must be considered in the design. According to Israelson (22) the criteria for a well-designed irrigation system is as follows:

1. Store the required water in the root zone.
2. Obtain reasonably uniform application of water.

3. Minimize soil erosion.
4. Minimize run-off of irrigation water from the field.
5. Provide for beneficial use of run-off water.
6. Minimize labor requirement for irrigation.
7. Minimize land used for ditches and other controls to distribute the water.
8. Fit irrigation system to field boundaries.
9. Adapt system to soil and topographic changes.
10. Facilitate use of machinery for land preparation, cultivating, furrowing, harvesting, etc.

Many irrigation systems have been designed using part of the above criteria. An irrigation system of considerable merit was designed by Garton (14). Garton's proposed cut-back irrigation system is shown in Figure 10. The concrete lined channel was constructed as a series of level bays with short outlet tubes set at a predetermined distance from the channel bottom. The size of the tubes are predetermined by the size of furrow stream. Garton stated that the labor requirement for irrigating could be drastically reduced for cut-back furrow irrigation. Further reduction in labor could be obtained by completely automating the system with time clocks or moisture sensing elements to trip the check gates at the ends of the bays.

The operation cycle of the system is (1) use a high initial flow to wet the soil over the length of the furrow

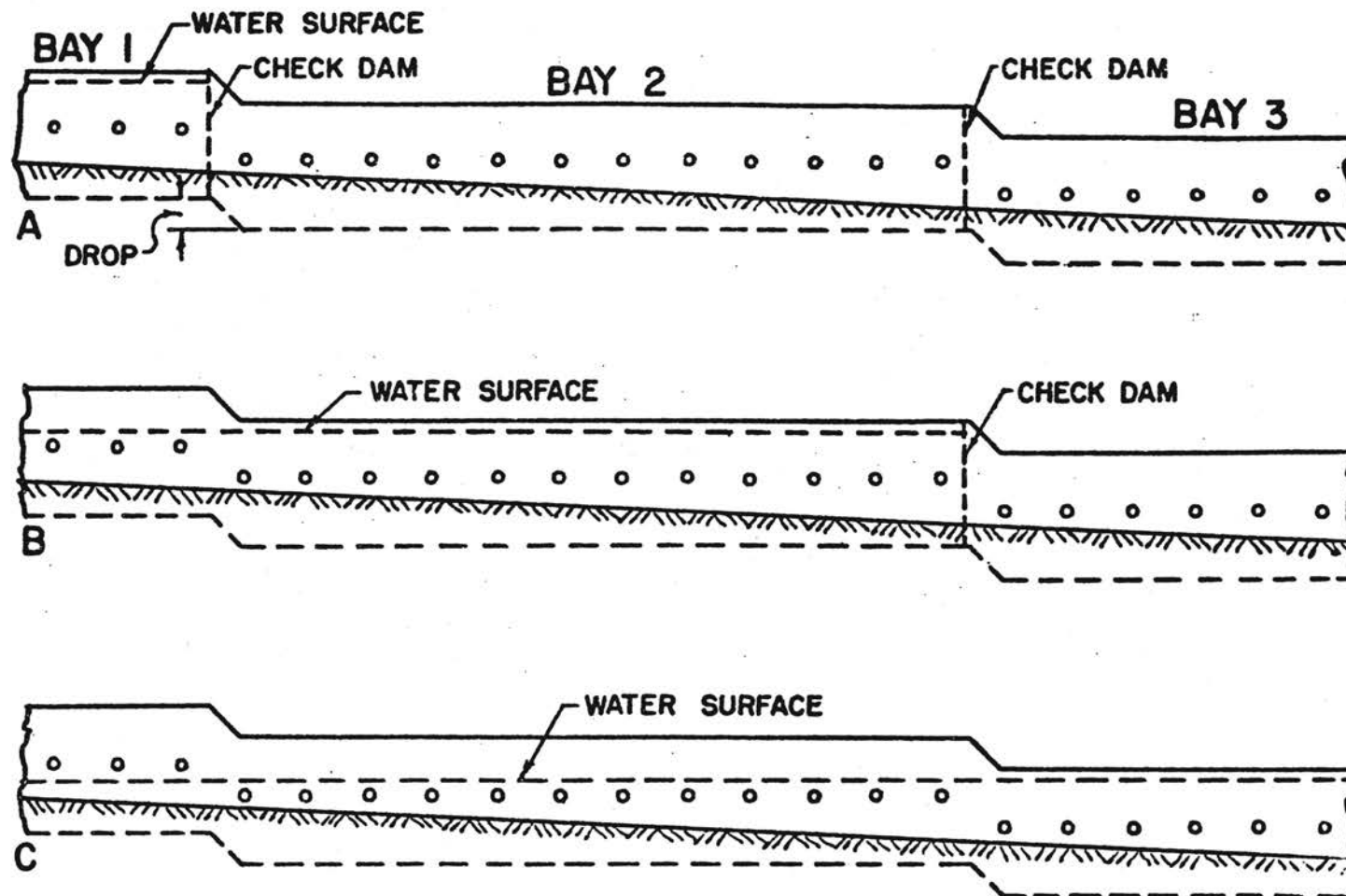


Figure 10. Elevation Drawing Showing the System of Cut-Back Furrow Irrigation Using One Cut-Back

(2) then cut back the discharge of the tubes to the approximate intake rate of the soil and (3) cut off the flow after applying the desired quantity of water to the soil.

The limitation of the proposed system is perhaps flexibility. This limitation is brought about by the uncertainty of row spacing of different row crops and a probable change in the intake rate of the soil with respect to time. In the future, cut-back irrigation systems such as that proposed by Garton may be accepted in furrow irrigation. However, at present, concrete lined channels with siphon tubes are widely used by many row crop farmers.

The Concrete Lined Channel

Concrete slip form channels are popular with surface irrigators. As a result of this popularity the American Society of Agricultural Engineers proposed a standard for concrete slip form canal and ditch linings. The proposed standard section for a trapezoidal channel is shown in Figure 11. If the channel is used for conveyance, the open channel formulas can be used for flow computations. An n value of .014 was used in calculating the flow in the recommended standard section. When the channel is used for distribution, the water surface profile is supposedly represented by the decreasing spatially varied flow equation (10). The accuracy with which the decreasing

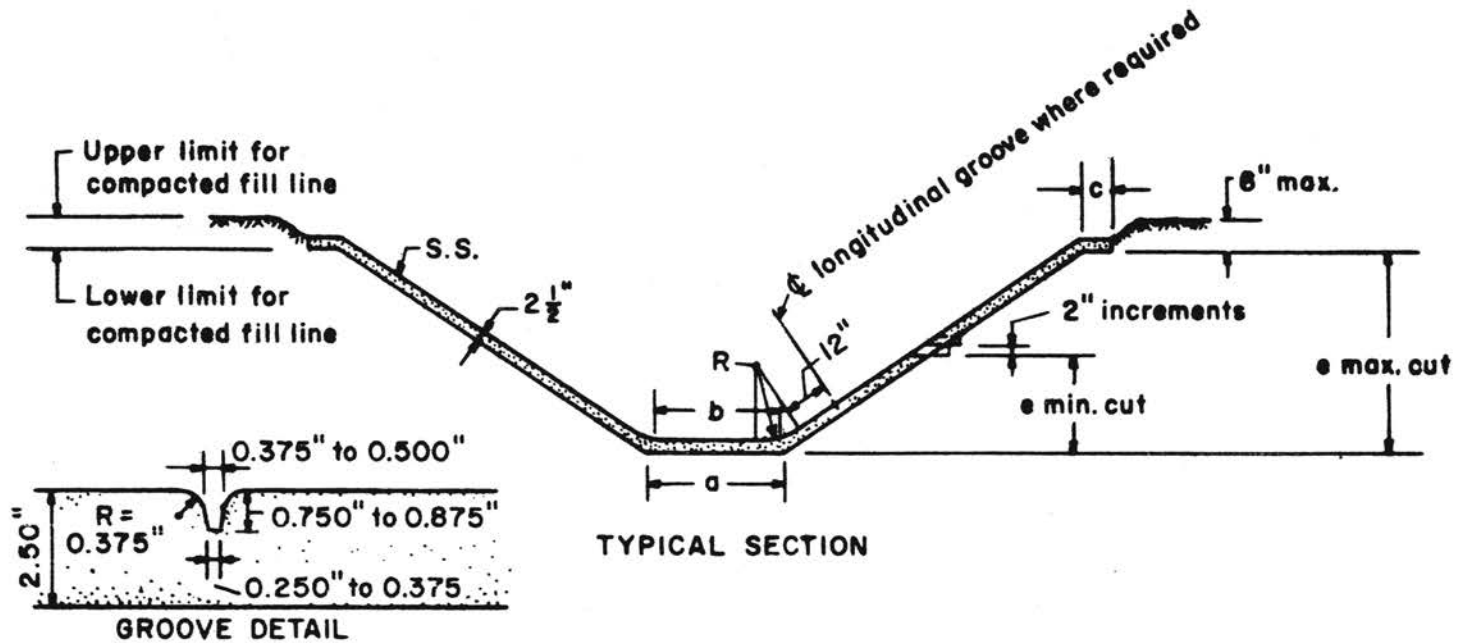


TABLE OF DIMENSIONS

SECTION	S.S.	a	b	c	e Min.	e Max.	R
A-1	1:1	14.07"	12.00"	4.00"	15.00"	30.00"	9.00"
A-2	1:1	26.07"	24.00"	4.00"	15.00"	30.00"	9.00"
B-2	1 1/2 : 1	25.51"	24.00"	6.00"	24.00"	48.00"	18.00"
B-3	1 1/2 : 1	37.51"	36.00"	6.00"	27.00"	54.00"	18.00"
B-4	1 1/2 : 1	49.51"	48.00"	6.00"	33.00"	66.00"	18.00"
B-5	1 1/2 : 1	61.51"	60.00"	6.00"	36.00"	72.00"	18.00"
B-6	1 1/2 : 1	73.51"	72.00"	6.00"	42.00"	84.00"	18.00"

Figure 11. Proposed Standard Trapezoidal Canal and Ditch Sections

spatially varied flow equation will predict the water surface profile is of primary concern in this paper because of the direct relationship of the water surface elevation with respect to the discharge of the siphon tubes.

Siphon Tubes

Siphon tubes are a means of transferring water from an irrigation distribution channel to the furrow. Siphon tubes are available in different lengths, diameters, configurations, and materials. Aluminum and plastic tubes are generally preferred over the other types.

The flow through a siphon tube is proportional to area (or diameter) and the square root of the head h on the tube. The head on a siphon tube is the distance from the water surface in the distribution channel to the point where the hydraulic grade line pierces the plane of the tube outlet provided the tube is not submerged. The head for a submerged tube is the distance between the water surface in the distribution channel and the water surface at the outlet end of the tube. The quantity of water Q flowing through a tube can be expressed theoretically by the equation $Q = A \sqrt{2gh}$. The actual flow is somewhat less than the Q predicted by the equation. To account for the apparent loss in Q due to pipe loss, entrance loss, and exit loss, a coefficient is necessary. The correction factor or coefficient applied to the theoretical equation is $C = \frac{Q_{\text{actual}}}{A \sqrt{2gh}}$

Johnson (25) observed that plastic tubes had a higher efficiency than metallic tubes, where efficiency was defined as $C = \frac{Q_{\text{actual}}}{Q_{\text{theoretical}}} \times 100$. The difference in efficiency was said to be due to the difference in roughness of the siphon tubes.

Tovey and Myers (51) tested aluminum and plastic siphon tubes. The diameters ranged from .5 to 2.0 inches with a variation in head of .15 to 2.0 feet. They found that the coefficient C increases as length and diameter decreased. This would be expected since one would not expect fully established flow in a short tube, and with the same physical roughness the flow in the small diameter tube would become fully established in a shorter length of tube.

Garton (16) constructed a nomograph from Tovey's data, shown in Figure 12. The nomograph is expected to estimate Q within 5 to 10 per cent. The error is due to different materials, lengths, and outlet losses.

Keflemariam (26) obtained a discharge relationship for double-bend plastic siphon tubes 5 feet in length.

$$Q = K D^{2.14} h^{.571}$$

where

D = Average inside diameter

h = Head in feet measured from the water surface in the supply reservoir to the center line of the outlet.

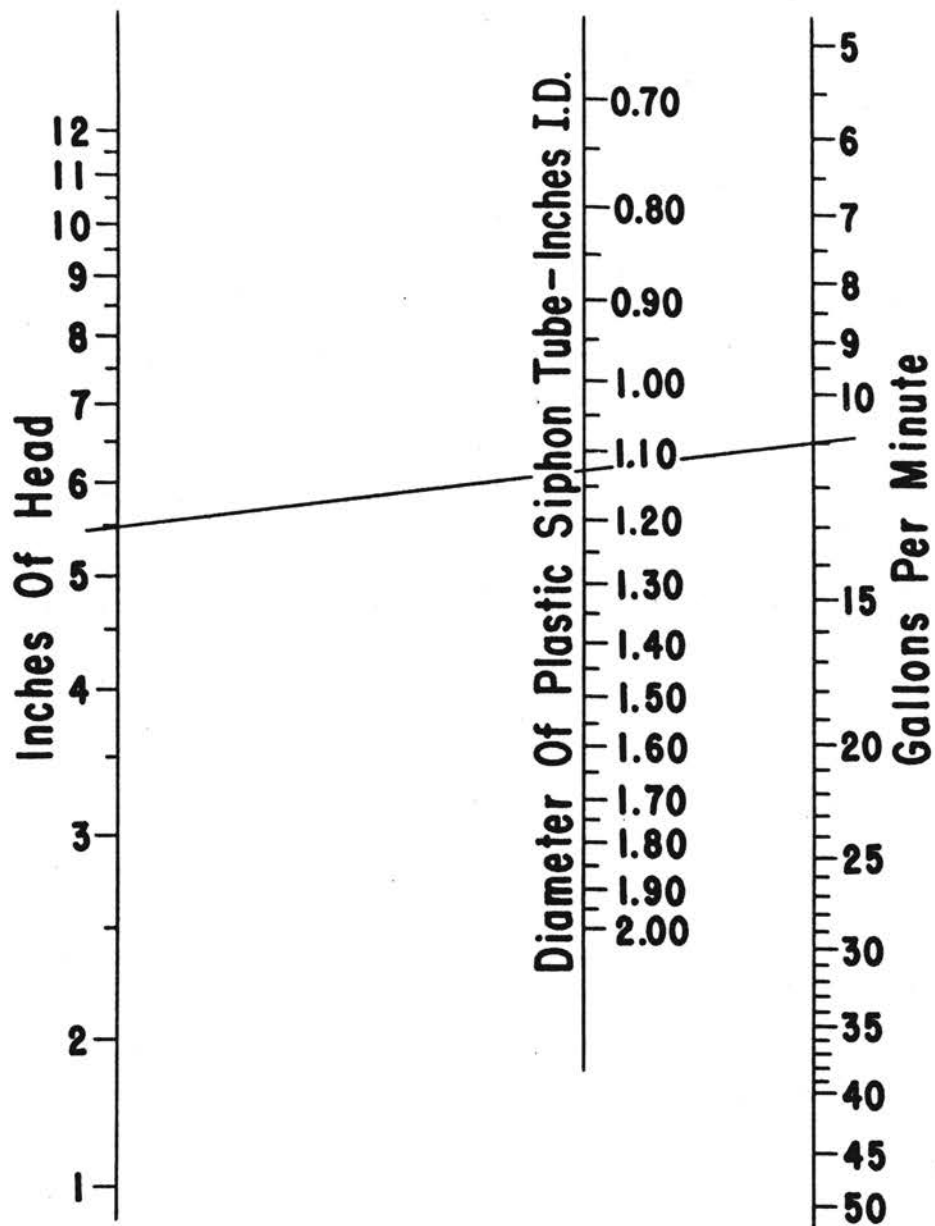


Figure 12. The Discharge of Plastic Siphon Tubes as a Function of Tube Diameter and Head

The equation was obtained from six tube sizes (.75, 1.0, 1.25, 1.5, 2.0, and 3.0) that were available for the study. A random sample of 5 tubes per size was selected from a lot of 90 tubes. An arithmetic average of four measurements 45 degrees apart at the outlet and inlet of the tubes was used as the inlet and outlet diameter. The tubes were placed in an apparatus simulating a trapezoidal channel. The discharge from three heads with four replications per head was measured on a weight basis. The head was held within $\pm .0025$ feet of the selected head values of .25, .50, and .75 feet.

Irregularities and indentations in the tubes had no apparent influence on tube discharge.

CHAPTER III

THEORY

The methods of describing fluid motion are the so-called Lagrangean method after J. L. Lagrange and the Eulerian method after L. Euler. The Lagrangean method describes the paths of individual fluid particles while the Eulerian method describes the velocity, pressure, and other characteristics at a section in the fluid. In the Eulerian method it is not known which particles pass the section, but the description gives the fluid characteristics at various points at the station. The energy equation derived in this section will be based on the Eulerian method.

Part of the material in this chapter will be repetitious of that in the literature review. The theoretical analysis will begin with the Bernoulli equation as developed along a streamline without the consideration of frictional resistance. This equation will be modified and a general energy equation developed. The energy equation will be used to develop an expression for decreasing spatially varied flow. A method for numerically solving the decreasing spatially varied flow equation will be presented and followed by a discussion of the equation.

General Energy Equation

Consider the Bernoulli equation in differential form along a streamline for an incompressible fluid

$$\left[\frac{d}{ds} \left(\frac{v_s^2}{2g} + \frac{P}{\gamma} + Z \right) \right] = \frac{dH}{ds}$$

where Z is the elevation of the water. Multiplying the equation by the weight of a fluid element yields

$$\left[\frac{d}{ds} \left(\frac{v_s^2}{2g} + \frac{P}{\gamma} + Z \right) \right] dw = \frac{dH}{ds} dw \quad (12)$$

where dH is the energy loss in total head along the distance ds . Integrating Equation 12 along a streamline gives

$$\int_1^2 \left[d \left(\frac{v_s^2}{2g} + \frac{P}{\gamma} + Z \right) \right] dw = dw \int_1^2 dH$$

Thus, the general expression along a streamline is

$$\left(\frac{v_s^2}{2g} + \frac{P}{\gamma} + Z \right)_1 dw - \left(\frac{v_s^2}{2g} + \frac{P}{\gamma} + Z \right)_2 dw = dw(H_1 - H_2) \quad (13)$$

A general expression between the boundaries can be obtained by integrating across the section under consideration. Substituting

$$dw = \gamma ds dA = \gamma v dt dA$$

into Equation 13 integration is impossible unless v is constant or unless the relationship $v = f(A)$ is known.

Substituting

$$dw = \gamma dQ dt$$

Equation 13 becomes

$$\left(\frac{v^2}{2g} + \frac{P}{\gamma} + Z\right)_1 \gamma dQ dt - \left(\frac{v^2}{2g} + \frac{P}{\gamma} + Z\right)_2 \gamma dQ dt = \gamma dQ dt (H_1 - H_2)$$

which is an expression with the units of energy. Now dividing by dt and integrating gives

$$\begin{aligned} & \gamma \int^Q \left(\frac{v_1^2}{2g} - \frac{v_2^2}{2g}\right) dQ + \gamma \int^Q \left(\frac{P}{\gamma} + Z\right)_1 dQ - \gamma \int^Q \left(\frac{P}{\gamma} + Z\right)_2 dQ \\ & = \gamma \int^Q (H_1 - H_2) dQ \end{aligned}$$

This expression has the units of power and could really be called the power equation. However, dividing through by γQ the equation becomes

$$\begin{aligned} & \frac{1}{Q} \int^Q \left(\frac{v_1^2}{2g} - \frac{v_2^2}{2g}\right) dQ + \frac{1}{Q} \int^Q \left(\frac{P}{\gamma} + Z\right)_1 dQ - \frac{1}{Q} \int^Q \left(\frac{P}{\gamma} + Z\right)_2 dQ = \\ & \frac{1}{Q} \int^Q (H_1 - H_2) dQ \end{aligned}$$

If $\frac{1}{Q} \int^Q (H_1 - H_2) dQ$ is defined as h_L , then the general energy equation is

$$\begin{aligned} & \frac{1}{Q} \left[\int^Q \frac{v_1^2}{2g} dQ - \int^Q \frac{v_2^2}{2g} dQ + \left(\frac{P}{\gamma} + Z\right)_1 - \right. \\ & \left. \left(\frac{P}{\gamma} + Z\right)_2 \right] = h_L \end{aligned} \tag{14}$$

The only constraint on Equation 14 is that the acceleration normal to the streamline is equal to zero which guarantees hydrostatic pressure.

The velocity head term can be approximated by

$$\frac{1}{Q} \int^Q \frac{v^2}{2g} dQ \sim \frac{1}{Q} \sum^Q \frac{v^2}{2g} \Delta Q$$

Multiplying the equation by γ yields

$$\frac{\gamma}{Q} \int^Q \frac{v^2}{2g} dQ \sim \frac{\gamma}{Q} \sum^Q \frac{v^2}{2g} \Delta Q$$

which is an expression of energy. If one assumes that the total kinetic energy at a station is approximately equal the sum of the kinetic energies of the incremental sections then

$$\sum^Q \gamma \frac{v^2}{2g} \Delta Q \sim \frac{V^2}{2g} m$$

or that

$$\sum^Q \gamma \frac{v^2}{2g} \Delta Q = \alpha \frac{V^2}{2g} m$$

where α is an energy coefficient. Substituting $m = \frac{\gamma}{g} Q$ the equation becomes

$$\alpha \frac{V^2}{2g} = \frac{1}{Q} \sum^Q \frac{v^2}{2g} \Delta Q \sim \frac{1}{Q} \int^Q \frac{v^2}{2g} dQ \quad (15)$$

Substituting Equation 15 into Equation 14 yields

$$\left(\frac{\alpha_1 V_1^2}{2g} - \frac{\alpha_2 V_2^2}{2g} \right) + \left(\frac{P}{\gamma} + Z \right)_1 - \left(\frac{P}{\gamma} + Z \right)_2 = h_L \quad (16)$$

Alpha (α) is dependent on the velocity distribution and can be computed by

$$\alpha = \frac{1}{QV^2} \int^Q v^2 \Delta Q = \frac{\int^A v^3 \Delta A}{V^3 A}$$

For open channel flow the pressure head $\frac{P}{\gamma}$ is constant and can be eliminated from Equation 16 leaving

$$\left(\frac{\alpha V_1^2}{2g} + Z_1 \right) - \left(\frac{\alpha V_2^2}{2g} + Z_2 \right) = h_L$$

Thus, the evaluation of the head loss for a channel reach is only as accurate as the determination of α , V , and Z .

Decreasing Spatially Varied Flow Equation

Take the expression of energy at a section of the channel

$$H = z + y + \frac{\alpha V^2}{2g} = z + y + \frac{\alpha Q^2}{2gA^2} \quad (17)$$

Now, consider a differential distance dx down the channel as shown in Figure 13. Differentiating Equation 17 with respect to x and assuming α is constant yields

$$\frac{dH}{dx} = \frac{dz}{dx} + \frac{dy}{dx} + \frac{\alpha}{2g} \left(\frac{2Q}{A^2} \frac{dQ}{dx} - \frac{2Q^2}{A^3} \frac{dA}{dx} \right) \quad (18)$$

Substituting

$$\frac{dH}{dx} = -S_s, \quad \frac{dQ}{dx} = q, \quad \frac{dz}{dx} = -S_o$$

and

$$\frac{da}{dx} = \frac{dA}{dx} \frac{dy}{dy} = T \frac{dy}{dx}$$

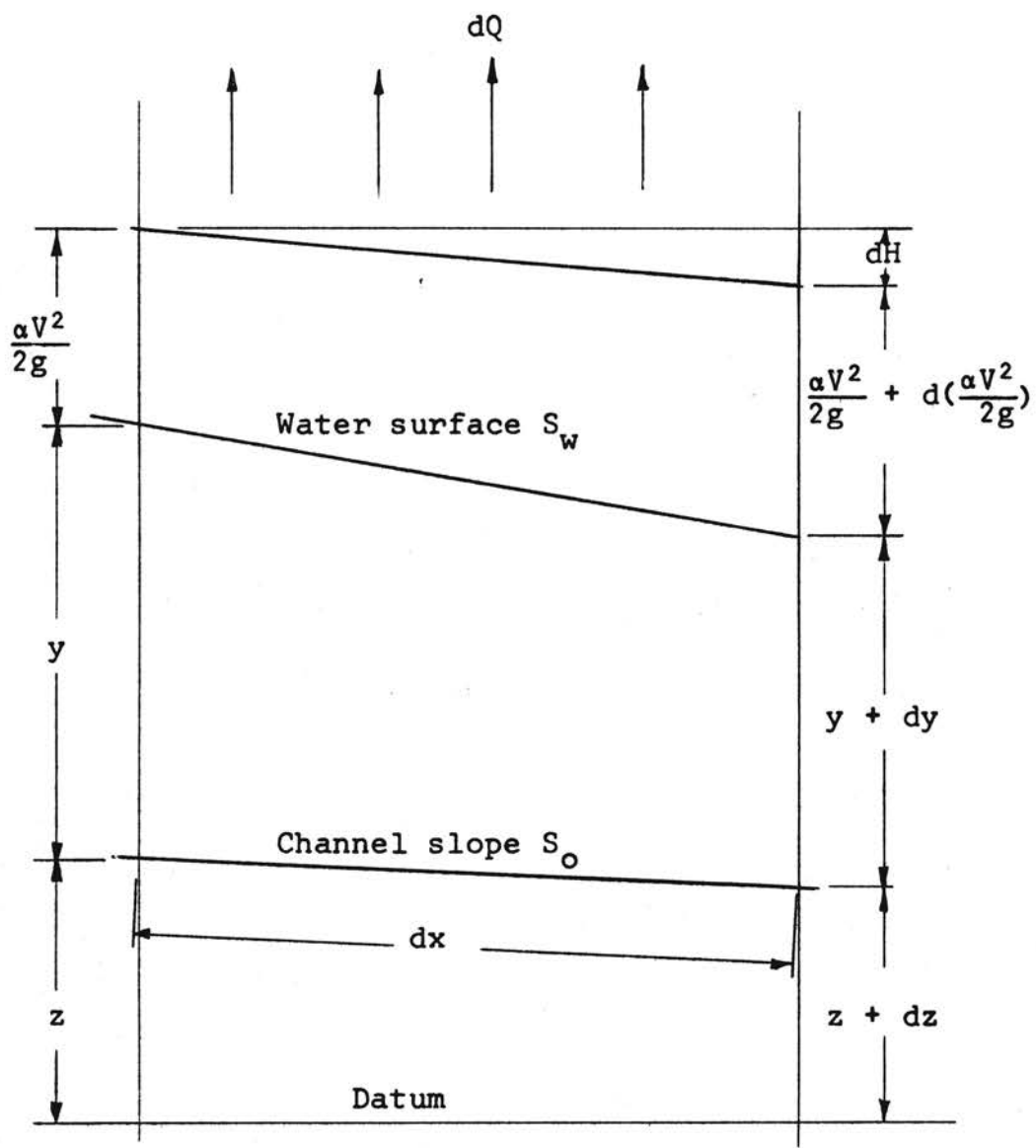


Figure 13. Graphic Illustration of Decreasing Spatially Varied Flow

into Equation 18 gives

$$-S_s = -S_o + \frac{dy}{dx} + \frac{\alpha}{2g} \left(\frac{2Qq}{A^2} - \frac{2Q^2}{A^3} T \frac{dy}{dx} \right)$$

Substituting $D = \frac{A}{T}$ and collecting terms the equation becomes

$$\frac{dy}{dx} = \frac{S_o - S_f - \frac{\alpha Qq}{gA^2}}{1 - \alpha \frac{Q^2}{gA^2 D}} \quad (10)$$

Equation 10 is an expression for the rate of change of the water surface with respect to distance down the channel. The ordinary first degree, first order, non-linear differential equation is not readily integrable for most channels. The assumptions made in deriving the equation are listed in the literature review under spatially varied flow.

The denominator in Equation 10 is $1 - \alpha N_F$. As the flow approaches critical depth, i.e., as N_F approaches 1.0 and if α is approximately 1.0 the derivative is undefined. Thus, the accuracy of the quantities on the right side of the equation become extremely important in calculating the slope of the water surface near a point of critical flow because small erroneous magnitudes could result in a large computative error.

To numerically integrate the decreasing spatially varied flow equation, Chow (11) considered the differential as finite increments and assumed the

velocity and discharge at Section 1 as V_1 and Q_1 and at 2 as $V_1 - \Delta V$ and $Q_1 - \Delta Q$. He expressed the lost momentum as $\frac{\gamma \Delta Q}{g} (V_1 - \frac{\Delta V}{2})$. The lost momentum was added to the momentum at Section 2. The change in momentum was written as

$$\frac{\gamma}{g} [Q_1 V_1 - ((Q_1 - \Delta Q)(V_1 - \Delta V) + \Delta Q(V_1 - \frac{\Delta V}{2}))] = F_p + F_g + F_s$$

expanding and collecting terms yields

$$\frac{\gamma}{g} [Q \Delta V - \frac{\Delta V \Delta Q}{2}] = -\gamma \int_0^{\Delta y} A dy + \gamma S_o \int_0^{\Delta x} A dx - \gamma S_s \int_0^{\Delta x} A dx = \gamma A_{avg} (-\Delta y + S_o \Delta x - S_s \Delta x)$$

Substituting $A_{avg} = \frac{Q_1 + Q_2}{V_1 + V_2}$ into the equation yields

$$\frac{\gamma}{g} [Q_1 \Delta V - \frac{\Delta V \Delta Q}{2}] = w \left(\frac{Q_1 + Q_2}{V_1 + V_2} \right) (-\Delta y + S_o \Delta x - S_s \Delta x)$$

The drop in the water surface is equal

$$-\Delta y + S_o \Delta x = \frac{Q_1 \Delta V}{g} \left(\frac{V_1 + V_2}{Q_1 + Q_2} \right) \left(1 - \frac{\Delta Q}{2Q_1} \right) + S_s \Delta x \quad (19)$$

An energy coefficient α is then added to the equation because α is evaluated by an energy loss formula. When the change in water $\Delta y' = -\Delta y + S_o \Delta x$ is substituted into Equation 19 the equation is

$$\Delta y' = \frac{\alpha Q_1 \Delta V}{g} \left(\frac{V_1 + V_2}{Q_1 + Q_2} \right) \left(1 - \frac{Q}{2Q_1} \right) + S_s \Delta x \quad (20)$$

where ΔQ is the discharge per Δx distance along the channel.

The numerical solution seems to have eliminated the undefined condition that appeared in the total derivative, Equation 10. However, small finite increments should be used in the region of the critical flow section, unless the possible error for a longer reach can be tolerated.

Discussion

As noted, the differential Equation 10 for decreasing spatially varied flow is not integrable except in the simplest cases and the numerical Equation 20 for decreasing spatially varied flow was derived from the momentum concept with an energy coefficient α introduced after the development of the equation. Thus, it appears that the computations of the water surface of a channel from the general energy Equation 16 would be as reliable as the computations from Equation 20. The general energy equation is definitely as sound theoretically.

The general energy equation was used in a preliminary investigation of a level concrete trapezoidal distribution channel with siphon tubes. The results of the investigation are summarized and discussed in Chapter IV.

CHAPTER IV

PRELIMINARY INVESTIGATION

A level irrigation distribution channel with siphon tubes was analyzed in a preliminary investigation. The channel was trapezoidal with a 1 foot bottom width and 1-to-1 side slopes. This type of channel was selected because of its popularity in the western states.

The general energy equation was used in the computations

$$z_2 - z_1 = H_L - \left(\alpha_2 \frac{V_2^2}{2g} - \frac{\alpha_1 V_1^2}{2g} \right)$$

where

z_1 = water surface elevation at Section 1 (the downstream section)

$\frac{V_1^2}{2g}$ = velocity head at Section 1

α_1 = energy coefficient at Section 1

H_L = energy loss between Sections 1 and 2 due to resistance

A siphon tube spacing of 40 inches was considered. The range in n values selected was .010 to .015 while alpha (α) values of 1.0 and 1.1 were used. These values

are compatible with those found in the literature. The variation in tube discharge was from .01 to .10 cfs and the number of tubes varied from 25 to 100.

Results

A relationship of the difference in water surface elevations at the end of a bay and the entering Q is shown in Figure 14. The initial depths at the downstream section were varied from .6 to 2.1 feet, while assuming a value of $n = .012$, $\alpha = 1.0$ and N (number of tubes) = 100. It can be seen that for depths between 1.1 feet and 2.1 feet the variation in the water surface at the ends of the bay is $\Delta w_s = \pm 0.01$. This is important because the entering discharge for a distribution channel in the field is usually covered by the range of 0 to 6 cfs and a .01 foot change in head on siphon tubes at high initial flow would probably result in less than a 2 per cent variation in tube discharge. When Δw_s is negative, the figure indicates that the water surface would appear to have a positive slope (or uphill slope) as viewed downstream. This would imply that the velocity head energy is greater than the loss in energy due to resistance with the differences in energies resulting in an increase in the water surface elevation.

The effect of a variation in n from .010 to .014 upon the change in water surface for a downstream depth of 1.2 feet is shown in Figure 15. This figure in

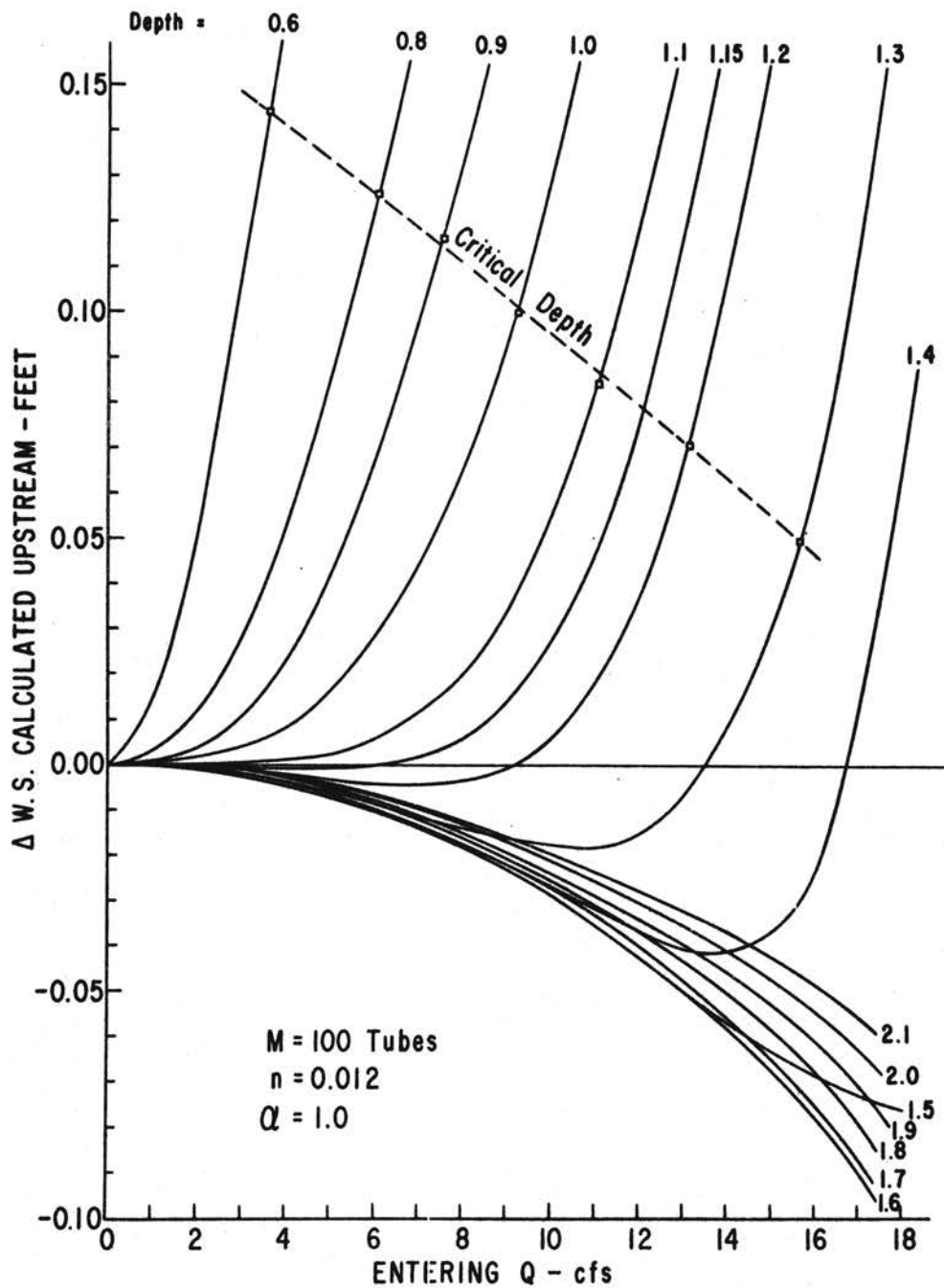


Figure 14. Change in the Water Surface Between the Ends of Level Distribution Bays of Various Depths Having 100 Tubes with a 3.33 Foot Spacing, a Manning n of 0.012 and $\alpha = 1.0$

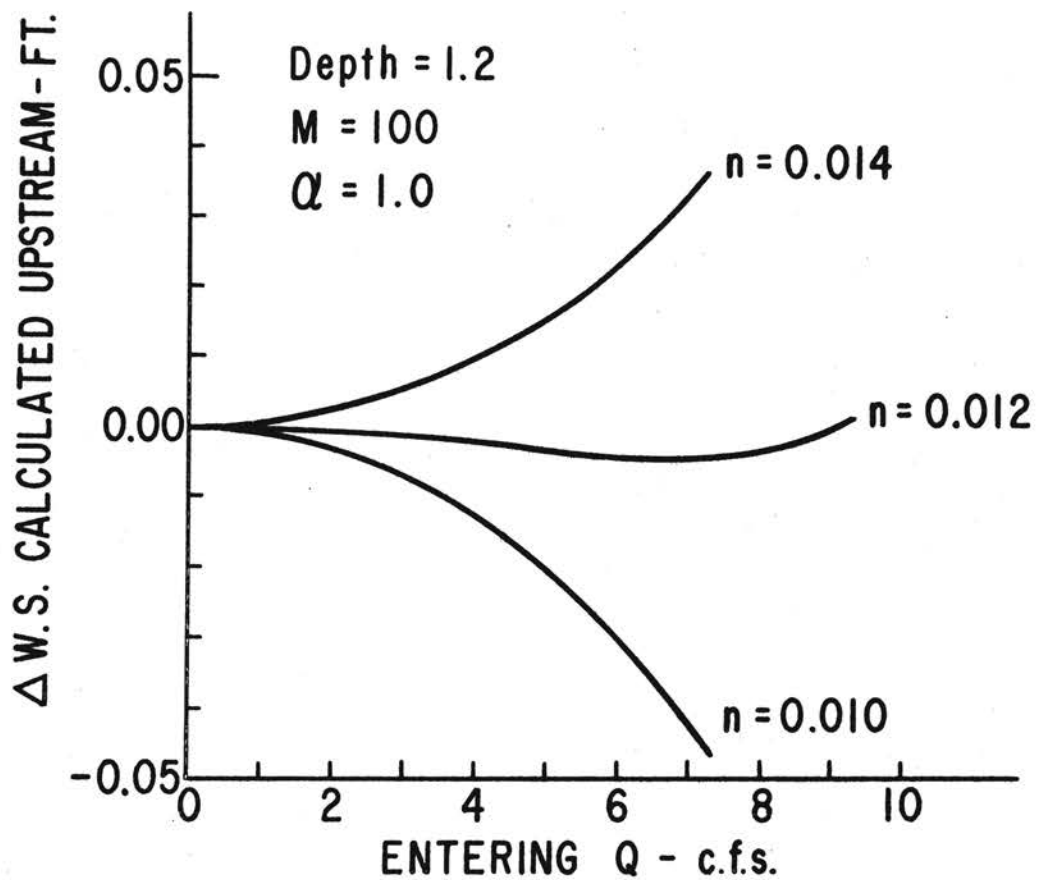


Figure 15. Change in the Water Surface Between the Ends of Level Distribution Bays Having Different Roughness

conjunction with Figure 14 would indicate that as the value of n increases so must the depth of flow in the channel if a level water surface is to be maintained.

Figure 16 shows that the depth at a given Manning's n is a function of the number of tubes and the tube discharge. The results of the figure are not astonishing since the channel length and the entering Q are determined by the number of tubes.

The number of tubes as a function of channel depth for equal water surface elevations at different values of Manning's N is shown in Figure 17. Graphs of this type were plotted for $\alpha = 1.0$, $QT = .01, .02, .06, .10$ and for $\alpha = 1.1$, $QT = .01, .02, .06, .10$. From these plots a generalized relationship was constructed as shown in Figure 18.

Figure 18 shows the relationship between the number of tubes, Manning's n , tube discharge, energy coefficients, and the depth for equal water surface elevation.

As the crossing lines approach tangency to the QT curves, the depth in the channel approaches critical depth.

Summary

Decreasing spatially varied flow in a trapezoidal irrigation channel with siphon tubes was analyzed with values of α and n considered to be constant along the length of the channel.

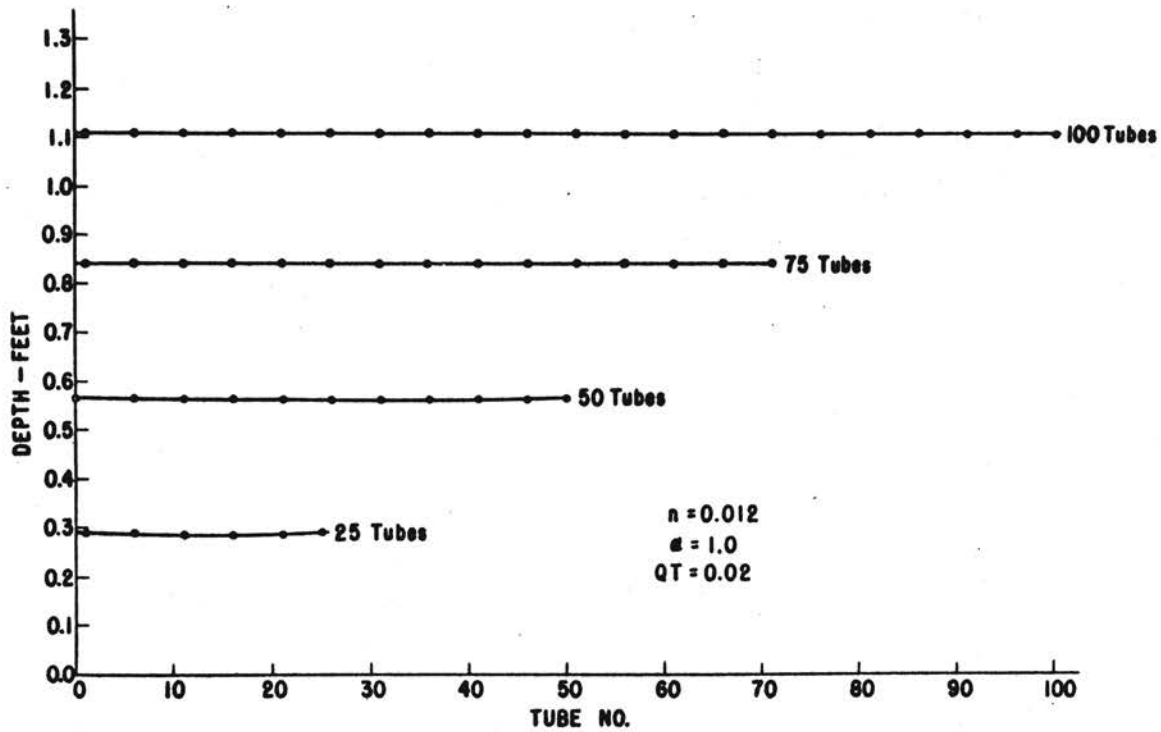


Figure 16. The Effect of the Number of Tubes on the Depth Required for Equal Water Surface Elevation Between the Ends of a Distribution Bay. Tube Discharge = 0.02 cfs. Tube Spacing, 40 Inches.

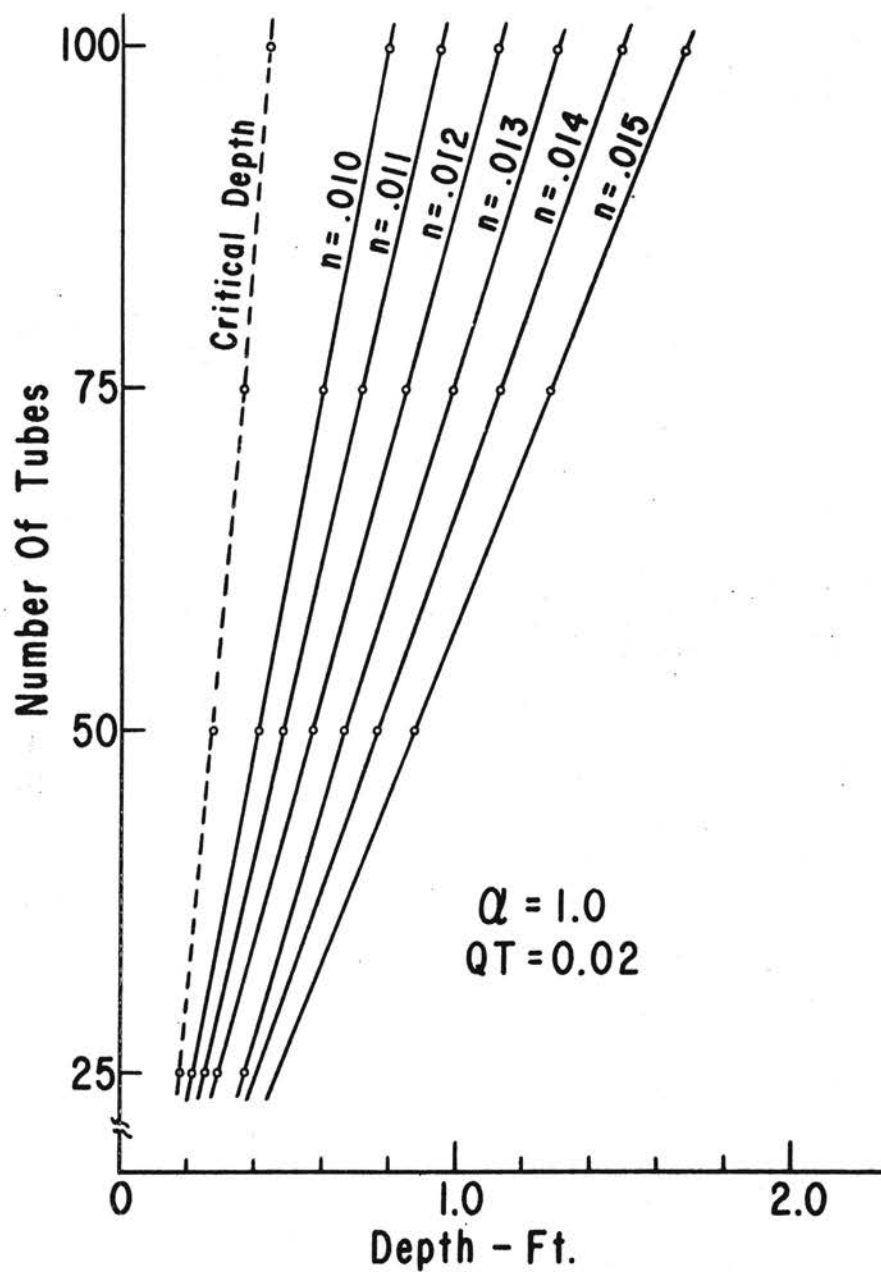


Figure 17. The Depth Required for the Same Water Surface Elevation Between the Ends of a Level Distribution Bay for Different Numbers of Tubes and Different Roughness

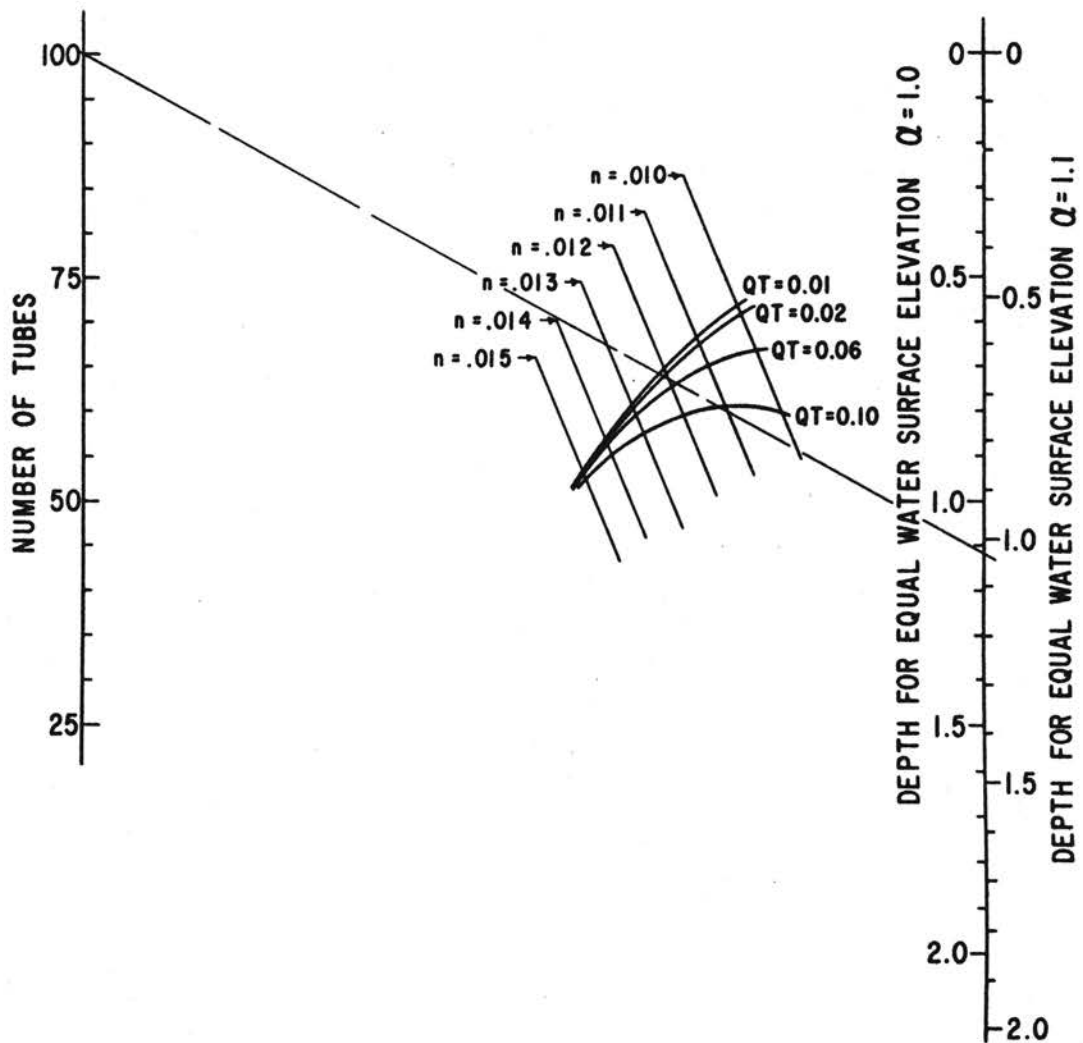


Figure 18. A Generalized Relationship of Depth Required for the Same Water Surface Elevation Between the Ends of Level Distribution Bays for Different Numbers of Tubes, Roughness, Tube Discharge and α

Equal water surface elevations at the ends of the bay were calculated for various values of roughness, tube discharge, tube number and α .

This theoretical investigation indicates that irrigation channels can be constructed in the field as a series of level bays with (1) expected uniformity in water application and (2) shallower depths than are currently used, provided the computed values are realistic. Accurate values of the variables α and n were not available for use in the calculations.

CHAPTER V

EXPERIMENTAL DISTRIBUTION CHANNEL SETUP

The preliminary investigation showed that water could be applied to the soil uniformly with more shallow channels than are commonly used where the inflow rates at the upstream end of the bay were from 0 to 6 cfs. However, the immediate questions arise, (1) how reliable were the estimates of α and n for the channel (2) can the general energy equation be used to calculate the water surface profiles? In an effort to answer these questions a concrete lined trapezoidal distribution channel was constructed at the Outdoor Hydraulic Laboratory near Stillwater, Oklahoma. The channel was instrumented to give an expected accuracy of measurement of .001 foot which was used in the preliminary investigation.

A general view of the experimental setup is shown in Appendix A and Figure 19. The setup consisted of (1) a 12 inch inlet pipe with an orifice meter and 60 inch manometer to measure the discharge into the channel, (2) the level concrete trapezoidal channel, (3) gauge wells to measure the depth of water in the channel, (4) a check gate at the downstream end of the channel, and (5) siphon

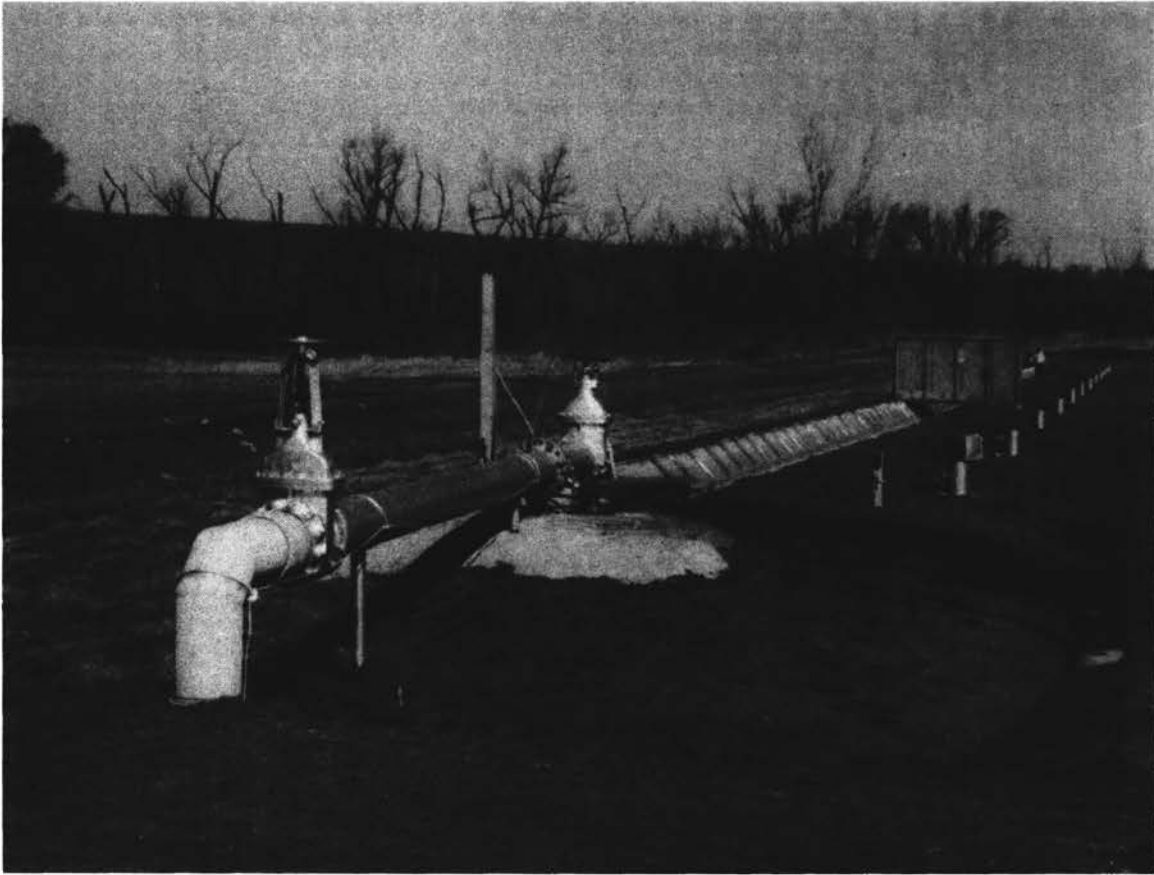


Figure 19. A General View of the Experimental Setup Showing the Water Supply Line, Orifice, Manometer, Gauge Wells, and Channel With the 2 in. Tubes in Place for a Roughness Test

tubes. The siphon tube mounts and the wind panels are shown in Figure 20.

Distribution Channel

A level concrete trapezoidal channel was constructed at the Stillwater Hydraulic Laboratory. The channel covered the range of dimensions currently used for small irrigation distribution channels. The channel is 320 feet in length, 2 feet deep with a 1 foot bottom width and 1 to 1 side slopes. Figure 21 shows the 300-foot test section of the channel used in the roughness and spatially varied flow test.

Gauge Wells and Reference System

The gauge wells were fabricated from 10-inch steel pipe and mounted in concrete. The wells were located 30 feet apart and connected to the channel with 1/2-inch plastic pipe. The gauge well at upstream station 0 + 00 was equipped with a FW - 1 water stage recorder and a 3-foot Lory point gauge. Lory point gauges 2-feet in length were mounted at the other stations. The point gauges were read to .001 foot. Figures 22 and 23 show the gauge wells at upstream stations 0 + 00 and 0 + 90, respectively. The gauge wells at the other nine stations along the channel are similar to the gauge well at station 0 + 90.

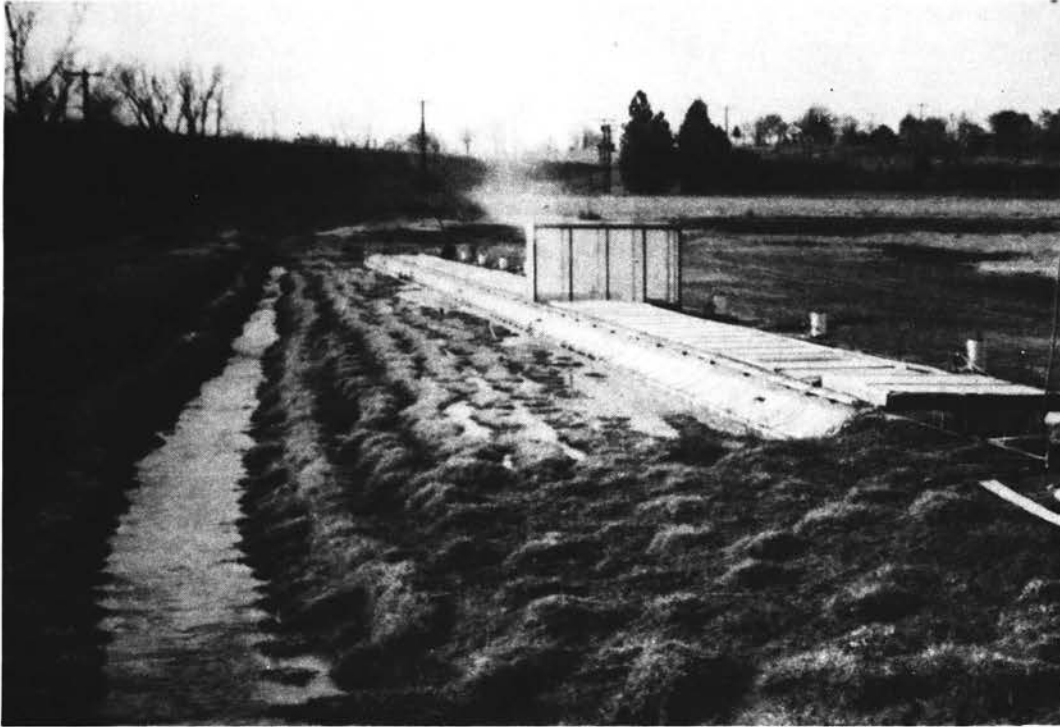


Figure 20. A View of the Wind Panels in Place During a Spatially Varied Flow Test. The Panels Were Used to Eliminate Wind Effects on the Water Surface Profile

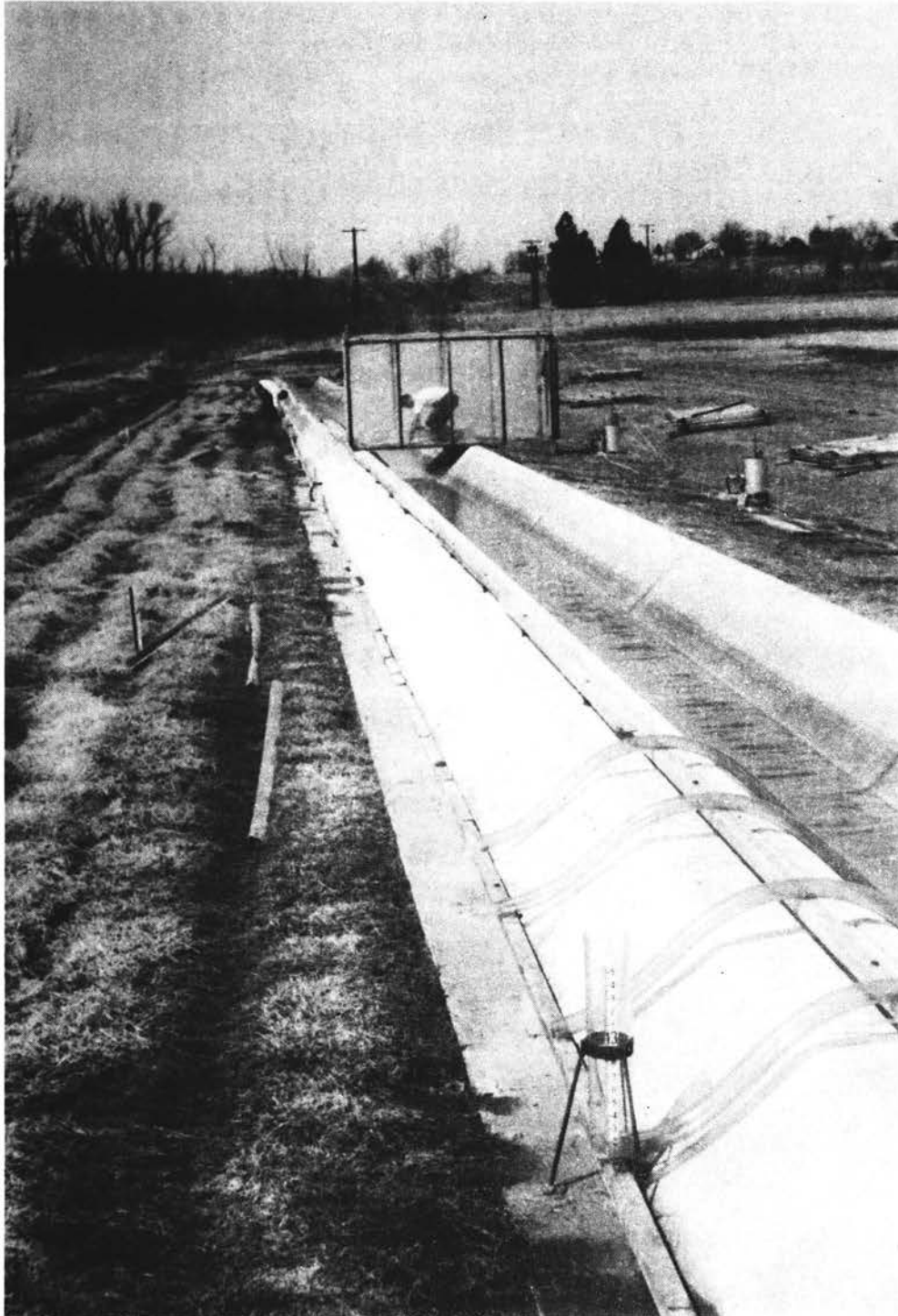


Figure 21. A View of the Test Section of the Channel, the Siphon Tube Mounts, and the Concrete Apron

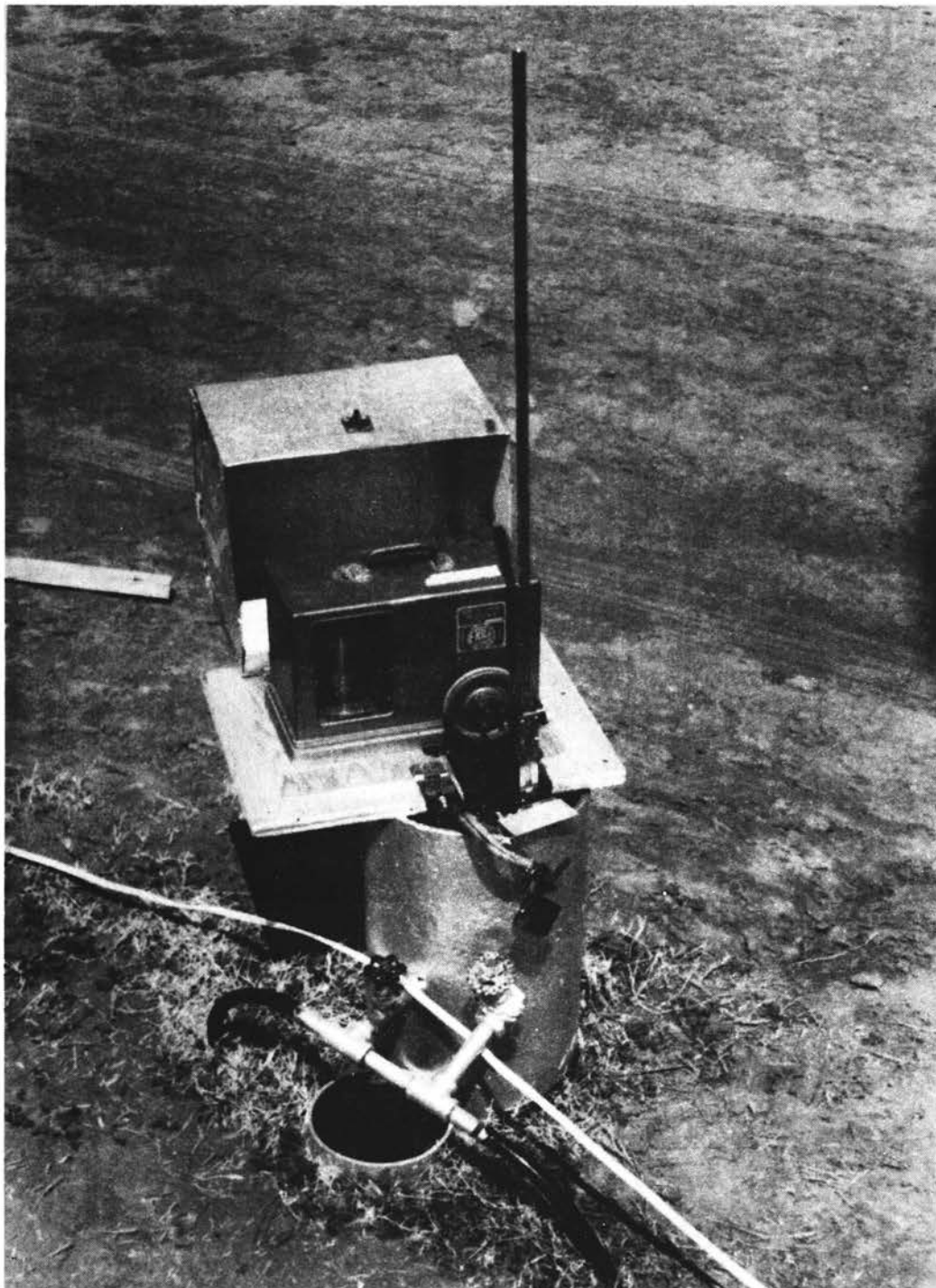


Figure 22. The Gauge Well at Station 0 + 00 With a FW-1 Water Stage Recorder and a 3 ft. Point Gauge. The Plumbing Seen on the Well Was Used to Obtain Gauge Zeros From a Common Water Surface



Figure 23. The Gauge Well at Station 0 + 90 With a 2 ft. Point Gauge. The Gauge Well Is Typical of the Wells at the Other 9 Stations Along the Test Channel

The plumbing above ground in the figures was used to determine gauge zeros from a water surface common to all gauge wells. The wells were filled with water and allowed to drain to an arbitrary elevation. This provided a water surface in the wells less sensitive to wind effects than the water surface in the channel.

The water surface in the well at station 0 + 00 was referenced to a bench mark called Hub #1, located approximately 120 feet from the station. The water surface elevation at the other gauge wells was assumed to be the same as the water surface at station 0 + 00. The elevation of the channel bottom and the siphon tube mounts were referenced to the water surface in the gauge wells.

The elevation of the channel bottom was obtained from the elevation of a brass plug embedded in the bottom of the channel at each station. A brass plug is shown in Figure 24.

Siphon Tube Mount

The siphon tube mount was designed such that the outlet end of the siphon tube could be adjusted to a desired elevation. The mounts consisted of a 1 1/2 by 1 1/2 by 3/16 inch structural steel angle 18 feet long which was held by 1/2 inch bolts and 1 1/4 inch tube adjustment shanks. The shanks were secured by a 1 1/2 inch collar and 1 1/2 inch pipe embedded in the concrete apron as shown in Appendix A.



Figure 24. A Brass Plug Embedded in the Channel Bottom. The Plug Was Used to Determine the Bottom Elevation of the Channel

Check Gate

The check gate shown in Figure 25 was cut from a plastic covered tarpaulin. The gate was secured to the channel with 1/4 inch lag screws and 3/8 inch molding material. This type of gate is used by Garton (15) on an automatic cut-back irrigation system at the Agricultural Experiment Station at Altus, Oklahoma. The gate has the advantages of being practically leak proof, economical, and offers little resistance to flow while in the down position. The gate was used in this investigation to control the depth of flow for a given discharge in the resistance tests as shown in Figure 26.

Velocity Distribution Measurements

A portable apparatus was built for the purpose of taking velocity distribution measurements at any station along the channel. The component parts of the apparatus are an H beam, a carriage, and a point gauge mount. The 8-inch aluminum H beam is 6 foot in length. The carriage rolls along a level edge of the H beam. A point gauge was mounted on the carriage. An Ott Laboratory current meter was attached to the point gauge. The carriage arrangement gave an accurate measurement of the location of the current meter with reference to the channel cross section. An Ott F-4 digital counter was connected to the current meter.



Figure 25. The Overflow Check Dam at the Downstream End of the Channel. In the Down Position the Dam Offers Little Resistance to Flow



Figure 26. The Check Dam in an Up Position. The Dam Was Used to Control the Depth in the Steady Flow Tests

The counter recorded the number of revolutions of the propeller. The velocity distribution measuring apparatus is shown in Figure 27.

Orifice Meter and Manometer

The inflow of water into the channel was measured with a sharp-edged orifice and U-tube manometer arrangement shown in Figures 28 and 29. The orifice plates are the property of the Outdoor Hydraulic Laboratory. The error of measurement using the orifice and manometer arrangement is considered to be less than 1 per cent.



Figure 27. Point Velocity Measuring Apparatus. The Component Parts Are: 8 in. Aluminum H Beam, Carriage, 3 ft. Point Gauge, OTT Laboratory Current Meter, and OTT F-4 Revolution Counter

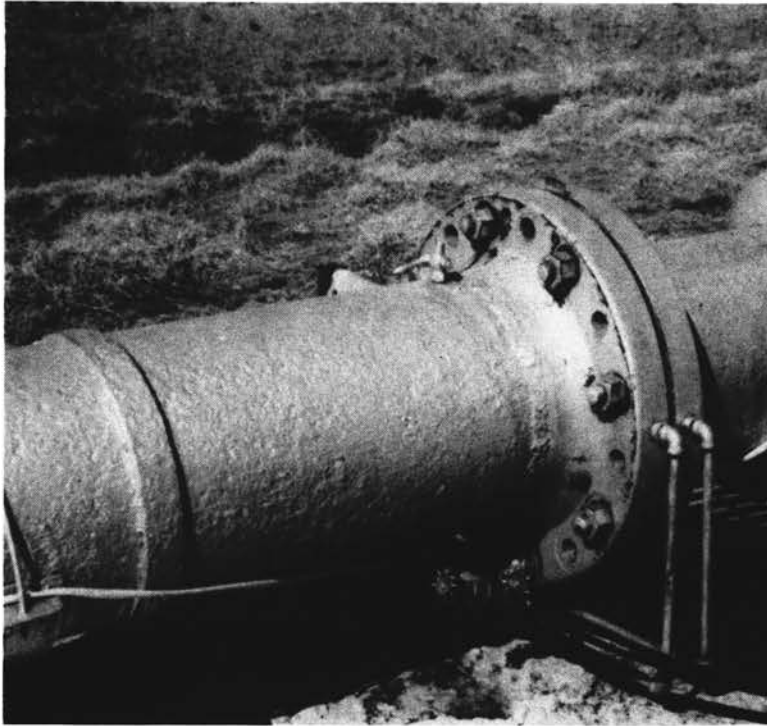


Figure 28. The Orifice Meter Used to Measure the Inflow

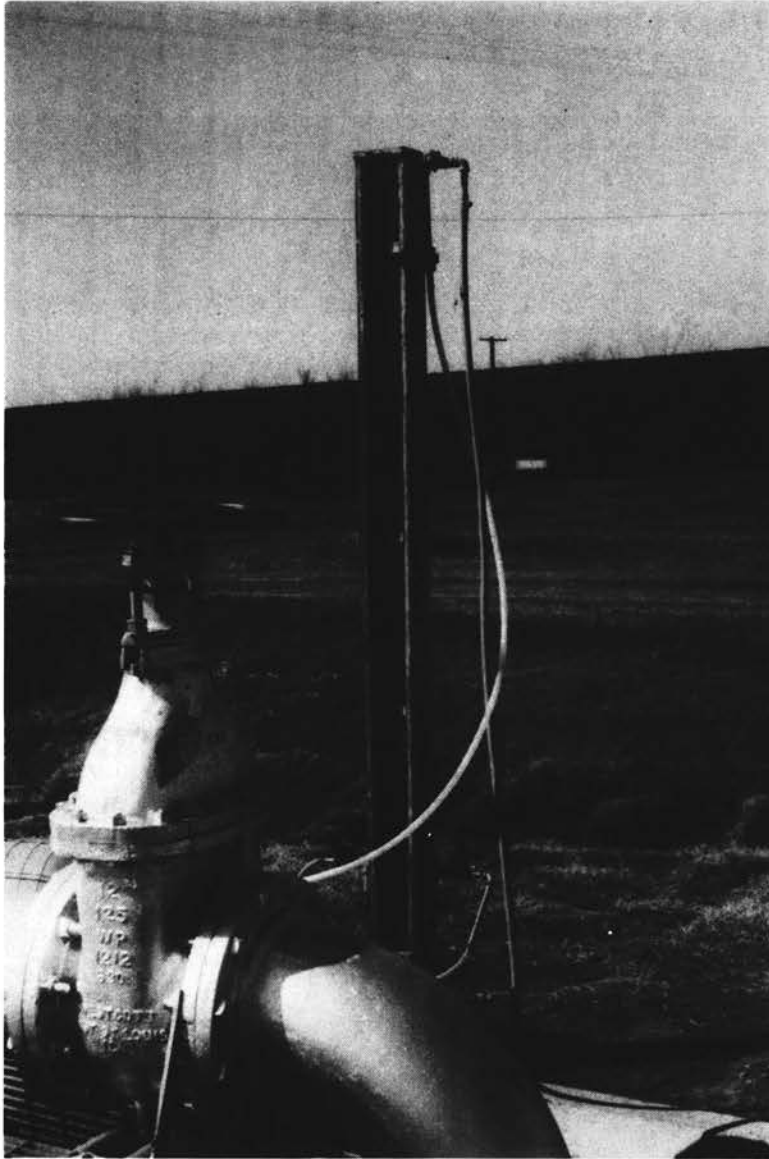


Figure 29. The Discharge Control Valve and
60 in. Manometer

CHAPTER VI

EXPERIMENTAL PROCEDURE

In order to calculate water surface profiles for a decreasing spatially varied flow condition values of channel resistance and nonuniformity coefficient (α) must be known. When siphon tubes are added to the channel, the values for resistance and α would be expected to change. Thus, a series of steady flow tests with different tube sizes, tube submergence, depth of flow, and discharges were conducted in an effort to relate resistance and α to the hydraulic properties of the system.

The hypothesis was that the relationships obtained from the gradually varied flow experiments used in conjunction with the spatially varied flow equation would predict the water surface profile as measured at the gauge wells in the spatially varied flow tests.

Gauge Zero and Channel Bottom

The soil at the Outdoor Hydraulic Laboratory shrinks and swells due to high montmorillonite content. As a result, the channel and gauge wells were subject to elevation changes. Computations for a change in H_L of .001 foot could result from a .05 foot error in the

channel bottom elevation or in a .001 foot error in the gauge zero. Thus, gauge zeros were taken more frequently than the bottom elevations. Plots of the elevation of the gauge zeros and bottom elevations are shown in Appendix C.

In general, two methods were used in determining gauge zero. One method was to reference the water surface at station 0 + 00 to a local bench mark then assume the water surface elevation was the same in the other wells. The gauge zeros were obtained by subtracting the gauge water surface reading from the water surface elevation at each station. The other method of determining gauge zeros was to assume that the gauge zero at 0 + 90 did not change in the time between determination of gauge zeros. With a known gauge zero the water surface elevation could be calculated and the other gauge zeros determined.

The channel bottom elevation was referenced to the water surface elevation in the wells.

Geometric Channel Elements

The geometric elements of the channel were obtained by placing the H-beam perpendicular to the channel and measuring the elevation at .1 foot intervals along the profile of the channel. These readings were taken at each station of the channel.

The geometric elements of a trapezoidal channel can be expressed in terms of depth measured from the bottom of

the channel to the water surface. Regression equations were obtained for area, wetted perimeter, and top width as a function of depth where depth is measured from the lowest elevation at the channel section. The equations were of the type

$$\text{Area} = (a_0 + a_1 y)y$$

$$\text{Wet perimeter} = b_0 + b_1 y$$

$$\text{Top} = c_0 + c_1 y$$

The coefficients for the equations at the beginning (9-20-65) and end (4-19-66) of the test period are shown in Appendix B.

Counter Test

Two revolution counters were available with the Ott Current Meter. One counter was a digital counter (F-4) which recorded the number of revolutions of the current meter. The other was an impulse counter (F-10) which permitted a direct reading in revolutions per second.

Since many hundred velocity measurements were to be taken, the time involved in taking the readings was considered. An analysis of the variation for five time treatments at five different velocities is shown in Table III. The five treatments were as follows:

(F-10) Impulse Counter

	<u>Elapsed Time</u>
T1. The average of the high and low reading	20 seconds
T2. Average of 10 readings	15 seconds

TABLE III
AN ANALYSIS OF THE VARIATION OF THE FIVE
TIME TREATMENTS AT FIVE VELOCITIES

		F-10				F-4					
		Avg. H-L	Avg. 10 Rdg	T3 15	T4 30	T5 60	Total	Mean			
		3.73	3.79	3.89	3.88	3.90	B ₁ 19.19	b ₁ 3.84			
		5.40	5.41	5.33	5.34	5.32	B ₂ 26.80	b ₂ 5.36			
		1.18	1.14	1.10	1.16	1.16	B ₃ 5.74	b ₃ 1.15			
		3.0	3.02	3.08	3.05	3.04	B ₄ 15.19	b ₄ 3.04			
		1.95	1.89	1.90	1.92	1.91	B ₅ 9.57	b ₅ 1.91			
Total	T ₁	15.26	T ₂ 15.25	T ₃ 15.30	T ₄ 15.35	T ₅ 15.33	G 76.49				
Mean	t ₁	3.05	t ₂ 3.05	t ₃ 3.06	t ₄ 3.07	t ₅ 3.07					

AOV Randomized Block

<u>Source</u>	<u>Degrees of Freedom</u>	<u>Sum Squares</u>	<u>Mean Square</u>	<u>F</u>	<u>Tabulated F (.01)</u>
Total	24	54.36			
Treat.	4	0.00	0.00	0.16	4.77
Block	4	54.32	13.58	5430.00	4.77
Error	16	0.04	0.00		

(F-4) Digital Counter

	<u>Elapsed Time</u>
T3. Revolutions	15 seconds
T4. Revolutions	30 seconds
T5. Revolutions	60 seconds

An average of four replications for each velocity was used in the analysis. The analysis showed the variation in the treatments was not significant at the .01 level of probability. As a result of this analysis, the F-4 digital counter was used with a 15 second elapsed time.

Velocity Distribution and Resistance

The purpose for taking velocity measurements was to obtain the nonuniformity coefficients α and β . The procedure for taking velocity data was the same for the channel with and without siphon tubes. The velocity measurements were taken at predetermined intervals. The intervals were partially determined by the size of propeller on the current meter. The vertical intervals used were .2 feet and .3 feet for the 30 mm and 50 mm propeller, respectively. The procedure for taking the velocity measurements was as follows:

1. Place velocity measuring apparatus in position across channel.
2. Place current meter one-half of vertical interval up from the point of the point gauge.

3. Set the desired flow in the channel.
4. Raise or lower check gate to obtain desired depth.
5. Take the water surface elevations after the flow had become steady.
6. Obtain center of water surface by taking reading at water's edge on each side of the channel.
7. Move current meter from water edge in increments equal to the vertical intervals and take readings at each location, also take readings along channel profile.

A typical cross section of velocity measurements is shown in Figure 30. The dots in the figure are locations of the current meter where the velocity measurements were taken.

Resistance

To predict the water surface profile for decreasing spatially varied flow, the energy loss due to channel resistance must be known. The energy loss was determined for steady flow conditions and was used in calculating the water surface profile for the spatially varied flow test.

After the velocity readings were taken , the water surface elevations at the gauge wells were recorded. The energy loss can be obtained by calculating the difference in energy at the ends of channel reach under consideration.

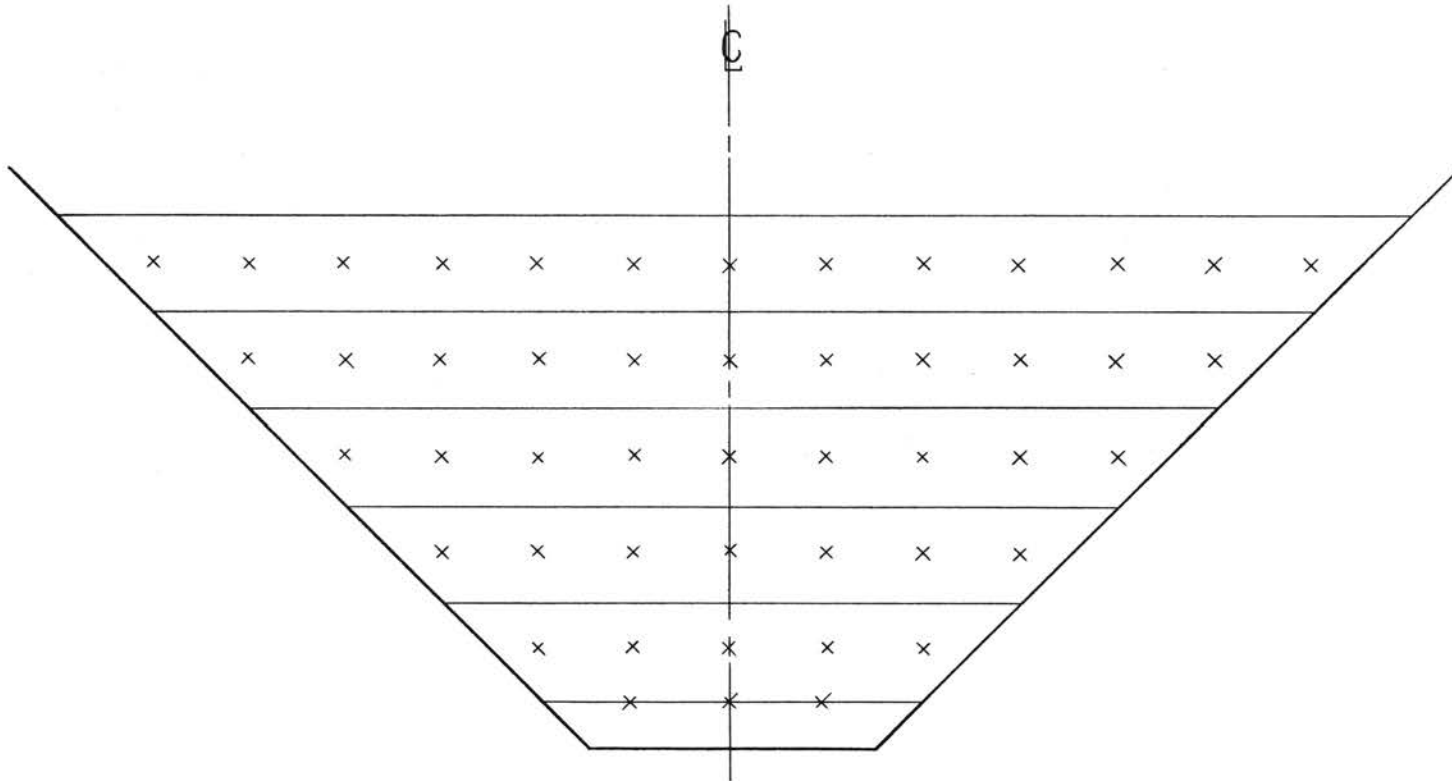


Figure 30. An Arrangement for a Typical Velocity Traverse

The energy loss of the channel reach was used to calculate S_g which was used to calculate the channel resistance where Manning's n was used as a measure of the channel resistance.

The resistance to flow was expected to change with depth, discharge, tube submergence and tube size. The experimental design that was expected to yield a functional relationship of resistance as a function of the variables is shown in Table IV. The number of tests conducted with and without tubes was 60 and 81, respectively.

Siphon Tubes

A relationship of $Q = f(h)$ was needed for the siphon tubes which were to be used as the means of transferring the water from the channel in the spatially varied flow tests. Since the siphon tubes were to be placed on the siphon tube mounts, a desirable relationship seemed to be that of tube discharge as a function of h' . Where h' is measured from the water surface in the distribution channel to the siphon tube mount.

The data taken by Keflemariam (26) were used to determine such a relationship.

Spatially Varied Flow Tests

Spatially varied flow tests were conducted for each tube size. The tube size, entering discharge, and the

TABLE IV
EXPERIMENTAL DESIGN WITH SIPHON TUBES

$S_1 = 0.0 \text{ ft.}$									$S_2 = 0.5 \text{ ft.}$									$S_3 = 1.0 \text{ ft.}$								
D_{11}			D_{12}			D_{13}			D_{21}			D_{22}			D_{23}			D_{31}			D_{32}			D_{33}		
Q_{111}	Q_{112}	Q_{113}	Q_{121}	Q_{122}	Q_{123}	Q_{131}	Q_{132}	Q_{133}	Q_{211}	Q_{212}	Q_{213}	Q_{221}	Q_{222}	Q_{223}	Q_{231}	Q_{232}	Q_{233}	Q_{311}	Q_{312}	Q_{313}	Q_{321}	Q_{322}	Q_{323}	Q_{331}	Q_{332}	Q_{333}
X	X	X	X	X	X	X	X	X	X	X	X	X	X	X	X	X	X	X	X	X	X	X	X	X	X	X
X	X	X	X	X	X	X	X	X	X	X	X	X	X	X	X	X	X	X	X	X	X	X	X	X	X	X
X	X	X	X	X	X	X	X	X	X	X	X	X	X	X	X	X	X	X	X	X	X	X	X	X	X	X

S - Vertical distance of the tube from the channel bottom D - Nominal diameter of the tube

(a) $Q_{nm1} = 1.0 \text{ cfs}$

(b) $Q_{nm2} = 3.0 \text{ cfs}$

(c) $Q_{nm3} = 4.5 \text{ cfs}$

(a) $D_{n1} = 1.0 \text{ in.}$

(b) $D_{n2} = 1.5 \text{ in.}$

(c) $D_{n3} = 2.0 \text{ in.}$

approximate depth in the channel for the tests are shown in Table V. The siphon tube mounts were set to within $\pm .003$ foot of an elevation 923.897 feet measured from mean sea level. The siphon tubes were spaced 40 inches apart, and secured to the mounts and were then primed with the apparatus shown in Figure 31. The wind panels were placed over the channel and when the flow had stabilized, the water surface elevations were recorded at the gauge wells.

For high inflow, velocity distributions were taken at stations 0 + 90 and 2 + 10.

TABLE V
 SPATIALLY VARIED FLOW TESTS

Tube location 12 inches from bottom of channel.

Tube Size (in.)	Inflow (cfs)	Depth (ft.)
3.00	3.671	1.768
3.00	3.405	1.631
3.00	3.130	1.557
2.00	3.733	1.897
2.00	3.318	1.763
2.00	2.925	1.624
2.00	2.552	1.536
1.50	4.225	1.890
1.50	3.612	1.741
1.50	3.240	1.598
1.50	2.700	1.463
1.25	2.785	1.888
1.25	2.341	1.717
1.25	1.858	1.555
1.25	1.408	1.444
1.00	1.769	1.897
1.00	1.558	1.763
1.00	1.303	1.605
1.00	.985	1.475
.75	.882	1.898
.75	.763	1.744
.75	.703	1.598

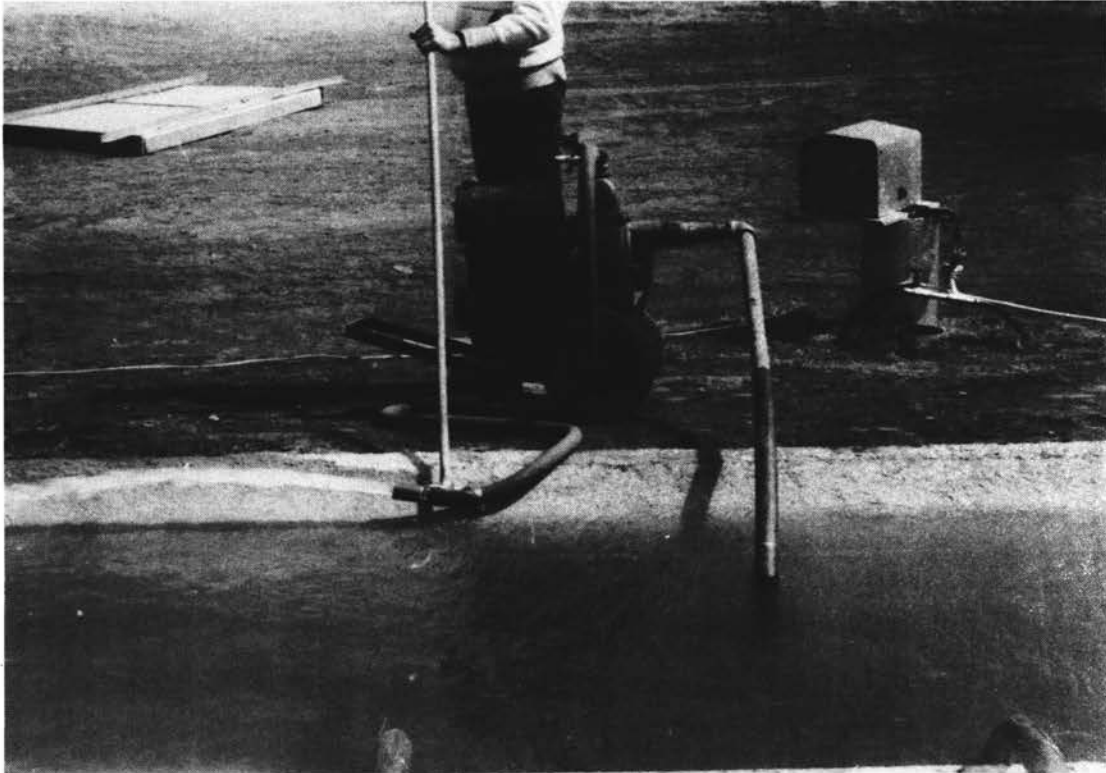


Figure 31. The Pump and Flexible Hose Used to Prime the Siphon Tube in the Spatially Varied Flow Tests

CHAPTER VII

ANALYSIS AND DISCUSSION OF DATA

The purpose of the steady flow tests with the siphon tubes secured in the channel was to obtain resistance and energy coefficients for the spatially varied flow tests. A relationship for siphon tube discharge as a function of the tube diameter and head was necessary also. Therefore, the data from the steady flow tests and the siphon tube experiment will be analyzed before the spatially varied flow tests. The steady flow test without siphon tubes will be analyzed in the section with the steady flow tests with siphon tubes.

The functional relationships of the hydraulic properties obtained in the steady flow test will be used to compute theoretical water surface profiles. The predicted profiles will be compared to the measured water surface profiles. The theoretical equation will be modified if necessary.

Siphon Tubes

A regression analysis was applied to the data taken by Keflemariam (26) for double-bend plastic siphon tubes. The generalized expression that best fit the data was

$$Q = 0.0245 D^{2.111} h_o^{0.6121} \quad (21)$$

where

D = the nominal tube diameter

h_o = the head in feet on the siphon tube

The head was measured from the water surface in the distribution channel to the siphon tube mount.

The generalized expression was obtained from Figures 32 and 33. The relationships of Q versus h_o for different tube sizes are shown in Figure 32. The slope of the curve for the 3-inch tube is distinguishably different from the slopes of the .75- to 2.0-inch tubes. The difference in slope is probably due to the different lengths of the tubes and the measurement of the h_o instead of a head measurement from the hydraulic grade line. The 3-inch tubes were 6 feet and the .75- to 2.0-inch tubes were 5 feet in length.

The hypothesis was made that the slopes of the tube curves were the same as the average slope of the curves of 0.6557. A Student "t" was calculated for each tube slope minus the average slope. The calculated values of "t" are shown in Table VI. The "t" values for the .75-, 1.0-, 1.25-, 1.50- and 3.0-inch tubes were larger than the "t" values at .05 level of probability. Thus, the hypothesis was rejected that the slope of the curves were the same.

The $Q = Ch_o^n$ relationship shown in Table VI was used in the spatially varied flow tests because a reliable

TABLE VI

VALUES OF THE Q VERSUS h_o RELATIONSHIPS FOR DIFFERENT
SIPHON TUBE DIAMETERS

Tube Diameter (in.)	Constant C	Exponent n	Correlation Coefficient r	Standard Deviation	s_n	Calculated "t"
0.75	0.01292	0.60697	0.999	0.000073	0.0026	18.58
1.0	0.02511	0.58794	0.999	0.000176	0.0030	22.80
1.25	0.03986	0.60844	0.999	0.000181	0.0025	19.11
1.50	0.05806	0.62449	0.986	0.002152	0.0138	2.26
2.0	0.10639	0.65513	0.991	0.001924	0.0119	2.05
3.0	0.24450	0.85109	0.996	0.003644	0.0101	19.27

$$\text{Calculated "t"} = \frac{n - n_{avg}}{s_n}$$

$$\text{"t"}_{(.05)} @ 58 \text{ d.f.} = 2.004$$

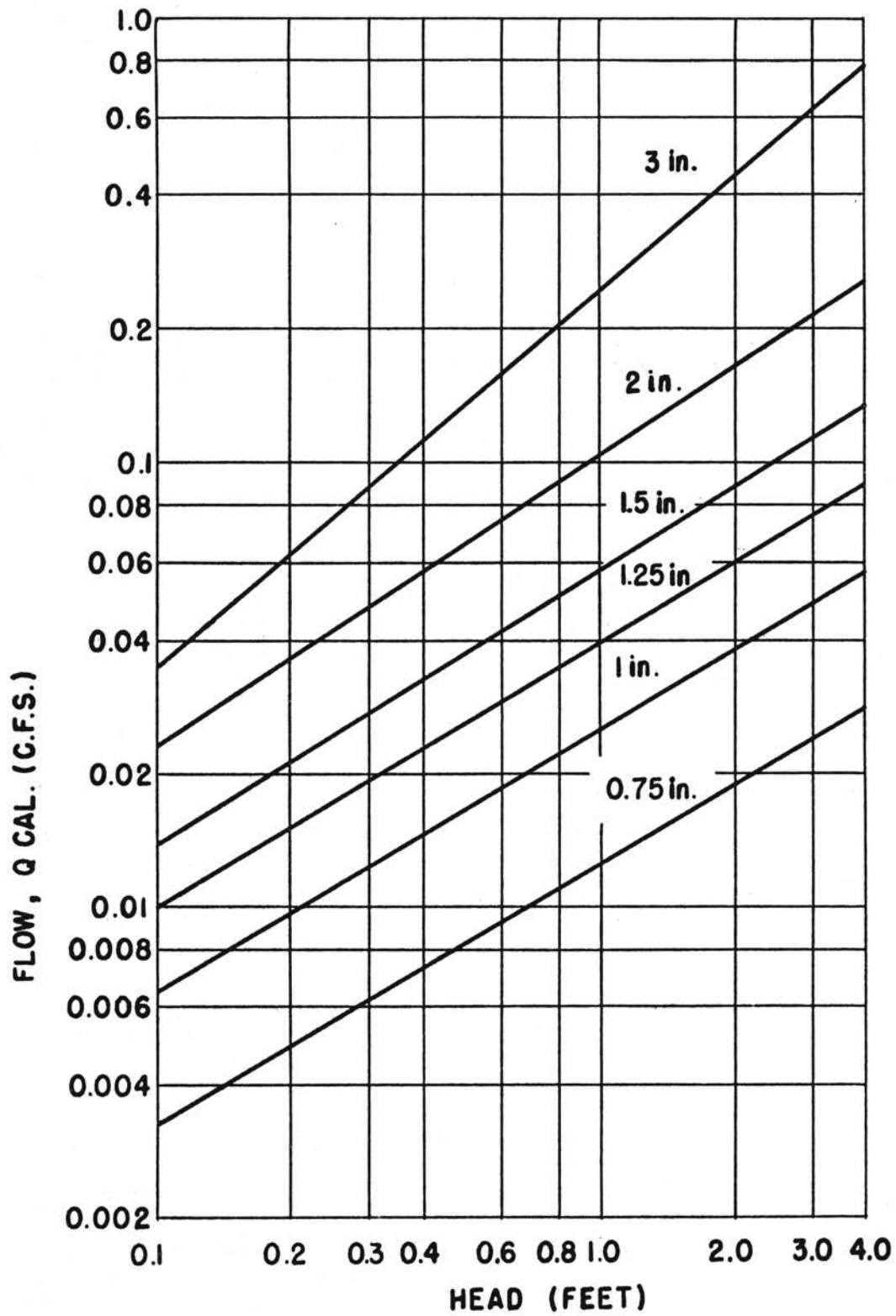


Figure 32. Relationship of Discharge Versus Head for Plastic Siphon Tubes

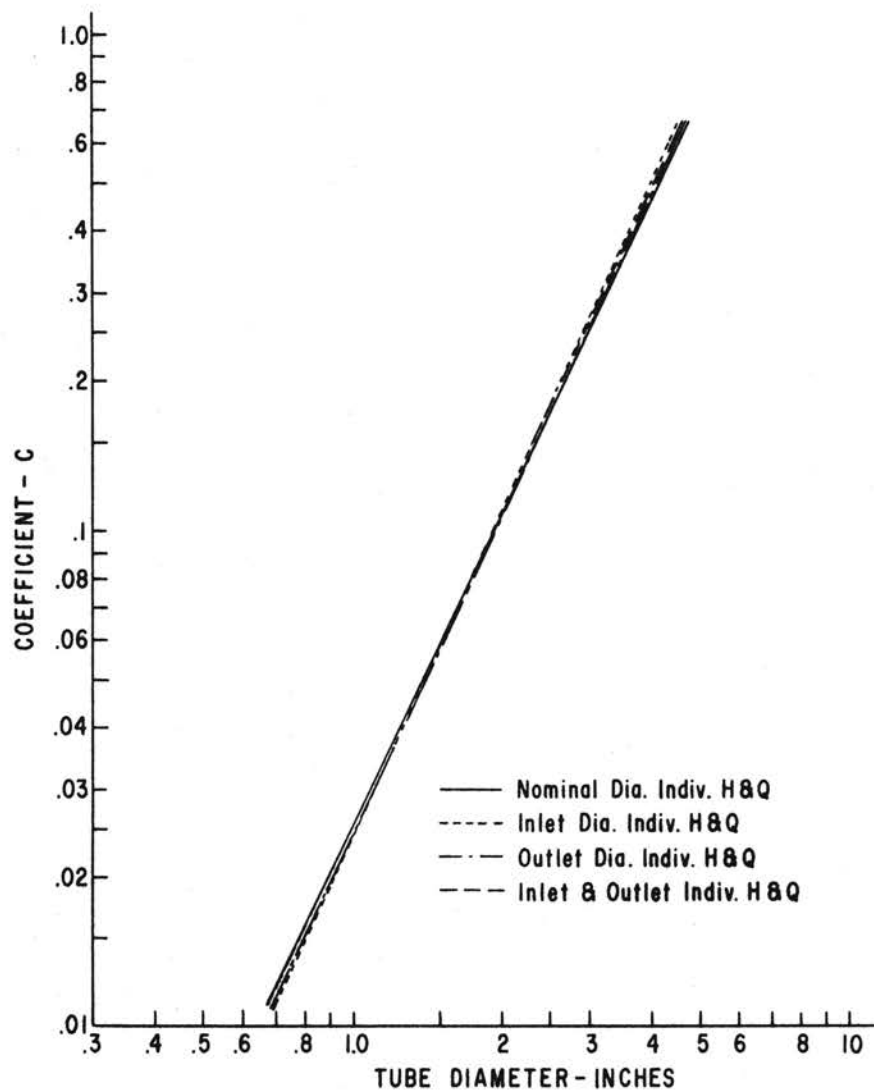


Figure 33. Relationship of C Versus Tube Diameter for Plastic Siphon Tubes

estimate for tube discharge was needed in the prediction of the water surface profiles and the majority of the tube slopes were different. The tube sizes (1.25- and 3.0-inch) indicating minimum and maximum derivation within tube size are shown in Appendix D.

Non-uniformity Coefficients

The non-uniformity coefficients α and β were obtained by numerically integrating the mass area curves v^3 and v^2 versus area. This is a modification of the O'Brien and Johnson method described in Chapter II.

The computer facilities at Oklahoma State University were utilized in calculating the non-uniformity coefficients. A program was written that transformed the raw data into velocities and computed the non-uniformity coefficients.

The data in revolutions per second from the current meter was transformed as follows:

1. The revolutions per second at the point locations across the channel were changed into equivalent velocities in feet per second.
2. The velocities were arranged in descending order with associated incremental areas.
3. The discharge ratio, α , and β were computed by:

$$\begin{aligned}
 \text{(a) Discharge Ratio} &= \left[\sum_{i=1}^n \left(\frac{v_i + v_{i+1}}{2} \right) \Delta A_i \right] / Q \\
 \text{(b) } \beta &= \left[\sum_{i=1}^n \left(\frac{v_i^2 + v_{i+1}^2}{2} \right) \Delta A_i \right] \frac{A_T}{Q} \\
 \text{(c) } \alpha &= \left[\sum_{i=1}^n \left(\frac{v_i^3 + v_{i+1}^3}{2} \right) \Delta A_i \right] \frac{A_T^2}{Q^3}
 \end{aligned}$$

where Q is the quantity of fluid flowing past the section. The discharge (Q) was considered to be measured without error. The total area of the cross section is A_T . The quantity $\frac{v_i + v_{i+1}}{2}$ is the average velocity through the incremental area ΔA_i .

4. The computation was continued until the discharge ratio was 0.005 cfs or less. When the error was outside the limit of 0.005 cfs, the magnitude of incremental velocities was adjusted. As a constant time period was used for the velocity measurements, the error due to instrument register was greater at the low velocities. Hence, the lower velocities were adjusted relatively more than the higher velocities.

The computed α and β values for the steady flow tests with and without siphon tubes are shown in Tables VII and VIII. The non-uniformity coefficients taken during the steady varied flow tests are shown in Table IX.

TABLE VII

NON-UNIFORMITY COEFFICIENTS FOR THE EXPERIMENTAL
CHANNEL WITHOUT SIPHON TUBES
(STEADY GRADUALLY VARIED FLOW)

Station	Average Depth (ft.)	Q (cfs)	Discharge Ratio	Beta	Alpha
2	0.795	1.005	1.000	1.022	1.060
2	1.307	0.993	0.996	1.047	1.144
2	0.680	1.021	1.001	1.044	1.086
2	0.889	1.985	1.002	1.026	1.064
2	1.143	1.971	1.002	1.027	1.064
2	1.514	1.942	0.998	1.028	1.081
2	1.606	2.963	1.000	1.021	1.058
2	1.338	2.998	1.003	1.028	1.068
2	1.093	2.988	1.001	1.028	1.070
2	1.681	4.039	1.000	1.018	1.047
2	1.398	4.017	1.000	1.020	1.053
2	1.220	3.991	1.002	1.029	1.072
2	1.478	4.975	1.001	1.017	1.041
2	1.305	5.006	1.001	1.022	1.055
2	1.739	5.046	1.002	1.020	1.049
4	1.828	4.943	1.002	1.022	1.057
4	1.507	4.974	1.004	1.030	1.074
4	1.291	4.895	1.005	1.034	1.081
10	1.417	4.895	1.002	1.025	1.061
10	1.066	4.862	1.004	1.027	1.062
10	1.802	4.911	0.998	1.012	1.038
9	1.127	3.995	1.004	1.031	1.070
9	1.816	3.994	0.999	1.016	1.047
9	1.335	4.003	1.001	1.022	1.057
8	1.730	3.008	1.000	1.030	1.083
8	1.361	2.964	0.999	1.021	1.058
8	0.979	2.998	1.002	1.035	1.089
2	1.605	1.999	0.997	1.041	1.120
2	1.199	2.003	0.998	1.027	1.078
2	0.931	2.001	1.003	1.034	1.084
7	0.969	0.998	1.003	1.052	1.135
7	0.834	1.006	0.997	1.036	1.102
7	0.616	0.998	1.006	1.046	1.119

TABLE VII (Continued)

Station	Average Depth (ft.)	Q (cfs)	Discharge Ratio	Beta	Alpha
4	1.524	1.999	0.997	1.036	1.103
4	1.161	2.001	0.999	1.071	1.110
4	0.929	1.999	1.004	1.040	1.096
4	1.442	2.992	0.998	1.022	1.065
4	1.107	2.987	1.005	1.041	1.097
4	1.804	2.984	1.004	1.045	1.110
4	1.693	4.010	1.002	1.024	1.060
4	1.373	4.004	1.004	1.035	1.084
4	1.200	4.006	1.004	1.036	1.088
6	1.672	2.997	1.004	1.033	1.082
6	1.302	2.977	1.000	1.021	1.058
6	1.013	2.982	1.001	1.030	1.078
6	1.575	2.009	1.000	1.036	1.100
6	1.207	1.998	0.999	1.019	1.053
6	0.906	2.011	1.003	1.035	1.083
6	1.086	1.005	0.998	1.060	1.132
6	0.858	1.007	0.996	1.022	1.065
6	0.660	1.000	1.004	1.037	1.082
8	1.362	2.008	1.003	1.039	1.100
8	0.997	2.008	1.005	1.039	1.093
8	0.820	2.007	1.002	1.038	1.094
8	0.613	1.003	0.999	1.031	1.078
8	0.861	1.017	1.004	1.043	1.104
8	1.052	1.005	0.998	1.060	1.160
10	0.548	1.004	1.005	1.042	1.091
10	0.813	1.006	0.998	1.028	1.077
10	1.006	1.005	0.996	1.031	1.093

TABLE VIII

NON-UNIFORMITY COEFFICIENTS AT STATION 0 + 60 FOR
THE EXPERIMENTAL CHANNEL WITH SIPHON TUBES
(STEADY GRADUALLY VARIED FLOW)

Tube Diameter 2 Inches

Average Depth (ft.)	Q (cfs)	Tube Location From Bottom (ft.)	Discharge Ratio	Beta	Alpha	Submergence
1.410	1.001	1.0	1.000	1.077	1.156	0.410
0.982	0.998	1.0	1.000	1.037	1.088	0.000
0.690	1.002	1.0	1.004	1.055	1.117	0.000
1.707	2.981	1.0	1.002	1.067	1.158	0.707
1.319	3.019	1.0	1.004	1.043	1.099	0.319
1.061	2.998	1.0	1.005	1.042	1.084	0.061
1.811	4.499	1.0	1.003	1.058	1.144	0.811
1.359	4.524	1.0	0.998	1.031	1.082	0.359
1.233	4.521	1.0	1.001	1.029	1.069	0.233
1.812	2.998	0.5	1.002	1.077	1.197	1.312
1.379	3.123	0.5	0.996	1.052	1.138	0.879
1.126	3.004	0.5	1.004	1.082	1.190	0.626
1.724	1.005	0.5	0.999	1.096	1.256	1.224
1.113	1.002	0.5	0.998	1.097	1.218	0.613
0.708	1.002	0.5	1.002	1.054	1.121	0.208
1.823	4.503	0.5	1.001	1.066	1.171	1.323
1.493	4.529	0.5	1.002	1.063	1.149	0.993
1.316	4.537	0.5	0.999	1.057	1.144	0.816
1.767	4.530	0.0	0.999	1.076	1.202	1.767
1.555	4.526	0.0	1.001	1.086	1.222	1.555
1.400	4.559	0.0	0.999	1.078	1.206	1.400
1.729	1.003	0.0	1.002	1.119	1.308	1.729
1.227	1.004	0.0	1.005	1.141	1.331	1.227
0.783	0.996	0.0	1.002	1.148	1.364	0.783
1.820	2.996	0.0	0.998	1.111	1.273	1.820
1.403	2.986	0.0	0.995	1.165	1.339	1.403
1.209	2.996	0.0	1.001	1.132	1.323	1.209

Tube Diameter 1.5 Inches

1.514	1.007	1.0	1.002	1.097	1.180	0.514
1.115	1.007	1.0	0.996	1.030	1.085	0.115
0.695	1.004	1.0	1.003	1.056	1.125	0.000
1.707	3.027	1.0	1.000	1.060	1.141	0.707
1.354	3.010	1.0	1.004	1.047	1.109	0.354
1.067	3.011	1.0	1.004	1.042	1.094	0.067

TABLE VIII (Continued)

Average Depth (ft.)	Q (cfs)	Tube Location From Bottom (ft.)	Discharge Ratio	Beta	Alpha	Submergence
1.736	4.633	1.0	1.004	1.055	1.127	0.736
1.435	4.659	1.0	1.004	1.043	1.099	0.435
1.266	4.639	1.0	1.001	1.026	1.062	0.266
1.748	4.738	0.5	0.995	1.036	1.107	1.248
1.569	4.776	0.5	1.000	1.050	1.131	1.069
1.339	4.795	0.5	1.005	1.063	1.153	0.839
1.714	2.983	0.5	1.000	1.167	1.279	1.214
1.367	2.975	0.5	1.004	1.078	1.179	0.867
1.308	1.002	0.5	1.004	1.102	1.234	0.808
0.990	0.996	0.5	1.004	1.066	1.153	0.490
0.702	1.003	0.5	1.004	1.063	1.141	0.202
1.768	4.784	0.0	1.000	1.054	1.144	1.768
1.507	4.750	0.0	0.999	1.071	1.191	1.587
0.839	1.002	0.0	1.004	1.163	1.375	0.839
1.129	0.999	0.0	1.003	1.161	1.406	1.129
0.745	0.996	0.0	1.003	1.154	1.344	0.745
1.721	2.983	0.0	1.001	1.157	1.326	1.721
1.323	2.991	0.0	1.005	1.103	1.247	1.323
1.173	2.972	0.0	1.005	1.101	1.253	1.173
Tube Diameter 1 Inch						
1.721	4.492	1.0	1.000	1.032	1.081	0.721
1.411	4.514	1.0	1.003	1.034	1.079	0.411
1.233	4.526	1.0	0.996	1.020	1.057	0.233
1.711	3.002	1.0	1.000	1.042	1.108	0.711
1.313	2.995	1.0	1.003	1.037	1.086	0.313
1.065	3.010	1.0	1.002	1.035	1.079	0.065
1.509	1.006	1.0	1.003	1.059	1.141	0.509
1.108	1.000	1.0	1.000	1.043	1.110	0.108
0.718	1.000	1.0	1.005	1.059	1.129	0.000
1.518	1.000	0.5	0.997	1.083	1.201	1.018
1.080	1.004	0.5	0.998	1.041	1.105	0.580
0.696	1.003	0.5	1.002	1.055	1.121	0.196
1.327	2.996	0.5	1.005	1.057	1.135	0.827
1.620	2.994	0.5	1.000	1.051	1.135	1.120
1.097	2.998	0.5	1.005	1.058	1.133	0.597
1.817	4.502	0.5	0.999	1.041	1.114	1.317
1.462	4.504	0.5	1.000	1.043	1.110	0.962
1.272	4.504	0.5	0.996	1.034	1.093	0.772

TABLE VIII (Continued)

Average Depth (ft.)	Q (cfs)	Tube Location From Bottom (ft.)	Discharge Ratio	Beta	Alpha	Submergence
1.519	1.005	0.0	0.998	1.091	1.220	1.519
1.122	1.003	0.0	1.001	1.071	1.185	1.122
0.734	1.012	0.0	1.001	1.099	1.246	0.734
1.689	2.997	0.0	0.999	1.053	1.146	1.689
1.307	3.029	0.0	1.005	1.077	1.191	1.307
1.134	3.012	0.0	1.003	1.076	1.188	1.134
1.744	4.523	0.0	0.997	1.034	1.097	1.744
1.448	4.494	0.0	1.000	1.047	1.123	1.448
1.312	4.521	0.0	0.999	1.051	1.134	1.312

TABLE IX
 NON-UNIFORMITY COEFFICIENTS
 SPATIALLY VARIED FLOW TESTS
 TUBE LOCATION 1.0 FOOT
 FROM CHANNEL BOTTOM

Station	Depth	Entering Q	Tube Size	Discharge Ratio	Beta	Alpha	S_u
0 + 90	1.948	3.788	2.0	0.999	1.083	1.179	0.948
2 + 10	1.885	3.788	2.0	0.999	1.091	1.232	0.885
2 + 10	1.877	4.226	1.5	1.004	1.069	1.174	0.877
0 + 90	1.768	2.241	1.25	0.995	1.096	1.167	0.768
2 + 10	1.710	2.241	1.25	0.995	1.060	1.180	0.710
0 + 90	1.526	0.985	1.0	1.002	1.083	1.215	0.526

Alpha Without Tubes

According to Kindsvater (30), the energy coefficient α is a function of Reynolds number N_R and the boundary geometry. Supposedly the boundary of the channel was the same at each station. Thus, a functional relationship between α and N_R was obtained for each station. The relationship found to best fit the data was of the type

$$\alpha = \frac{N_R}{a + b N_R}$$

The coefficients (a and b) for the stations down the channel are shown in Table X. A hypothesis was made that the slopes of the equations were not different from the average slope. This information is given in Table X, also. At the 0.01 level of probability the slope of the equation for station 0 + 90 was significantly different from the average; that is, the variation between the slopes was not due to chance alone.

Station 0 + 90 is located immediately behind a small, but noticeable constriction in the channel. The side of the channel was accidentally pushed inward during the construction of the experimental setup. The data of station 0 + 90 were eliminated from the analysis. The energy coefficients of the remaining stations were lumped together, and a relationship of α and N_R is shown in Figure 34. The relationship can be expressed as

TABLE X

COEFFICIENTS FOR α VERSUS N_R FOR THE
EXPERIMENTAL CHANNEL WITHOUT TUBES

Station	Intercept	Degrees Of Freedom	Deviation Of Slope s_{b_1}	Slope b_1	Slope-0.9466	t_c	$t(0.01)$
2	-1492.0	16	0.00975	0.9737	0.0271	2.78	2.921
4	- 176.0	10	0.00596	0.9369	0.0197	3.30	3.169
6 & 7	- 311.0	10	0.00648	0.9339	0.0127	1.96	3.169
8 & 9	- 225.0	8	0.00828	0.9344	0.0122	1.47	3.355
10	- 106.0	4	0.00463	0.9433	0.0033	0.71	4.604

$$t_c = \frac{b_1 - b_{avg}}{s_{b_1}}$$

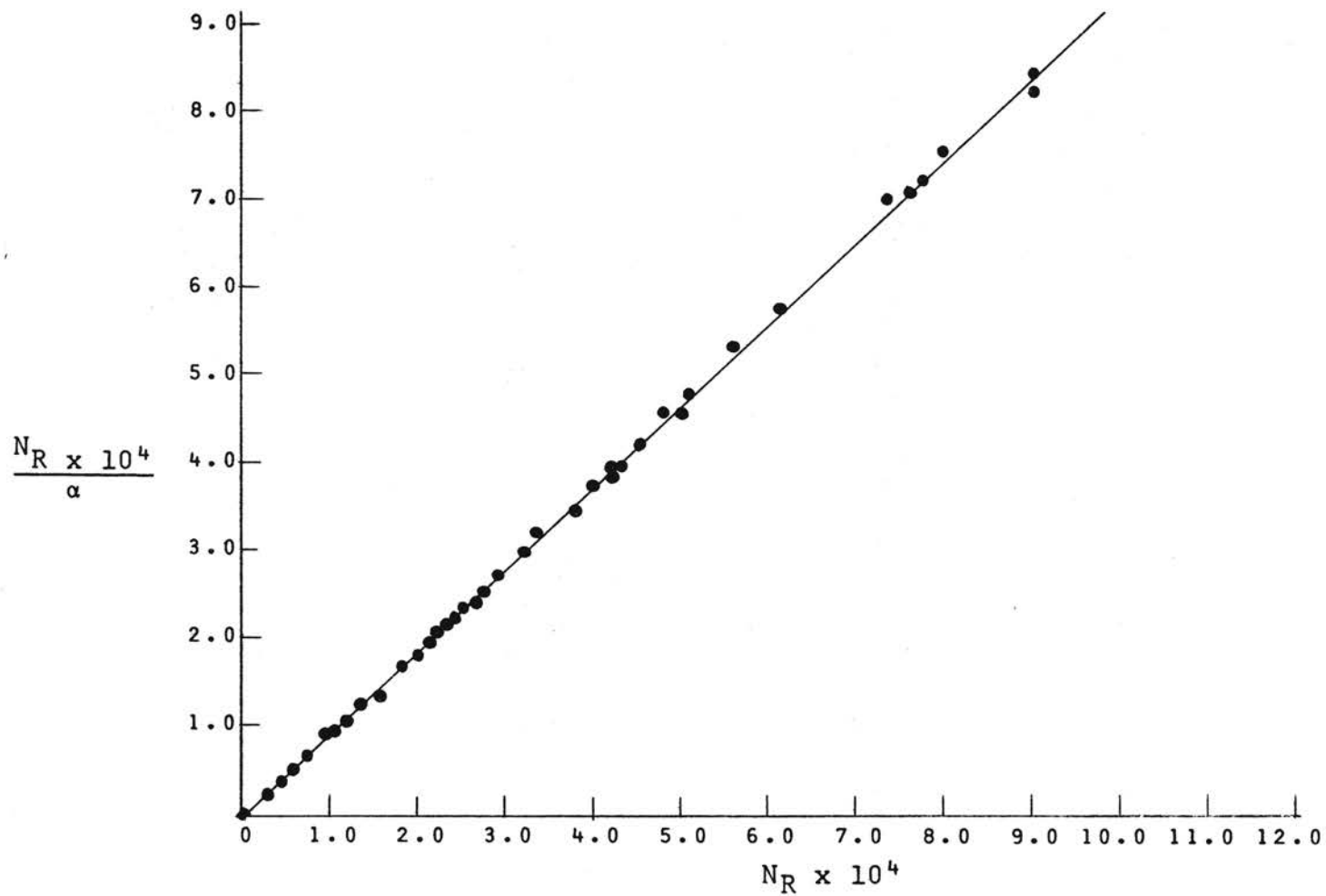


Figure 34. N_R/α Versus N_R for Channel Without Tubes

$$\alpha = \frac{N_R}{-634 + 0.95 N_R}$$

This expression is believed to be adequate for describing α when the limits on the Reynolds number are $3000 \leq N_R \leq 10^7$. The lower limit of $N_R = 3000$ is the approximate beginning of laminar flow region as shown in Figure 8. In the laminar flow region, the velocity distribution becomes more parabolic. In a circular pipe α is equal to 2.0 in the laminar flow region (Rouse, 46). An alpha value of 2.00 was used to obtain the lower limit of N_R . As the flow becomes extremely turbulent or as $N_R \rightarrow \infty$, $\alpha \rightarrow 1.050$. Generally, in turbulent flow the magnitude of the average velocity approaches that of the maximum velocity and α is expected to decrease.

Alpha With Siphon Tubes

Linear Model

Efforts to find a functional relationship of α as a function of depth of flow (y), discharge (Q), tube location from bottom of channel (TL), and tube diameter (D) resulted in a linear model of

$$\alpha = 1.1782 + 0.04270Y - 0.03455Q - 0.11983TL + 0.05947D$$

A plot of α_{obs} versus α_{cal} for the above expression is shown in Figure 35. As y increased, α increased which was expected because the quantity $\frac{v_{max}}{V}$ in the expression

$$\alpha = \int_0^A \left(\frac{v}{V}\right)^3 dA$$

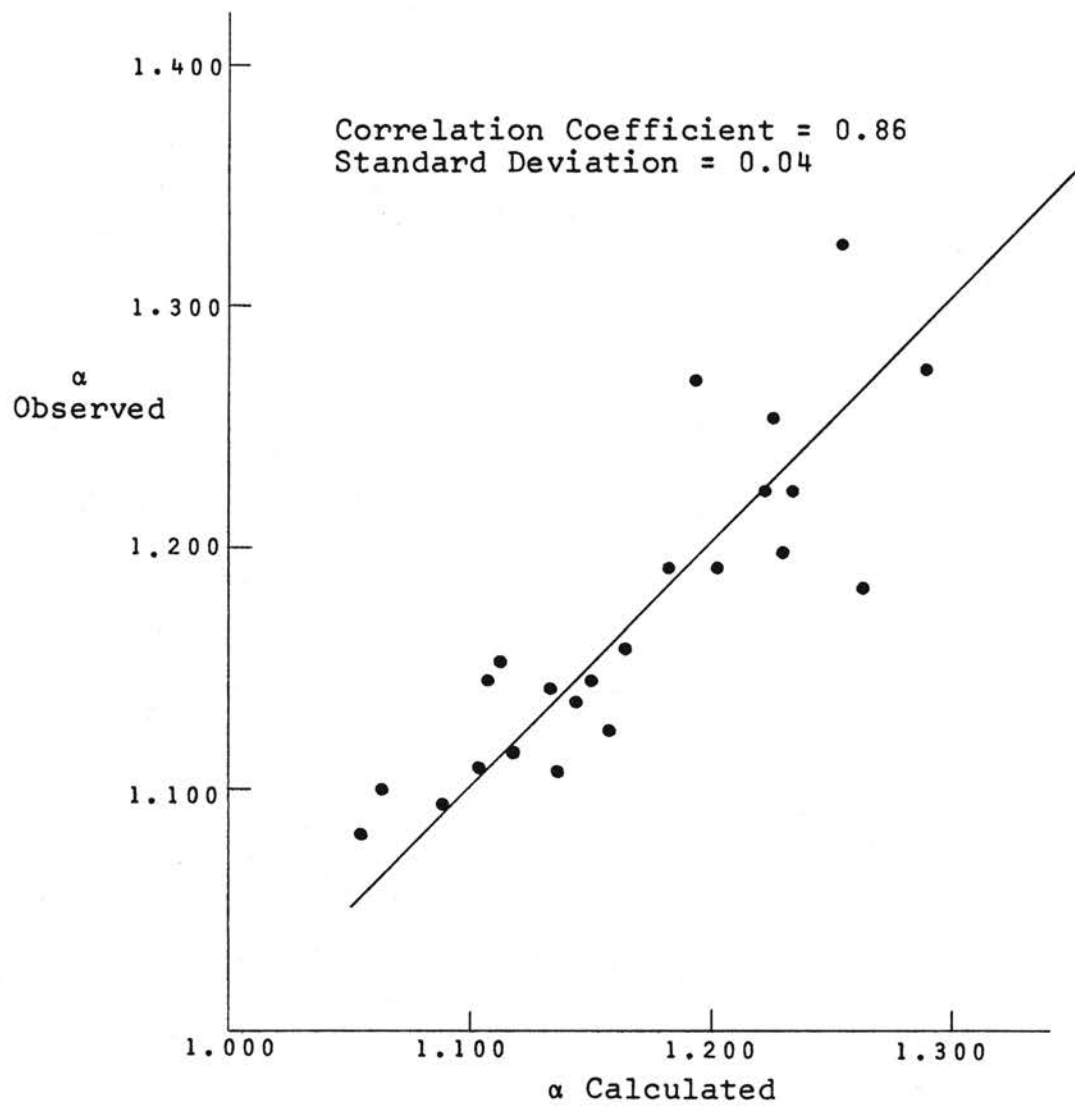


Figure 35. A Plot of the Alpha Observed Versus Alpha Calculated from the Linear Model

increased. The tubes decreased the effective cross-sectional area of the channel. The velocity and area measurements were taken 1.50 feet behind the tubes; thus, the measurements of V were lower than the V at the tube locations. The insertion of the tubes would be expected to create a zone of relative stagnation and, in effect, increase the v_{\max} in the channel for the same depth and Q . This increase in v_{\max} would result in a higher v_{\max}/V ratio which would increase α . The same reasoning follows for the tube location (TL) from the channel bottom for a given Q and y . The submergence increased as TL decreased, and the cross-sectional area at the tube was less than the area where α was measured.

Alpha would be expected to vary with Q and D because it is a function of the dimensionless parameter N_R .

Dimensionless Model

Alpha can be written as a function of the pertinent quantities ($y, Q, S_u, D, \mu, \rho, g$) where S_u is the tube submergence. Arranging the dimensions of the quantities in a matrix form results in the following:

	g	μ	S_u	D	α	y	Q	ρ
M	0	1	0	0	0	0	0	1
L	1	-1	1	1	0	1	3	-3
T	-2	-1	0	0	0	0	1	0

The rank of the matrix is equal to 3. According to the Buckingham Pi Theorem, there are (8) the number of pertinent

quantities - (3) the rank of the matrix = (5) the dimensionless independent parameters. The five parameters are:

$$\Pi_0 = \alpha$$

$$\Pi_1 = Q^2/gy^5 \text{ Discharge coefficient}$$

$$\Pi_2 = S_u/y \text{ Submergence parameter where } S_u = (y-TL)$$

$$\Pi_3 = D/y \text{ Size parameter}$$

$$\Pi_4 = Vy/\nu \text{ Reynolds number}$$

The dimensionless parameters are supposedly independent; thus, an interaction term would result in a different independent parameter. The number of dimensionless parameters must remain constant according to the Buckingham Pi Theorem. If more terms were added, the function would be redundant.

The dimensionless model found to best fit the data was

$$\alpha = 1.07468 + 0.17469\Pi_2 + 0.61324\Pi_3 - 1.619 \times 10^{-6} \Pi_4 \quad (22)$$

Figure 36 shows α_{obs} versus α_{cal} from Equation 22. The expression is unrealistic in the sense that the effect of tube diameter contributes to the values of α when there is no submergence, i.e., $\Pi_2 = 0$. Attempts were made to find a more realistic model for α that surpassed Equation 22; however, the attempts were unsuccessful.

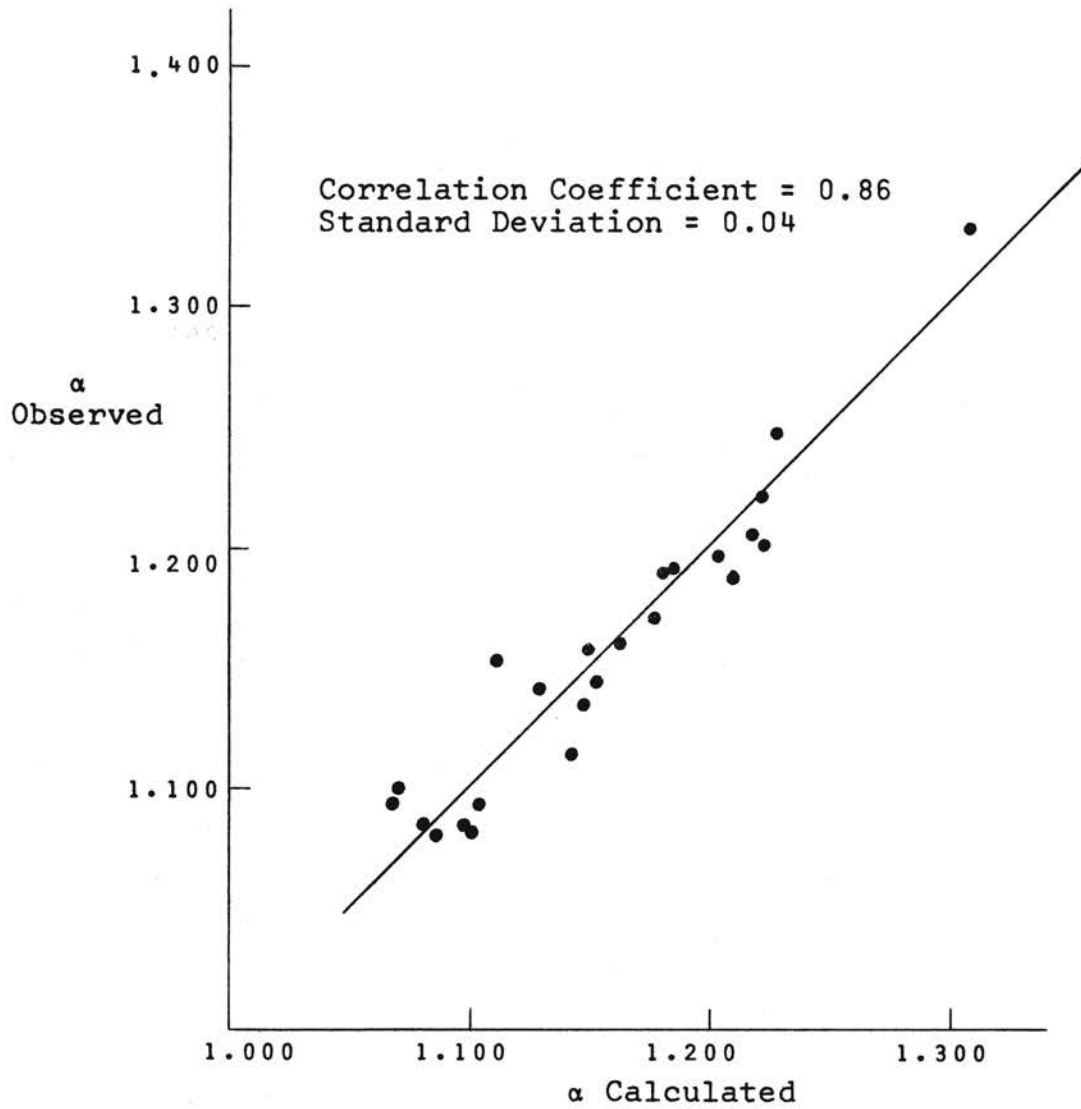


Figure 36. Alpha Observed Versus Alpha Calculated From the Dimensionless Model

Multivariant Model

A multivariant model of $\alpha = f(Y, Q, TL, D)$ with interactions gave the smallest standard deviation (0.02) and the highest correlation coefficient (0.94). The terms and their coefficients are as follows:

<u>Terms</u>	<u>Coefficient</u>
Constant	0.9150
y	-0.0939
y ²	-0.0506
Q	0.0151
Q ²	-0.0036
D	-0.1697
D ²	0.0757
TL	0.4768
TL ²	-0.1209
TLD	-0.1138
TLQ	0.0338
TLy	0.0662
QD	0.0126
YD	0.0032
YQ	-0.0156
DTLQ	-0.3790
yTLQ	-0.0184
YDQ	-0.0106
DTLyQ	-0.2950

The equation gave reliable estimates of α when the range of data was $1 < Q < 4.5$, $0.5 < y < 2.0$, $0 < TL < 1.0$, and

1.0 < D < 2.0. Extrapolation with a multivariant function outside the range of the data can yield unrealistic values. Thus, the linear model was used for computation outside the range of the data.

Resistance

Resistance values (n) were found for the channel with and without tubes. These values were needed in the computation of the water surface profiles in the spatially varied flow tests. The hypothesis being that the resistance values for gradually varied flow conditions were applicable at the same depth (y) and (Q) in the spatially varied flow tests.

The values of n were calculated from the Manning formula

$$n = \frac{1.486}{V} R^{2/3} S_s^{1/2}$$

where S_s was computed from the energy equation

$$S_s = \left[\frac{1}{L} \left(\left(\frac{\alpha_1 V_1^2}{2g} - \frac{\alpha_2 V_2^2}{2g} \right) + (z_1 - z_2) \right) \right]$$

The alpha values were considered to be unity in the calculation of n . Alpha values from Equation 22 were used in calculating n_α . n_α is the value of n obtained when values of α are calculated and used in the expression for S_s .

The n values were calculated for the channel reach 0 + 00 to 0 + 180. This reach was selected because of the relative stability of the gauge zeros and channel bottom as shown in Appendix C.

The precision at which the water surface could be measured was believed to be ± 0.001 . Thus, a change in the water surface of $\Delta y = 0.04$ between the ends of the reach must be measured before the n calculated would be expected to be within 5 per cent of the true value. The n values computed from water surface differences less than $\Delta y = 0.04$ were not considered. In general, the flow of $Q \leq 1$ for $y > 1$ and $Q \leq 3$ for $y > 1.5$ were not considered in the analysis. The values of n , f and n_α , f_α with calculated α for the channel with and without tubes are shown in Tables XI and XII, where the Darcy-Weisbach f is the friction factor of the channel.

Resistance Without Tubes

A relationship of Manning's $n/R^{1/6}$ versus N_R for the channel without tubes is shown in Figure 37. The value of n varied from 0.0104 at $N_R = 27555$ to a value of 0.0117 $N_R = 59000$. The small hump in the curve shown in Figure 38 is similar in shape to the curves found by other hydraulicians. The equation that best represents this curve over the range of data was found to be

$$n = R^{1/6} \frac{N_R}{218,500 + 86.59 N_R}$$

TABLE XI
 VALUES OF n , n_α , f AND f_α FOR
 REACH 0 + 00 TO 1 + 80
 WITHOUT TUBES

Average Depth	Q	Reynolds Number	n	n_α	α	f	f_α
0.628	0.998	27554.99	0.0104	0.0104	1.081	0.01771	0.01754
0.839	1.999	46253.47	0.0108	0.0109	1.081	0.01790	0.01768
1.220	3.000	51201.24	0.0114	0.0115	1.077	0.01799	0.01785
0.995	3.002	59640.85	0.0112	0.0113	1.081	0.01854	0.01829
1.756	4.441	56653.12	0.0119	0.0119	1.066	0.01776	0.01767
1.386	4.447	68647.41	0.0110	0.0111	1.078	0.01625	0.01610
1.153	4.454	79345.12	0.0111	0.0112	1.081	0.01736	0.01706
1.747	4.285	72381.89	0.0106	0.0107	1.065	0.01422	0.01413
1.555	4.294	79766.92	0.0110	0.0111	1.073	0.01581	0.01570
1.211	4.331	97937.79	0.0109	0.0110	1.080	0.01660	0.01637
1.715	2.995	51357.12	0.0115	0.0115	1.050	0.01651	0.01643
1.448	3.002	59052.94	0.0117	0.0117	1.069	0.01793	0.01784
0.920	2.000	55462.26	0.0115	0.0115	1.080	0.01955	0.01937

TABLE XII

VALUES OF n , n_α , f AND f_α FOR REACH 0 + 00 TO 1 + 80
WITH TUBES

Average Depth	Q	Reynolds Number	n	n_α	α	f	f_α
TUBES TWELVE INCHES FROM BOTTOM							
Tube Size 2.0 Inches							
0.658*	1.002	23694.95	0.0105	0.0105	1.071	0.01785	0.01775
1.681	2.981	35305.74	0.0144	0.0144	1.158	0.02605	0.02605
1.290	3.019	44195.18	0.0126	0.0126	1.087	0.02158	0.02151
1.028	2.998	52121.28	0.0108	0.0108	1.071	0.01683	0.01668
1.782	4.499	50790.63	0.0144	0.0144	1.118	0.02573	0.02570
1.424	4.524	61260.07	0.0133	0.0133	1.081	0.02330	0.02319
1.106	4.521	70124.86	0.0118	0.0119	1.071	0.01939	0.01919
Tube Size 1.0 Inch							
0.679*	1.000	23560.13	0.0110	0.0111	1.072	0.01951	0.01942
1.083	1.000	17021.56	0.0108	0.0108	1.152	0.01650	0.01652
1.029	3.010	54029.41	0.0108	0.0108	1.071	0.01676	0.01662
1.282	2.995	45537.04	0.0118	0.0118	1.086	0.01876	0.01869
1.682	3.002	36727.08	0.0128	0.0128	1.157	0.02048	0.02049
1.190	4.526	75198.84	0.0109	0.0109	1.071	0.01650	0.01631
1.375	4.514	67034.75	0.0120	0.0120	1.078	0.01914	0.01903
1.691	4.492	56473.05	0.0132	0.0132	1.105	0.02186	0.02182
Tube Size 1.5 Inches							
0.664*	1.004	26372.94	0.0109	0.0109	1.071	0.01903	0.01893
1.678	3.027	39486.90	0.0117	0.0117	1.154	0.01736	0.01736
1.321	3.010	47549.65	0.0119	0.0119	1.090	0.01909	0.01904
1.038	3.011	55419.22	0.0114	0.0115	1.072	0.01887	0.01872
1.704	4.633	57871.62	0.0.33	0.0133	1.104	0.02232	0.02227
1.399	4.659	68268.41	0.0125	0.0125	1.078	0.02068	0.02057
1.224	4.639	75427.42	0.0117	0.0117	1.071	0.01881	0.01862

* Tubes were not submerged

TUBES SIX INCHES FROM BOTTOM
Tube Size 2.0 Inches

1.785	2.998	33799.47	0.0179	0.0179	1.200	0.03970	0.03963
1.346	3.123	44218.09	0.0169	0.0170	1.143	0.03862	0.03839
1.086	3.044	50104.01	0.0164	0.0165	1.133	0.03857	0.03807
1.088	1.002	16435.08	0.0134	0.0134	1.178	0.02536	0.02531
0.678	1.002	22865.66	0.0117	0.0118	1.132	0.02216	0.02193
1.792	4.503	50602.72	0.0179	0.0179	1.159	0.03968	0.03952
1.455	4.529	60278.59	0.0173	0.0174	1.138	0.03971	0.03936
1.270	4.537	67174.51	0.0166	0.0167	1.133	0.03800	0.03740

TABLE XII (Continued)

Average Depth	Q	Reynolds Number	n	n_α	α	f	f_α
Tube Size 1.5 Inches							
1.718	4.738	62467.03	0.0160	0.0160	1.150	0.03209	0.03192
1.433	4.776	74042.38	0.0158	0.0159	1.137	0.03319	0.03283
1.290	4.795	80749.54	0.0153	0.0154	1.133	0.03222	0.03168
1.682	2.983	40638.88	0.0164	0.0164	1.181	0.03402	0.03394
1.333	2.975	48856.31	0.0161	0.0161	1.143	0.03480	0.03459
1.074	2.978	57667.04	0.0149	0.0150	1.133	0.03182	0.03139
0.959	0.996	20632.98	0.0142	0.0142	1.154	0.02935	0.02925
0.667	1.003	26636.03	0.0119	0.0120	1.132	0.02288	0.02264
Tube Size 1.0 Inch							
1.054	1.004	17996.35	0.0135	0.0135	1.170	0.02611	0.02605
0.660	1.003	24850.39	0.0115	0.0115	1.131	0.02135	0.02111
1.593	2.994	39534.81	0.0127	0.0127	1.167	0.02058	0.02050
1.297	2.996	46584.98	0.0136	0.0137	1.141	0.02517	0.02499
1.057	2.998	54469.17	0.0135	0.0136	1.132	0.02650	0.02610
1.787	4.502	54076.97	0.0140	0.0141	1.159	0.02456	0.02444
1.428	4.504	64912.17	0.0135	0.0136	1.137	0.02437	0.02412
1.229	4.504	72982.75	0.0134	0.0135	1.132	0.02513	0.02466
TUBES ZERO INCHES FROM BOTTOM							
Tube Size 2.0 Inches							
1.722	4.530	52590.32	0.0217	0.0218	1.224	0.05956	0.05907
1.516	4.526	58278.82	0.0215	0.0216	1.224	0.06061	0.05981
1.351	4.559	64320.56	0.0213	0.0215	1.224	0.06212	0.06078
0.744	0.996	21734.74	0.0203	0.0204	1.224	0.06475	0.06405
1.792	2.996	33663.45	0.0215	0.0215	1.223	0.05744	0.05719
1.164	2.996	47430.68	0.0218	0.0220	1.224	0.06713	0.06600
1.370	2.986	41698.14	0.0218	0.0219	1.224	0.06399	0.06341
Tube Size 1.5 Inches							
1.093	1.003	17491.21	0.0156	0.0157	1.223	0.03458	0.03440
0.695	1.012	24239.55	0.0155	0.0157	1.224	0.03892	0.03832
1.657	2.997	37703.53	0.0170	0.0170	1.223	0.03660	0.03637
1.274	3.029	47009.42	0.0164	0.0165	1.224	0.03698	0.03649
1.092	3.012	54541.34	0.0164	0.0165	1.224	0.03870	0.03781
1.711	4.523	56329.59	0.0163	0.0164	1.224	0.03355	0.03322
1.412	4.494	65364.70	0.0160	0.0161	1.229	0.03437	0.03373
1.267	4.521	71551.08	0.0159	0.0161	1.224	0.03542	0.03440

TABLE XII (Continued)

Average Depth	Q	Reynolds Number	n	n_α	α	f	f_α
Tube Size 1.0 Inch							
1.733	4.784	63603.39	0.0179	0.0180	1.224	0.04060	0.04025
1.466	4.750	72332.45	0.0183	0.0184	1.224	0.04448	0.04371
1.352	4.805	77988.41	0.0181	0.0183	1.224	0.04506	0.04396
0.804	1.002	23880.75	0.0174	0.0175	1.224	0.04647	0.04605
0.710	0.996	25396.04	0.0170	0.0171	1.224	0.04637	0.04575
1.690	2.983	39853.17	0.0184	0.0185	1.223	0.04283	0.04259
1.286	2.991	49719.70	0.0186	0.0188	1.224	0.04756	0.04699
1.129	2.972	54551.37	0.0186	0.0188	1.224	0.04959	0.04865

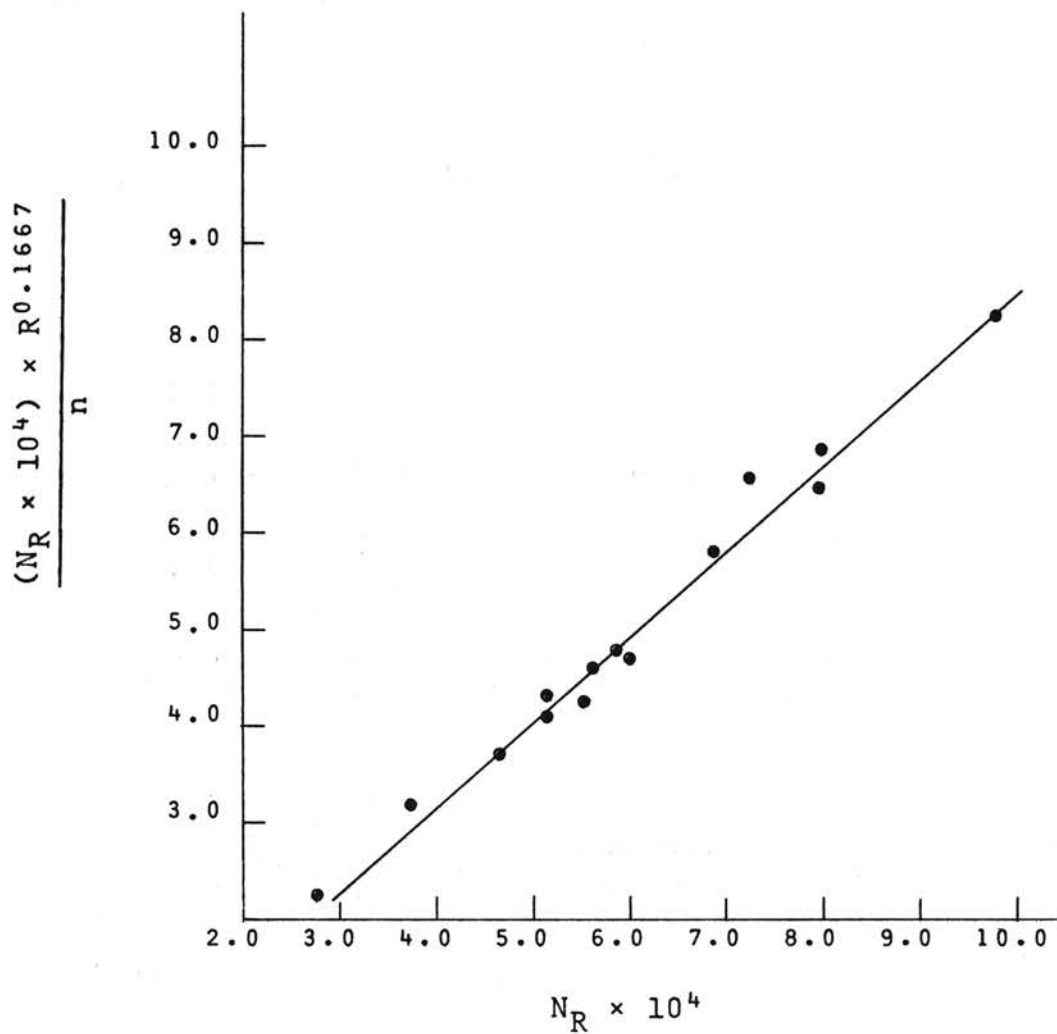


Figure 37. Relationships of $N_R R^{1/6}/n$ Versus N_R for the Channel Without Tubes

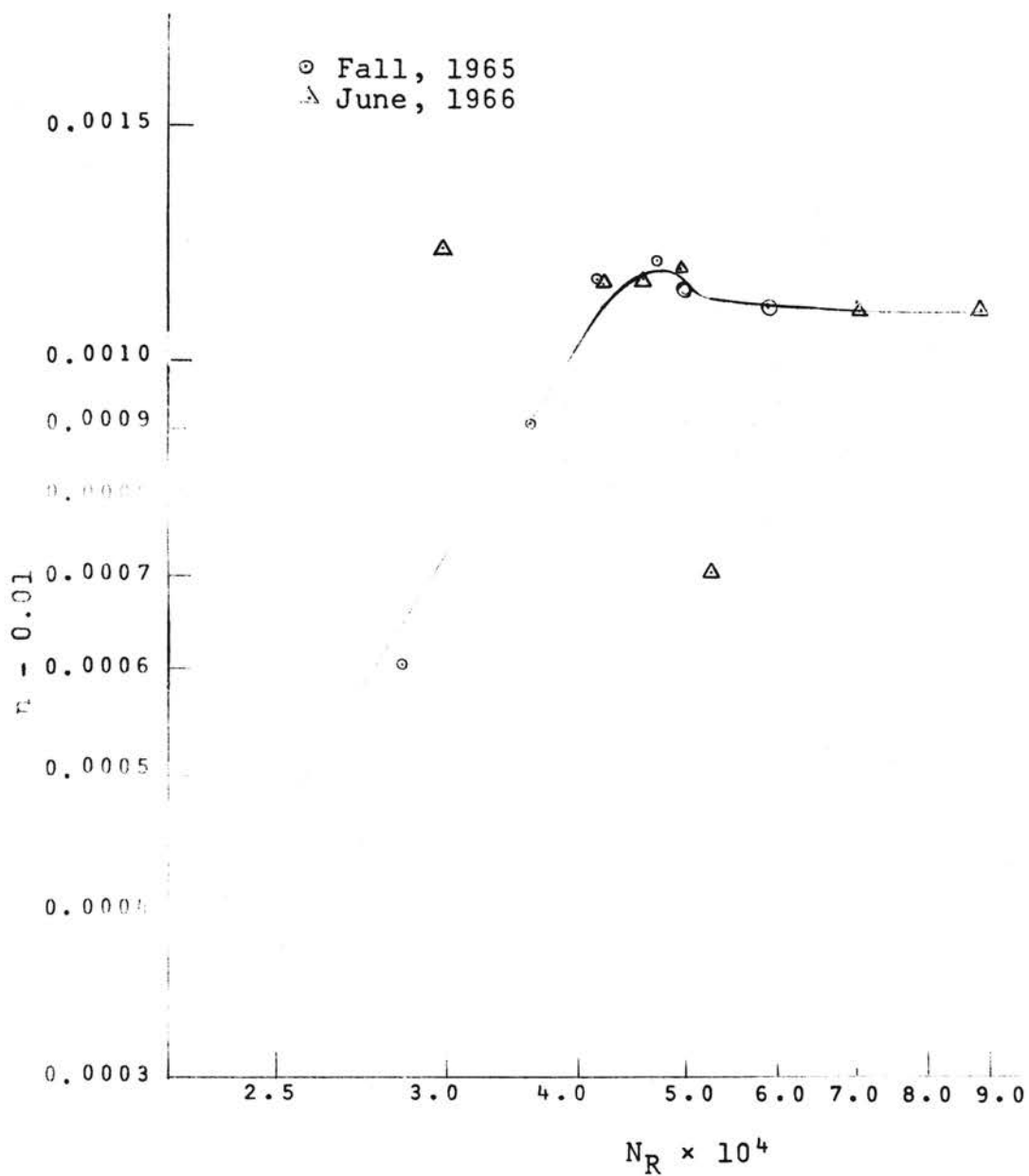


Figure 38. Relationship of n Versus N_R for the Data of the Fall, 1965 and June, 1966

The relationship is believed to be adequate for describing the roughness of the channel for $10^4 < N_R < 10^5$. It is probably good for $N_R > 10^5$ which is the highly turbulent flow region. The relationship reduces to $N_R = R^{1/6}(0.0115)$ as $N_R \rightarrow \infty$. The data plots in the vicinity of the curve for trapezoidal channels for $k = 0.04$ in Figure 8. The values of $N_R \leq 10^4$ from the curve with $k = 0.04$ cm in Figure 8 would probably give an adequate estimate for the values of f and n .

Resistance With Tubes

Many functional relationships of n as a function of depth (y), discharge (Q), tube diameter (D), tube location (TL) or submergence (S_u), and Reynolds number (N_R) were found from statistical models, plots and combinations of both. Only the models that were found to best predict n will be presented in the section.

Functional Model

To obtain an estimate of the magnitude of the contribution of the variables to the value of n , a multi-variant linear regression analysis was performed with n as a function of (y , Q , TL , D). The pertinent quantities making the majority of the contribution to resistance were tube diameter (D) and tube location (TL). Thus, n was plotted as a function of tube diameter with a fixed tube location as shown in Figure 39. The curves were forced

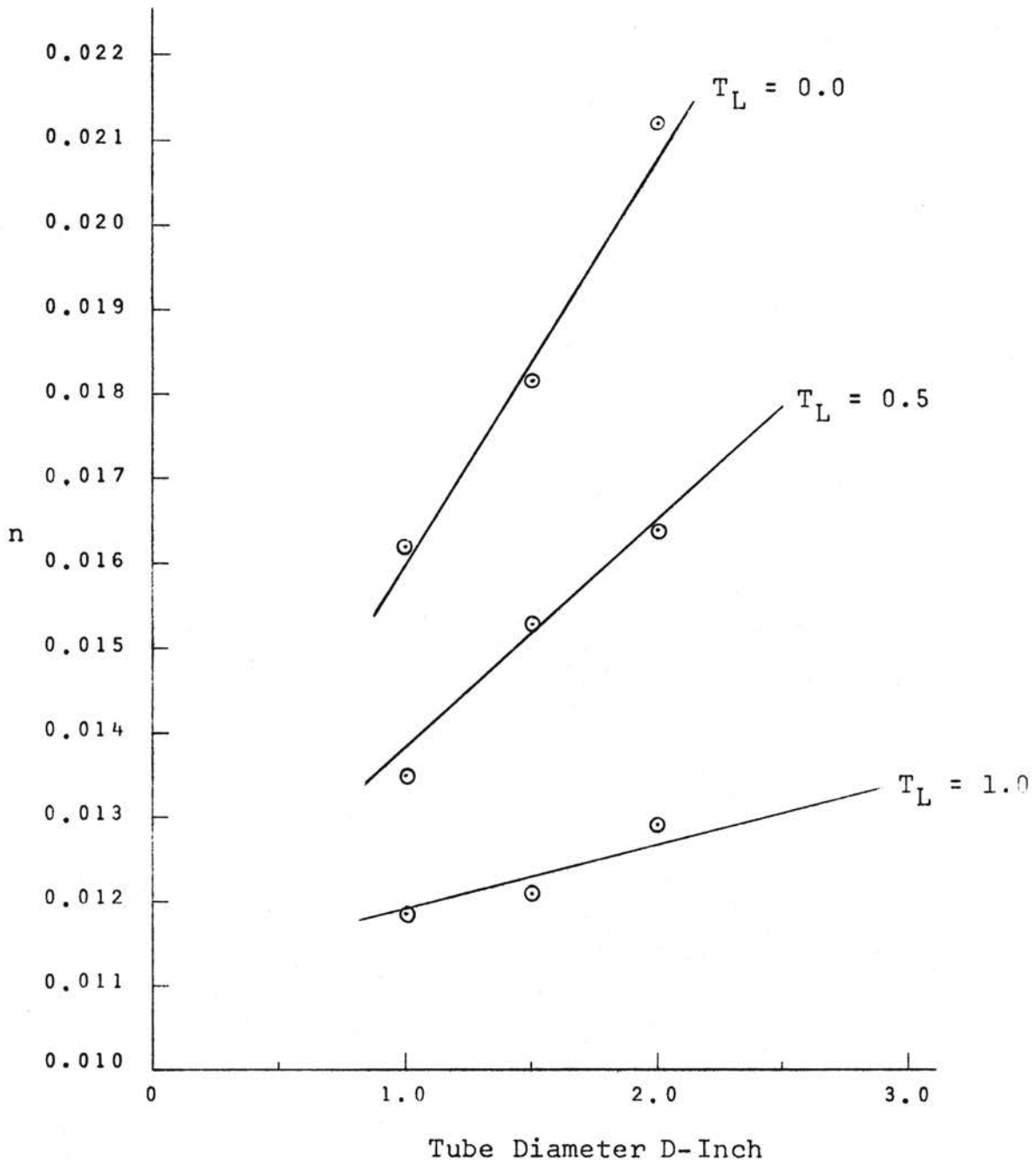


Figure 39. Average n as a Function of Tube Diameter at a Fixed Tube Location

through the point 0.01117 which was found to be the average n value for the channel without tubes. The slope of the three equations representing the relationships in Figure 39 were then plotted as a function of tube location (TL) as shown in Figure 40. These two relationships gave

$$n = 0.01117 + (0.00487 - 0.00417 \text{ TL}) D \quad (23)$$

The relationship for the residual of Equation 23 + 0.01117 as a function of N_R was found to be

$$(\text{Residual} + 0.01117) = \frac{N_R}{204300 + 85.61 N_R}$$

The equation becomes

$$n = (0.00487 - 0.00417 \text{ TL}) TS + \frac{N_R}{204300 + 85.61 N_R} \quad (24)$$

The observed n versus calculated n is shown in Figure 41, the correlation coefficient and standard deviation were $r = 0.95$ and $s = 0.001$. The expression indicates that as the tube size approaches zero the resistance is only a function of Reynolds number, which was the case of the channel without tubes. However, no provision is made for the case where the tube submergence is zero, i.e., $y < TL$. The relationship is believed to be adequate for expressing resistance in the channel for the condition of $0 < D \leq 3.0$, $TL < y$ and $N_R > 10^4$. The coefficients in the expression of N_R were not expected to be the same as those obtained for the channel without tubes because the dependent variable in the expression was the dimensionless parameter $n/R^{1/6}$

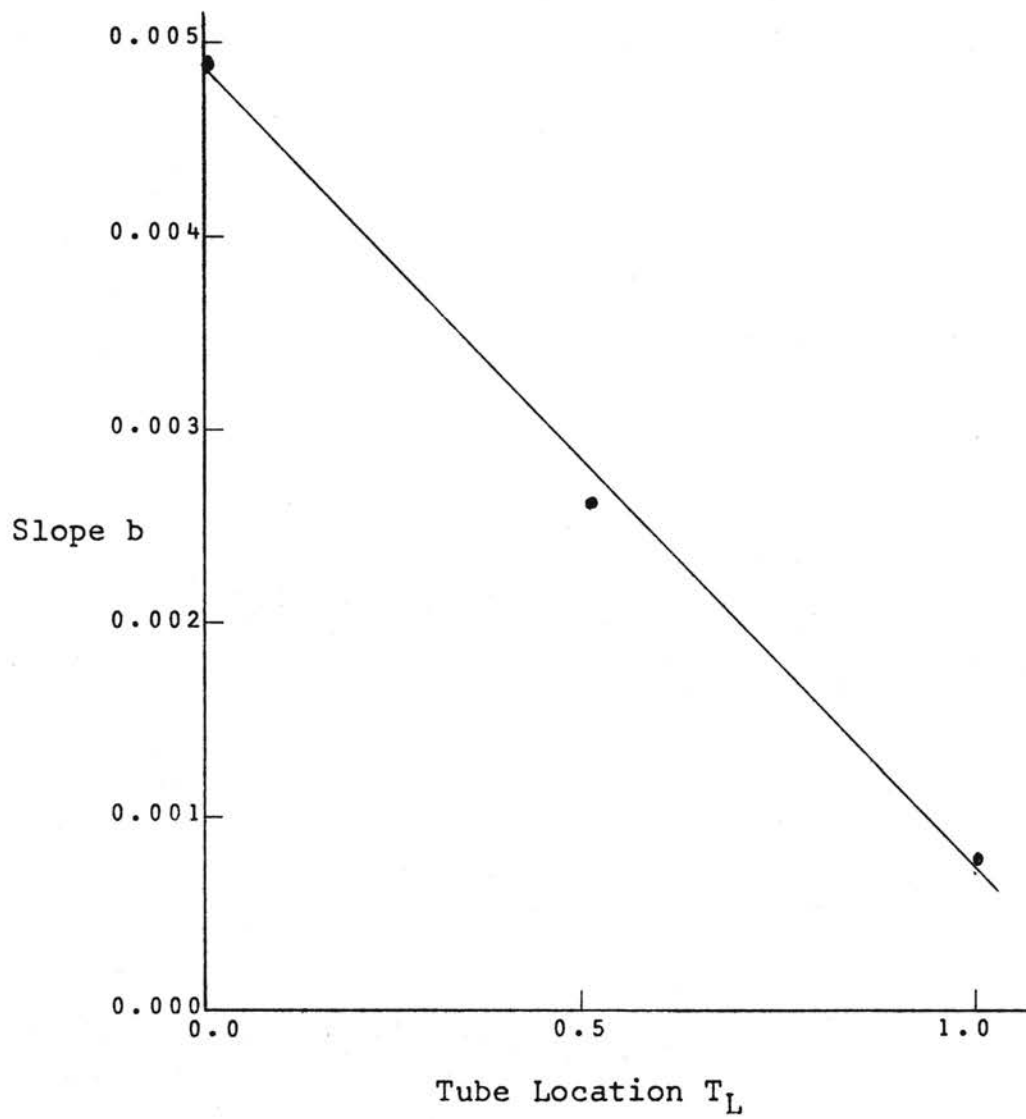


Figure 40. Slope Versus Tube Location From Channel Bottom

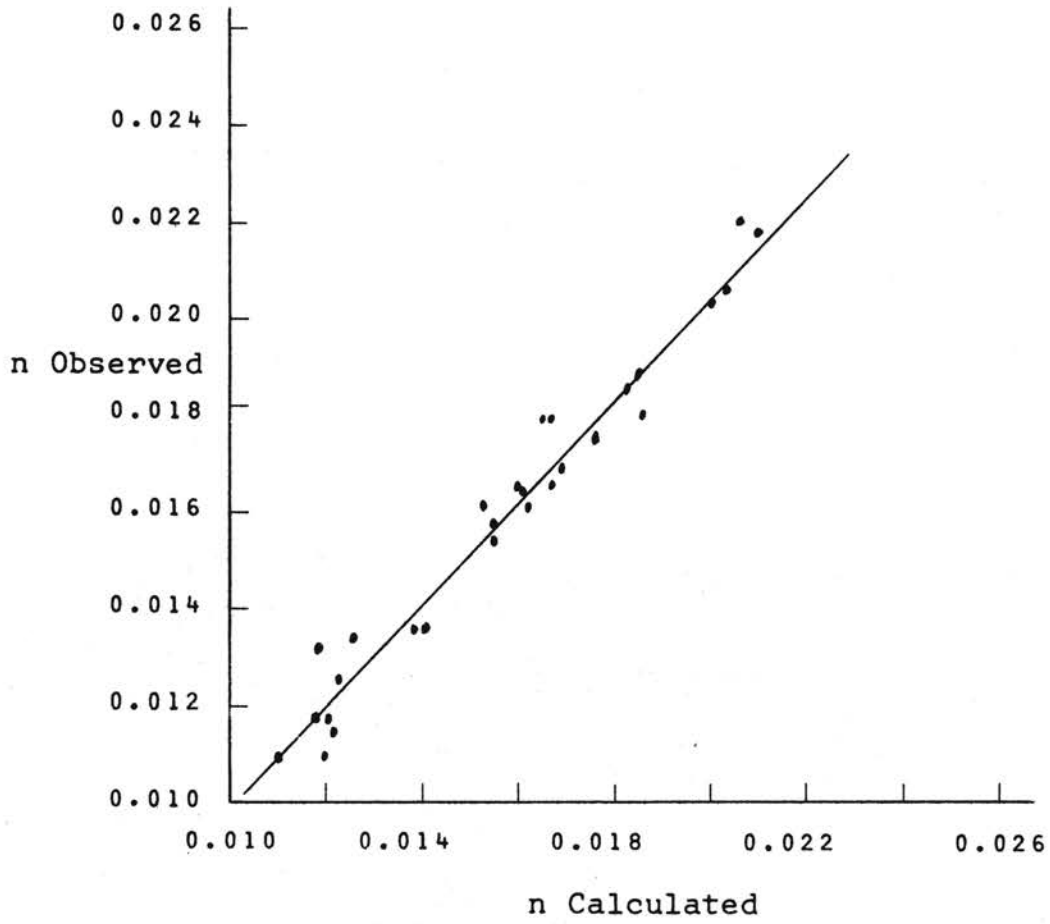


Figure 41. n Observed Versus n Calculated from Equation 24

and the contribution of $R^{1/6}$ is probably distributed throughout the coefficients of the expression. Equation 24 was used to calculate n in the spatially varied flow test for $N_R > 2.0 \times 10^4$.

Dimensionless Model

Considering n as a function of the pertinent quantities $n = f(y, Q, S_u, D, \mu, \rho, g)$ in accordance with Buckingham's Pi Theorem. The expression can be written as

$$\Pi_0 = Cf(\Pi_1, \Pi_2, \Pi_3, \Pi_4)$$

where

$$\Pi_0 = n/R^{1/6} \text{ resistance parameter}$$

$$\Pi_1 = Q/gR^5 \text{ discharge coefficient}$$

$$\Pi_2 = S_u/R \text{ submergence parameter } S_u = (y-TL)$$

$$\Pi_3 = D/R \text{ tube size parameter}$$

$$\Pi_4 = VR/\nu \text{ Reynolds number}$$

A plot of Π_0 versus Π_2 for fixed Q 's are shown in Figure 42. The slope of the lines were plotted as a function of Π_3 as shown in Figure 43. The resulting equation was

$$\Pi_0 = 0.01114 + (0.0021 + 0.0110\Pi_3) \Pi_2$$

The coefficients were computed statistically for the model with the resistance equation without tubes included, and the equation became

$$n = 0.00510 + R^{1/6} \left[(0.00319 + 0.00821 \Pi_3) \Pi_2 + \frac{0.44175 N_R}{218500 + 85.61 N_R} \right] \quad (25)$$

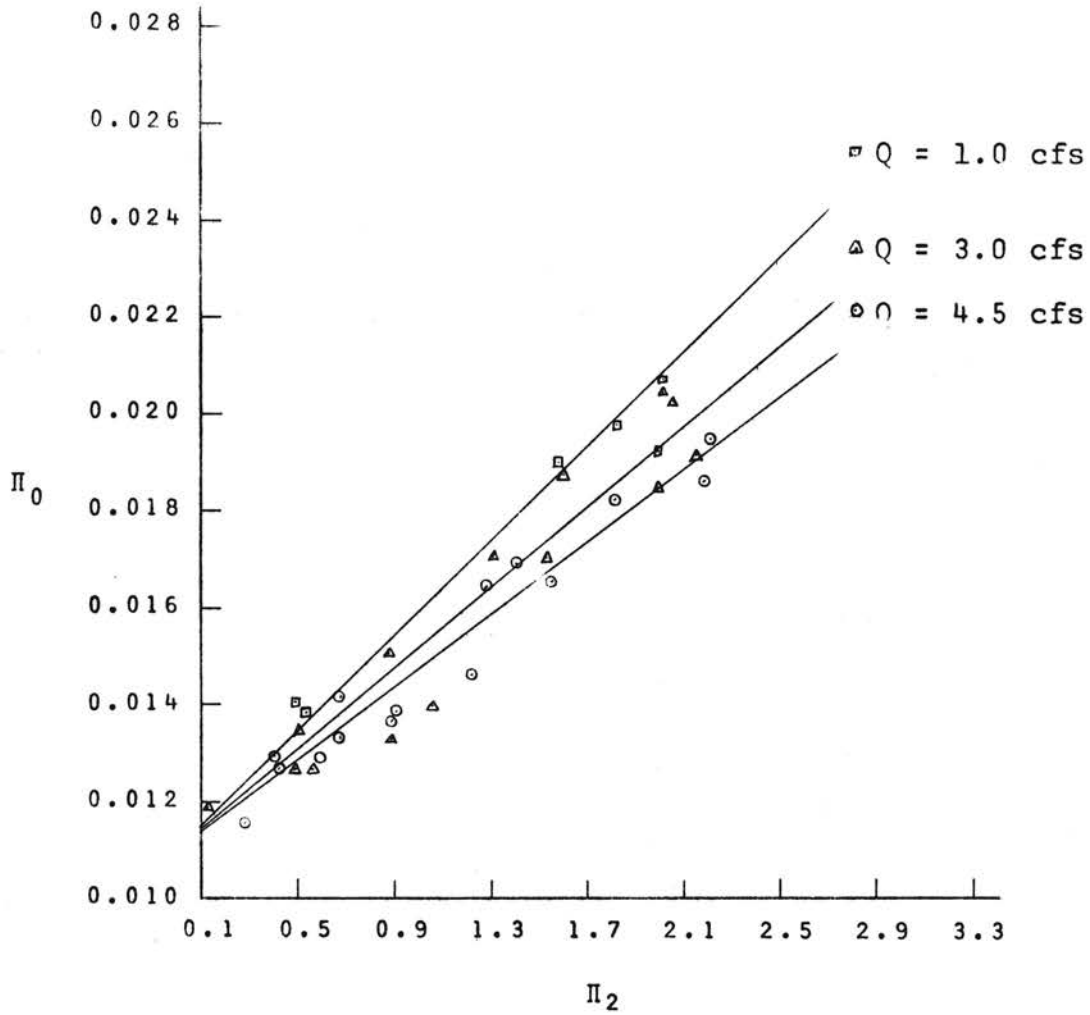


Figure 42. Π_0 Versus Π_2 for Various Values of Q

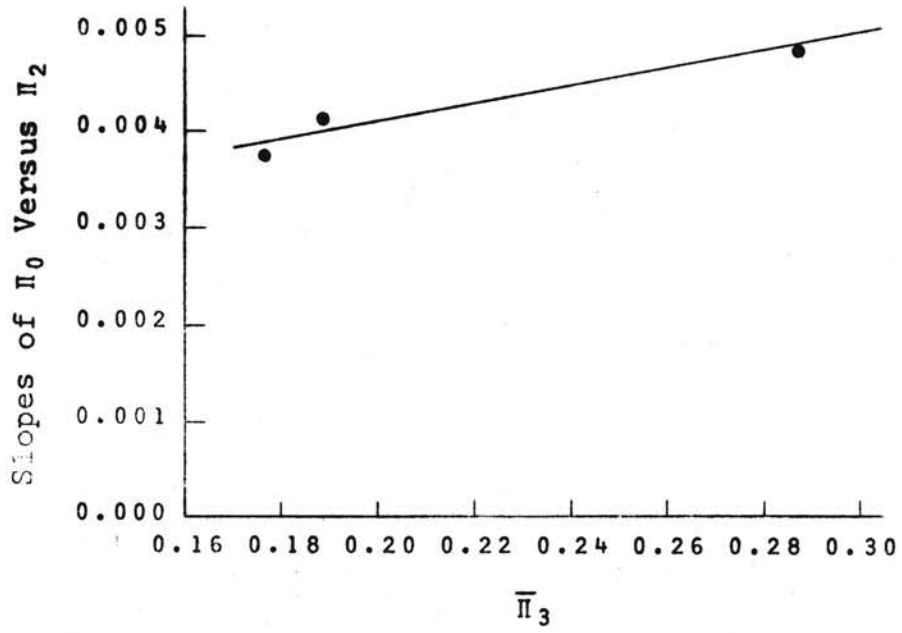


Figure 43. Slopes from Figure 42 Versus $\bar{\Pi}_3$

The residual of the above equation was not found to be a function of Π_1 . The observed n versus the calculated n is shown in Figure 44. The expression for n is realistic in the sense that (1) as the submergence parameter decreases to zero, n becomes a function of R and N_R which occurred without tubes in the channel, and (2) as Π_3 increases the value of resistance n becomes larger.

One would think a model similar to the drag force equation $F_D = C_D \rho A V^2 / 2.0$ would be applicable. However, equations of this type failed to yield an adequate estimate of the resistance.

Multivariant Model

A multivariable regression analysis including interactions was applied to the data. The coefficients of the expression are as follows:

Correlation Coefficient $r = 0.95$	Standard Deviation $s = 0.001$
<u>Coefficients</u>	<u>Terms</u>
0.00510	Constant
0.01990	y
-0.00229	y^2
0.00212	Q
0.00007	Q^2
-0.01095	TL
0.00278	TL^2
0.00252	D

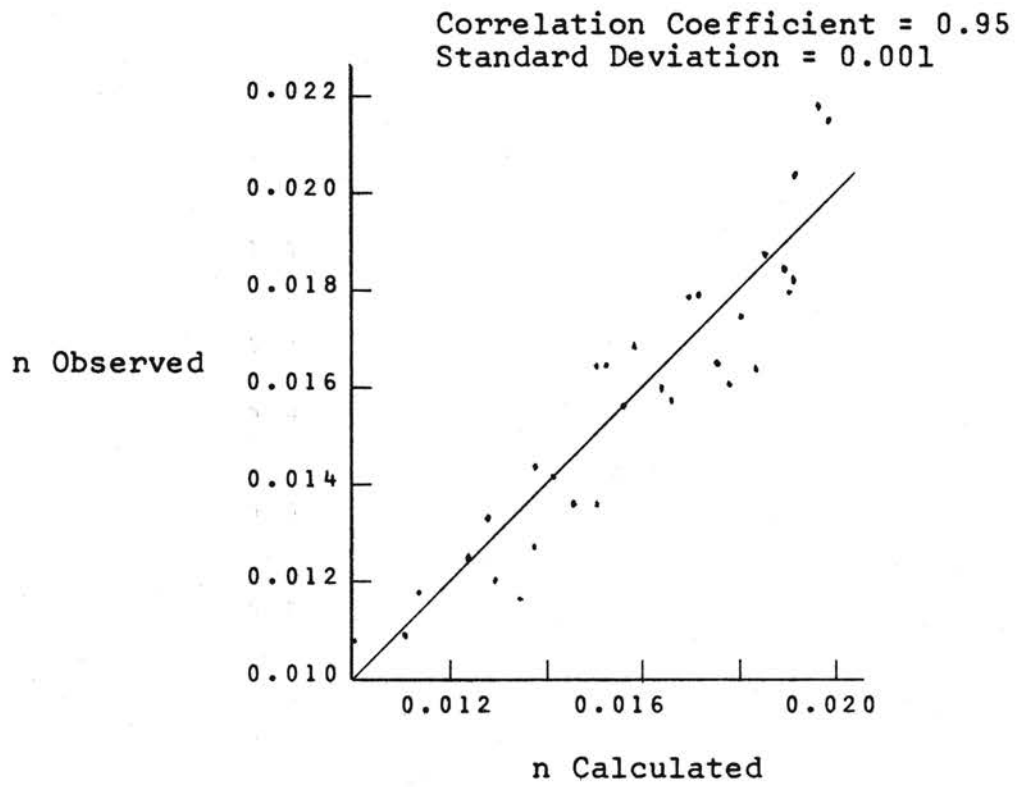


Figure 44. n Observed Versus n As
Calculated from
Equation 25

<u>Coefficients</u>	<u>Terms</u>
0.00119	D ²
0.00697	TLD
0.00155	TLQ
-0.00645	TLD
0.0008	DQ
-0.00409	yTS
-0.00250	yQ
-0.00364	QTL
0.00201	yQTL
0.00087	yQD
0.00052	yQTLD

According to this expression, (1) the resistance decreases as the depth and location of the tube from the bottom increases, and (2) the resistance increases as the discharge and tube diameter increases as in previous relationships.

The use of the equation in estimating the resistance would be a laborious task without the aid of a computer. Thus, Equation 24 or 25 could be used just as effectively and with the same expected accuracy of prediction since the correlation coefficient and the standard deviation are of the same magnitude for all three models.

Spatially Varied Flow Tests

The water surface profiles for the experimental channel were calculated with the siphon tube inlets 1.0

foot from the channel bottom. The water surfaces were computed with n calculated (n -cal) and $\alpha = 1$, n -cal and α -cal, and \bar{n} or adjusted n . The adjusted n was used for calculating the water surface profiles for a prismatic channel with variable slope at the same Q 's used in the experimental channel.

A program was written to compute the water surface profiles. The assumptions and basic operation of the program are listed as follows:

1. The area at each of the 11 stations was calculated. The area between stations was assumed to vary linearly, then the areas for the increments between the stations were calculated. The same procedure was used for computing the wetted perimeter.
2. Initial water surface
 - a. The initial water surface was taken as the measured value during the calculation of the water surface with n -cal and $\alpha = 1$.
 - b. In the calculation of the water surface to find \bar{n} , a regression curve was fitted to the observed water surface profile and the value for the downstream end of the channel was used as the initial water surface.
 - c. The initial water surface for the sloping channel was obtained by adding the tube

head necessary to discharge the entering Q to the elevation of the tube outlets. When the calculations had progressed to the upstream end of the channel, the total QT out the tubes was checked against the entering Q -in. Iteration of the initial head was continued until

$$-0.5\% \leq \frac{Q\text{-in} - QT}{Q\text{-in}} \times 100 \leq 0.5\%$$

3. The energy equation was used in calculating the water surface profile

$$\left(\frac{\alpha_1 V_1^2}{2g} - \frac{\alpha_2 V_2^2}{2g} \right) + (y_1 - y_2) = L(S_s - S_o)$$

To start the computation, V_1 and y_1 must be known. Then the equation was applied to successive increments up the channel. The depth y_2 was adjusted within each increment until the energy equation

$$\left(\frac{\alpha_1 V_1^2}{2g} - \frac{\alpha_2 V_2^2}{2g} \right) + (y_1 - y_2) - L(S_s - S_o) = \pm 0.00001$$

Spatially Varied Profile n -cal and $\alpha = 1$

The resistance values obtained for the channel under gradually varied flow conditions were obtained for values of $2.0 \times 10^4 \leq N_R \leq 10^5$. For the spatially varied flow the expected range of N_R was from 0 to 10^5 . Thus, a small portion of the spectrum of N_R was covered by the gradually

varied flow data. Resorting to experimental results obtained by other hydraulicians in Figure 8, the resistance values n were obtained. The value of f can be calculated from the expression

$$f = \frac{8gn^2}{(1.486)^2 R^{1/3}}$$

This expression and Equation 24 for n were used for $0.715 \leq R \leq 0.901$ foot to calculate f in terms of n . The relationship is shown in Figure 45. The values of $0.715 \leq R \leq 0.901$ covers the range of hydraulic radii used in the spatially varied flow tests.

The average slope of the curves for trapezoidal channels in Figure 8 with k values of 0.20 and 0.04 cm (mean sand grain diameter) were found to be approximately 0.270. A curve with this slope was fitted through the mean f from Figure 45 at $N_R = 2.0 \times 10^4$ as shown in Figure 46. The relationships from Figure 46 were used in calculating n in the spatially varied flow tests. The resistance values of n used in the spatially varied flow tests were computed from the relationship

$$n = 1.486 \sqrt{\frac{f R^{1/3}}{8g}}$$

The f values within limits of N_R from Figure 46 used in computing n are as follows:

$$f = 0.1, N_R < 45$$

$$f = 45/N_R, 45 \leq N_R \leq 1000$$

$$f = 0.292/N_R^{0.270}, 1000 < N_R \leq 2.0 \times 10^4$$

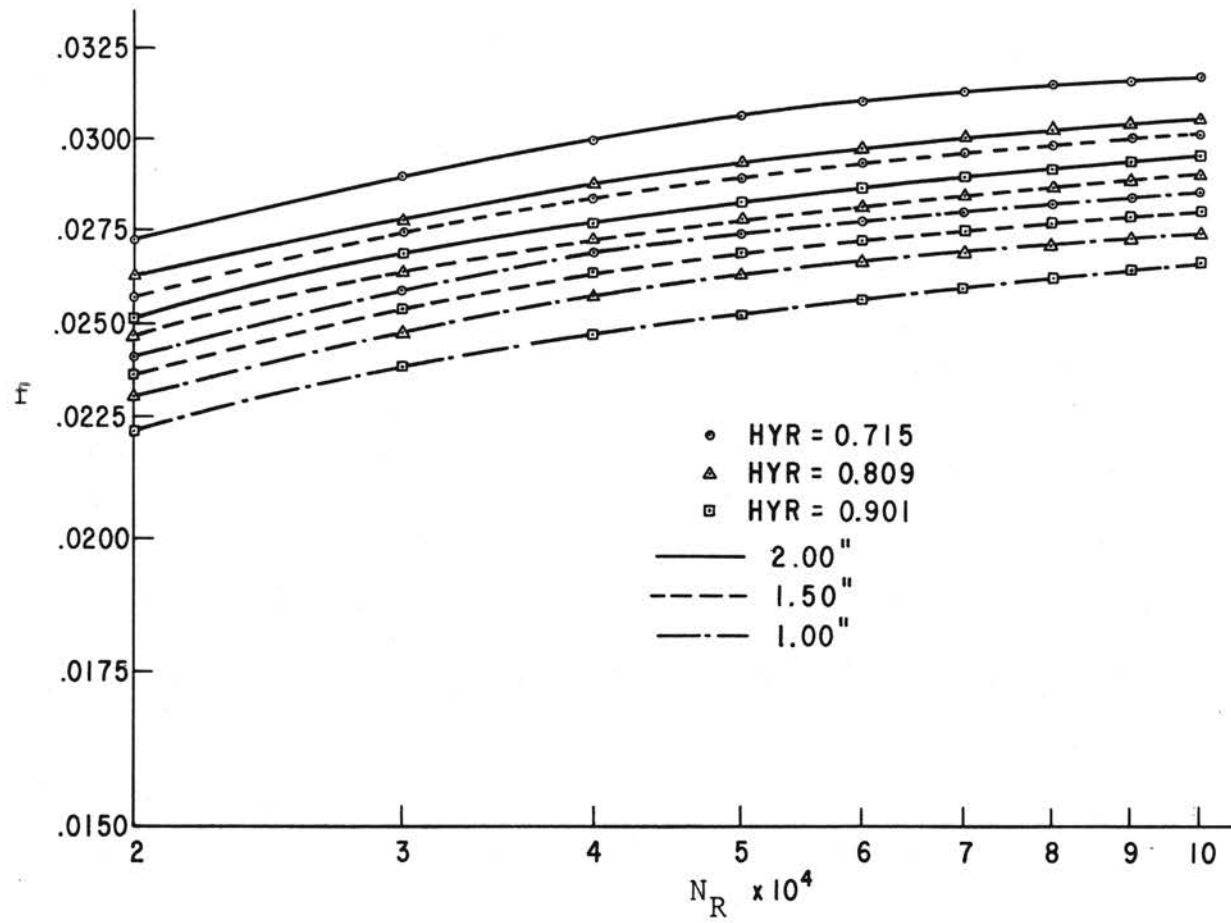


Figure 45. f Versus N_R For Various Tube Diameters and Hydraulic Radii

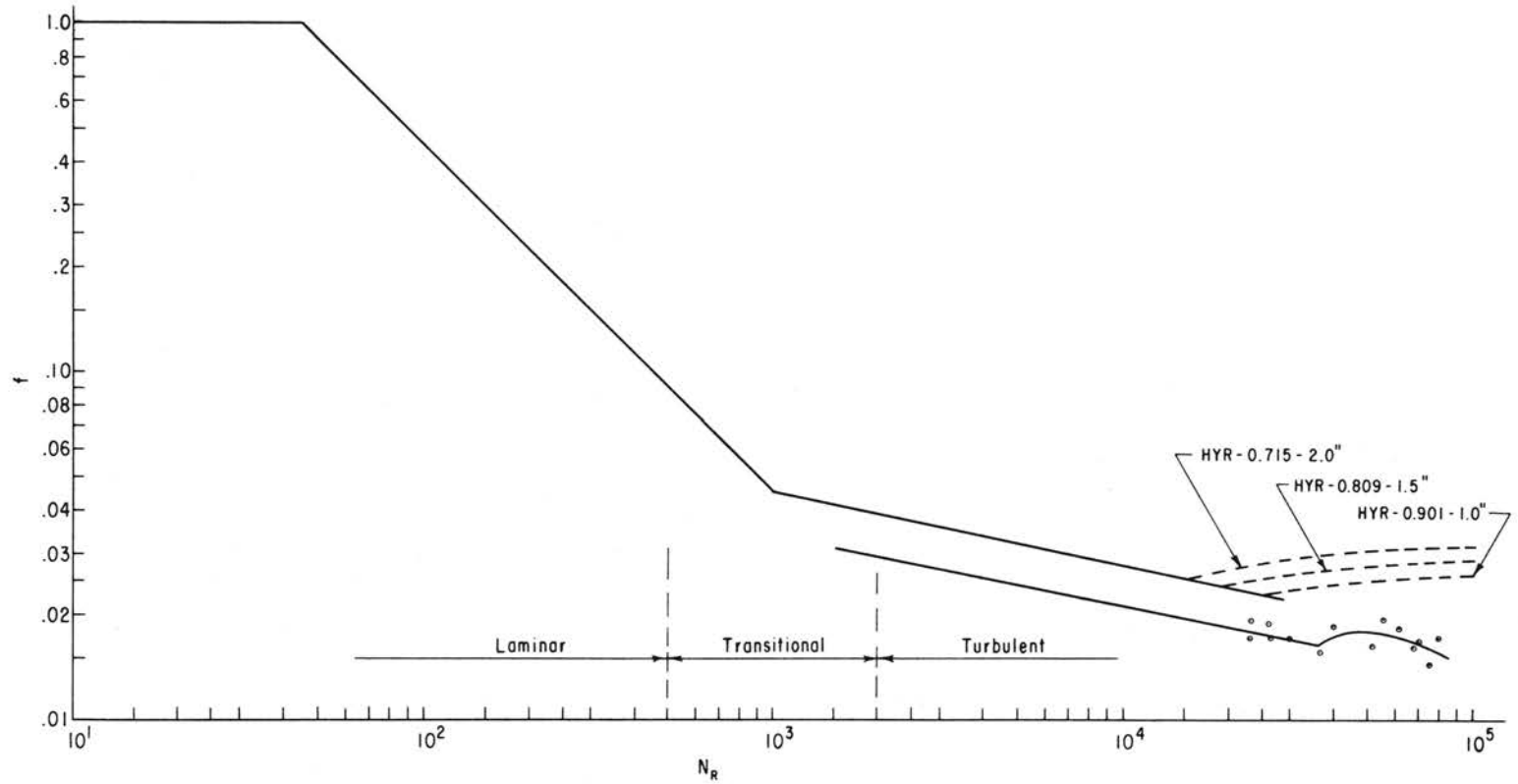


Figure 46. The Relationship of f Versus N_R Used in the Water Surface Profile Computations

Computed values from Equation 24 were used for $N_R > 2.0 \times 10^4$.

The calculated water surface profiles for n -cal and $\alpha = 1$ are shown in Column 3 of Appendix E. In general, the calculated water surface profiles underestimated the observed profiles. The water surface profiles are shown in Figures 47 to 50.

The underprediction of the water surface profiles indicates that the values of n obtained for gradually varied flow conditions are lower than the values of n for spatially varied flow or that the resistance values from Figure 46 are low.

Water Surface Profile with Adjusted \bar{n}

The water surface profiles were calculated with an adjusted value of n which is called \bar{n} . The value of \bar{n} was obtained by fitting a curve to the observed measurements of the water surface elevation. The downstream and upstream elevations as calculated from the curve were used in computing \bar{n} . The \bar{n} that would yield an upstream water surface within ± 0.0001 foot of the calculated elevation was found. The values of \bar{n} are shown in Table XIII. The resulting water surface profiles are shown in Column 5 of Appendix E. The water surface elevations calculated from \bar{n} were compared with the observed values of the water surface profiles in Figures 47 to 50. These figures

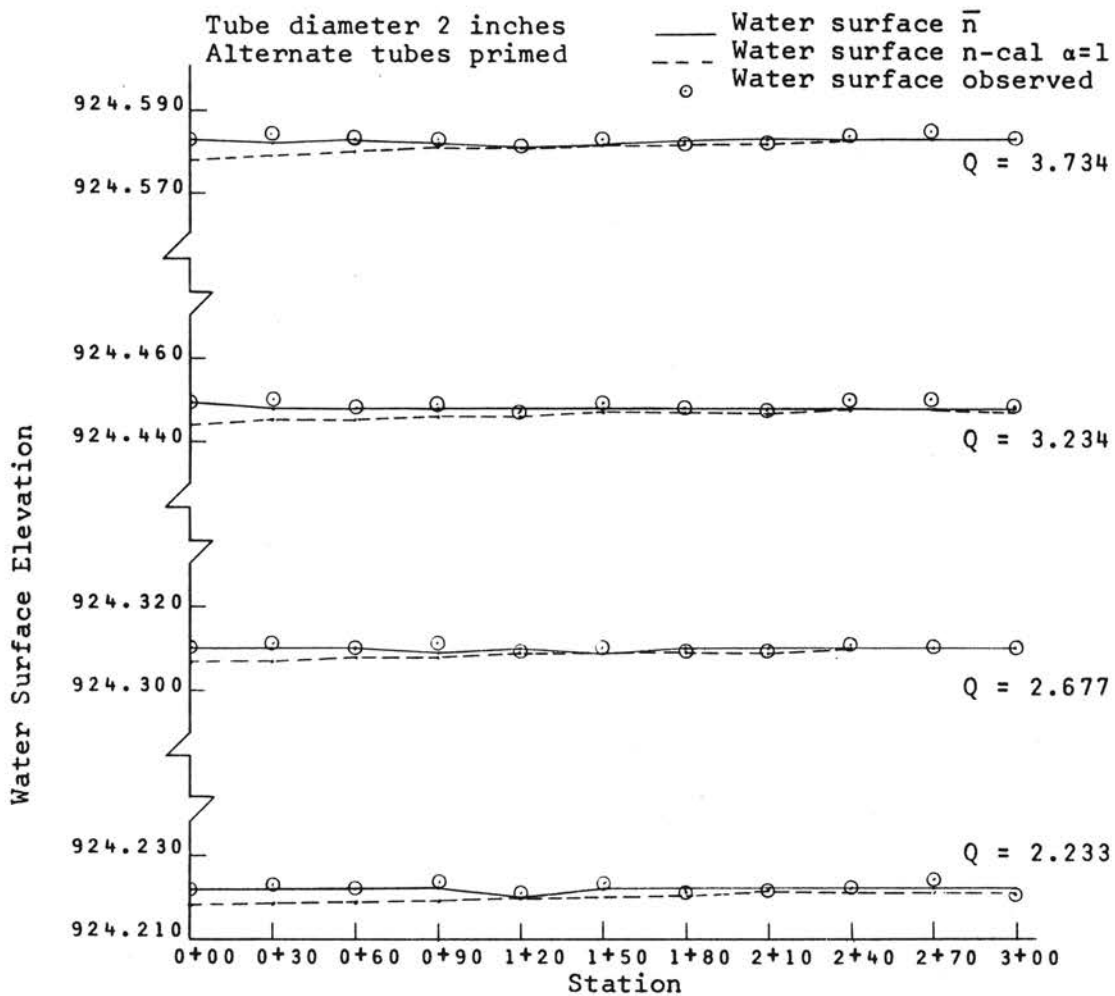


Figure 47. Water Surface Elevations as Observed and Calculated for the Channel with 2-Inch Tubes in the Spatially Varied Flow Tests

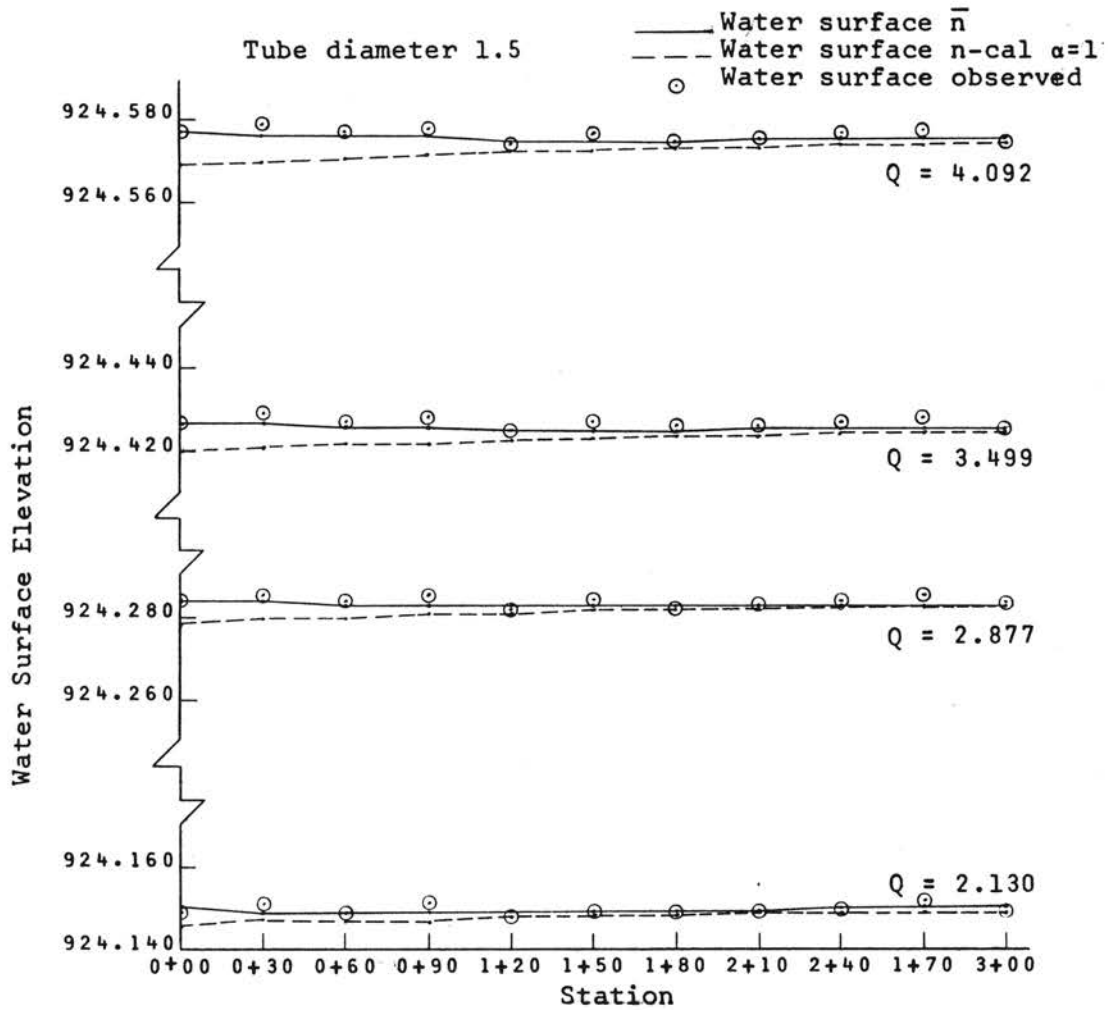


Figure 48. Water Surface Elevations as Observed and Calculated for the Channel with 1.5-Inch Tubes in the Spatially Varied Flow Tests

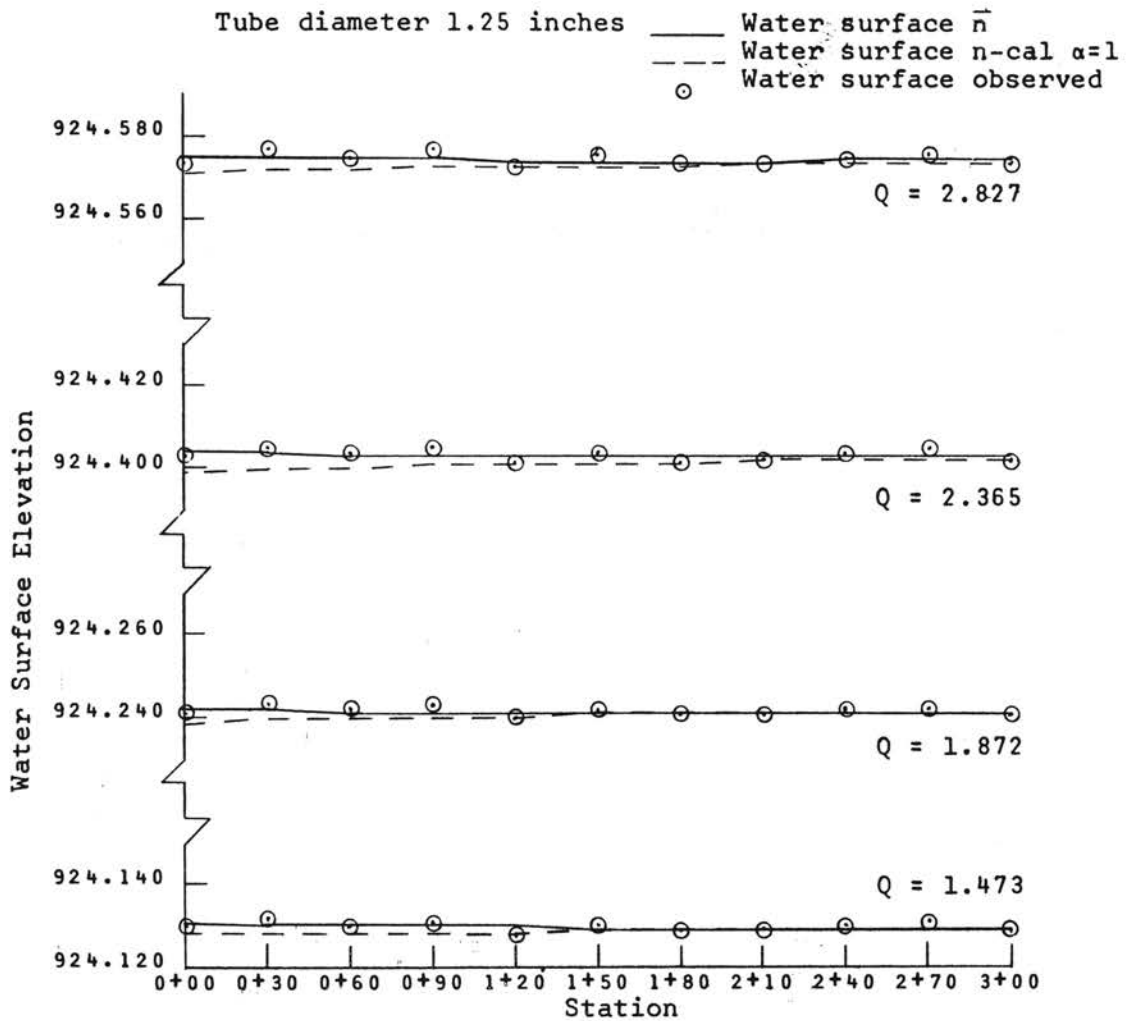


Figure 49. Water Surface Elevations as Observed and Calculated for the Channel with 1.25-Inch Tubes in the Spatially Varied Flow Tests

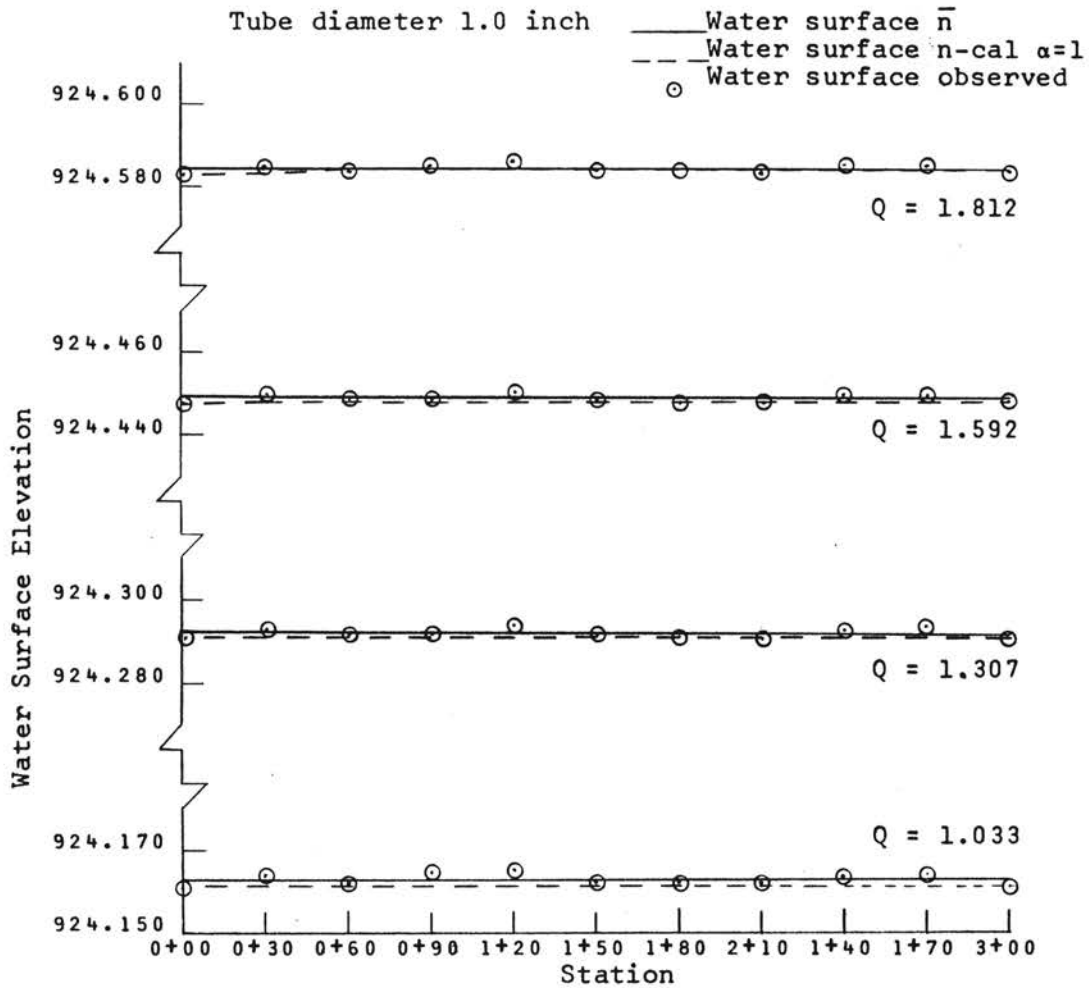


Figure 50. Water Surface Elevations as Observed and Calculated for the Channel with 1.0-Inch Tubes in the Spatially Varied Flow Tests

TABLE XIII

RESISTANCE VALUES, DEPTHS, WATER SURFACE ELEVATIONS
AND ENTERING Q'S FOR VARIOUS TUBE DIAMETERS IN
THE SPATIALLY VARIED FLOW TESTS
90 TUBES, 40-INCH SPACING

Tube Diameter	Entrance Elevation	Downstream Elevation	Depth Upstream	Depth Downstream	Flow (cfs)	Effective n	Adjusted \bar{n}	n-avg From n-cal	$\alpha=1$	VR
2.000	924.5827	924.5833	1.909	1.9093	3.738	0.01126	0.02016	0.01291		0.57933
2.000	924.4487	924.4485	1.775	1.7745	3.240	0.01145	0.02012	0.01287		0.53541
2.000	924.3101	924.3100	1.636	1.6360	2.680	0.01086	0.01869	0.01282		0.47326
2.000	924.2223	924.2221	1.548	1.5481	2.239	0.01065	0.01805	0.01280		0.41318
1.500	924.5771	924.5760	1.903	1.9020	4.101	0.01249	0.02247	0.01272		0.63858
1.500	924.4276	924.4260	1.754	1.7520	3.510	0.01225	0.02156	0.01269		0.61178
1.500	924.2841	924.2833	1.610	1.6093	2.863	0.01125	0.01942	0.01267		0.55352
1.500	924.1496	924.1496	1.476	1.4756	2.137	0.01016	0.01719	0.01269		0.41517
1.250	924.4039	924.4029	1.730	1.7289	2.369	0.01246	0.02187	0.01287		0.39934
1.250	924.5754	924.5746	1.901	1.9006	2.830	0.01284	0.02291	0.01291		0.44107
1.250	924.2420	924.2413	1.568	1.5673	1.874	0.01155	0.01943	0.01293		0.35122
1.250	924.1304	924.1294	1.456	1.4554	1.476	0.01184	0.02007	0.01307		0.27154
1.000	924.1631	924.1625	1.489	1.4885	1.036	0.01249	0.02188	0.01388		0.20018
1.000	924.2922	924.2920	1.618	1.6180	1.309	0.01140	0.01968	0.01368		0.23372
1.000	924.4492	924.4490	1.775	1.7750	1.593	0.01198	0.02160	0.01360		0.26364
1.000	924.5843	924.5844	1.910	1.9104	1.813	0.01142	0.01662	0.01362		0.27964

indicate that the \bar{n} considered to exist all along the channel is a good estimate of the average n under spatially varied flow conditions.

Effective n For the Experimental Channel

The values of n_e shown in Table XIII were calculated from the Manning formula.

$$n_e = \frac{1.486}{V} R^{2/3} S_s^{1/2}$$

where

$$S_s = \left[\frac{1}{L} \left(\frac{V_i^2}{2g} - 0 \right) + (y_i - y_o) \right]$$

and

V_i = Average entering velocity

y_i = Upstream depth

y_o = downstream depth

Thus, for a given depth, Q , tube diameter and submergence the water surface elevation at the downstream end of the bay can be calculated as if gradually varied flow occurred.

Figure 51 shows \bar{n} as a function of n_e . The figure shows $n_e = 0.0019 + 0.4830 \bar{n}$.

Water Surface Profiles With n -cal and α -cal

Water surface profiles for the channel were computed using a calculated value for n and α . The values for n were calculated in the same manner as those used in calculating the water surface with n -cal and $\alpha=1$. The alpha (α) values were calculated from Equation 22. The values of the water surface are shown in Column 4 of

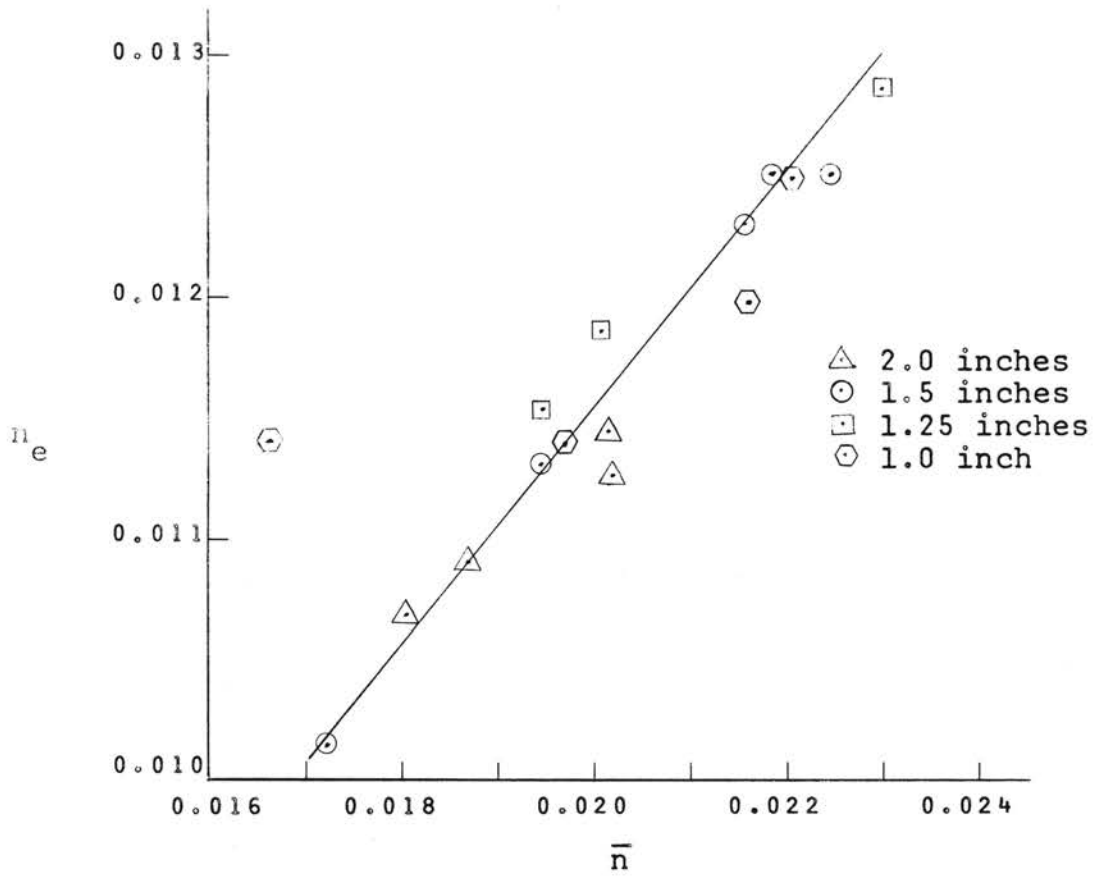


Figure 51. The Functional Relationship of n_e Versus \bar{n}

Appendix E. The predicted water surface profiles are lower than those predicted with n -cal and $\alpha=1$ which indicates that n became smaller. This was not true in gradually varied flow because n increased when α was used in computing n_α . However, n would be expected to decrease in spatially varied flow because n is calculated from the equation

$$n = \frac{1.486}{V} R^{2/3} \left[\frac{1}{L} \left(\left(\frac{\alpha_1 V_1^2}{2g} - \frac{\alpha_2 V_2^2}{2g} \right) + (y_1 - y_2) + (z_1 - z_2) \right) \right]^{1/2}$$

The velocity head term for reach L for gradually varied flow is

$$\left(\frac{\alpha_u V_u^2}{2g} - \frac{\alpha_D (V_u + \Delta V)^2}{2g} \right)^2$$

where the subscript u and D stand for upstream and downstream stations. The velocity changes slightly over the length of the reach for gradually varied flow. The magnitude of α_u is expected to be larger than α_D from Equation 22. Thus, a slight increase in n might be expected because the velocity head at u was slightly larger than at D .

In spatially varied flow all the energy is dissipated over the length of the channel by flow out the tubes, resistance along the channel, and an increase in turbulence (or eddies) expected with decreasing flow. The difference in velocity heads at the upstream and downstream

ends of the channel is

$$\left(\frac{\alpha_D V_D^2}{2g} - \frac{\alpha_u V_u^2}{2g} \right) = - \frac{\alpha_u V_u^2}{2g}$$

because $V_D = 0$ at the downstream end of the channel. Thus, the water surface profile for spatially varied flow would be expected to decrease when α is used.

The underprediction of the water surface profile indicates that the n values obtained in gradually varied flow were not representative of the n values obtained from spatially varied flow.

The available alpha data obtained during the spatially varied flow test were of the same order of magnitude as the data obtained in gradually varied flow tests. The alpha values for gradually varied flow appear to be representative of those in spatially varied flow.

However, when the value of n computed with $\alpha=1$ is used in the water surface computations, the values of alpha are not needed because the effects of α are absorbed in calculated values of n .

Water Surface Profile for Sloping Prismatic Channels

Constant Tube Elevation

The values of \bar{n} obtained from the water surface calculations of the actual channel were used in the calculation of water surface profiles for a prismatic channel with slopes from 0.000 to 0.0025. The same entering Q 's were used as in the actual channel. The

tube elevations were constant with respect to the channel bottom at the downstream end of the channel. The values of the computed water surface profiles are shown in Appendix E.

The prismatic channel with 0.000 slope had almost exactly the same surface profiles as was obtained in the actual channel. The actual channel was not exactly prismatic and the channel bottom undulated ± 0.05 foot. As discussed in the procedure section, a change in bottom elevation of 0.05 foot would change the H_L approximately 0.002 foot. This change in H_L corresponds closely with the values actually observed.

Δw_s (or the difference in the upstream and downstream elevations) as a function of slope are shown in Figures 52 to 55. In general, the figures indicate that as the slope increases the difference in water surface between the ends of the channel increases, with the upstream water surface being higher than the downstream water surface for a given tube diameter. The change in elevations Δw_s decreases as Q decreases, which was expected as a result of the preliminary investigation.

The channel with the siphon tubes at a constant elevation is highly fictitious for a slope of 0.0025 because at the upstream end of the channel the tube outlets would be 0.474 foot above the bottom of the channel. To place the tube outlets 0.474 foot above the bottom of the channel would require a different type of siphon tube

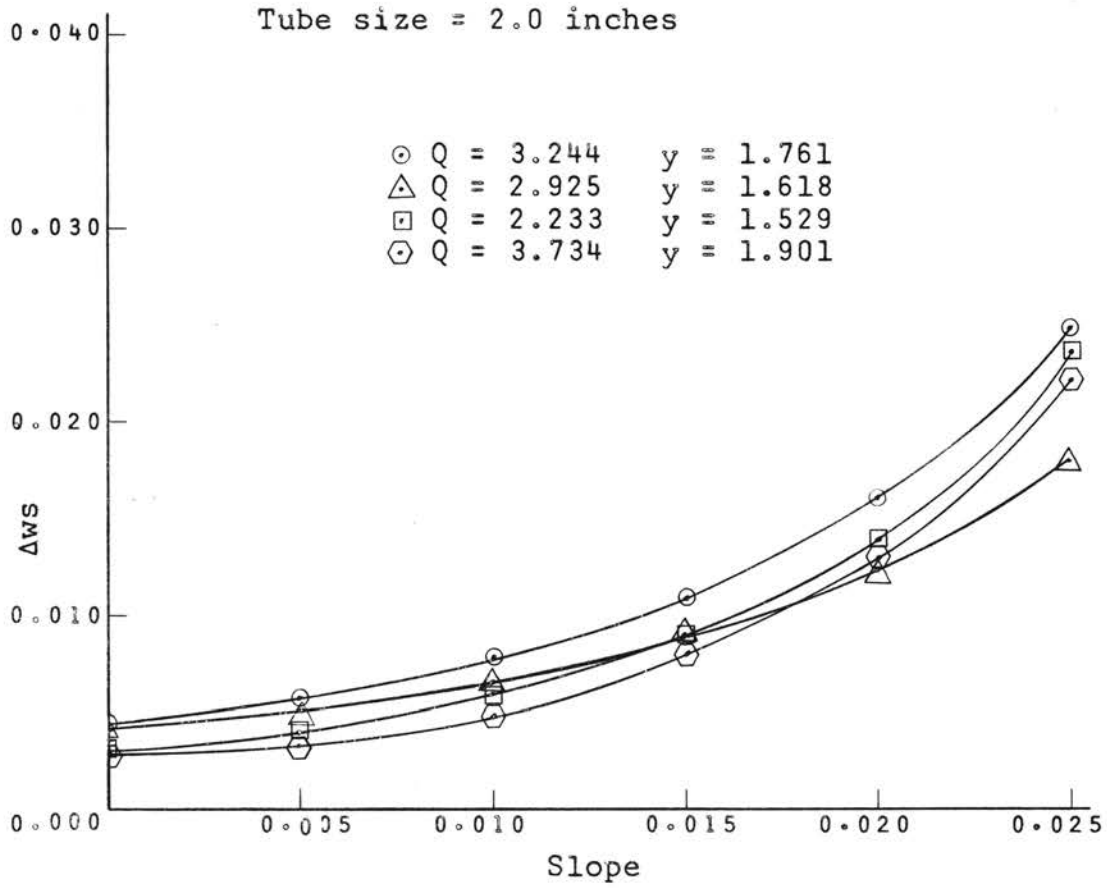


Figure 52. Change in Water Surface Elevation Between the Upstream and Downstream End of the Prismatic Channel as a Function of Slope for the 2-Inch Tubes with Various Depths and Entering Q's

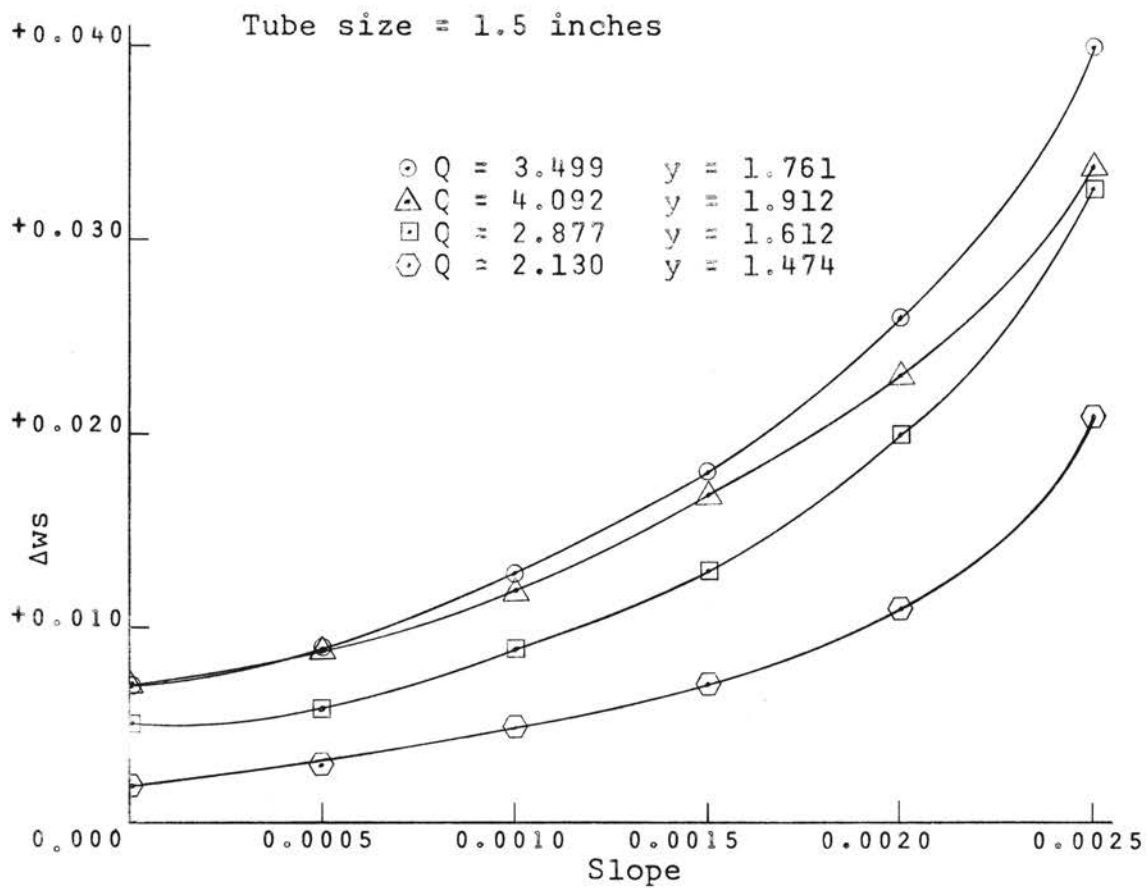


Figure 53. Change in Water Surface Elevation Between the Upstream and Downstream End of the Prismatic Channel as a Function of Slope for the 1.5-Inch Tubes with Various Depths and Entering Q's

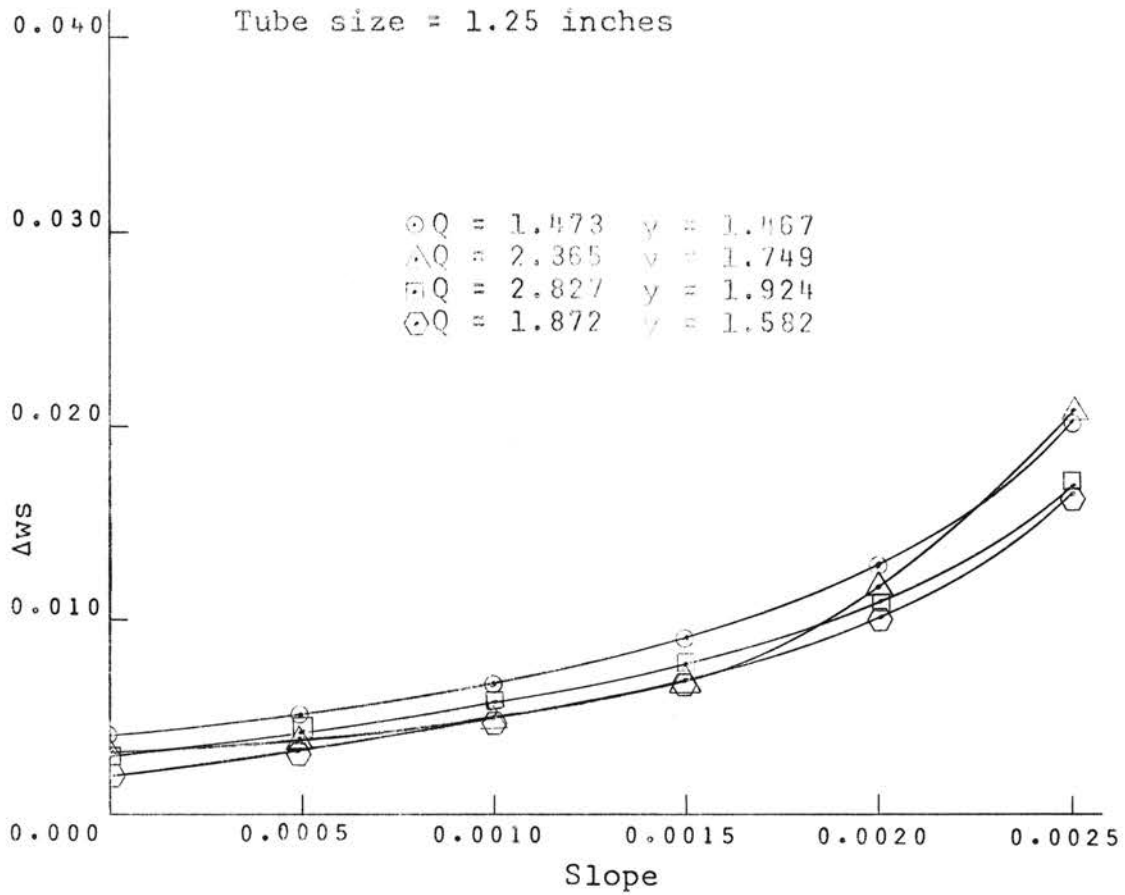


Figure 54. Change in Water Surface Elevation Between the Upstream and Downstream End of the Prismatic Channel as a Function of Slope for the 1.25-Inch Tubes with Various Depths and Entering Q's

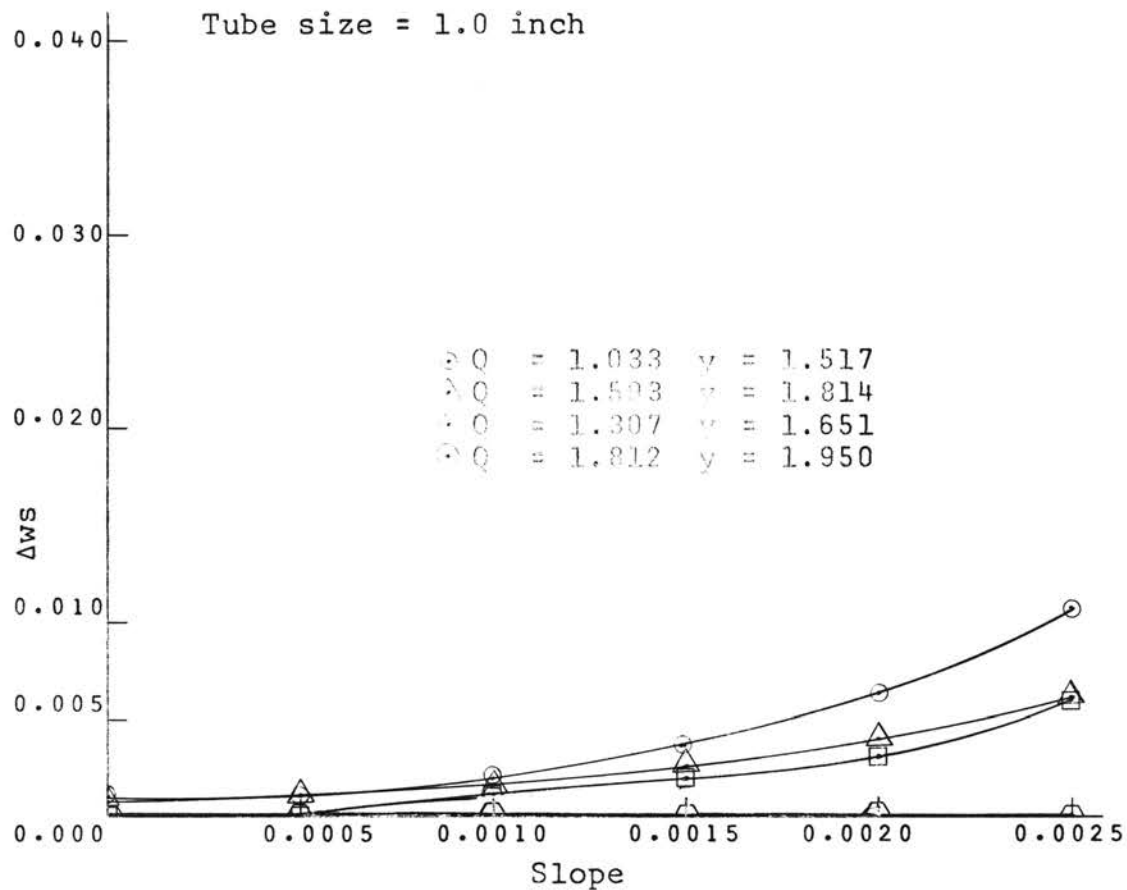


Figure 55. Change in Water Surface Elevation Between the Upstream and Downstream End of the Prismatic Channel as a Function of Slope for the 1.0-Inch Tubes with Various Depths and Entering Q's

than is currently available. Generally, the channels are constructed along the slope of the land and the prevailing situation would put the outlets below the furrow elevation.

The percentage change in tube discharge as a function of slope and tube diameter for a constant entering Q is shown in Figures 56 to 59. The calculated values are given in Appendix F. The figures are for sloping prismatic channels with the tube outlets at the same elevation of 1.224 feet above the channel bottom at the downstream end of the channel. The largest change in discharge obtained was 5 per cent for the 1.5-inch tubes. For practical purposes a change of 5 per cent would not warrant a change in channel design to yield a more uniform flow from the tubes. Thus, a level channel has little, if any, advantages of uniform water application over a sloping channel with tubes at a constant elevation. This is assuming that the elevation of the tubes can be placed above the elevation of the furrows.

Tube Elevation 1.224 Feet Above Channel Bottom

Water surface profiles for prismatic channels with tubes the same distance from the bottom were calculated. The tube outlet elevations were 1.224 feet above the channel bottom. The calculated values for the water surface at 30 foot intervals are shown in Appendix G.

Figures 60 to 63 show the change in water surface (Δw_s) as a function of slope for different entering Q 's

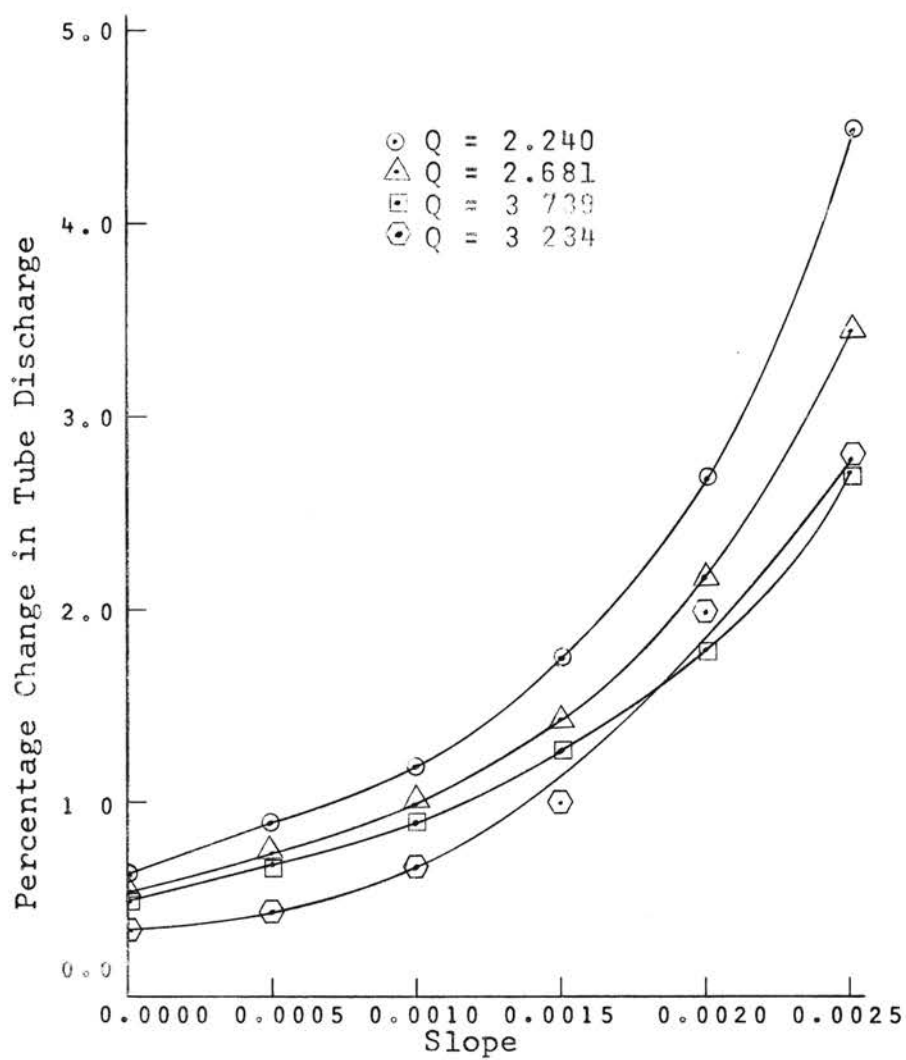


Figure 56. Percentage Change in the 2.00-Inch Tube Discharge for Tubes At a Constant Elevation in a Prismatic Channel with Various Slopes

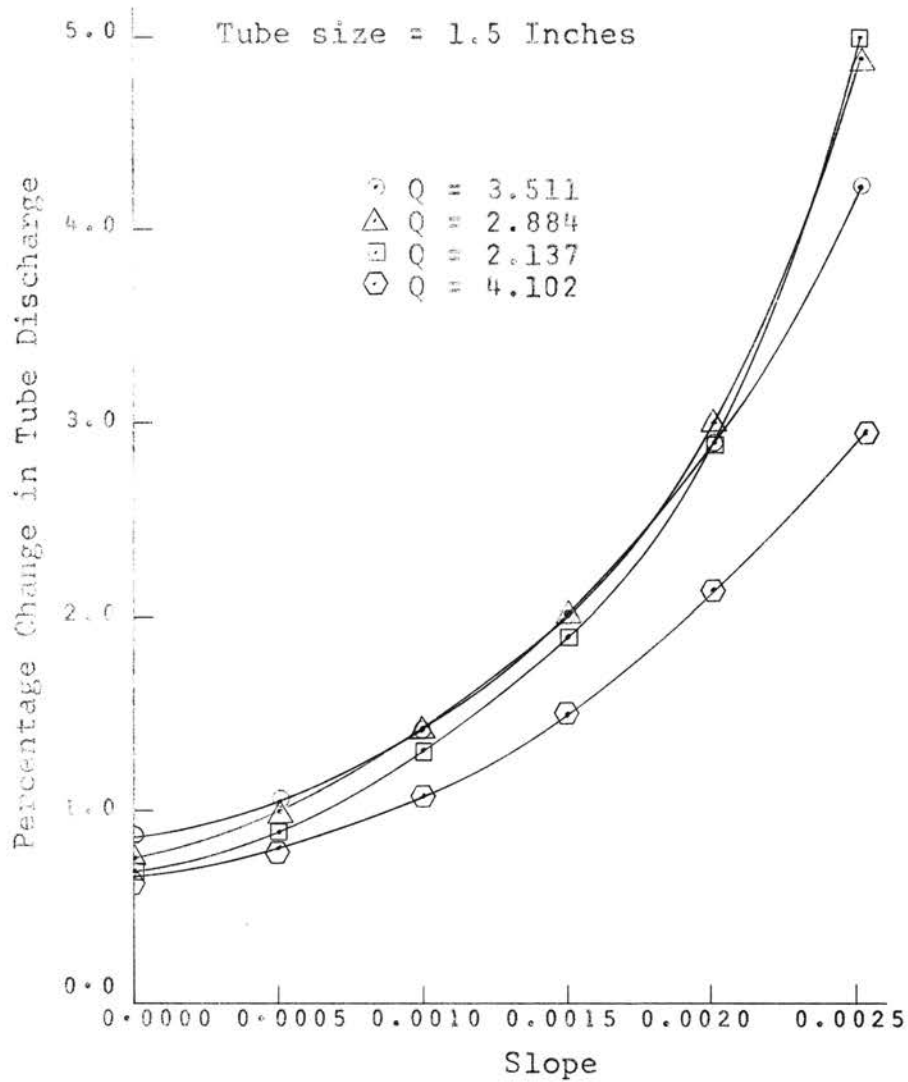


Figure 57. Percentage Change in the 1.5-Inch Tube Discharge for Tubes At a Constant Elevation in a Prismatic Channel with Various Slopes

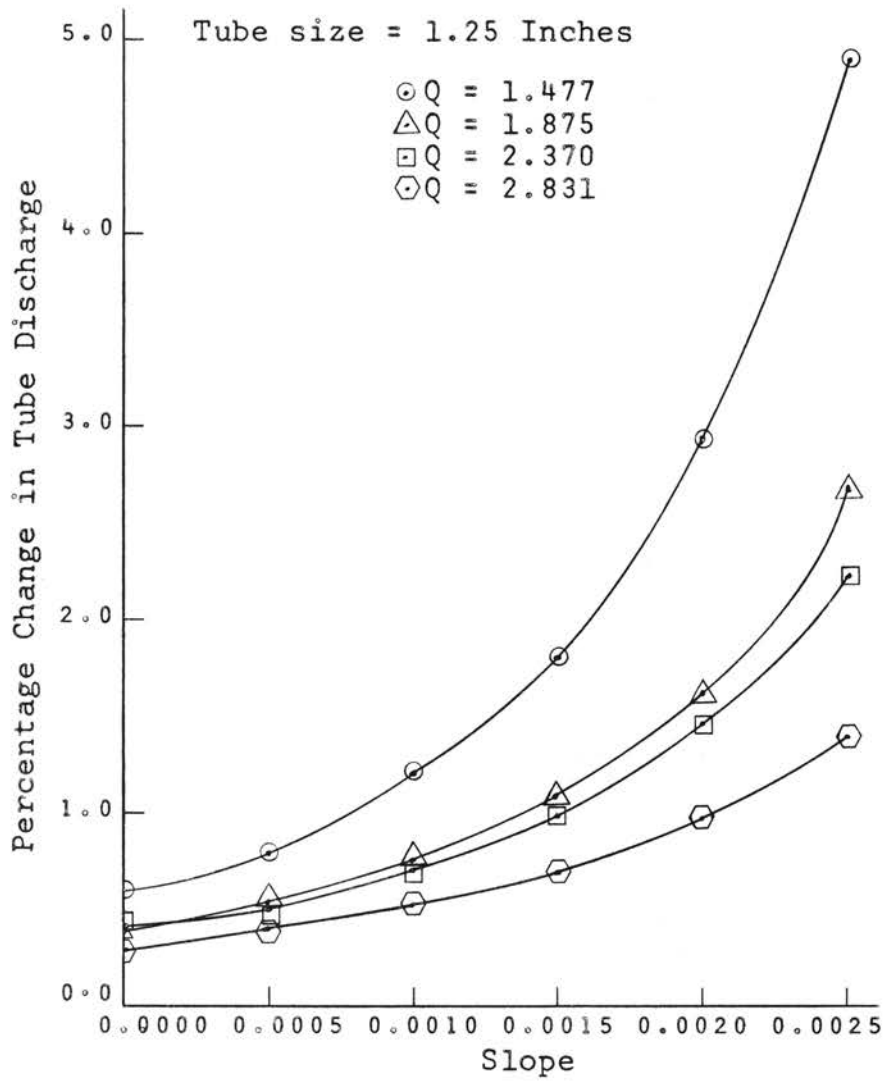


Figure 58. Percentage Change in the 1.25-Inch Tube Discharge for Tubes At a Constant Elevation in a Prismatic Channel with Various Slopes

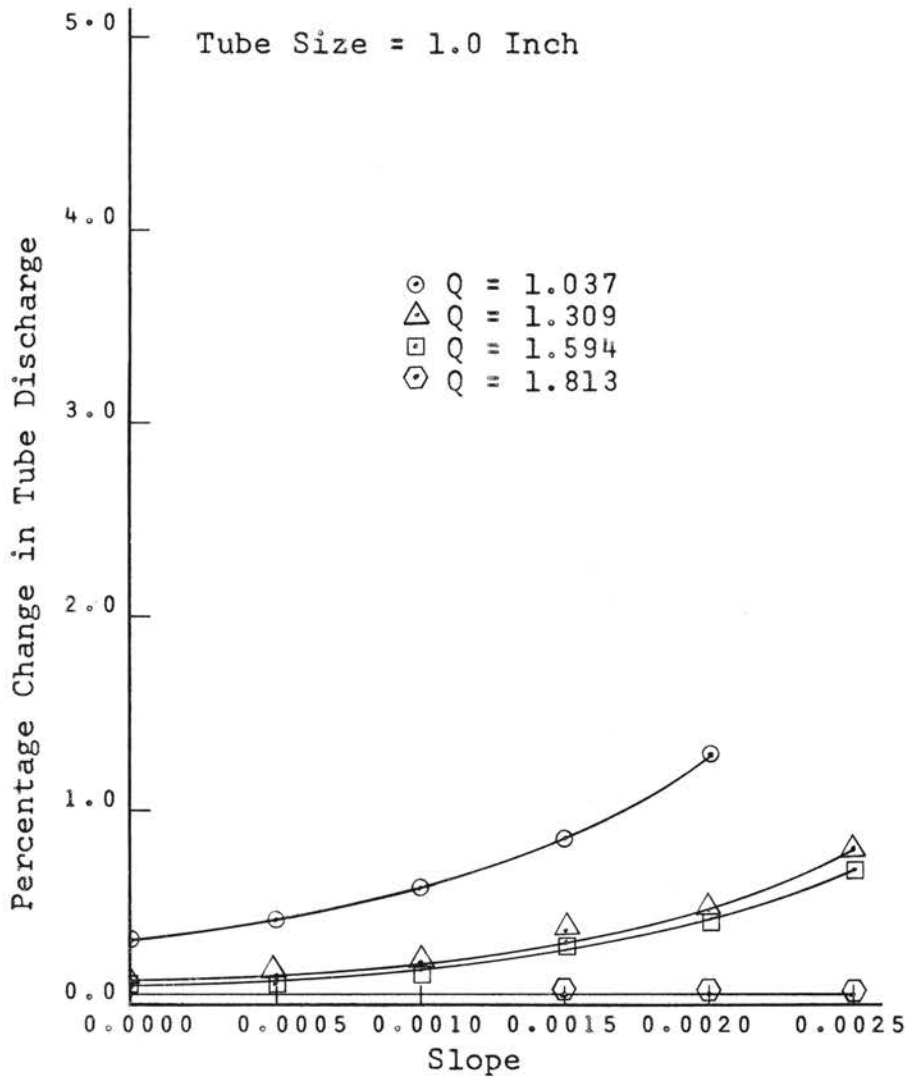


Figure 59. Percentage Change in the 1.0-Inch Tube Discharge for Tubes At a Constant Elevation in a Prismatic Channel with Various Slopes

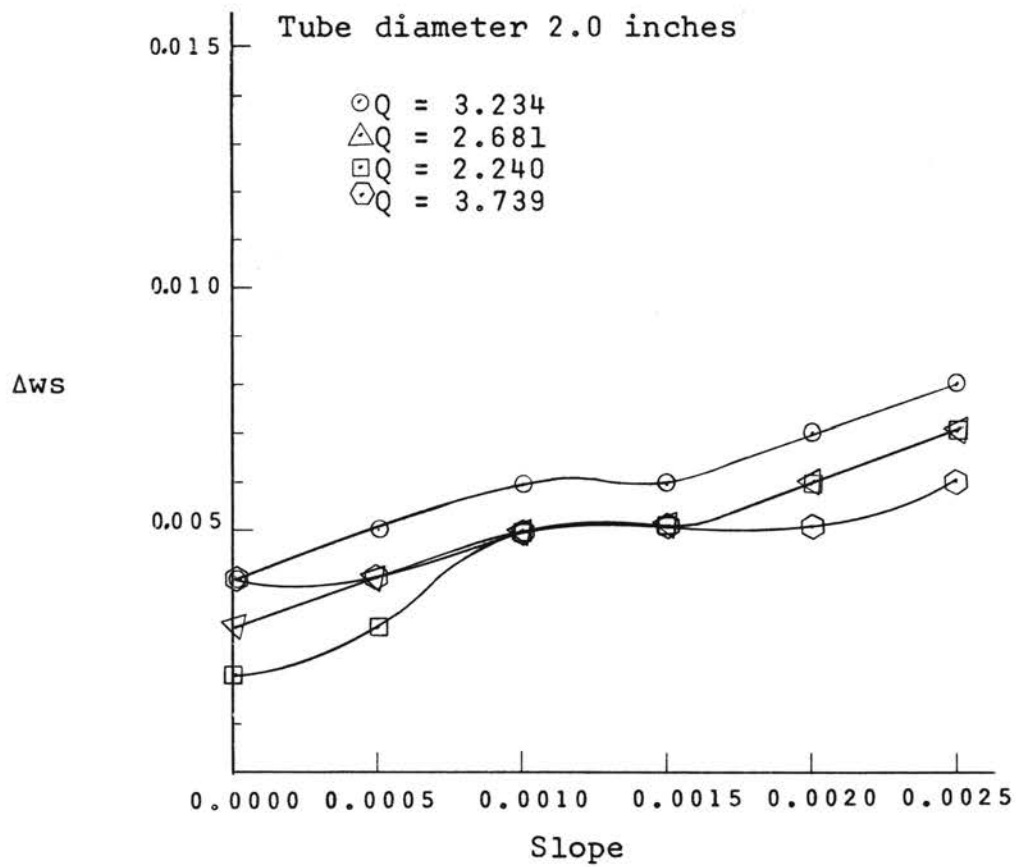


Figure 60. Δw_s As a Function of Slope for a Prismatic Channel With 2.0-Inch Siphon Tubes. The Tube Outlets Were 1.224 Feet Above the Channel Bottom

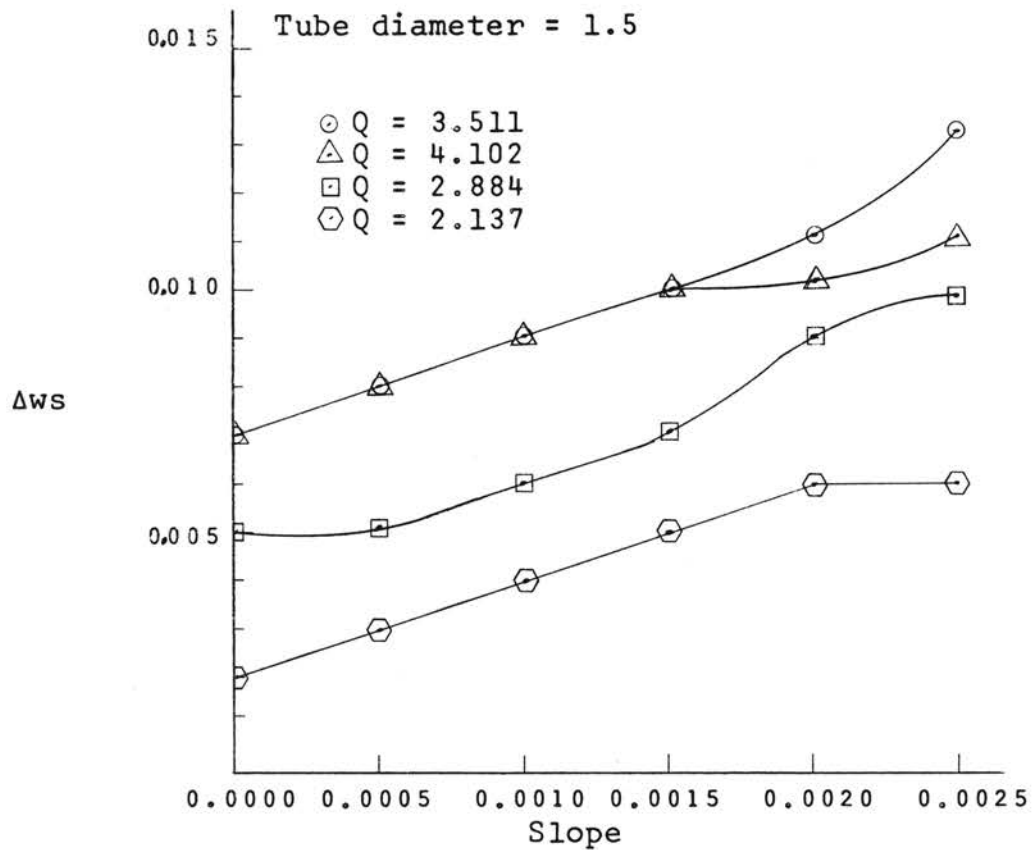


Figure 61. Δw_s As a Function of Slope for a Prismatic Channel with 1.5-Inch Siphon Tubes. The Tube Outlets Were 1.224 Feet Above the Channel Bottom

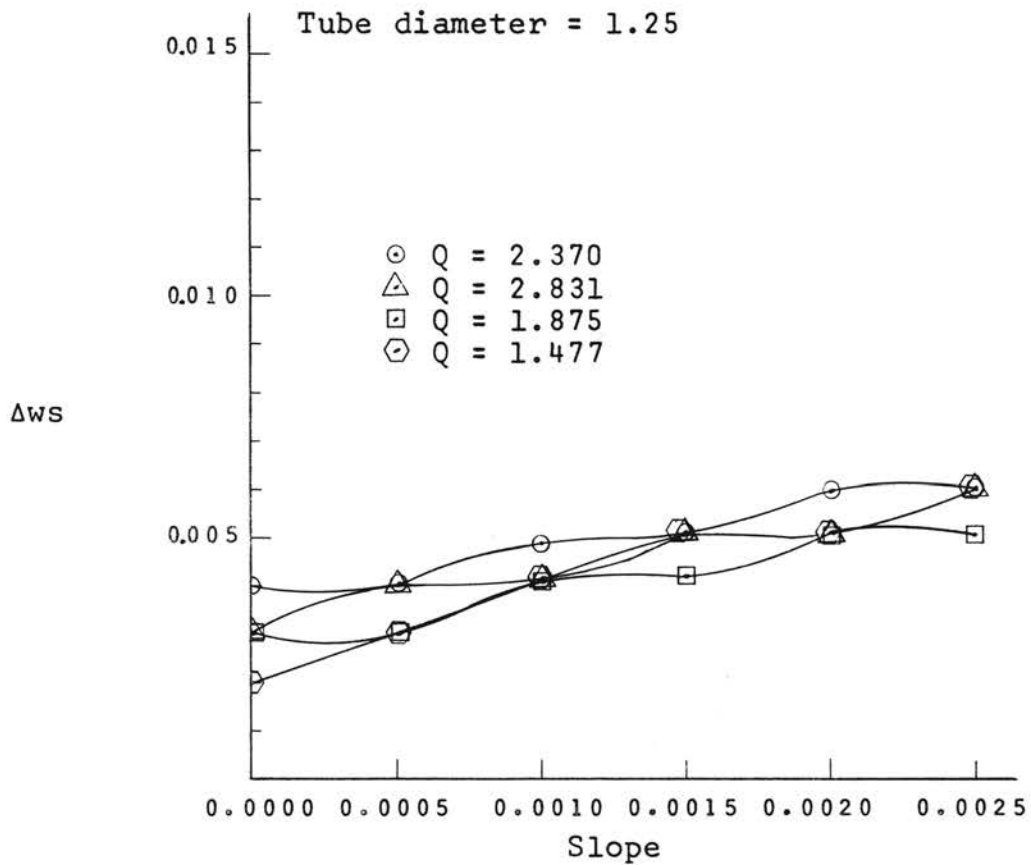


Figure 62. Δw_s As a Function of Slope for a Prismatic Channel with 1.25-Inch Siphon Tubes. The Tube Outlets Were 1.224 Feet Above the Channel Bottom

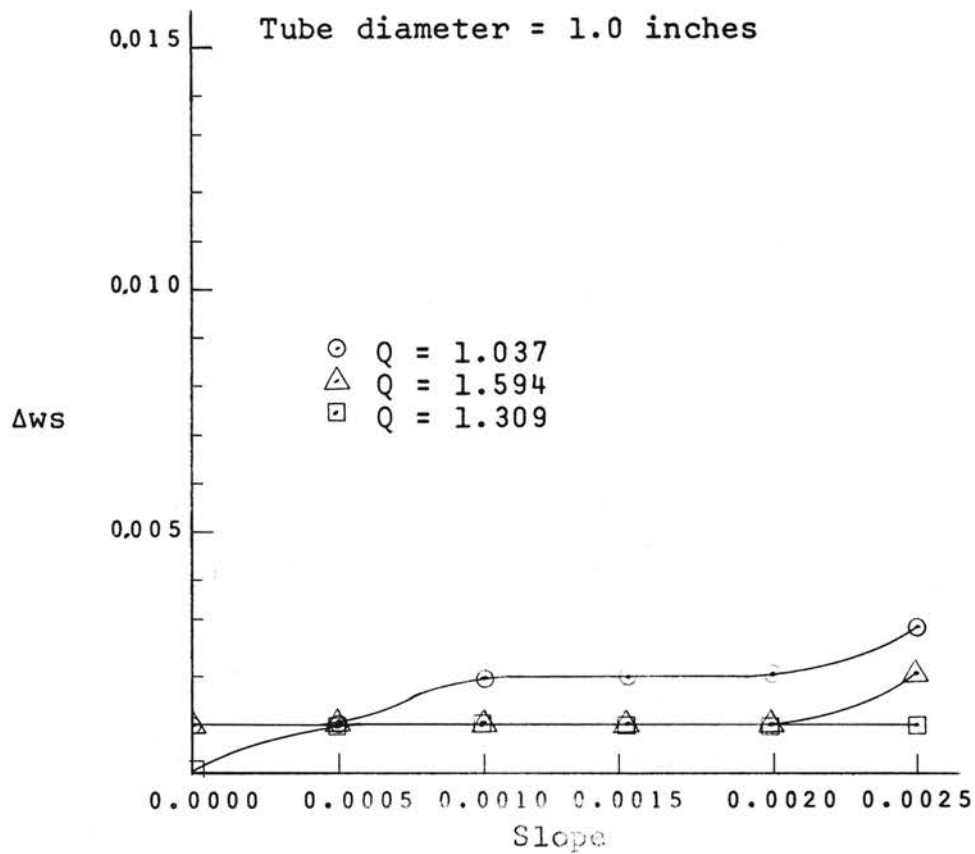


Figure 63. Δw_s As a Function of Slope for a Prismatic Channel with 1.0-Inch Siphon Tubes. The Tube Outlets Were 1.224 Feet Above the Channel Bottom

and a fixed tube diameter. The changes in water surface elevations Δw_s were slightly smaller than the changes for the channel with the tube outlets at a constant elevation because the head on the tubes at the upstream end was not sufficient to produce flow from the tubes at the low entering Q 's.

The drastic change occurred in the percentage change in tube flow. The range was from 0.2 per cent at the small slopes and large Q 's to 100.0 per cent at the large slope and small Q 's. The percentage change in tube discharge as a function of slope is shown in Figures 64 and 67, and calculated values are given in Appendix H.

When the allowable variation in discharge which can be tolerated is decided, the limiting slope for a given tube diameter can be determined from the graphs.

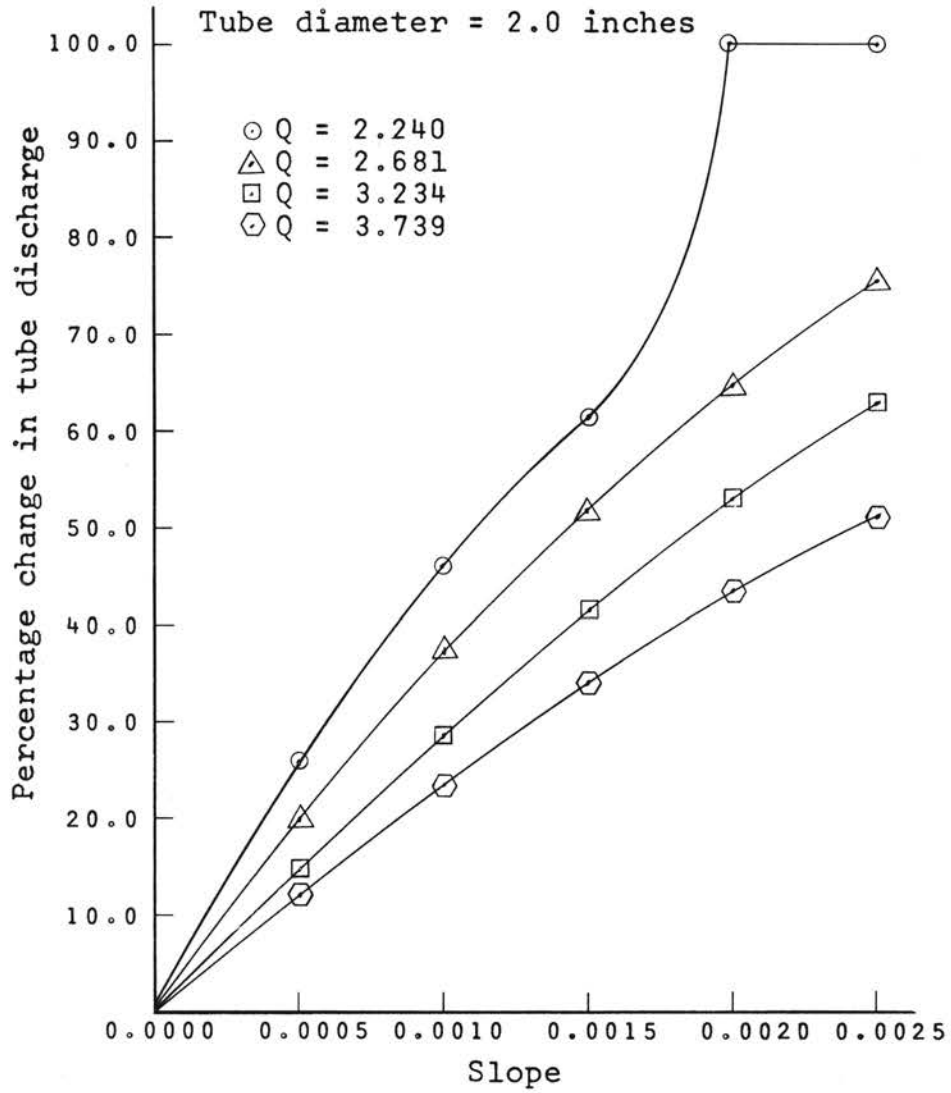


Figure 64. Percentage Change in the 2.00-Inch Tube Discharge for a Prismatic Channel with Various Slopes. The Tube Outlets Were 1.224 Feet From the Channel Bottom

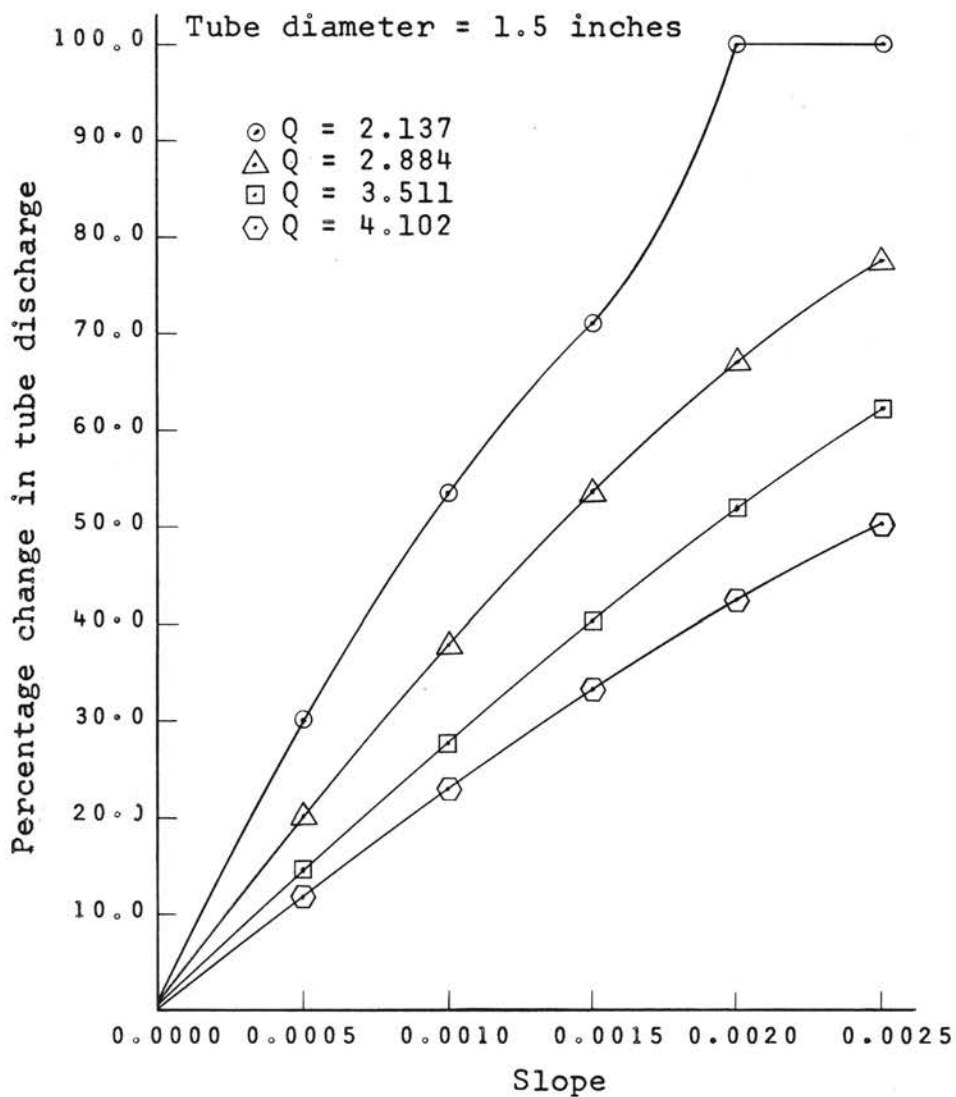


Figure 65. Percentage Change in the 1.5-Inch Tube Discharge for a Prismatic Channel with Various Slopes. The Tube Outlets Were 1.224 Feet From the Channel Bottom

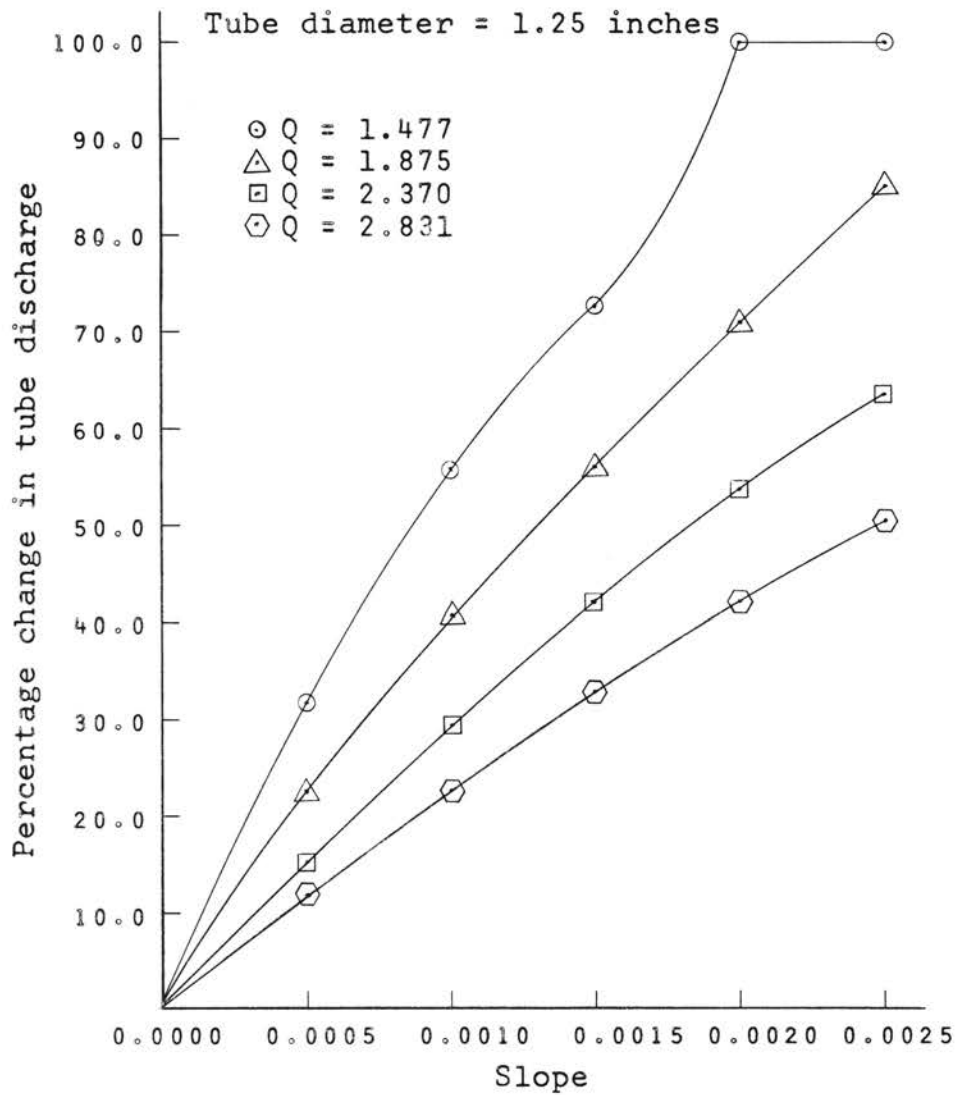


Figure 66. Percentage Change in the 1.25-Inch Tube Discharge for a Prismatic Channel with Various Slopes. The Tube Outlets Were 1.224 Feet From the Channel Bottom

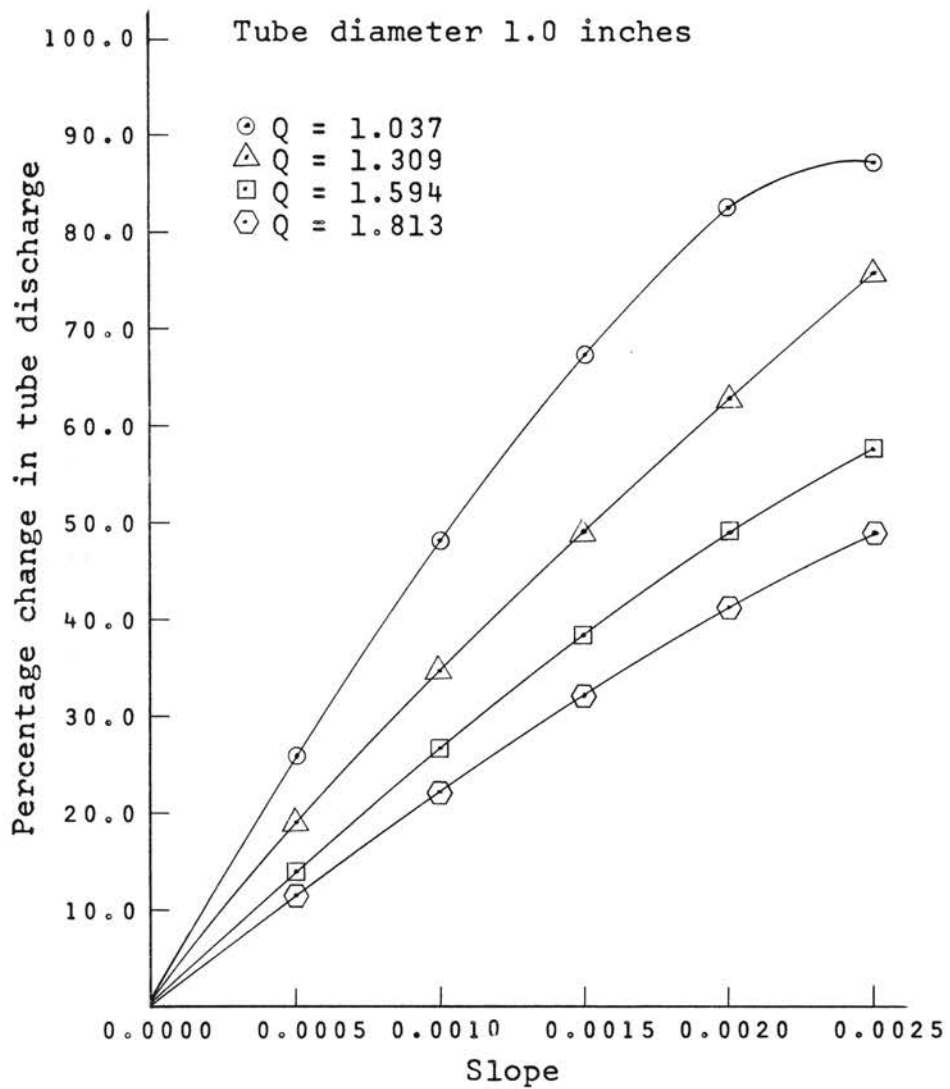


Figure 67. Percentage Change in the 1.00-Inch Tube Discharge for a Prismatic Channel with Various Slopes. The Tube Outlets Were 1.224 Feet From the Channel Bottom

CHAPTER VIII

SUMMARY AND CONCLUSIONS

Summary

Ordinarily, irrigation distribution channels have slope. Sloping channels were believed to result in non-uniform water distribution. The hypothesis was made that a level channel would distribute the water more uniformly. The hypothesis was confirmed by a preliminary computer analysis using assumed values of α and n . A weakness of the theoretical study was a lack of knowledge of the values α and n , and the effects of their variation on the hydraulic behavior of the channel.

A 320-foot distribution channel was constructed at the Stillwater Outdoor Hydraulic Laboratory. The hydraulic properties of the channel with and without siphon tubes were obtained from gradually varied flow tests. The hypothesis being that these hydraulic properties were applicable for spatially varied flow.

Relationships were found for α as a function of tube diameter, submergence, and Reynolds number. The functional relationships of α were used for calculating n_α and a set of water surface profiles. The inclusion of

alpha increased the value of resistance and decreased the predicted water surface profiles. Computations with n and $\alpha = 1$ gave improved estimates of the water surface elevations. The maximum difference between the predicted and observed profiles at the upstream end was 0.007 foot for n -cal $\alpha=1$ and 0.009 foot for n -cal α -cal.

The resistance (n) of the channel was shown to be a function of the hydraulic radius, tube diameter, submergence and the Reynolds number for the gradually varied flow tests.

The value of resistance \bar{n} that would yield the water surface profile as found by statistically fitting curves to the observed measurements of the water surface was calculated for each spatially varied flow test with the associated entering Q . This value of \bar{n} predicted the spatially varied flow water surface profiles closer than any other values of n .

The values of \bar{n} were used for predicting the water surface profiles in sloping trapezoidal channels with (1) the tube outlets elevated 1.224 feet from the bottom of the channel, and (2) the tube outlets set at a constant elevation of 1.224 feet above the channel bottom at the downstream end.

A maximum of 5 per cent variation in tube discharge was found to exist with the sloping channel with a constant tube outlet elevation. This variation is within acceptable limits for uniform water distribution. Such

a system could be limited physically because of the slope of the land and the furrow elevations.

A large variation in tube discharge was found for the sloping channel with the tube outlet placed 1.224 feet from the channel bottom. This system does not distribute the water uniformly along the length of the channel.

This study confirmed the hypothesis that a level distribution channel results in a more uniform water application.

Conclusions

The following conclusions are based on the interpretation of the experimental results.

1. The value of the energy coefficient α increased as the Reynolds number (N_R) increased for the channel with siphon tubes. For gradually varied flow with siphon tubes, α increased as the tube diameter (D), submergence (S_u), and the Reynolds number (N_R) increased. This indicated that α was indeed a function of the Reynolds number and the boundary geometry.
2. An α value of unity should be used in computing water surface profiles while using an n value that was calculated with an α of unity from the gradually varied flow tests. The effects of α are absorbed in the resistance term when α is considered to

be unity in calculating S_s . The alpha values obtained in the spatially varied flow test were of the same magnitude as those found in the gradually varied flow test.

3. The resistance n was a function of the Reynolds number and the values of n obtained for the channel without tubes were of the same magnitude as the n values for concrete channels found in text books.
4. Equations 24 and 25 are adequate for estimating the resistance for gradually varied flow for the experimental channel with siphon tubes. However, the n values for gradually varied flow did not accurately predict the water surface profiles as observed at the high flow rates in the spatially varied flow tests.
5. The energy equation in conjunction with a correct \bar{n} can be used to predict the water surface profiles for decreasing spatially varied flow.
6. The effective resistance value (n_e) calculated from Manning's equation based on uniform flow and hydraulic properties at the upstream end of the experimental channel is equal to $0.0019 + 0.483 \bar{n}$.
7. A sloping channel with the siphon tube outlets set 1.224 feet above the downstream channel

bottom distributed the water uniformly. Land slope and furrow elevation would limit the application of this type of system.

8. A sloping channel with the siphon tube outlets 1.224 feet above the channel bottom did not distribute the water uniformly.
9. A level channel with the siphon tube outlets 1.224 feet above the channel bottom distributed the water uniformly along the length of the channel. The maximum observed difference in the water surface elevation in the spatially varied flow test was 0.007. Considering the physical limitations of (7) and the nonuniform distribution of (8) a level distribution channel with a constant tube elevation is the most desirable of the three systems.

Suggestions For Further Research

The results from this study and the limitations of the experimental setup suggest the following items as possible subjects for investigation:

1. A functional relationship for resistance \bar{n} which includes tube diameter, tube spacing, tube submergence, entering discharge, channel length, and depth is needed to predict the water surface profiles for decreasing spatially varied flow.
2. Since the cost of a channel is largely determined by the depth, and the channel resistance is a major factor in determining the depth, the possibility of distributing the water through slots in the side of the channel should be investigated.
3. A long distribution channel could be constructed as a series of level bays. The drop between bays and the length of the bays may determine the depth of channel needed.
4. As shown in the preliminary investigation, the resistance of the channel for a given depth definitely affects the water surface elevation. Thus, the minimum depth for a given Q which will still distribute the water uniformly needs to be determined.

BIBLIOGRAPHY

1. Aris, R. Vectors, Tensors, and the Basic Equations of Fluid Mechanics. Prentice-Hall, 1962.
2. Bakhmeteff, Boris A. Hydraulics of Open Channels. New York: McGraw-Hill, 329, 1932.
3. Bazin. H. E. "Recherches Hydrauliques." Paris, 1865.
4. Beij, K. Hilding. "Flow in Roof Gutters." Journal of Research of the National Bureau of Standards. 12:193-213, 1934.
5. Bettess, F. "Non-Uniform Flow in Channels." Civil Engineering and Public Works Review. No. 610. 52(1):434-436, March, 1957.
6. Bettess, F. "Non-Uniform Flow in Channels." Civil Engineering and Public Works Review. No. 610. 52(2), April, 1957.
7. Binder, R. C. Advanced Fluid Mechanics. Prentice-Hall, 1958.
8. Boyer, M. C. "Estimating the Manning Coefficient from an Average Bed Roughness in Open Channels." Transactions of the American Geophysical Union. 35(6):957-961, December, 1954.
9. Camp, Thomas R. "Lateral Spillway Channels." Transactions of the American Society of Civil Engineers. 105:606-617, 1940.
10. Chow, Ven Te. "A Note on Manning Formula." Transactions of the American Geophysical Union. 36(4), August, 1955.
11. Chow, Ven Te. Open Channel Hydraulics. New York: McGraw-Hill, 680, 1959.
12. Cunningham, Allen J. C. "Recent Hydraulic Experiments." Proceedings Institute of Civil Engineering. London: 71(1), 1882.

13. Eisenlohr, William S., Jr. "Coefficients for Velocity Distribution in Open Channel Flow." Transactions of the American Society of Civil Engineers. 110:633-644, 1945.
14. Garton, J. E. "Automation of Cut-Back Furrow Irrigation." Unpublished Ph.D. dissertation, University of Missouri, 1964.
15. Garton, J. E. "Automation of Cut-Back Furrow Irrigation." Paper No. 63-719. Presented to Annual Meeting, American Society of Agricultural Engineers, Chicago, Illinois, December, 1963.
16. Garton, J. E. and A. L. Mink. "Spatially Varied Flow in an Irrigation Distribution Ditch." Transactions of the American Society of Agricultural Engineers. 8(4):530-531, 1965.
17. Hanson, V. E. "New Concepts in Irrigation Efficiency." Presented to the Annual Meeting of the American Society of Agricultural Engineers, East Lansing, Michigan, June 25, 1957.
18. Hanson, V. E., J. L. Haddock, and S. A. Taylor. "Irrigation Fertilization and Soil Management of Crops in Rotation." 1941 Annual Progress Report, Utah Agricultural Experiment Station, Logan, Utah: November, 1952.
19. Hinds, Julian. "Side Channel Spillways: Hydraulic Theory, Economic Factors, and Experimental Determination of Losses." Transactions of the American Society of Civil Engineers. 89:881-927, 1926.
20. Horton, R. E. "Separate Roughness Coefficients for Channel Bottom and Sides." Engineering News-Record. November 30, 1933.
21. Houk, Ivan E. "Calculation of Flow in Open Channels." Technical Reports, Part IV, Dayton, Ohio. The Miami Conservancy District, State of Ohio, 1918.
22. Israelson, O. W. and V. E. Hanson. Irrigation Principles and Practices. III. New York, John Wiley and Sons, Inc., 1962.

23. Israelson, O. W. and H. F. Blaney. Water Application Efficiencies in Irrigation. United States Department of Agriculture, February, 1946.
24. Jaeger, Charles. Engineering Fluid Mechanics. Trans. P. O. Wolf. London: Blackie and Son, 1956.
25. Johnson, C. N. "Comparison Performances of Metallic and Plastic Siphon Tubes." Agricultural Engineering. 469-470, October, 1946.
26. Keflemariam, Joseph. "Flow Through Plastic Siphon Tubes." Special Report, Agricultural Engineering Department, Oklahoma State University, 1966.
27. Keulegan, Garbis H. "Equation of Motion for the Steady Mean Flow of Water in Open Channels." Journal of Research of the National Bureau of Standards. 29:97-111, 1942.
28. Keulegan, Garbis H. "Laws of Turbulent Flow in Open Channels." Journal of Research of the National Bureau of Standards. 21:707-741, 1938.
29. Keulegan, Garbis H. "Spatially Variable Discharge Over a Sloping Plane." Transactions, American Geophysical Union. VI:956-959, 1944.
30. Kindsvater, C. E. "Selected Topics of Fluid Mechanics." Geological Survey Water-Supply Paper. 1369A, 2nd, 1962.
31. King, Horace W. Handbook of Hydraulics. 4th ed. New York: McGraw-Hill, 1954.
32. Long, Horace W. and Ernest F. Brater. Handbook of Hydraulics. 5th ed. New York: McGraw-Hill, 1963.
33. Kolupaila, Steponas. "Methods of Determination of the Kinetic Energy Factor." The Port Engineer. Calcutta, India: 5:12-18, 1956.
34. Kruse, G. E. "The Hydraulics of Small Rough Irrigation Channels. International Commission on Irrigation and Drainage, Fifth Congress. R.11, Question 16.
35. Li, Wen-Hsiung. "Open Channels with Nonuniform Discharge." Transactions of the American Society of Civil Engineers. 120:255-274, 1955.

36. Manning, Robert. "On the Flow of Water in Open Channels and Pipes." Transactions of the Institute of Civil Engineering. 20: 1891.
37. McCool, D. K. "Spatially Varied Steady Flow in a Vegetated Channel." Unpublished Ph.D. dissertation, Oklahoma State University, 1965.
38. Murphy, Glenn. Similitude in Engineering. New York: Ronald Press, 302, 1950.
39. Nielson, Kaj. L. Methods in Numerical Analysis. New York: Macmillan, 382, 1956.
40. Natrella, M. G. "Experimental Statistics." Handbook 91, National Bureau of Standards. Government Printing Office, 1963.
41. "Nomenclature for Hydraulics." ASCE-Manuals and Reports on Engineering Practice No. 43. New York: American Society of Civil Engineers, 501, 1962.
42. O'Brien, Morrrough P. and Joe W. Johnson. "Velocity-Head Correction for Hydraulic Flow." Engineering News-Record. 113:214-216, 1934.
43. Page, L. Introduction to Theoretical Physics. 2nd ed. Van horstead, 21-22, 1935.
44. Robinson, A. R. and M. L. Albertson. "Artificial Roughness Standard for Open Channels." Transactions, American Geophysical Union. 33(6): 881-887, December, 1952.
45. Rouse, Hunter. Elementary Fluid Mechanics. New York: Wiley, 1946.
46. Rouse, Hunter. Engineering Hydraulics. New York: Wiley, 1039, 1950.
47. Rouse, Hunter and John S. McNown. "Discussion of 'Coefficients for Velocity Distribution in Open Channel Flow' by William S. Eisenlohr, Jr." Transactions of the American Society of Civil Engineers. 110:651-657, 1945.
48. Stoker, J. J. "Water Waves, the Mathematical Theory with Applications." Pure and Applied Mathematics. ed. R. Courant, L. Bers, J. J. Stoker. New York: Interscience. IV:567, 1957.

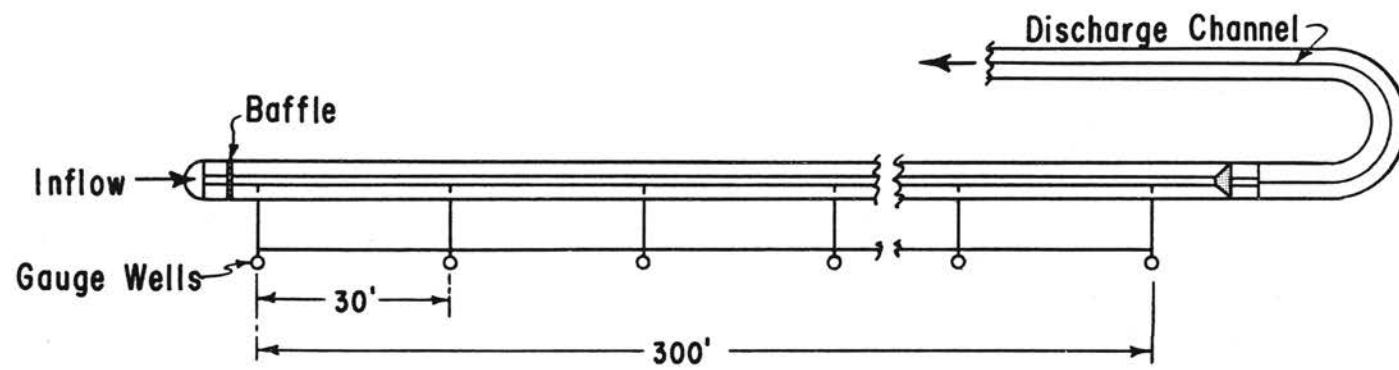
49. Straub, L. G., E. Silberman, and H. C. Nelson. "Open Channel Flow at Small Reynolds Numbers." Transactions of the American Society of Civil Engineers. 123:685-706, 1958.
50. Streeter, V. L. "The Kinetic Energy and Momentum Correction Factors for Pipes and for Open Channels of Great Width." Civil Engineering. 12(4):212-214, April, 1942.
51. Tovey, R. and V. I. Myers. "Evaluation of Some Irrigation Water Control Devices." Idaho Agricultural Experiment Station Bulletin No. 319, December, 1959.
52. Van Driest, E. R. "Discussion of 'Coefficients for Velocity Distribution in Open Channel Flow' by William S. Eisenlohr, Jr." Transactions of the American Society of Civil Engineers. 110:648-651, 1945.
53. Woo, Dah-Cheng and Ernest F. Brater. "Spatially Varied Flow from Controlled Rainfall." Proceedings of the American Society of Civil Engineers, Journal of the Hydraulics Division. 88(6-1):31-56, 1962.

APPENDIX A

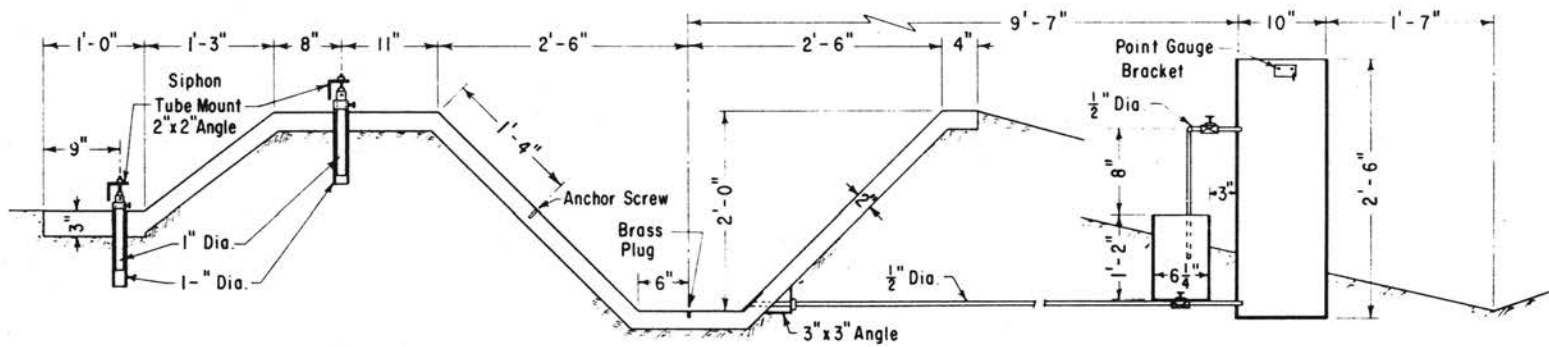
SKETCH OF THE EXPERIMENTAL SETUP

A TYPICAL CROSS-SECTION OF THE EXPERIMENTAL SETUP

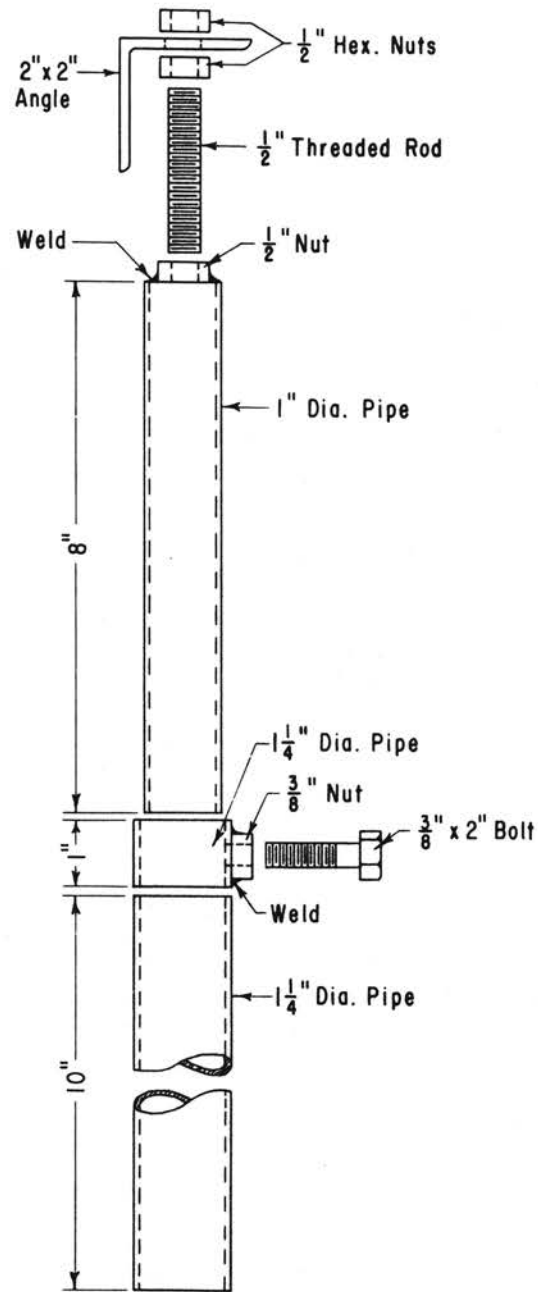
DETAILED VIEW OF THE SIPHON TUBE MOUNT



Sketch of Experimental Setup



A Typical Cross-Section of the Experimental Setup



Detailed View of the Siphon Tube Mount

APPENDIX B

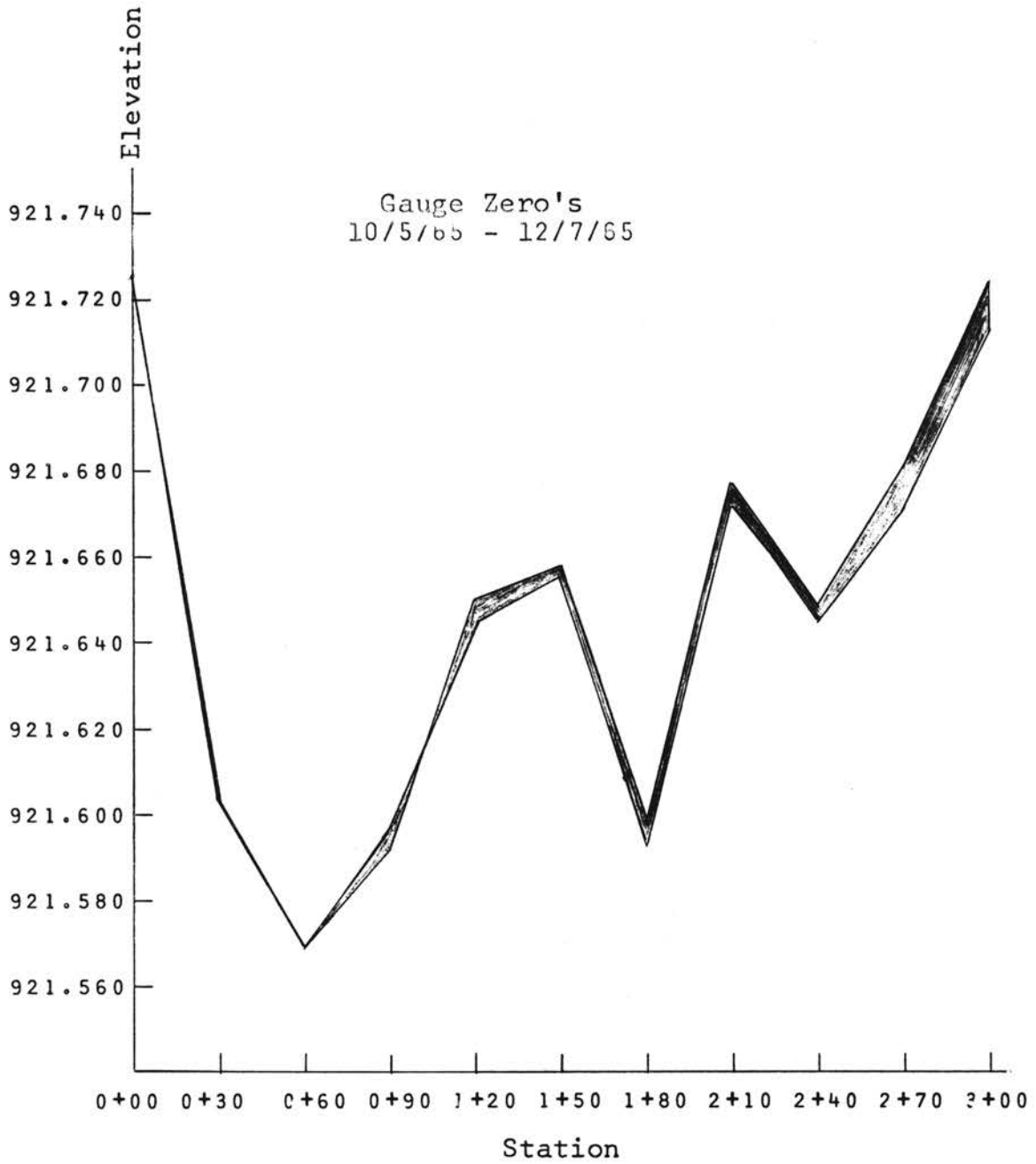
COEFFICIENTS FOR THE AREA, WETTED PERIMETER,
AND TOP WIDTH EQUATIONS FOR THE
EXPERIMENTAL CHANNEL

Station	Data Set	Areas				Top Width			
		a ₀	a ₁	Correlation Coefficient	Standard Deviation	b ₀	b ₁	Correlation Coefficient	Standard Deviation
0 + 00	I-9-20-65	1.023	1.014	1.000	0.002	1.034	2.021	1.000	0.007
	II-4-19-66	1.036	1.004	1.000	0.001	1.044	2.005	1.000	0.006
0 + 30	I	1.038	1.010	1.000	0.001	1.041	2.021	1.000	0.010
	II	1.043	1.002	1.000	0.002	1.050	2.000	1.000	0.007
0 + 60	I	1.041	1.006	1.000	0.001	1.042	2.014	1.000	0.011
	II	1.048	1.001	1.000	0.001	1.053	1.999	1.000	0.005
0 + 90	I	1.043	1.007	1.000	0.001	1.050	2.013	1.000	0.006
	II	1.050	1.002	1.000	0.001	1.054	2.002	1.000	0.004
1 + 20	I	1.044	1.005	1.000	0.001	1.047	2.010	1.000	0.005
	II	1.045	1.003	1.000	0.001	1.054	1.998	1.000	0.004
1 + 50	I	1.035	1.013	1.000	0.001	1.044	2.019	1.000	0.006
	II	1.041	1.007	1.000	0.001	1.049	2.008	1.000	0.005
1 + 80	I	1.041	1.006	1.000	0.000	1.047	2.008	1.000	0.004
	II	1.051	0.997	1.000	0.000	1.055	1.992	1.000	0.004
2 + 10	I	1.036	1.012	1.000	0.002	1.049	2.014	1.000	0.005
	II	1.046	1.002	1.000	0.002	1.057	1.995	1.000	0.005
2 + 40	I	1.020	1.033	1.000	0.008	1.069	2.022	1.000	0.017
	II	1.013	1.023	1.000	0.008	1.066	2.001	1.000	0.007
2 + 70	I	1.053	1.011	1.000	0.002	1.058	2.018	1.000	0.009
	II	1.054	1.003	1.000	0.002	1.062	2.000	1.000	0.006
3 + 00	I	1.041	1.011	1.000	0.001	1.046	2.019	1.000	0.010
	II	1.041	1.006	1.000	0.001	1.048	2.007	1.000	0.006
Between and 0 + 60 and 0 + 90	I	1.053	0.961	1.000	0.001	1.053	1.926	1.000	0.010
		1.061	0.956	1.000	0.000	1.067	1.909	1.000	0.004

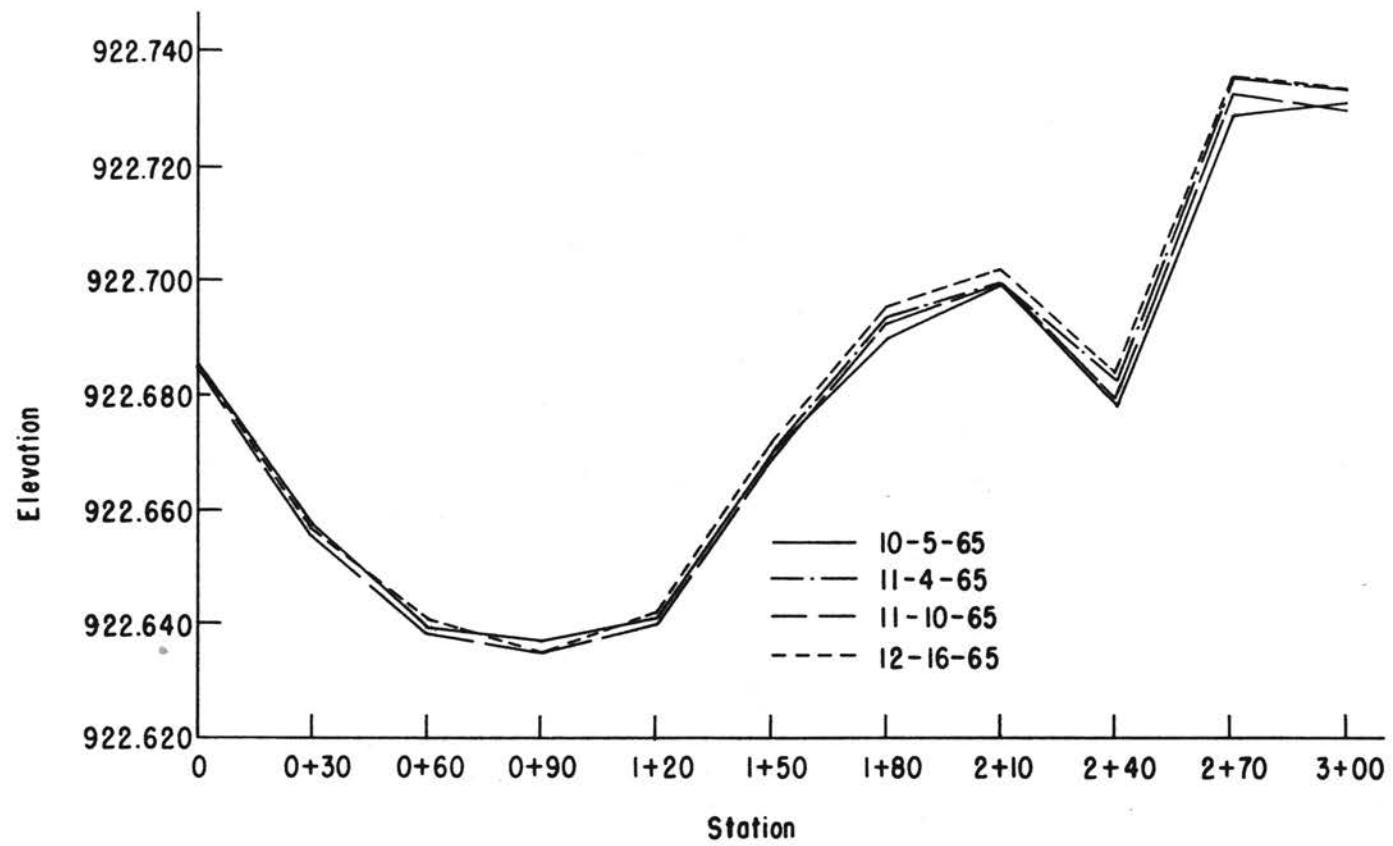
Station	Data Set	Wetted Perimeter			
		c_0	c_1	Correlation Coefficient	Standard Deviation
0 + 00	I	1.016	2.844	1.000	0.005
	II	1.031	2.832	1.000	0.005
0 + 30	I	1.028	2.843	1.000	0.007
	II	1.032	2.829	1.000	0.005
0 + 60	I	1.031	2.839	1.000	0.008
	II	1.037	2.828	1.000	0.004
0 + 90	I	1.040	2.838	1.000	0.004
	II	1.043	2.830	1.000	0.003
1 + 20	I	1.037	2.836	1.000	0.004
	II	1.036	2.828	1.000	0.003
1 + 50	I	1.030	2.843	1.000	0.004
	II	1.036	2.835	1.000	0.004
1 + 80	I	1.036	2.834	1.000	0.003
	II	1.047	2.823	1.000	0.002
2 + 10	I	1.028	2.839	1.000	0.004
	II	1.041	2.826	1.000	0.004
2 + 40	I	1.052	2.847	1.000	0.015
	II	1.041	2.830	1.000	0.006
2 + 70	I	1.045	2.842	1.000	0.007
	II	1.048	2.829	1.000	0.005
3 + 00	I	1.042	2.843	1.000	0.008
	II	1.039	2.835	1.000	0.004
Between 0 + 60 and 0 + 90	I	1.037	2.778	1.000	0.008
	II	1.053	2.766	1.000	0.003

APPENDIX C

GAUGE ZERO'S AND BRASS PLUG ELEVATION
FOR THE EXPERIMENTAL CHANNEL



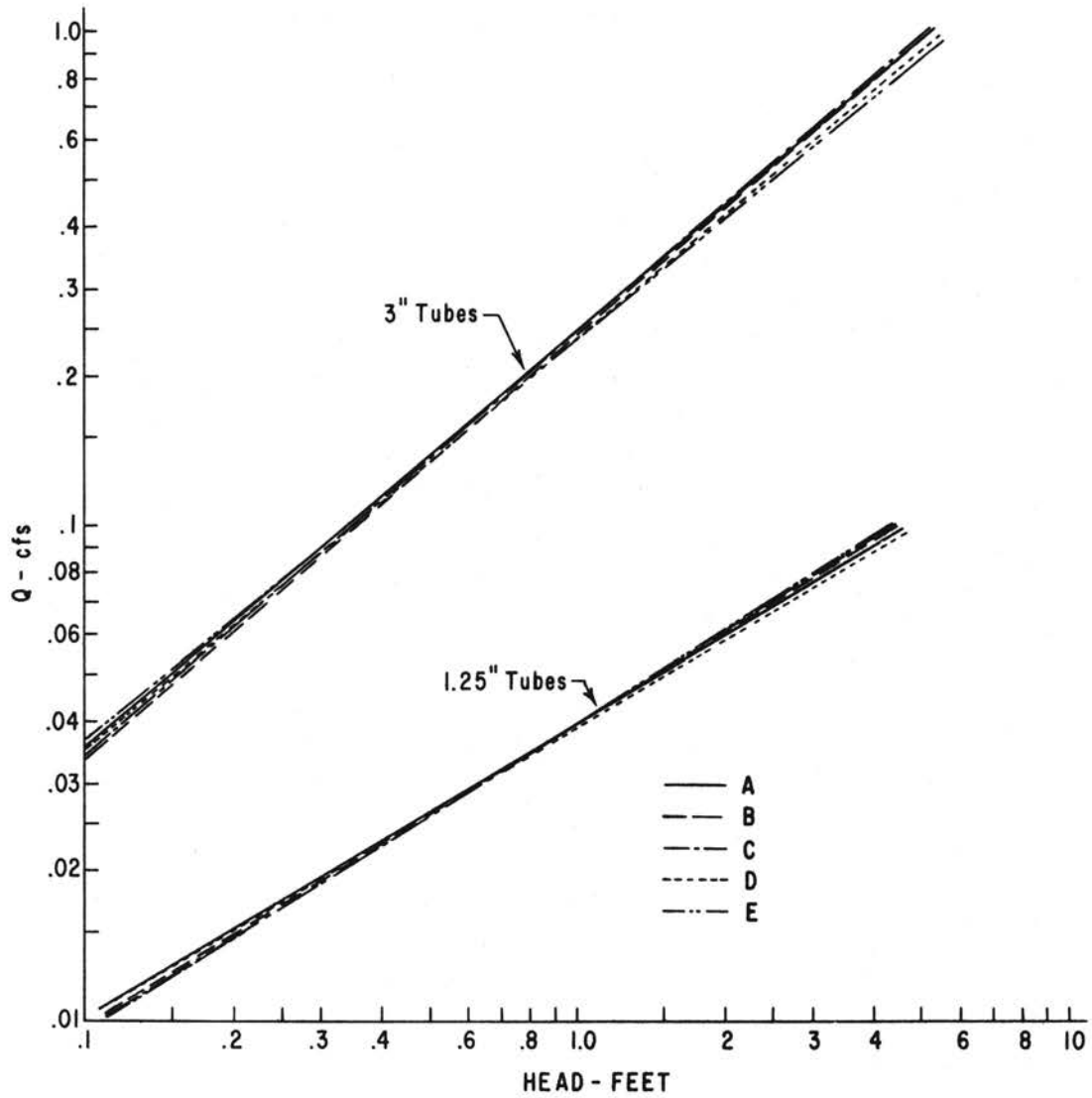
Gauge Zero's For the Gradually Varied Flow Test



Brass Plug Elevation, Fall 1965, Referenced to Station 0 + 00

APPENDIX D

DISCHARGE VERSUS HEAD RELATIONSHIP FOR THE
3.00- AND 1.25-INCH PLASTIC SIPHON TUBES
SHOWING THE VARIATION IN DISCHARGE
WITHIN A TUBE SIZE



Discharge Versus Head Relationship for the 3.00- And 1.25-Inch Plastic Siphon Tubes Showing the Variation in Discharge Within a Tube Size

APPENDIX E

OBSERVED AND CALCULATED WATER SURFACE ELEVATIONS
FOR THE ACTUAL AND PRISMATIC CHANNEL WITH
THE TUBES AT A CONSTANT ELEVATION

SVF 4

Q = 2.130

TUBE DIAMETER = 1.50 INCHES

TUBE LOCATION = 1.0 FOOT

ALL TUBES PRIMED

STATION	W.S. OBS.	W.S. NCAL ALPHA=1.0	W.S. N CAL ALPHA CAL	W.S. NBAR
0+00	924.149	924.146	924.146	924.150
0+30	924.151	924.147	924.146	924.149
0+60	924.149	924.147	924.147	924.149
0+90	924.151	924.147	924.147	924.149
1+20	924.148	924.148	924.148	924.149
1+50	924.150	924.148	924.148	924.149
1+80	924.149	924.148	924.148	924.149
2+10	924.149	924.149	924.148	924.149
2+40	924.150	924.149	924.149	924.150
2+70	924.151	924.149	924.149	924.150
3+00	924.149	924.149	924.149	924.150

SLOPE

STATION	0.0000	0.0005	0.0010	0.0015	0.0020	0.0025
0+00	101.474	101.475	101.477	101.479	101.486	101.496
0+30	101.473	101.474	101.475	101.476	101.480	101.483
0+60	101.473	101.473	101.473	101.473	101.476	101.477
0+90	101.472	101.472	101.472	101.472	101.475	101.475
1+20	101.472	101.472	101.472	101.471	101.474	101.474
1+50	101.472	101.472	101.472	101.471	101.474	101.474
1+80	101.472	101.472	101.472	101.471	101.474	101.474
2+10	101.472	101.472	101.472	101.472	101.474	101.474
2+40	101.472	101.472	101.472	101.472	101.474	101.474
2+70	101.472	101.472	101.472	101.472	101.475	101.475
3+00	101.472	101.472	101.472	101.472	101.475	101.475

APPENDIX F

CHANGES IN TUBE DISCHARGE FOR A SLOPING
PRISMATIC CHANNEL WITH THE SIPHON
TUBES AT THE SAME ELEVATION

Tube Size 2.0 Inches

Slope	Q _{in}	Q _{Tmax}	Q _{Tmin}	ΔQ	ΔQ/Q _{Tmax} ×100
SVF 1					
0.0000	3.739	0.08334	0.08305	0.00029	0.3479
0.0005	3.739	0.08335	0.08299	0.00036	0.4319
0.0010	3.739	0.08348	0.08292	0.00056	0.6708
0.0015	3.739	0.08350	0.08285	0.00065	0.7784
0.0020	3.739	0.08370	0.08278	0.00092	1.0991
0.0025	3.739	0.08405	0.08270	0.00235	1.6140
SVF 2					
0.0000	3.240	0.07233	0.7197	0.00036	0.4977
0.0005	3.240	0.07239	0.07190	0.00049	0.6769
0.0010	3.240	0.07247	0.07182	0.00065	0.8969
0.0015	3.240	0.07260	0.07174	0.00092	1.2661
0.0020	3.240	0.07298	0.07167	0.00131	1.7950
0.0025	3.240	0.07360	0.07159	0.00201	2.7309
SVF 3					
0.0000	2.6810	0.05986	0.05954	0.00032	0.5346
0.0005	2.6810	0.05990	0.05946	0.00044	0.7345
0.0010	2.6810	0.05997	0.05937	0.00060	1.0005
0.0015	2.6810	0.60160	0.05929	0.00087	1.4461
0.0020	2.6810	0.06051	0.05920	0.00131	2.1649
0.0025	2.6810	0.06123	0.05911	0.00212	3.4623
SVF 4					
0.0000	2.240	0.05120	0.05087	0.00033	0.6445
0.0005	2.240	0.05122	0.05078	0.00044	0.8590
0.0010	2.240	0.05130	0.05060	0.00061	1.1890
0.0015	2.240	0.05150	0.05059	0.00091	1.7669
0.0020	2.240	0.05189	0.05049	0.00140	2.6980
0.0025	2.240	0.05276	0.05039	0.00237	4.4920

Tube Size 1.5 Inches

Slope	Q_{in}	$Q_{T_{max}}$	$Q_{T_{min}}$	ΔQ	$\Delta Q/Q_{T_{max}} \times 100$
SVF 1					
0.0000	4.102	0.04586	0.04556	0.00030	0.6541
0.0005	4.102	0.04590	0.04553	0.00037	0.8061
0.0010	4.102	0.04599	0.04550	0.00049	1.0654
0.0015	4.102	0.04614	0.04546	0.00068	1.4737
0.0020	4.102	0.04636	0.04542	0.00094	2.0276
0.0025	4.102	0.04676	0.04538	0.00138	2.9512
SVF 2					
0.0000	3.511	0.03931	0.03900	0.00031	0.7886
0.0005	3.511	0.03937	0.03896	0.00041	1.0414
0.0010	3.511	0.03948	0.03892	0.00056	1.4184
0.0015	3.511	0.03967	0.03888	0.00079	1.9914
0.0020	3.511	0.03998	0.03883	0.00115	2.8764
0.0025	3.511	0.04053	0.03879	0.00174	4.2931
SVF 3					
0.0000	2.884	0.03227	0.03203	0.00024	0.7437
0.0005	2.884	0.03231	0.03198	0.00033	1.0213
0.0010	2.884	0.03240	0.03194	0.00046	1.4197
0.0015	2.884	0.03256	0.03189	0.00067	2.9577
0.0020	2.884	0.03286	0.03184	0.00102	3.1040
0.0025	2.884	0.03344	0.03179	0.00165	4.9342
SVF 4					
0.0000	2.137	0.02471	0.02454	0.00017	0.6879
0.0005	2.137	0.02471	0.02449	0.00022	0.8903
0.0010	2.137	0.02475	0.02443	0.00032	1.2929
0.0015	2.137	0.02484	0.02437	0.00047	1.8921
0.0020	2.137	0.02519	0.02445	0.00073	2.8979
0.0025	2.137	0.02569	0.02440	0.00129	4.0214

Tube Size 1.25 Inches

Slope	Q_{in}	QT_{max}	QT_{min}	ΔQ	$\Delta Q/QT_{max} \times 100$
SVF 1					
0.0000	2.370	0.02644	0.02633	0.00011	0.4177
0.0005	2.370	0.02645	0.02631	0.00014	0.5293
0.0010	2.370	0.02647	0.02628	0.00019	0.7177
0.0015	2.370	0.02652	0.02626	0.00026	0.9803
0.0020	2.370	0.02662	0.02623	0.00039	1.4650
0.0025	2.370	0.02680	0.02620	0.00060	2.2388
SVF 2					
0.0000	2.831	0.03155	0.03146	0.00009	0.2852
0.0005	2.831	0.03156	0.03143	0.00013	0.4119
0.0010	2.831	0.03158	0.03141	0.00017	0.5383
0.0015	2.831	0.03161	0.03139	0.00022	0.6959
0.0020	2.831	0.03167	0.03136	0.00031	0.9788
0.0025	2.831	0.03179	0.03134	0.00045	1.4155
SVF 3					
0.0000	1.875	0.02091	0.02083	0.00008	0.3825
0.0005	1.875	0.02091	0.02080	0.00011	0.5260
0.0010	1.875	0.02093	0.02077	0.00016	0.7644
0.0015	1.875	0.02097	0.02074	0.00023	1.0968
0.0020	1.875	0.02105	0.02071	0.00034	1.6152
0.0025	1.875	0.02124	0.02067	0.00057	2.6836
SVF 4					
0.0000	1.477	0.01651	0.01641	0.00010	0.6056
0.0005	1.477	0.01651	0.01638	0.00013	0.8440
0.0010	1.477	0.01654	0.01634	0.00020	1.2091
0.0015	1.477	0.01661	0.01631	0.00030	1.8061
0.0020	1.477	0.01676	0.01627	0.00049	2.9236
0.0025	1.477	0.01708	0.01624	0.00084	4.9180

Tube Size 1.0 Inch

Slope	Q_{in}	$Q_{T_{max}}$	$Q_{T_{min}}$	ΔQ	$\Delta Q/Q_{T_{max}} \times 100$
SVF 1					
0.0000	1.0370	0.01156	0.01152	0.00004	0.3460
0.0005	1.0370	0.01155	0.01150	0.00005	0.4329
0.0010	1.0370	0.01155	0.01148	0.00007	0.6060
0.0015	1.0370	0.01156	0.01146	0.00010	0.8650
0.0020	1.0370	0.01159	0.01144	0.00015	1.2942
0.0025					
SVF 2					
0.0000	1.309	0.01456	0.01454	0.00002	0.1373
0.0005	1.309	0.01455	0.01453	0.00002	0.1374
0.0010	1.309	0.01454	0.01451	0.00002	0.2063
0.0015	1.309	0.01454	0.01449	0.00005	0.3438
0.0020	1.309	0.01455	0.01448	0.00007	0.4810
0.0025	1.309	0.01458	0.01446	0.00012	0.8230
SVF 3					
0.0000	1.594	0.01773	0.01771	0.00002	0.1128
0.0005	1.594	0.01772	0.01770	0.00002	0.1128
0.0010	1.594	0.01772	0.01761	0.00004	0.2257
0.0015	1.594	0.01772	0.01767	0.00005	0.2841
0.0020	1.594	0.01773	0.01765	0.00008	0.4512
0.0025	1.594	0.01775	0.01763	0.00012	0.6760
SVF 4					
0.0000	1.813	0.02015	0.02014	0.00001	0.0496
0.0005	1.813	0.02013	0.02013	0.00000	0.0000
0.0010	1.813	0.02012	0.02012	0.00000	0.0000
0.0015	1.813	0.02011	0.02010	0.00001	0.0497
0.0020	1.813	0.02009	0.02008	0.00001	0.0497
0.0025	1.813	0.02007	0.02006	0.00001	0.0498

APPENDIX G

WATER SURFACE ELEVATIONS FOR A PRISMATIC CHANNEL
WITH THE SIPHON TUBES 1.224 FEET
ABOVE THE CHANNEL BOTTOM

SVF 1 Q = 3.734

TUBE DIAMETER = 2.00 INCHES TUBE LOCATION = 1.0 FOOT
EVERY OTHER TUBE PRIMED

STATION	SLOPE					
	0.0000	0.0005	0.0010	0.0015	0.0020	0.0025
0+00	101.901	101.981	102.052	102.132	102.212	102.293
0+30	101.899	101.979	102.050	102.130	102.210	102.290
0+60	101.898	101.978	102.048	102.128	102.208	102.288
0+90	101.898	101.977	102.047	102.127	102.207	102.287
1+20	101.897	101.977	102.047	102.127	102.207	102.287
1+50	101.897	101.977	102.047	102.127	102.207	102.287
1+80	101.897	101.977	102.047	102.127	102.207	102.287
2+10	101.897	101.977	102.047	102.127	102.207	102.287
2+40	101.897	101.977	102.047	102.127	102.207	102.287
2+70	101.897	101.977	102.047	102.127	102.207	102.287
3+00	101.897	101.977	102.047	102.127	102.207	102.287

SVF 2 Q = 3.234

TUBE DIAMETER = 2.00 INCHES TUBE LOCATION = 1.0 FOOT
EVERY OTHER TUBE PRIMED

STATION	SLOPE					
	0.0000	0.0005	0.0010	0.0015	0.0020	0.0025
0+00	101.759	101.835	101.916	101.991	102.072	102.153
0+30	101.758	101.833	101.913	101.988	102.069	102.149
0+60	101.757	101.832	101.912	101.987	102.067	102.147
0+90	101.756	101.831	101.911	101.985	102.065	102.145
1+20	101.755	101.830	101.910	101.985	102.065	102.145
1+50	101.755	101.830	101.910	101.985	102.065	102.145
1+80	101.755	101.830	101.910	101.985	102.065	102.145
2+10	101.755	101.830	101.910	101.985	102.065	102.145
2+40	101.755	101.830	101.910	101.985	102.065	102.145
2+70	101.755	101.830	101.910	101.985	102.065	102.145
3+00	101.755	101.830	101.910	101.985	102.065	102.145

SVF 3 Q = 2.677

TUBE DIAMETER = 2.00 INCHES TUBE LOCATION = 1.0 FOOT
EVERY OTHER TUBE PRIMED

STATION	SLOPE					
	0.0000	0.0005	0.0010	0.0015	0.0020	0.0025
0+00	101.618	101.694	101.775	101.855	101.959	102.055
0+30	101.617	101.692	101.772	101.853	101.955	102.050
0+60	101.616	101.691	101.771	101.851	101.953	102.048
0+90	101.615	101.690	101.770	101.850	101.952	102.047
1+20	101.615	101.690	101.770	101.850	101.952	102.047
1+50	101.615	101.690	101.770	101.849	101.952	102.047
1+80	101.615	101.690	101.770	101.850	101.952	102.047
2+10	101.615	101.690	101.770	101.850	101.952	102.047
2+40	101.615	101.690	101.770	101.850	101.952	102.047
2+70	101.615	101.690	101.770	101.850	101.953	102.048
3+00	101.615	101.690	101.770	101.850	101.953	102.048

SVF 4 Q = 2.233

TUBE DIAMETER = 2.00 INCHES TUBE LOCATION = 1.0 FOOT
EVERY OTHER TUBE PRIMED

STATION	SLOPE					
	0.0000	0.0005	0.0010	0.0015	0.0020	0.0025
0+00	101.529	101.605	101.688	101.791	101.892	101.973
0+30	101.528	101.603	101.685	101.788	101.889	101.969
0+60	101.527	101.602	101.684	101.787	101.887	101.967
0+90	101.527	101.602	101.683	101.786	101.885	101.965
1+20	101.526	101.601	101.683	101.785	101.885	101.965
1+50	101.526	101.601	101.683	101.785	101.885	101.965
1+80	101.526	101.601	101.683	101.785	101.885	101.965
2+10	101.526	101.601	101.683	101.785	101.885	101.965
2+40	101.526	101.601	101.683	101.786	101.886	101.966
2+70	101.526	101.601	101.683	101.786	101.886	101.966
3+00	101.527	101.602	101.683	101.786	101.886	101.966

SVF 1 Q = 4.092

TUBE DIAMETER = 1.50 INCHES TUBE LOCATION = 1.0 FOOT
ALL TUBES PRIMED

STATION	SLOPE					
	0.0000	0.0005	0.0010	0.0015	0.0020	0.0025
0+00	101.912	101.993	102.064	102.145	102.225	102.306
0+30	101.909	101.990	102.060	102.141	102.221	102.301
0+60	101.907	101.988	102.058	102.138	102.218	102.298
0+90	101.906	101.986	102.056	102.136	102.216	102.296
1+20	101.905	101.985	102.055	102.135	102.215	102.295
1+50	101.905	101.985	102.055	102.135	102.214	102.294
1+80	101.905	101.985	102.055	102.135	102.214	102.294
2+10	101.905	101.985	102.055	102.135	102.214	102.294
2+40	101.905	101.985	102.055	102.135	102.215	102.295
2+70	101.905	101.985	102.055	102.135	102.215	102.295
3+00	101.905	101.985	102.055	102.135	102.215	102.295

SVF 2 Q = 3.499

TUBE DIAMETER = 1.50 INCHES TUBE LOCATION = 1.0 FOOT
ALL TUBES PRIMED

STATION	SLOPE					
	0.0000	0.0005	0.0010	0.0015	0.0020	0.0025
0+00	101.759	101.835	101.916	101.997	102.078	102.160
0+30	101.756	101.832	101.912	101.993	102.073	102.154
0+60	101.755	101.830	101.910	101.990	102.070	102.150
0+90	101.753	101.828	101.908	101.988	102.068	102.148
1+20	101.752	101.827	101.907	101.987	102.067	102.147
1+50	101.752	101.827	101.907	101.987	102.067	102.146
1+80	101.752	101.827	101.907	101.987	102.067	102.146
2+10	101.752	101.827	101.907	101.987	102.067	102.147
2+40	101.752	101.827	101.907	101.987	102.067	102.147
2+70	101.752	101.827	101.907	101.987	102.067	102.147
3+00	101.752	101.827	101.907	101.987	102.067	102.147

SVF 3 Q = 2.877

TUBE DIAMETER = 1.50 INCHES TUBE LOCATION = 1.0 FOOT
ALL TUBES PRIMED

STATION	SLOPE					
	0.0000	0.0005	0.0010	0.0015	0.0020	0.0025
0+00	101.612	101.687	101.768	101.849	101.941	102.042
0+30	101.610	101.685	101.766	101.846	101.936	102.036
0+60	101.608	101.684	101.764	101.844	101.934	102.034
0+90	101.608	101.683	101.763	101.842	101.932	102.032
1+20	101.607	101.682	101.762	101.842	101.931	102.031
1+50	101.607	101.682	101.762	101.841	101.931	102.031
1+80	101.607	101.682	101.762	101.841	101.931	102.031
2+10	101.607	101.682	101.762	101.841	101.931	102.031
2+40	101.607	101.682	101.762	101.842	101.932	102.032
2+70	101.607	101.682	101.762	101.842	101.932	102.032
3+00	101.607	101.682	101.762	101.842	101.932	102.032

SVF 4 Q = 2.130

TUBE DIAMETER = 1.50 INCHES TUBE LOCATION = 1.0 FOOT
ALL TUBES PRIMED

STATION	SLOPE					
	0.0000	0.0005	0.0010	0.0015	0.0020	0.0025
0+00	101.474	101.550	101.641	101.742	101.833	101.916
0+30	101.473	101.549	101.639	101.740	101.830	101.913
0+60	101.473	101.548	101.638	101.738	101.828	101.910
0+90	101.472	101.547	101.637	101.737	101.827	101.909
1+20	101.472	101.547	101.636	101.736	101.826	101.908
1+50	101.472	101.547	101.636	101.736	101.826	101.908
1+80	101.472	101.547	101.636	101.736	101.826	101.909
2+10	101.472	101.547	101.637	101.737	101.826	101.909
2+40	101.472	101.547	101.637	101.737	101.827	101.909
2+70	101.472	101.547	101.637	101.737	101.827	101.909
3+00	101.472	101.547	101.637	101.737	101.827	101.910

SVF 1 Q = 2.365

TUBE DIAMETER = 1.25 INCHES TUBE LOCATION = 1.0 FOOT
ALL TUBES PRIMED

STATION	SLOPE					
	0.0000	0.0005	0.0010	0.0015	0.0020	0.0025
0+00	101.749	101.829	101.900	101.980	102.061	102.151
0+30	101.747	101.828	101.898	101.978	102.058	102.149
0+60	101.747	101.827	101.897	101.977	102.057	102.147
0+90	101.746	101.826	101.896	101.976	102.056	102.146
1+20	101.745	101.825	101.895	101.975	102.055	102.145
1+50	101.745	101.825	101.895	101.975	102.055	102.145
1+80	101.745	101.825	101.895	101.975	102.055	102.145
2+10	101.745	101.825	101.895	101.975	102.055	102.145
2+40	101.745	101.825	101.895	101.975	102.055	102.145
2+70	101.745	101.825	101.895	101.975	102.055	102.145
3+00	101.745	101.825	101.895	101.975	102.055	102.145

SVF 2 Q = 2.827

TUBE DIAMETER = 1.25 INCHES TUBE LOCATION = 1.0 FOOT
ALL TUBES PRIMED

STATION	SLOPE					
	0.0000	0.0005	0.0010	0.0015	0.0020	0.0025
0+00	101.924	102.005	102.075	102.156	102.236	102.317
0+30	101.923	102.002	102.074	102.154	102.234	102.314
0+60	101.922	102.002	102.072	102.152	102.232	102.312
0+90	101.922	102.001	102.072	102.152	102.231	102.311
1+20	101.921	102.001	102.071	102.151	102.231	102.311
1+50	101.921	102.001	102.071	102.151	102.231	102.311
1+80	101.921	102.001	102.071	102.151	102.231	102.311
2+40	101.921	102.001	102.071	102.151	102.231	102.311
2+70	101.921	102.001	102.071	102.151	102.231	102.311
3+00	101.921	102.001	102.071	102.151	102.231	102.311

SVF 3 Q = 1.872

TUBE DIAMETER = 1.25 INCHES TUBE LOCATION = 1.0 FOOT
ALL TUBES PRIMED

STATION	SLOPE					
	0.0000	0.0005	0.0010	0.0015	0.0020	0.0025
0+00	101.582	101.657	101.738	101.818	101.914	102.009
0+30	101.581	101.656	101.736	101.817	101.912	102.007
0+60	101.580	101.655	101.735	101.815	101.910	102.005
0+90	101.580	101.655	101.735	101.815	101.910	102.005
1+20	101.580	101.655	101.735	101.814	101.909	102.004
1+50	101.579	101.654	101.734	101.814	101.909	102.004
1+80	101.579	101.654	101.734	101.814	101.909	102.004
2+10	101.579	101.654	101.734	101.814	101.909	102.004
2+40	101.579	101.654	101.734	101.814	101.909	102.004
2+70	101.579	101.654	101.734	101.814	101.909	102.004
3+00	101.579	101.654	101.734	101.814	101.909	102.004

SVF 4 Q = 1.473

TUBE DIAMETER = 1.25 INCHES TUBE LOCATION = 1.0 FOOT
ALL TUBES PRIMED

STATION	SLOPE					
	0.0000	0.0005	0.0010	0.0015	0.0020	0.0025
0+00	101.467	101.543	101.627	101.733	101.825	101.911
0+30	101.466	101.542	101.626	101.731	101.823	101.909
0+60	101.466	101.541	101.625	101.730	101.821	101.907
0+90	101.465	101.540	101.624	101.729	101.820	101.905
1+20	101.465	101.540	101.624	101.729	101.820	101.905
1+50	101.465	101.540	101.624	101.728	101.820	101.904
1+80	101.465	101.540	101.623	101.728	101.820	101.904
2+10	101.465	101.540	101.623	101.728	101.820	101.904
2+40	101.465	101.540	101.623	101.728	101.820	101.905
2+70	101.465	101.540	101.623	101.728	101.820	101.905
3+00	101.465	101.540	101.623	101.728	101.820	101.905

SVF 1 Q = 1.033

TUBE DIAMETER = 1.00 INCHES TUBE LOCATION = 1.0 FOOT
ALL TUBES PRIMED

STATION	SLOPE					
	0.0000	0.0005	0.0010	0.0015	0.0020	0.0025
0+00	101.517	101.592	101.673	101.758	101.858	101.949
0+30	101.516	101.592	101.672	101.757	101.857	101.948
0+60	101.516	101.591	101.671	101.756	101.857	101.947
0+90	101.516	101.591	101.671	101.756	101.856	101.946
1+20	101.516	101.591	101.671	101.756	101.856	101.946
1+50	101.516	101.591	101.671	101.756	101.856	101.946
1+80	101.516	101.591	101.671	101.756	101.856	101.946
2+10	101.516	101.591	101.671	101.756	101.856	101.946
2+40	101.516	101.591	101.671	101.756	101.856	101.946
2+70	101.516	101.591	101.671	101.756	101.856	101.946
3+00	101.516	101.591	101.671	101.756	101.856	101.946

SVF 2 Q = 1.307

TUBE DIAMETER = 1.00 INCHES TUBE LOCATION = 1.0 FOOT
ALL TUBES PRIMED

STATION	SLOPE					
	0.0000	0.0005	0.0010	0.0015	0.0020	0.0025
0+00	101.651	101.732	101.807	101.807	101.967	102.057
0+30	101.651	101.731	101.806	101.806	101.966	102.057
0+60	101.651	101.731	101.806	101.806	101.966	102.056
0+90	101.651	101.731	101.806	101.806	101.966	102.056
1+20	101.651	101.731	101.806	101.806	101.966	102.056
1+50	101.651	101.731	101.806	101.806	101.966	102.056
1+80	101.651	101.731	101.806	101.806	101.966	102.056
2+10	101.651	101.731	101.806	101.806	101.966	102.056
2+40	101.651	101.731	101.806	101.806	101.966	102.056
2+70	101.651	101.731	101.806	101.806	101.966	102.056
3+00	101.651	101.731	101.806	101.806	101.966	102.056

SVF 3 Q = 1.592

TUBE DIAMETER = 1.00 INCHES TUBE LOCATION = 1.0 FOOT
ALL TUBES PRIMED

STATION	SLOPE					
	0.0000	0.0005	0.0010	0.0015	0.0020	0.0025
0+00	101.814	101.894	101.964	102.044	102.124	102.210
0+30	101.813	101.893	101.963	102.044	102.124	102.209
0+60	101.813	101.893	101.963	102.044	102.124	102.208
0+90	101.813	101.893	101.963	102.044	102.124	102.208
1+20	101.813	101.893	101.963	102.044	102.124	102.208
1+50	101.813	101.893	101.963	102.044	102.124	102.208
1+80	101.813	101.893	101.963	102.044	102.124	102.208
2+10	101.813	101.893	101.963	102.044	102.124	102.208
2+40	101.813	101.893	101.963	102.044	102.124	102.208
2+70	101.813	101.893	101.963	102.044	102.124	102.208
3+00	101.813	101.893	101.963	102.044	102.124	102.208

SVF 4 Q = 1.812

TUBE DIAMETER = 1.00 INCHES TUBE LOCATION = 1.0 FOOT
ALL TUBES PRIMED

STATION	SLOPE					
	0.0000	0.0005	0.0010	0.0015	0.0020	0.0025
0+00	101.950	102.030	102.100	102.180	102.260	102.340
0+30	101.950	102.030	102.100	102.180	102.260	102.340
0+60	101.950	102.030	102.100	102.180	102.260	102.340
0+90	101.950	102.030	102.100	102.180	102.260	102.340
1+20	101.950	102.030	102.100	102.180	102.260	102.340
1+50	101.950	102.030	102.100	102.180	102.260	102.340
1+80	101.950	102.030	102.100	102.180	102.260	102.340
2+10	101.950	102.030	102.100	102.180	102.260	102.340
2+40	101.950	102.030	102.100	102.180	102.260	102.340
2+70	101.950	102.030	102.100	102.180	102.260	102.340
3+00	101.950	102.030	102.100	102.180	102.260	102.340

APPENDIX H

CHANGES IN TUBE DISCHARGE FOR A SLOPING PRISMATIC
CHANNEL WITH THE SIPHON TUBES 1.224 ABOVE
THE CHANNEL BOTTOM

Tube Size 2.0 Inches

Slope	Q_{in}	$Q_{T_{max}}$	$Q_{T_{min}}$	ΔQ	$\Delta Q/Q_{T_{max}} \times 100$
SVF 1					
0.0000	3.739	0.083343	0.083053	0.000290	0.348
0.0005	3.739	0.088878	0.077976	0.010902	12.266
0.0010	3.739	0.093739	0.071549	0.022190	23.672
0.0015	3.739	0.099122	0.065603	0.033519	33.816
0.0020	3.739	0.104326	0.059298	0.045028	43.161
0.0025	3.739	0.109370	0.052552	0.056818	51.951
SVF 2					
0.0000	3.234	0.072198	0.071833	0.000365	0.505
0.0005	3.234	0.077785	0.065877	0.011908	15.309
0.0010	3.234	0.083807	0.059611	0.241960	28.871
0.0015	3.234	0.089206	0.052401	0.036805	41.258
0.0020	3.234	0.094753	0.045059	0.049694	52.446
0.0025	3.234	0.100101	0.036874	0.112921	63.163
SVF 3					
0.0000	2.681	0.059864	0.059539	0.000325	0.543
0.0005	2.681	0.066186	0.052672	0.013514	20.419
0.0010	2.681	0.072812	0.045341	0.027471	37.728
0.0015	2.681	0.079075	0.037182	0.041893	52.979
0.0020	2.681	0.086702	0.031014	0.055688	64.229
0.0025	2.681	0.093400	0.022621	0.070779	75.781
SVF 4					
0.0000	2.240	0.051198	0.050874	0.000324	0.632
0.0005	2.240	0.058143	0.043147	0.014996	25.791
0.0010	2.240	0.065451	0.034948	0.030503	46.605
0.0015	2.240	0.073964	0.028495	0.045469	61.475
0.0020	2.240	0.077561	0.000000	0.077569	100.000

Tube Size 1.5 Inches

<u>Slope</u>	<u>Q_{in}</u>	<u>Q_T_{max}</u>	<u>Q_T_{min}</u>	<u>ΔQ</u>	<u>ΔQ/Q_T_{max} × 100</u>
SVF 1					
0.0000	4.102	0.045855	0.045564	0.000291	0.635
0.0005	4.102	0.048719	0.042969	0.005750	11.801
0.0010	4.102	0.051358	0.039516	0.011842	23.058
0.0015	4.102	0.054281	0.036335	0.017946	33.060
0.0020	4.102	0.057107	0.032965	0.024142	42.276
0.0025	4.102	0.059847	0.029368	0.034790	50.928
SVF 2					
0.0000	3.511	0.039310	0.038997	0.000313	0.796
0.0005	3.511	0.042243	0.035882	0.006361	15.057
0.0010	3.511	0.045530	0.032486	0.013044	28.649
0.0015	3.511	0.048673	0.028856	0.019817	40.714
0.0020	3.511	0.051692	0.024915	0.026777	51.802
0.0025	3.511	0.054604	0.020540	0.034064	62.384
SVF 3					
0.0000	2.884	0.032273	0.032026	0.000247	0.767
0.0005	2.884	0.035672	0.028339	0.007333	20.557
0.0010	2.884	0.039304	0.024328	0.014976	38.104
0.0015	2.884	0.042735	0.019842	0.022893	53.570
0.0020	2.884	0.046406	0.015442	0.030964	66.723
0.0025	2.884	0.050287	0.011092	0.039195	77.942
SVF 4					
0.0000	2.137	0.024706	0.024540	0.000166	0.669
0.0005	2.137	0.028783	0.019914	0.008869	30.815
0.0010	2.137	0.033396	0.015503	0.017893	53.579
0.0015	2.137	0.038096	0.011137	0.026959	70.767

Tube Size 1.25 Inches

Slope	Q _{in}	Q _{Tmax}	Q _{Tmin}	ΔQ	ΔQ/Q _{Tmax} × 100
SVF 1					
0.0000	2.370	0.026438	0.026333	0.000105	0.398
0.0005	2.370	0.028690	0.024235	0.004455	15.529
0.0010	2.370	0.030649	0.021548	0.009101	29.695
0.0015	2.370	0.032802	0.019013	0.013789	42.037
0.0020	2.370	0.034869	0.016244	0.018625	53.416
0.0025	2.370	0.037111	0.013607	0.023504	63.334
SVF 2					
0.0000	2.831	0.031551	0.031456	0.000095	0.303
0.0005	2.831	0.033575	0.029591	0.003984	11.866
0.0010	2.831	0.035357	0.027248	0.008109	22.935
0.0015	2.831	0.037333	0.025086	0.012247	32.804
0.0020	2.831	0.039244	0.022803	0.016441	41.895
0.0025	2.831	0.041098	0.020361	0.020737	50.457
SVF 3					
0.0000	1.875	0.020913	0.020833	0.000080	0.381
0.0005	1.875	0.023368	0.018126	0.005242	22.433
0.0010	1.875	0.025896	0.015253	0.010643	41.097
0.0015	1.875	0.028276	0.011982	0.016294	57.624
0.0020	1.875	0.030955	0.008960	0.021995	71.054
0.0025	1.875	0.033495	0.005088	0.028437	84.901
SVF 4					
0.0000	1.477	0.016510	0.016411	0.000099	0.601
0.0005	1.477	0.019312	0.013202	0.006110	31.637
0.0010	1.477	0.222620	0.009772	0.012490	56.104
0.0015	1.477	0.025656	0.006958	0.018698	72.880
0.0020	1.477	0.026780	0.000000	0.026780	100.000

Tube Size 1.0 Inch

Slope	Q_{in}	$Q_{T_{max}}$	$Q_{T_{min}}$	ΔQ	$\Delta Q/Q_{T_{max}} \times 100$
SVF 1					
0.0000	1.037	0.011555	0.011522	0.000033	0.280
0.0005	1.037	0.013218	0.009648	0.003570	27.008
0.0010	1.037	0.014889	0.007625	0.007264	48.791
0.0015	1.037	0.016545	0.005375	0.011170	67.511
0.0020	1.037	0.018373	0.003112	0.015261	83.062
0.0025	1.037	0.019922	0.002572	0.017350	87.091
SVF 2					
0.0000	1.309	0.014562	0.014544	0.000018	0.122
0.0005	1.309	0.016125	0.013055	0.003070	19.038
0.0010	1.309	0.017521	0.011309	0.006212	35.457
0.0015	1.309	0.018938	0.009506	0.009432	49.803
0.0020	1.309	0.020291	0.007456	0.012835	63.255
0.0025	1.309	0.021750	0.005354	0.016396	75.382
SVF 3					
0.0000	1.594	0.017732	0.017711	0.000021	0.120
0.0005	1.594	0.019119	0.016416	0.002703	14.138
0.0010	1.594	0.020295	0.014823	0.005472	26.964
0.0015	1.594	0.021593	0.013335	0.008258	38.242
0.0020	1.594	0.022843	0.011734	0.011109	48.632
0.0025	1.594	0.024126	0.010112	0.014014	58.086
SVF 4					
0.0000	1.813	0.020146	0.020144	0.000002	0.010
0.0005	1.813	0.021448	0.018935	0.002513	11.717
0.0010	1.813	0.022545	0.017487	0.005058	22.435
0.0015	1.813	0.023763	0.016155	0.007608	32.016
0.0020	1.813	0.024942	0.014749	0.010193	40.867
0.0025	1.813	0.026087	0.013247	0.012840	49.218

VITA

Albert Lee Mink

Candidate for the Degree of
Doctor of Philosophy

Thesis: THE HYDRAULICS OF AN IRRIGATION DISTRIBUTION
CHANNEL

Major Field: Engineering

Biographical:

Personal Data: Born in Jonesboro, Arkansas,
September 17, 1936, the son of Albert L.
and Lorene Mink.

Education: Graduated from Brookland High School
in Brookland, Arkansas in 1955; graduated from
Arkansas State College with a Bachelor of Science
in Agriculture degree in 1961; received the
Master of Science in Agricultural Engineering
degree from Louisiana State University, 1963;
completed the requirements for the Doctor of
Philosophy degree from Oklahoma State University
in May, 1967.

Professional Experience: Worked in Maintenance
Department of General Motors Corporation in
1956; worked in Maintenance for Emerson Electric
Company in 1957; worked as a carpenter for
Cooper Construction Corporation in the summers
of 1958 and 1959; taught chemistry and physical
science for Brookland School District in 1960;
research assistant for the Agricultural Engineer-
ing Department, Louisiana State University,
1961-1963 and at Oklahoma State University,
1963-1966.

Professional and Honorary Organizations: Member of
Gamma Sigma Delta, Phi Kappa Phi, American
Society of Agricultural Engineers, and an honorary
member of American Society of Testing Materials,
1963-1964.